

Induction and suppression of
the innate antiviral responses
by picornaviruses

Qian Feng

Cover illustrations

This thesis has a strong emphasis on the battle between viruses and their hosts – how the host recognizes the enemy, and how the virus tries to evade the host defense system. However, it is not to be forgotten that viruses and their hosts have also come to an agreement, or a common understanding, if you like, during their very long co-evolution. Viruses do not wipe off their host species, and the host also lends resources to allow the virus to replicate, once in a while.

Cover designed by Qian Feng
Cover executed by Nikki Vermeulen, Ridderprint BV
Printed by Ridderprint BV, Ridderkerk, The Netherlands

Printing of this thesis was partially sponsored by
Graduate School Infection & Immunity Utrecht

Copyright 2014 Qian Feng

All rights reserved. No part of this publication may be reproduced or transmitted in any form or by any means without written permission of the author and the publisher holding the copyrights of the published articles.

ISBN
978-90-393-6160-3

致韩宪耀同志 😊

For my grandpa

who was never given the chance to become a scientist,
but has always remained a man of science at heart

Induction and suppression of the innate antiviral responses by picornaviruses

Inductie en onderdrukking van de aangeboren
antivirale responsen door picornavirussen

(met samenvattingen in het Nederlands en Chinees)

Proefschrift

ter verkrijging van de graad van doctor aan de Universiteit Utrecht
op gezag van de rector magnificus, prof. dr. G.J. van der Zwaan,
ingevolge het besluit van het college voor promoties
in het openbaar te verdedigen op
maandag 30 juni 2014 des middags te 12.45 uur

door

Qian Feng

geboren op 21 juni 1985
te Beijing, China

Promotor: Prof. dr. F.J.M. van Kuppeveld

This thesis was financially supported by a Mozaïek grant from the Netherlands Organisation for Scientific Research (NWO).

CONTENTS

Chapter 1	General Introduction	9
Chapter 2	MDA5 Detects the Double-Stranded RNA Replicative Form in Picornavirus-Infected Cells <i>Cell Reports. 2012. 2(5):1187-96.</i>	31
Chapter 3	Coxsackievirus Cloverleaf RNA Containing a 5' Triphosphate Triggers an Antiviral Response via RIG-I Activation <i>PLoS One. 2014. 9(4): e95927.</i>	55
Chapter 4	Enteroviruses 2A ^{pro} Targets MDA5 and MAVS in Infected Cells <i>Journal of Virology. 2014. 88(6):3369-78.</i>	75
Chapter 5	MDA5 Localizes to Stress Granules, but This Localization Is Not Required for the Induction of Type I Interferon <i>Journal of Virology. 2013. 87(11):6314-25.</i>	95
Chapter 6	Summary and General Discussion <i>Cytokine and Growth Factors Review. 2014. Submitted upon invitation.</i>	119
Chapter 7	Nederlandse en Chinese samenvattingen	143
	Dankwoord / Acknowledgements / 致谢词	153
	Curriculum Vitae	160
	List of publications	161

Chapter 1

General Introduction

PICORNAVIRUSES

Viral diseases have long accompanied mankind. An ancient Egyptian stele dated to 1403-1365 BC depicts a man with a withered leg, a symptom rather typical to that of poliomyelitis caused by poliovirus (PV), may very well be one of the earliest documentations of a viral disease (1). *Picornaviridae* is a large family of human and animal pathogens comprising of 17 genera, including *Enterovirus*, *Cardiovirus*, *Parechovirus*, and *Aphthovirus*. These viruses were traditionally classified based on their pathogenicity in humans and animals, and defined as serotypes. However, with increasing advancements in sequence analysis, picornaviruses are currently grouped based on their genetic relationships. For instance, many coxsackievirus A (CVA) serotypes are split into the species *Enterovirus A* and *C*, and species *Enterovirus B* contains many CVB serotypes and many echoviruses. Furthermore, rhinoviruses, which cause pathology in the respiratory systems, were initially recognized as a separate genus, but have been grouped into the *Enterovirus* genus since their genomic sequences are known. Figure 1 represents the classification of picornaviruses according to the International Committee of Taxonomy of Viruses (ICTV) as of 28 February, 2014, specially featuring the genera *Enterovirus* and *Cardiovirus*.

Among the large picornavirus family, the *Enterovirus* genus contains a large number of human pathogens. PV is the etiological agent of the paralytic disease poliomyelitis and caused large scale epidemics worldwide prior to the introduction of vaccines in the late 1950's and early 1960's, which tremendously helped to keep poliovirus under control in developed countries, but it continues to cause outbreaks in parts of the world even today. Since 1988, PV has become the subject of a global eradication campaign launched by the WHO, a multibillion dollar international operation that was intended to end in 2000 but is still not completed in 2014 (1). Other enteroviruses collectively cause a number of diseases in humans. Enterovirus 71 (EV71) and others are known to cause the so-called hand, foot and mouth disease (HFMD) in small children, a mostly mild clinical manifestation including fever, diarrhea and blisters in the palms of hands and foot, but can also cause central nervous system infections leading to serious neurological symptoms and even death (2, 3). Many HFMD outbreaks have occurred in the past decade, mostly concentrated in Southeast Asia. In addition, enteroviruses are also leading causes of encephalitis, aseptic meningitis, pancreatitis and myocarditis (reviewed in (4–6)), and have also been implicated in the development of type I diabetes (7). Human rhinoviruses (HRVs) are responsible for approximately one third to one half of common colds in adults, posing a huge economic impact on our society, and are also associated with asthma exacerbations and chronic obstructive pulmonary disease (COPD) (8, 9). Furthermore, members of the *Parechovirus* genus, especially Human Parechovirus 3, have been found to cause severe neonatal infections associated with neonatal sepsis, encephalitis and hepatitis (10). Hepatitis A virus (HAV), from the *Hepatovirus* genus, is also an important human pathogen, causing hepatitis A, as the name suggests (11, 12).

Besides these human-tropic viruses, the picornavirus family also contains a number of important animal pathogens, such as members of the *Cardiovirus* and *Aphthovirus* genera. *Encephalomyocarditis virus (EMCV)* and *Theilovirus* are two species under the *Cardiovirus* genus and are primarily rodent pathogens. However, EMCV also causes severe, sometimes lethal, infections in a wide variety of other animals such as pigs, elephants, lions and primates, posing

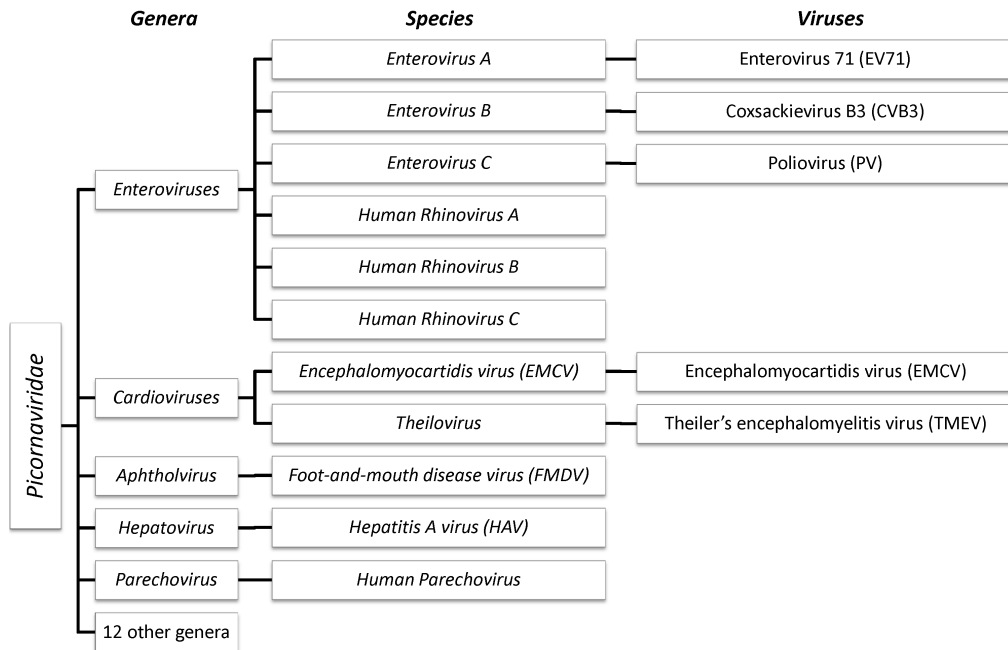


Figure 1. Classification of picornaviruses specially featuring members of the *Enterovirus* and *Cardiovirus* genera, and other viruses mentioned in this thesis.

problems in zoos and national parks (13, 14). Recently, a new cardiovirus that infects humans has been discovered, namely the Saffold virus, which has been associated with gastroenteritis and respiratory and neurological infections (reviewed in (6)). Another genus, *Aphthovirus*, also contains a highly relevant virus – the foot-and-mouth disease virus (FMDV). FMDV causes foot-and-mouth disease (not to be confused with HFMD caused by some enteroviruses in humans) in cloven-hoofed animals, and have severe implications on animal farms since outbreak control often requires slaughter of large numbers of animals, leading to tremendous economic loss.

Currently, no vaccines (with a few exceptions such as for PV, EV71 and HAV) or licensed antivirals are available to combat picornavirus infections. Further research that may lead to new targets and/or antiviral strategies are in need to aid future development of antiviral interventions against this large family of pathogens.

The life cycle of picornaviruses

Picornaviruses are small, non-enveloped, positive-strand RNA viruses. The viral genome, a single-stranded (ss) RNA molecule of 7.5-8.5 kb, is tightly packaged in an icosahedral protein shell of approximately 30 nm, formed by the viral structural proteins VP1-4. The viral RNA contains a single open reading frame (ORF), a untranslated region (UTR) at each terminus, and a poly(A) tail at the extreme 3' end. The 5' terminus of the viral RNA is coupled to a small viral peptide VPg (also known as 3B) via a phosphodiester bond, as a result of VPg-primed viral RNA replication (the replication cycle will be discussed in more details below). The genomic RNA also contains several structured RNA elements that are crucial for virus replication. The internal

ribosomal entry site (IRES) in the 5' UTR drives viral cap-independent translation. Stem-loop structures in the UTRs and a *cis*-acting RNA element (CRE) – the position of which varies across different genera – are indispensable for viral RNA replication.

Picornaviruses share a similar life cycle. Below, the replication life cycle of enteroviruses is described (Figure 2) (15, 16). Relevant differences in the replication cycle of other genera will be indicated later. Upon receptor-mediated endocytosis, the viral particle uncoats, releasing the genomic RNA into the cytoplasm of the host cell. Next, a cellular enzyme releases the VPg peptide from the genomic RNA, for reasons not yet understood. As a positive-strand RNA, the viral genome is immediately translated by the host translation machinery, driven by the viral IRES. A large polyprotein is produced which subsequently undergoes proteolytic processing by the virally encoded proteinases 2A^{pro}, 3C^{pro} and 3CD^{pro} to produce precursor and mature viral proteins. 2A^{pro} autocleaves at its own N terminus releasing the P1 (capsid) region from the rest of the polyprotein. 3C^{pro} then performs all the intramolecular cleavage events within and between the P2 and P3 regions, while its precursor 3CD^{pro} processes the capsid proteins within the P1 region *in trans*. Besides the viral polyprotein processing, 2A^{pro} and 3C^{pro}/3CD^{pro} also cleave a number of host factors to aid virus RNA replication and/or to evade the host antiviral responses (will be discussed in more detail in the section **Picornavirus evasion mechanism**). Next, several viral non-structural proteins including 2B, 2C, 3A and their precursors hijack regulatory mechanisms of membrane metabolism of the host cell, and induce extensive remodeling of the intracellular membranous structures to form the so-called replication organelles (ROs), tubulovesicular membranous networks where viral RNA replication takes place. The process of RNA replication is carried out by the virally encoded RNA-dependent RNA polymerase (3D^{pol}). First, 3D^{pol} uridylylates VPg, and uses the resulting VPg-pU-pU as a primer to transcribe the positive-strand RNA into a complementary, negative-strand RNA molecule. During this process,

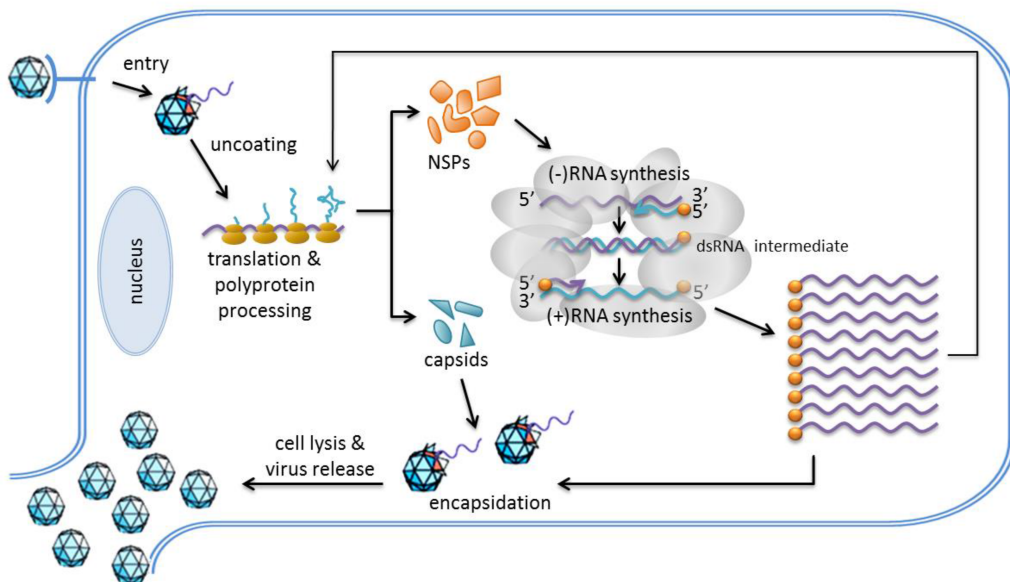


Figure 2. Illustration of the replication cycle of picornaviruses.

a long dsRNA intermediate product is produced, which is referred to as the replicative form (RF) (Figure 3). Next, $3D^{pol}$ uses the negative-strand RNA as a template, and again VPg-pU-pU as a primer, to produce a large number of new positive strands. This step leads to the production of another intermediate product, namely the replicative intermediate (RI), which comprises of a single negative-strand RNA and multiple incomplete positive-strand RNAs that are undergoing active transcription. The completed nascent positive-strand RNAs can then either enter a new round of translation and RNA replication or be encapsidated to form new virions. At the end of the replication cycle, progeny virus particles are released by cell lysis, though non-lytic virus release has also been proposed for some picornaviruses (17–20).

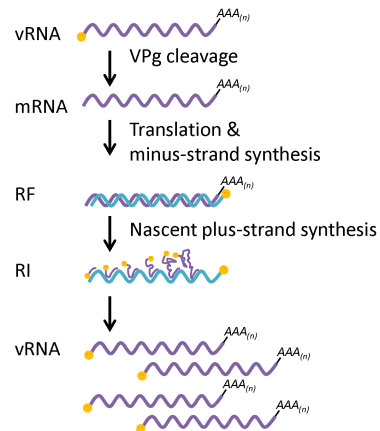


Figure 3. Systematic illustration of steps of picornavirus RNA replication (taken from **Chapter 2**).

Not all picornaviruses encode for a 2A protein with proteinase activity. The 2A proteins of cardioviruses and aphthoviruses are not proteases, however, they contain a small peptide motif at their C termini that induces a so-called ribosome slippage (or StopGo) phenomenon. At this motif, the ribosome releases the P1-2A precursor, and continues translating the rest of the polyprotein. The P1/2A cleavage is carried out by the $3C^{pro}$ of these viruses. The 2A proteins of hepatitis A virus and human parechoviruses are neither proteases themselves, nor do they induce ribosome slippage. Polyprotein processing is believed to be carried out by the 3C proteinase. (15, 16)

In addition, some picornaviruses encode an additional viral protein at the 5' end of the ORF. Because of this position, these proteins have all been named Leader (L), though they share little sequence or functional similarities across genera. The L protein of aphthoviruses acts as a proteinase, can release itself from the rest of the polyprotein, and cleaves a number of host factors during infection. The L protein of cardioviruses possesses no protease activity, is non-essential for virus replication in cell culture, but is an important virulence factor *in vivo*. (15, 16)

ANTIVIRAL INNATE IMMUNE RESPONSES

Viral infections stimulate responses of our immune system. The adaptive immune reactions, such as antibody and T cell responses, are specifically directed to the invading pathogen, and are often very important in eventually clearing the pathogen from the host organism. However, upon infection of a previously unencountered pathogen, these reactions can take days to weeks to develop. The innate immunity is a more responsive system. Although non-specific, these reactions can be mounted immediately after infection. However, these reactions still rely on specific cell types such as natural killer (NK) cells, macrophages, DCs and more to function, which must first be recruited to the site of infection. A yet faster reacting system is the cell-based antiviral responses such as the type I interferon system, which can be mounted by virtually all nucleated cells in our body. They form the first line of defense against invading pathogens and act as an early warning system to the innate and adaptive immune systems.

Type I interferons

A group of key players in the innate antiviral responses are the type I interferons (IFNs). Type I IFNs are class II α -helical cytokines, and include 13 subtypes of IFN- α and a single IFN- β in humans (21). IFN- α/β can be produced by virtually all nucleated cell types, and bind to the ubiquitously expressed receptor IFNAR in autocrine as well as paracrine manners (Figure 4). Activated IFNAR then initiates a signaling cascade via the JAK/STAT pathway, eventually leading to activation of the interferon-stimulated response element promoter. This drives the expression of hundreds of interferon-stimulated genes (ISGs), the products of which establish a so-called antiviral state in the target cell (22). Well known examples of ISGs include protein kinase R (PKR), which, upon dsRNA activation, phosphorylates eukaryotic initiation factor 2 α (eIF2 α) and thereby halts host translation. Another example of ISG is 2'-5' oligo(A) synthetase (OAS), which produces 2'-5' adenosine (A) upon activation. 2'-5'(A) then activates RNase L, which then non-specifically digests intracellular RNAs. Besides ISG induction, IFN- α/β also help orchestrate the innate and adaptive immune responses by activating NK cells, macrophages and dendritic cells (DCs), as well as promoting iNOS production (21, 23, 24).

Pattern recognition receptors

To mount a timely immune response, our cells must efficiently and correctly recognize an invading pathogen. In this regard, our cells rely heavily on specialized pattern recognition receptors (PRRs), which recognize specific pathogen-associated molecular patterns (PAMPs) produced by pathogens including bacteria, viruses, parasites, and fungi.

Toll-like receptors (TLRs) are a family of well-studied PRRs that can recognize various PAMPs including lipopolysaccharide, flagellin, nucleic acids, *etc.* TLRs are expressed in specific immune cell types, such as macrophages and DCs, and function either at the plasma membrane or in endosomes, surveying the extracellular environment (reviewed in (25, 26)). Among all known mammalian TLRs, TLR3, 7, 8 and 9 are particularly important for detection of viruses. TLR3 and TLR7/8 recognize dsRNAs and ssRNAs, respectively, while TLR9 recognizes non-methylated CpG-containing DNAs. Upon activation, these TLRs induce activation of transcription factors such as NF- κ B and IRF3 to activate transcription of proinflammatory cytokine and IFN- α/β genes (Figure 4).

RIG-I-like receptors (RLRs) form another important group of PRRs, a family of DExH/D box helicases including RIG-I (retinoic acid-inducible gene I) (27), MDA5 (melanoma differentiation factor 5) (28–30), and LGP2 (laboratory of genetics and physiology 2) (31). Unlike TLRs, RLRs are ubiquitously expressed, and function in the cytoplasm of cells to detect intracellular RNA molecules that carry “non-self” molecular motifs.

All three members of the RLR family contain a DExH/D helicase domain, which is highly conserved within the RLR family (31) (Figure 5). RIG-I and MDA5 also contain tandem caspase activation and recruitment domains (CARDs) at their N termini, which are responsible for initiating downstream signaling cascades via protein-protein interaction (31). LGP2 lacks the CARD domains and thereby the ability to signal to downstream molecules, but instead, plays regulatory roles on RIG-I and MDA5 (31–35). Additionally, RIG-I contains a C terminal domain (CTD) that binds to the CARD domains during resting conditions, preventing RIG-I from interacting with downstream molecules (36).

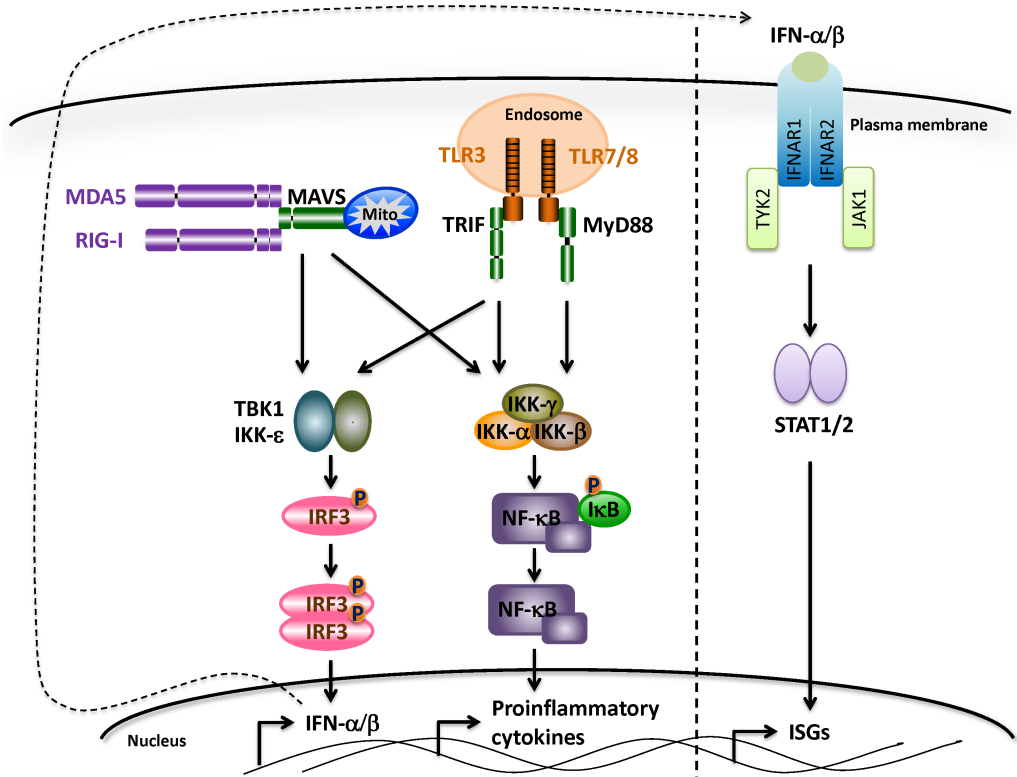


Figure 4. Type I interferon (IFN- α/β) induction and signaling pathways. (Left) RIG-I-like receptors (RLRs) and Toll-like receptors (TLRs) that are important for viral RNA recognition and their downstream signaling cascades leading to transcription activation of IFN- α/β and proinflammatory cytokine genes. (Right) The IFN- α/β signaling pathway leading to transcription activation of interferon-stimulated genes (ISGs).

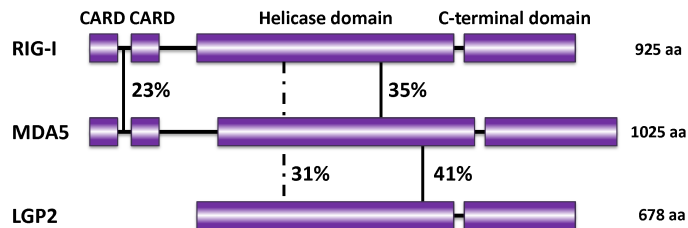


Figure 5. Systematic representation of the domain structures of RLRs. Numbers indicate the percentage of amino acid identities shared by connected domains. Figure drawn based on (31).

Chapter 1

Upon ligand recognition, RIG-I and MDA5 interact with an adaptor molecule MAVS (also known as VISA, Cardif and IPS-1) (37–40), which is localized to the outer membrane of mitochondria. MAVS then oligomerizes (41) and activates the TBK1/IKK- ϵ and IKK- $\alpha/\beta/\gamma$ pathways. TBK1 phosphorylates and activates IRF3, leading to transcription activation of IFN- α/β genes, whereas the IKK- $\alpha/\beta/\gamma$ complex leads to NF- κ B activation and the transcription of many proinflammatory cytokine genes (26) (Figure 4).

RLR ligands

Although RIG-I and MDA5 share a high level of sequence homology (31), they detect distinct groups of viruses. RIG-I mediates IFN- α/β response against many RNA viruses such as influenza virus (42), Japanese encephalitis virus (43), hepatitis C virus (36), and rabies virus (44), whereas MDA5 recognizes a variety of picornaviruses including EMCV, Theiler's murine encephalomyelitis Virus (TMEV), CVs, HRV and PV (45–49), mouse norovirus (50), mouse hepatitis virus (51) and defective interfering particles of paramyxoviruses (52). In other cases, RIG-I and MDA5 appear to collaborate to sense pathogens such as rotavirus (32), Sindbis virus (53), West Nile virus (54, 55), dengue virus (56) and measles virus (57).

Lots of effort has been invested into characterizing RIG-I and MDA5 ligands. *In vitro* studies using synthetic ligands showed that RIG-I requires relatively short dsRNAs, or ssRNAs with double-stranded regions, containing 5' triphosphate groups (5'ppp) for activation (58–62). An exception to the 5'ppp requirement is the synthetic dsRNA mimic polyinosinic:polycytidylic acid (poly(I:C)), which is a potent RIG-I activator (when it is shorter than 1-2 kb) but does not have 5'ppp (27, 59, 63). In agreement with these *in vitro* findings, the 5'ppp-containing, pan-handle RNA structures of many negative-strand RNA viruses such as influenza virus and Sendai virus have been shown to potently activate RIG-I (64, 65). However, other RIG-I-stimulating RNAs have been described which do not share the classic RIG-I ligand characteristics. These include RNase L digestion products, which are very small (< 200 nt) RNAs carrying 5' hydroxyl and 3' monophosphoryl groups (66), as well as a 5'ppp-containing polyuridine RNA motif derived from hepatitis C virus 3' UTR, a linear stretch of RNA (67). Together, these results demonstrate the variety of RNA motifs that can potentially activate RIG-I, and suggest that there is still much to learn about the mode of activation of this RNA receptor.

MDA5 recognizes long dsRNAs as evidenced by data from transfection experiments using poly(I:C) (46, 59, 68). In addition, it has been reported that the L segments of the reovirus genome, which includes several dsRNAs of approximately 4 kbp, induced an IFN- α/β response that is partially dependent on MDA5 (Kato et al., 2006). To date, there is no evidence that specific terminal groups are required on the RNA ligand to activate MDA5. *In vitro* electron microscopy (EM) studies revealed that MDA5 actually scans/binds to different types of nucleic acids including ssRNA, dsRNA and DNA. However, only dsRNA binding could induce a cooperative assembly of MDA5 molecules to form a filamentous oligomer along the length of the dsRNA *in vitro*. The stability of this MDA5 filament was found to be directly related to the length of the dsRNA (69), providing a possible mechanistic explanation for the requirement of long dsRNA molecules for MDA5 activation. What MDA5 recognizes during viral infections is not yet clear.

PRR ligands as potential broad-spectrum antivirals and vaccine adjuvants

It is long known that IFN- α/β are potent antiviral agents. In fact, pegylated recombinant IFN- α

and IFN- β have been used for decades in the clinic to treat infections of hepatitis B and C viruses (70, 71). However, IFN therapy causes prolonged, severe side effects including, among others, nausea, hematological toxicity and depression (72), which makes it less desirable for future use. Recently, major efforts have been directed towards utilizing PRR ligands as antiviral agents, as this may mimic the induction of antiviral responses during a natural viral infection. Many TLR ligands such as synthetic CpG oligodeoxynucleotides and poly(I:C) have been shown effective in eliciting protective immune responses and combating various viral infections (73–76). Recently, a few RIG-I agonists have also been shown to exert potent antiviral activities, including a short, 5'ppp-containing RNA derived from the 3' UTR of FMDV and two 5'ppp-containing RNA hairpins derived from Sendai virus and vesicular stomatitis virus (VSV) (77–79). Importantly, employing a systems analysis approach, Goulet et al. demonstrated that the VSV hairpin RNA induced an extensive spectrum of RIG-I responsive genes, including not only the classical ISGs as a result of IRF3-mediated IFN- α/β induction, but also many proinflammatory cytokine and chemokine genes due to NF- κ B activation, thus providing a much more complete and balanced immune activation (79). This study encourages further research aimed at better understanding of RIG-I-ligand interaction, and exploiting the RLR pathway as a means of immune stimulation in disease.

Cellular stress response

Besides the IFN- α/β and inflammatory responses, cells also employ various other mechanisms to cope with undesirable conditions. One of such mechanisms is the formation of stress granules (SGs) in the presence of external stress such as oxidative, heat, or nutrient stress, UV radiation and viral infections. SGs are cytoplasmic aggregates of many translation initiation factors, 40S ribosomes, mRNAs, and numerous other RNA-binding proteins (Figure 6), and function as a means of temporary storage of pre-initiation complexes. SGs are very dynamic structures that form quickly when cellular translation rate declines, and disassemble again when the stress condition is resolved, releasing mRNAs and translation factors (reviewed in (80)). In most cases, SG formation is triggered by the phosphorylation of eIF2 α , and thus inactivation of translation, by one of four kinases –PKR, PKR-like endoplasmic reticulum kinase (PERK), heme-regulated kinase (HRI), and general control non-depressible 2 kinase (GCN2). However, eIF2 α phosphorylation-independent SG formation after oxidative stress or direct inhibition of eIF4G or eIF4A has also been reported (81–83), indicating that eIF2 α phosphorylation is not an absolute prerequisite for SG assembly. Several marker proteins such as Ras GTPase-activating protein-binding protein (G3BP), T-cell intracellular antigen (TIA) and TIA-related protein (TIAR) are commonly used to identify SGs, but several other proteins have been reported to associate with SGs formed under specific types of stress (80), indicating that there is some level of specificity of the cellular stress response.

Although the SG pathway was initially thought to function independently of classical innate antiviral responses such as IFN- α/β , it was recently suggested that SGs may also directly or indirectly play a role in antiviral activities (80). The aggregation of host translation initiation factors may be detrimental for viruses that rely on cap-dependent translation machinery such as influenza virus. It is also conceivable that some viral mRNAs may be sequestered at SGs and therefore, cannot be used for viral translation. The possible antiviral effect of SGs is also indirectly supported by the fact that many viruses actively interfere with SG formation, including PV, TMEV, cricket paralysis virus, influenza A virus (IAV), mammalian orthoreovirus, and rotavirus (80). Curiously, two well established, unrelated recombinant viruses that can no

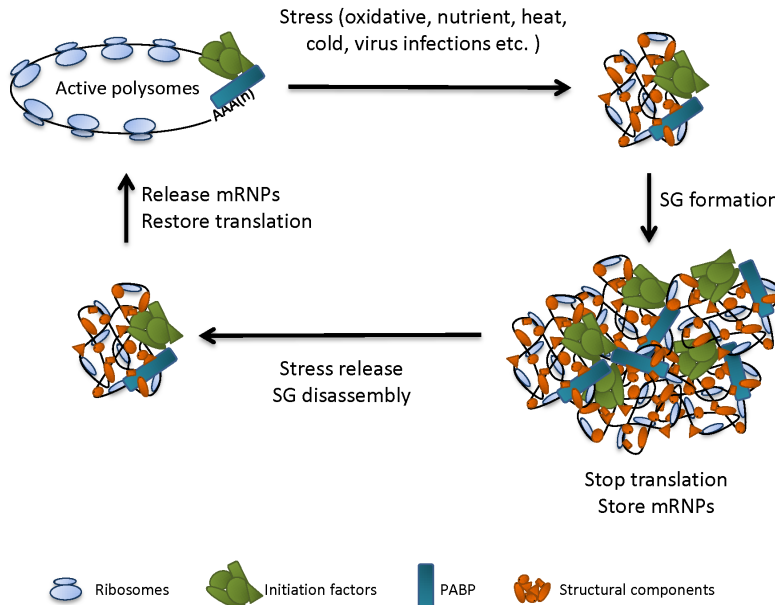


Figure 6. Illustration of the stress response. SG, Stress Granules.

longer suppress IFN- α/β induction, namely IAV- Δ NS1 and TMEV- Δ L, have also lost their abilities to inhibit SG formation during infection (84, 85). That IFN suppression and SG suppression phenotypes correlate with each other tentatively suggest that these two antiviral systems may be linked. Interestingly, a recent report suggested that both RIG-I and viral ssRNA (ligand of RIG-I) translocate to SGs during IAV- Δ NS1 infection, and artificial inhibition of SG formation, by G3BP knockdown or PKR knockout, resulted in a reduction in IFN- α/β response (86). These results suggest that SGs may be used by cytoplasmic sensors as a viral RNA detection platform.

PICORNAVIRUS MECHANISMS TO EVADE INNATE ANTIVIRAL RESPONSES

RLR pathway antagonization

Like most viruses, picornaviruses have evolved to actively circumvent host antiviral activities at multiple steps. Several enteroviruses have been reported to directly interfere with the RLR-mediated IFN- α/β induction pathway. Both MDA5 and MAVS seem to be targeted for cleavage or degradation during infection of some enteroviruses. However, different, and sometimes conflicting, mechanisms have been proposed for the inactivation of each of these factors (87–91). In addition, RIG-I is also reportedly cleaved during infection of several enteroviruses such as PV, echovirus, and HRV 16 and 1A, most likely via their 3C^{pro} activity (92), though it remains to be elucidated why these viruses would target a RNA sensor that does not participate in their recognition. It is somewhat surprising that enteroviruses seem to employ a wide variety of mechanisms to shut down the RLR pathway, since these viruses tend to utilize the same strategies to target a particular host factor or pathway. A systematic examination of RLR pathway factors during infection of various enteroviruses is required to provide a comprehensive overview.

EMCV, a cardiavirus, has also been reported to target RIG-I, either by direct cleavage by the viral 3C^{pro} (92) or via caspase-mediated degradation (93). Whether RIG-I targeting contributes to IFN- α/β suppression in EMCV-infected cells is unknown since this receptor is not implicated in EMCV detection (68). Furthermore, recombinant EMCVs or TMEVs carrying substitutions or deletions in the L protein were able to induce significantly higher levels of IFN- β as compared to wt EMCV (94–96), indicating that L, which has no protease activity, is the primary IFN antagonist of cardiaviruses. HAV, a member of the *Hepatovirus* genus, also proteolytically targets MAVS for cleavage. In this case, a precursor of the viral 3C^{pro} proteinase, namely the 3ABC, is responsible, and both the proteinase activity of 3C^{pro} and a transmembrane domain in 3A, which targets 3ABC to mitochondria where MAVS is localized, are required (97). Another picornavirus, FMDV from the *Aphthovirus* genus, also targets the RLR pathway. The 3C^{pro} of FMDV has been reported to cleave NF- κ B essential modulator (NEMO, also known as IKK- γ), a factor required for NF- κ B activation (98). In addition, the L protein of FMDV exerts deubiquitinating activity, and has been shown to reduce ubiquitination of both RIG-I and TBK1 (99), which is known to modulate the activity of these factors.

Stress pathway suppression

As mentioned above, SGs may also act as an antiviral mechanism, and their formation is actively suppressed by many viruses including members of the picornavirus family. PV induces eIF2 α phosphorylation and SG formation early on during infection, but gradually eliminate them, presumably by cleaving G3BP via their 3C^{pro} activity (100, 101). Artificially sustaining SGs in infected cells by overexpressing a 3C^{pro} cleavage-resistant G3BP leads to reduced virus replication, confirming that SGs exert antiviral roles during PV infection (100). TMEV also inhibits SG formation during infection, in this case by their L protein (84), although the biological consequence of TMEV-induced SG suppression remains to be demonstrated.

Other potential antagonization mechanisms

Besides the direct antagonization of the RLR pathway and SG formation, several other virus-induced events have also been suggested to play a role in viral immune evasion. It is well documented that several picornaviruses inhibit host transcription and cap-dependent translation (also referred to as host shutoff) (reviewed in (4)). In enterovirus-infected cells, this is achieved by cleavage of transcription and translation factors by viral proteinases. 2A^{pro} cleaves and inactivates eukaryotic initiation factor 4G (eIF4G) to inhibit host mRNA translation (102–104), while 3C^{pro} participates in both transcription and translation shutoff by cleaving TATA box-binding protein (TBP) (105, 106), CREB (107) and poly(A)-binding protein (PABP) (108, 109). The 2A proteins of aphthoviruses do not have proteinase activity. Instead, these viruses use another viral proteinase, namely the L^{pro}, to target eIF4G for cleavage (110). In addition, aphthoviruses also inhibit host transcription by inducing cleavage of histone H3 by their 3C^{pro} (111). Cardiaviruses also do not have 2A^{pro} activity, but induces host translation shutoff by activating 4E-BP1, and thereby repressing eIF4E activity (112). Host shutoff is most likely important for redirecting cellular resources for viral use. In addition, it may also reduce the production of virus-induced proteins such as IFN- α/β and other antiviral cytokines, but thus far no experimental evidence for this has been reported. Furthermore, picornaviruses induce the formation of ROs in infected cells (113–115). These densely packed tubulovascular membranous structures, where viral RNAs and proteins are concentrated, may not only be important for viral RNA replication but also help shield viral RNAs from RLRs. However, this

latter hypothesis remains to be experimentally supported. Further research is called upon to dissect, and demonstrate, the contribution of these various picornavirus-induced phenotypes in circumventing cellular antiviral activities.

AIM AND OUTLINE OF THIS THESIS

The interaction between an invading pathogen and the host immune system is extremely complex, and is a fierce arms race. And as in an arms race, seemingly insignificant changes from either part may shift the balance of forces and alter the net outcome. The aim of this thesis is to deepen our understanding of the interaction between picornaviruses and the cell-based innate antiviral responses, specifically, how picornavirus RNA is recognized by the RLR pathway, and how picornaviruses antagonize the RLR-mediated IFN- α/β response and stress response. In addition, we also set out to exploit the RLR pathway for potential pharmacological use.

When this thesis project was started, the natural MDA5 ligand(s) in virus-infected cells was unidentified. Long double-stranded replication intermediates of positive-strand RNA viruses seemed logical candidates since MDA5 can be activated by the synthetic dsRNA mimic poly(I:C), but no experimental evidence had been reported to support this hypothesis. In addition, picornavirus ssRNA is known to form stable double-stranded structures and carry a viral peptide at the 5' terminus, which may be recognized by MDA5 as non-self. **Chapter 2** focuses on picornavirus RNA recognition by MDA5. A systematic analysis of the IFN- α/β -stimulatory activities of different viral RNA species produced during picornavirus infection was carried out. In addition, we also set out to study viral RNA recognition during picornavirus infection, by using inhibitors that block RNA replication at different stages and thus allowing the presence of different RNA species in the cell.

In **Chapter 3**, we studied how artificial RNA ligands that resemble stem-loop structures in CVB3 genomic RNA interact with RIG-I, and identify the CL structure (when provided with 5' triphosphate) as a potent RIG-I ligand and potential antiviral agent.

In **Chapters 4** and **5**, we investigated how enteroviruses and cardioviruses antagonize the RLR signaling pathway and cellular stress pathway, as well as the relationship between these two cellular antiviral responses themselves. **Chapter 4** focuses on several components of the RLR-mediated IFN- α/β signaling pathway, and reveals their fate during infection of CVB3 and mengoviruses. Observations made with CVB3 were also broadened to viruses from other species of enteroviruses. In **Chapter 5**, we studied the stress response during CVB3 and mengovirus infections. Using a recombinant mengovirus carrying a mutant L, we further studied the relationship between the IFN- α/β induction pathway and SG formation. The antiviral activity of SGs during mengovirus infection is also investigated.

Chapter 6 provides a brief summary of the main findings of this thesis, a general discussion, as well as directions for future research.

REFERENCES

1. Chumakov K, Ehrenfeld E, Wimmer E, Agol VI. 2007. Vaccination against polio should not be stopped. *Nat. Rev. Microbiol.* 5:952–8.
2. Li Y, Zhu R, Qian Y, Deng J. 2012. The characteristics of blood glucose and WBC counts in peripheral blood of cases of hand foot and mouth disease in China: a systematic review. *PLoS One* 7:e29003.
3. Ooi MH, Wong SC, Lewthwaite P, Cardoso MJ, Solomon T. 2010. Clinical features, diagnosis, and management of enterovirus 71. *Lancet Neurol.* 9:1097–105.
4. Chase AJ, Semler BL. 2012. Viral subversion of host functions for picornavirus translation and RNA replication. *Future Virol.* 7:179–191.
5. Harris KG, Coyne CB. 2013. Enter at your own risk: How enteroviruses navigate the dangerous world of pattern recognition receptor signaling. *Cytokine* 63:230–6.
6. Tapparel C, Siegrist F, Petty TJ, Kaiser L. 2013. Picornavirus and enterovirus diversity with associated human diseases. *Infect. Genet. Evol.* 14:282–93.
7. Yeung W-CG, Rawlinson WD, Craig ME. 2011. Enterovirus infection and type 1 diabetes mellitus: systematic review and meta-analysis of observational molecular studies. *BMJ* 342:d35.
8. Kurai D, Saraya T, Ishii H, Takizawa H. 2013. Virus-induced exacerbations in asthma and COPD. *Front. Microbiol.* 4:293.
9. Tsukagoshi H, Ishioka T, Noda M, Kozawa K, Kimura H. 2013. Molecular epidemiology of respiratory viruses in virus-induced asthma. *Front. Microbiol.* 4:278.
10. Harvala H, Wolthers KC, Simmonds P. 2010. Parechoviruses in children: understanding a new infection. *Curr. Opin. Infect. Dis.* 23:224–30.
11. Martin A, Lemon SM. 2006. Hepatitis A virus: from discovery to vaccines. *Hepatology* 43:S164–72.
12. Debing Y, Neyts J, Thibaut HJ. 2013. Molecular Biology and Inhibitors of Hepatitis A Virus. *Med. Res. Rev.* Epub ahead of print.
13. Canelli E, Luppi A, Lavazza A, Lelli D, Sozzi E, Martin AMM, Gelmetti D, Pascotto E, Sandri C, Magnone W, Cordioli P. 2010. Encephalomyocarditis virus infection in an Italian zoo. *Virol. J.* 7:64.
14. Reddacliff LA, Kirkland PD, Hartley WJ, Reece RL. 1997. Encephalomyocarditis virus infections in an Australian zoo. *J. Zoo Wildl. Med.* 28:153–7.
15. Ehrenfeld E, Domingo E, Roos RP. 2010. The Picornaviruses. ASM Press, Washington , DC.
16. Semler BL, Wimmer E. 2002. Molecular biology of picornaviruses. ASM Press, Washington, D.C.
17. Jackson WT, Giddings TH, Taylor MP, Mulinyawe S, Rabinovitch M, Kopito RR, Kirkegaard K. 2005. Subversion of cellular autophagosomal machinery by RNA viruses. *PLoS Biol.* 3:e156.
18. Ponnuraj EM, John TJ, Levin MJ, Simoes EA. 1998. Cell-to-cell spread of poliovirus in the

- spinal cord of bonnet monkeys (*Macaca radiata*). *J. Gen. Virol.* 79 (Pt 10):2393–403.
19. Taylor MP, Burgon TB, Kirkegaard K, Jackson WT. 2009. Role of microtubules in extracellular release of poliovirus. *J. Virol.* 83:6599–609.
20. Vallbracht A, Hofmann L, Wurster KG, Flehmig B. 1984. Persistent infection of human fibroblasts by hepatitis A virus. *J. Gen. Virol.* 65 (Pt 3):609–15.
21. Theofilopoulos AN, Baccala R, Beutler B, Kono DH. 2005. Type I interferons (alpha/beta) in immunity and autoimmunity. *Annu. Rev. Immunol.* 23:307–36.
22. Schoggins JW, Wilson SJ, Panis M, Murphy MY, Jones CT, Bieniasz P, Rice CM. 2011. A diverse range of gene products are effectors of the type I interferon antiviral response. *Nature* 472:481–5.
23. Chen Y-L, Chen T-T, Pai L-M, Wesoly J, Bluysen HAR, Lee C-K. 2013. A type I IFN-Flt3 ligand axis augments plasmacytoid dendritic cell development from common lymphoid progenitors. *J. Exp. Med.* 210:2515–22.
24. Stackaruk ML, Lee AJ, Ashkar AA. 2013. Type I interferon regulation of natural killer cell function in primary and secondary infections. *Expert Rev. Vaccines* 12:875–84.
25. Kumar H, Kawai T, Akira S. 2011. Pathogen recognition by the innate immune system. *Int. Rev. Immunol.* 30:16–34.
26. Goubau D, Deddouche S, Reis E Sousa C. 2013. Cytosolic sensing of viruses. *Immunity* 38:855–69.
27. Yoneyama M, Kikuchi M, Natsukawa T, Shinobu N, Imaizumi T, Miyagishi M, Taira K, Akira S, Fujita T. 2004. The RNA helicase RIG-I has an essential function in double-stranded RNA-induced innate antiviral responses. *Nat. Immunol.* 5:730–737.
28. Kang D, Gopalkrishnan R V, Wu Q, Jankowsky E, Pyle AM, Fisher PB. 2002. mda-5: An interferon-inducible putative RNA helicase with double-stranded RNA-dependent ATPase activity and melanoma growth-suppressive properties. *Proc. Natl. Acad. Sci. U. S. A.* 99:637–42.
29. Kang D-C, Gopalkrishnan R V, Lin L, Randolph A, Valerie K, Pestka S, Fisher PB. 2004. Expression analysis and genomic characterization of human melanoma differentiation associated gene-5, mda-5: a novel type I interferon-responsive apoptosis-inducing gene. *Oncogene* 23:1789–800.
30. Andrejeva J, Childs KS, Young DF, Carlos TS, Stock N, Goodbourn S, Randall RE. 2004. The V proteins of paramyxoviruses bind the IFN-inducible RNA helicase, mda-5, and inhibit its activation of the IFN-beta promoter. *Proc. Natl. Acad. Sci. U. S. A.* 101:17264–17269.
31. Yoneyama M, Kikuchi M, Matsumoto K, Imaizumi T, Miyagishi M, Taira K, Foy E, Loo YM, Gale Jr. M, Akira S, Yonehara S, Kato A, Fujita T. 2005. Shared and unique functions of the DExD/H-box helicases RIG-I, MDA5, and LGP2 in antiviral innate immunity. *J. Immunol.* 175:2851–2858.
32. Broquet AH, Hirata Y, McAllister CS, Kagnoff MF. 2011. RIG-I/MDA5/MAVS are required to signal a protective IFN response in rotavirus-infected intestinal epithelium. *J. Immunol.* 186:1618–26.
33. Childs KS, Randall RE, Goodbourn S. 2013. LGP2 plays a critical role in sensitizing mda-5 to activation by double-stranded RNA. *PLoS One* 8:e64202.

34. Rothenfusser S, Goutagny N, DiPerna G, Gong M, Monks BG, Schoenemeyer A, Yamamoto M, Akira S, Fitzgerald KA. 2005. The RNA helicase Lgp2 inhibits TLR-independent sensing of viral replication by retinoic acid-inducible gene-I. *J. Immunol.* 175:5260–5268.
35. Satoh T, Kato H, Kumagai Y, Yoneyama M, Sato S, Matsushita K, Tsujimura T, Fujita T, Akira S, Takeuchi O. 2010. LGP2 is a positive regulator of RIG-I- and MDA5-mediated antiviral responses. *Proc. Natl. Acad. Sci. U. S. A.* 107:1512–1517.
36. Saito T, Hirai R, Loo Y-M, Owen D, Johnson CL, Sinha SC, Akira S, Fujita T, Gale M. 2007. Regulation of innate antiviral defenses through a shared repressor domain in RIG-I and LGP2. *Proc. Natl. Acad. Sci. U. S. A.* 104:582–7.
37. Seth RB, Sun L, Ea C-KK, Chen ZJ. 2005. Identification and characterization of MAVS, a mitochondrial antiviral signaling protein that activates NF-kappaB and IRF3. *Cell* 122:669–82.
38. Xu LG, Wang YY, Han KJ, Li LY, Zhai Z, Shu HB. 2005. VISA is an adaptor protein required for virus-triggered IFN-beta signaling. *Mol. Cell* 19:727–740.
39. Kawai T, Takahashi K, Sato S, Coban C, Kumar H, Kato H, Ishii KJ, Takeuchi O, Akira S. 2005. IPS-1, an adaptor triggering RIG-I- and Mda5-mediated type I interferon induction. *Nat. Immunol.* 6:981–988.
40. Meylan E, Curran J, Hofmann K, Moradpour D, Binder M, Bartenschlager R, Tschopp J. 2005. Cardif is an adaptor protein in the RIG-I antiviral pathway and is targeted by hepatitis C virus. *Nature* 437:1167–1172.
41. Hou F, Sun L, Zheng H, Skaug B, Jiang Q-X, Chen ZJ. 2011. MAVS forms functional prion-like aggregates to activate and propagate antiviral innate immune response. *Cell* 146:448–61.
42. Baum A, Sachidanandam R, García-Sastre A. 2010. Preference of RIG-I for short viral RNA molecules in infected cells revealed by next-generation sequencing. *Proc. Natl. Acad. Sci. U. S. A.* 107:16303–8.
43. Chang T-H, Liao C-L, Lin Y-L. 2006. Flavivirus induces interferon-beta gene expression through a pathway involving RIG-I-dependent IRF-3 and PI3K-dependent NF-kappaB activation. *Microbes Infect.* 8:157–71.
44. Faul EJ, Wanjalla CN, Suthar MS, Gale M, Wirblich C, Schnell MJ. 2010. Rabies virus infection induces type I interferon production in an IPS-1 dependent manner while dendritic cell activation relies on IFNAR signaling. *PLoS Pathog.* 6:e1001016.
45. Abe Y, Fujii K, Nagata N, Takeuchi O, Akira S, Oshiumi H, Matsumoto M, Seya T, Koike S. 2012. The toll-like receptor 3-mediated antiviral response is important for protection against poliovirus infection in poliovirus receptor transgenic mice. *J. Virol.* 86:185–94.
46. Gitlin L, Barchet W, Gilfillan S, Cella M, Beutler B, Flavell RA, Diamond MS, Colonna M. 2006. Essential role of mda-5 in type I IFN responses to polyriboinosinic:polyribocytidylic acid and encephalomyocarditis picornavirus. *Proc. Natl. Acad. Sci. U. S. A.* 103:8459–8464.
47. Jin Y-H, Kim SJ, So EY, Meng L, Colonna M, Kim BS. 2012. Melanoma differentiation-associated gene 5 is critical for protection against Theiler's virus-induced demyelinating disease. *J. Virol.* 86:1531–43.
48. Wang JP, Cerny A, Asher DR, Kurt-Jones EA, Bronson RT, Finberg RW. 2010. MDA5 and MAVS

Chapter 1

mediate type I interferon responses to coxsackie B virus. *J. Virol.* 84:254–260.

49. Wang Q, Miller DJ, Bowman ER, Nagarkar DR, Schneider D, Zhao Y, Linn MJ, Goldsmith AM, Bentley JK, Sajjan US, Hershenson MB. 2011. MDA5 and TLR3 initiate pro-inflammatory signaling pathways leading to rhinovirus-induced airways inflammation and hyperresponsiveness. *PLoS Pathog.* 7:e1002070.

50. McCartney SA, Thackray LB, Gitlin L, Gilfillan S, Virgin HW, Colonna M. 2008. MDA-5 recognition of a murine norovirus. *PLoS. Pathog.* 4:e1000108.

51. Roth-Cross JK, Bender SJ, Weiss SR. 2008. Murine coronavirus mouse hepatitis virus is recognized by MDA5 and induces type I interferon in brain macrophages/microglia. *J. Virol.* 82:9829–9838.

52. Yount JS, Gitlin L, Moran TM, López CB. 2008. MDA5 participates in the detection of paramyxovirus infection and is essential for the early activation of dendritic cells in response to Sendai Virus defective interfering particles. *J. Immunol.* 180:4910–8.

53. Burke CW, Gardner CL, Steffan JJ, Ryman KD, Klimstra WB. 2009. Characteristics of alpha/beta interferon induction after infection of murine fibroblasts with wild-type and mutant alphaviruses. *Virology* 395:121–32.

54. Fredericksen BL, Gale Jr. M. 2006. West Nile virus evades activation of interferon regulatory factor 3 through RIG-I-dependent and -independent pathways without antagonizing host defense signaling. *J. Virol.* 80:2913–2923.

55. Fredericksen BL, Keller BC, Fornek J, Katze MG, Gale Jr. M. 2008. Establishment and maintenance of the innate antiviral response to West Nile Virus involves both RIG-I and MDA5 signaling through IPS-1. *J. Virol.* 82:609–616.

56. Nasirudeen AMA, Wong HH, Thien P, Xu S, Lam K-P, Liu DX. 2011. RIG-I, MDA5 and TLR3 synergistically play an important role in restriction of dengue virus infection. *PLoS Negl. Trop. Dis.* 5:e926.

57. Ikegame S, Takeda M, Ohno S, Nakatsu Y, Nakanishi Y, Yanagi Y. 2010. Both RIG-I and MDA5 RNA helicases contribute to the induction of alpha/beta interferon in measles virus-infected human cells. *J. Virol.* 84:372–9.

58. Hornung V, Ellegast J, Kim S, Brzózka K, Jung A, Kato H, Poeck H, Akira S, Conzelmann KK, Schlee M, Endres S, Hartmann G. 2006. 5'-Triphosphate RNA is the ligand for RIG-I. *Science* 314:994–997.

59. Kato H, Takeuchi O, Mikamo-Satoh E, Hirai R, Kawai T, Matsushita K, Hiiragi A, Dermody TS, Fujita T, Akira S. 2008. Length-dependent recognition of double-stranded ribonucleic acids by retinoic acid-inducible gene-I and melanoma differentiation-associated gene 5. *J. Exp. Med.* 205:1601–10.

60. Pichlmair A, Schulz O, Tan CP, Naslund TI, Liljestrom P, Weber F, Reis e S. 2006. RIG-I-mediated antiviral responses to single-stranded RNA bearing 5'-phosphates. *Science* 314:997–1001.

61. Schlee M, Roth A, Hornung V, Hagmann CA, Wimmenauer V, Barchet W, Coch C, Janke M, Mihailovic A, Wardle G, Juranek S, Kato H, Kawai T, Poeck H, Fitzgerald KA, Takeuchi O, Akira S, Tuschl T, Latz E, Ludwig J, Hartmann G. 2009. Recognition of 5' triphosphate by RIG-I helicase

requires short blunt double-stranded RNA as contained in panhandle of negative-strand virus. *Immunity*. 31:25–34.

62. Schmidt A, Schwerdt T, Hamm W, Hellmuth JC, Cui S, Wenzel M, Hoffmann FS, Michallet MC, Besch R, Hopfner KP, Endres S, Rothenfusser S. 2009. 5'-triphosphate RNA requires base-paired structures to activate antiviral signaling via RIG-I. *Proc. Natl. Acad. Sci. U. S. A.* 106:12067–12072.

63. Cheng G, Zhong J, Chung J, Chisari F V. 2007. Double-stranded DNA and double-stranded RNA induce a common antiviral signaling pathway in human cells. *Proc. Natl. Acad. Sci. U. S. A.* 104:9035–40.

64. Rehwinkel J, Tan CP, Goubau D, Schulz O, Pichlmair A, Bier K, Robb N, Vreede F, Barclay W, Fodor E, Reis e Sousa C. 2010. RIG-I detects viral genomic RNA during negative-strand RNA virus infection. *Cell* 140:397–408.

65. Weber M, Gawanbacht A, Habjan M, Rang A, Borner C, Schmidt AMM, Veitinger S, Jacob R, Devignot S, Kochs G, García-Sastre A, Weber F. 2013. Incoming RNA virus nucleocapsids containing a 5'-triphosphorylated genome activate RIG-I and antiviral signaling. *Cell Host Microbe* 13:336–346.

66. Malathi K, Saito T, Crochet N, Barton DJ, Gale Jr. M, Silverman RH. 2010. RNase L releases a small RNA from HCV RNA that refolds into a potent PAMP. *RNA* 16:2108–2119.

67. Saito T, Owen DM, Jiang F, Marcotrigiano J, Gale Jr. M. 2008. Innate immunity induced by composition-dependent RIG-I recognition of hepatitis C virus RNA. *Nature* 454:523–527.

68. Kato H, Takeuchi O, Sato S, Yoneyama M, Yamamoto M, Matsui K, Uematsu S, Jung A, Kawai T, Ishii KJ, Yamaguchi O, Otsu K, Tsujimura T, Koh CS, Reis e S, Matsuura Y, Fujita T, Akira S. 2006. Differential roles of MDA5 and RIG-I helicases in the recognition of RNA viruses. *Nature* 441:101–105.

69. Peisley A, Lin C, Wu B, Orme-Johnson M, Liu M, Walz T, Hur S. 2011. Cooperative assembly and dynamic disassembly of MDA5 filaments for viral dsRNA recognition. *Proc. Natl. Acad. Sci. U. S. A.* 108:21010–5.

70. Dogan UB, Golge N, Akin MS. 2013. The comparison of the efficacy of pegylated interferon α -2a and α -2b in chronic hepatitis B patients. *Eur. J. Gastroenterol. Hepatol.* 25:1312–6.

71. Ploss A, Dubuisson J. 2012. New advances in the molecular biology of hepatitis C virus infection: towards the identification of new treatment targets. *Gut* 61 Suppl 1:i25–35.

72. Sleijfer S, Bannink M, Van Gool AR, Kruit WHJ, Stoter G. 2005. Side effects of interferon-alpha therapy. *Pharm. World Sci.* 27:423–31.

73. Zhao T, Wu X, Song D, Fang M, Guo S, Zhang P, Wang L, Wang L, Yu Y. 2012. Effect of prophylactically applied CpG ODN on the development of myocarditis in mice infected with Coxsackievirus B3. *Int. Immunopharmacol.* 14:665–73.

74. McCaskill JL, Marsh GA, Monaghan P, Wang L-F, Doran T, McMillan NAJ. 2013. Potent inhibition of Hendra virus infection via RNA interference and poly I:C immune activation. *PLoS One* 8:e64360.

75. Oosterhoff D, Heusinkveld M, Loughheed SM, Kosten I, Lindstedt M, Bruijns SCM, van Es T, van Kooyk Y, van der Burg SH, de Groot TD. 2013. Intradermal delivery of TLR agonists in a

human explant skin model: preferential activation of migratory dendritic cells by polyribosinic-polyribocytidylic acid and peptidoglycans. *J. Immunol.* 190:3338–45.

76. Arsenault RJ, Kogut MH, He H. 2013. Combined CpG and poly I:C stimulation of monocytes results in unique signaling activation not observed with the individual ligands. *Cell. Signal.* 25:2246–54.

77. Rodríguez-Pulido M, Borrego B, Sobrino F, Sáiz M. 2011. RNA structural domains in noncoding regions of the foot-and-mouth disease virus genome trigger innate immunity in porcine cells and mice. *J. Virol.* 85:6492–501.

78. Martínez-Gil L, Goff PH, Hai R, García-Sastre A, Shaw ML, Palese P. 2013. A Sendai virus-derived RNA agonist of RIG-I as a virus vaccine adjuvant. *J. Virol.* 87:1290–300.

79. Goulet M-L, Olganier D, Xu Z, Paz S, Belgnaoui SM, Lafferty EI, Janelle V, Arguello M, Paquet M, Ghneim K, Richards S, Smith A, Wilkinson P, Cameron M, Kalinke U, Qureshi S, Lamarre A, Haddad EK, Sekaly RP, Peri S, Balachandran S, Lin R, Hiscott J. 2013. Systems Analysis of a RIG-I Agonist Inducing Broad Spectrum Inhibition of Virus Infectivity. *PLoS Pathog.* 9:e1003298.

80. Reineke LC, Lloyd RE. 2013. Diversion of stress granules and P-bodies during viral infection. *Virology* 436:255–67.

81. Mazroui R, Sukarieh R, Bordeleau M-E, Kaufman RJ, Northcote P, Tanaka J, Gallouzi I, Pelletier J. 2006. Inhibition of ribosome recruitment induces stress granule formation independently of eukaryotic initiation factor 2 alpha phosphorylation. *Mol. Biol. Cell* 17:4212–9.

82. Dang Y, Kedersha N, Low W-K, Romo D, Gorospe M, Kaufman R, Anderson P, Liu JO. 2006. Eukaryotic initiation factor 2alpha-independent pathway of stress granule induction by the natural product pateamine A. *J. Biol. Chem.* 281:32870–8.

83. Emara MM, Fujimura K, Sciaranghella D, Ivanova V, Ivanov P, Anderson P. 2012. Hydrogen peroxide induces stress granule formation independent of eIF2 α phosphorylation. *Biochem. Biophys. Res. Commun.* 423:763–9.

84. Borghese F, Michiels T. 2011. The leader protein of cardioviruses inhibits stress granule assembly. *J. Virol.* 85:9614–22.

85. Khaperskyy D a, Hachette TF, McCormick C. 2012. Influenza A virus inhibits cytoplasmic stress granule formation. *FASEB J.* 26:1629–39.

86. Onomoto K, Jogi M, Yoo J-S, Narita R, Morimoto S, Takemura A, Sambhara S, Kawaguchi A, Osari S, Nagata K, Matsumiya T, Namiki H, Yoneyama M, Fujita T. 2012. Critical role of an antiviral stress granule containing RIG-I and PKR in viral detection and innate immunity. *PLoS One* 7:e43031.

87. Barral PM, Morrison JM, Drahos J, Gupta P, Sarkar D, Fisher PB, Racaniello VR. 2007. MDA-5 is cleaved in poliovirus-infected cells. *J. Virol.* 81:3677–84.

88. Kuo R-L, Kao L-T, Lin S-J, Wang RY-L, Shih S-R. 2013. MDA5 Plays a Crucial Role in Enterovirus 71 RNA-Mediated IRF3 Activation. *PLoS One* 8:e63431.

89. Drahos J, Racaniello VR. 2009. Cleavage of IPS-1 in cells infected with human rhinovirus. *J. Virol.* 83:11581–7.

90. Mukherjee A, Morosky S a, Delorme-Axford E, Dybdahl-Sissoko N, Oberste MS, Wang T, Coyne CB. 2011. The coxsackievirus B 3C protease cleaves MAVS and TRIF to attenuate host type I interferon and apoptotic signaling. *PLoS Pathog.* 7:e1001311.
91. Wang B, Xi X, Lei X, Zhang X, Cui S, Wang J, Jin Q, Zhao Z. 2013. Enterovirus 71 Protease 2Apro Targets MAVS to Inhibit Anti-Viral Type I Interferon Responses. *PLoS Pathog.* 9:e1003231.
92. Barral PM, Sarkar D, Fisher PB, Racaniello VR. 2009. RIG-I is cleaved during picornavirus infection. *Virology* 391:171–6.
93. Papon L, Oteiza A, Imaizumi T, Kato H, Brocchi E, Lawson TG, Akira S, Mehti N. 2009. The viral RNA recognition sensor RIG-I is degraded during encephalomyocarditis virus (EMCV) infection. *Virology* 393:311–8.
94. Hato S V, Ricour C, Schulte BM, Lanke KH, de Bruijini M, Zoll J, Melchers WJ, Michiels T, van Kuppeveld FJ. 2007. The mengovirus leader protein blocks interferon-alpha/beta gene transcription and inhibits activation of interferon regulatory factor 3. *Cell Microbiol.* 9:2921–2930.
95. Zoll J, Melchers WJG, Galama JMD, Kuppeveld FJM Van. 2002. The mengovirus leader protein suppresses alpha/beta interferon production by inhibition of the iron/ferritin-mediated activation of NF-kappa B. *J. Virol.* 76:9664–9672.
96. Van Pesch V, van Eyll O, Michiels T. 2001. The leader protein of Theiler's virus inhibits immediate-early alpha/beta interferon production. *J. Virol.* 75:7811–7.
97. Yang Y, Liang Y, Qu L, Chen Z, Yi M, Li K, Lemon SM. 2007. Disruption of innate immunity due to mitochondrial targeting of a picornaviral protease precursor. *Proc. Natl. Acad. Sci. U. S. A.* 104:7253–8.
98. Wang D, Fang L, Li K, Zhong H, Fan J, Ouyang C, Zhang H, Duan E, Luo R, Zhang Z, Liu X, Chen H, Xiao S. 2012. Foot-and-mouth disease virus 3C protease cleaves NEMO to impair innate immune signaling. *J. Virol.* 86:9311–22.
99. Wang D, Fang L, Li P, Sun L, Fan J, Zhang Q, Luo R, Liu X, Li K, Chen H, Chen Z, Xiao S. 2011. The leader proteinase of foot-and-mouth disease virus negatively regulates the type I interferon pathway by acting as a viral deubiquitinase. *J. Virol.* 85:3758–66.
100. White JP, Cardenas AM, Marissen WE, Lloyd RE. 2007. Inhibition of cytoplasmic mRNA stress granule formation by a viral proteinase. *Cell Host Microbe* 2:295–305.
101. White JP, Lloyd RE. 2011. Poliovirus unlinks TIA1 aggregation and mRNA stress granule formation. *J. Virol.* 85:12442–54.
102. Etchison D, Milburn SC, Edery I, Sonenberg N, Hershey JW. 1982. Inhibition of HeLa cell protein synthesis following poliovirus infection correlates with the proteolysis of a 220,000-dalton polypeptide associated with eucaryotic initiation factor 3 and a cap binding protein complex. *J. Biol. Chem.* 257:14806–10.
103. Lloyd RE. 2006. Translational control by viral proteinases. *Virus Res.* 119:76–88.
104. Liebig HD, Ziegler E, Yan R, Hartmuth K, Klump H, Kowalski H, Blaas D, Sommergruber W, Frasel L, Lamphear B. 1993. Purification of two picornaviral 2A proteinases: interaction with eIF-4 gamma and influence on in vitro translation. *Biochemistry* 32:7581–8.

Chapter 1

105. Kundu P, Raychaudhuri S, Tsai W, Dasgupta A. 2005. Shutoff of RNA polymerase II transcription by poliovirus involves 3C protease-mediated cleavage of the TATA-binding protein at an alternative site: incomplete shutoff of transcription interferes with efficient viral replication. *J. Virol.* 79:9702–13.
106. Das S, Dasgupta a. 1993. Identification of the cleavage site and determinants required for poliovirus 3CPro-catalyzed cleavage of human TATA-binding transcription factor TBP. *J. Virol.* 67:3326–31.
107. Yalamanchili P, Datta U, Dasgupta A. 1997. Inhibition of host cell transcription by poliovirus: cleavage of transcription factor CREB by poliovirus-encoded protease 3Cpro. *J. Virol.* 71:1220–6.
108. Joachims M, Van Breugel PC, Lloyd RE. 1999. Cleavage of poly(A)-binding protein by enterovirus proteases concurrent with inhibition of translation in vitro. *J. Virol.* 73:718–27.
109. Kuyumcu-martinez NM, Eden ME Van, Younan P, Lloyd RE. 2004. Cleavage of Poly (A) -Binding Protein by Poliovirus 3C Protease Inhibits Host Cell Translation : a Novel Mechanism for Host Translation Shutoff. *Mol. Cell Biol.* 24:1779-90.
110. Devaney MA, Vakharia VN, Lloyd RE, Ehrenfeld E, Grubman MJ. 1988. Leader protein of foot-and-mouth disease virus is required for cleavage of the p220 component of the cap-binding protein complex. *J. Virol.* 62:4407–9.
111. Falk MM, Grigera PR, Bergmann IE, Zibert A, Multhaup G, Beck E. 1990. Foot-and-mouth disease virus protease 3C induces specific proteolytic cleavage of host cell histone H3. *J. Virol.* 64:748–56.
112. Gingras AC, Svitkin Y, Belsham GJ, Pause A, Sonenberg N. 1996. Activation of the translational suppressor 4E-BP1 following infection with encephalomyocarditis virus and poliovirus. *Proc. Natl. Acad. Sci. U. S. A.* 93:5578–5583.
113. Limpens RWAL, van der Schaar HM, Kumar D, Koster AJ, Snijder EJ, van Kuppeveld FJM, Bárcena M. 2011. The transformation of enterovirus replication structures: a three-dimensional study of single- and double-membrane compartments. *MBio.* 2:e00166-11
114. Bienz K, Egger D, Pasamontes L. 1987. Association of polioviral proteins of the P2 genomic region with the viral replication complex and virus-induced membrane synthesis as visualized by electron microscopic immunocytochemistry and autoradiography. *Virology* 160:220–6.
115. Belov GA, Nair V, Hansen BT, Hoyt FH, Fischer ER, Ehrenfeld E. 2012. Complex dynamic development of poliovirus membranous replication complexes. *J. Virol.* 86:302–12.

Chapter 2

MDA5 Detects the Double-Stranded RNA Replicative Form in Picornavirus-Infected Cells

Qian Feng^{1,*}, Stanleyson V. Hato^{1,*}, Martijn A. Langereis¹,
Jan Zoll¹, Richard Virgen-Slane², Alys Peisley³, Sun Hur³,
Bert L. Semler², Ronald P. van Rij¹, Frank J.M. van Kuppeveld¹

¹Department of Medical Microbiology, Radboud University Nijmegen Medical Centre,
Nijmegen, PO Box 9101, 6500 HB, The Netherlands.

²Department of Microbiology and Molecular Genetics, School of Medicine,
University of California, Irvine, California, 92697, United States of America.

³The Immune Disease Institute, Children's Hospital Boston,
Boston, Massachusetts, 02115, United States of America.

* These authors contributed equally to this work

Cell Reports. 2012. 2(5):1187-96

ABSTRACT

RIG-I and MDA5 are cytosolic RNA sensors that play a critical role in innate antiviral responses. Major advances have been made in identifying RIG-I ligands, but our knowledge of the ligands for MDA5 remains restricted to data from transfection experiments mostly using poly(I:C), a synthetic dsRNA mimic. Here, we dissected the IFN- α/β -stimulatory activity of different viral RNA species produced during picornavirus infection, both by RNA transfection and in infected cells in which specific steps of viral RNA replication were inhibited. Our results show that the incoming genomic plus-strand RNA does not activate MDA5, but minus-strand RNA synthesis and production of the 7.5 kbp replicative form trigger a strong IFN- α/β response. IFN- α/β production does not rely on plus-strand RNA synthesis and thus generation of the partially double-stranded replicative intermediate. This study reports for the first time MDA5 activation by a natural RNA ligand under physiological conditions.

INTRODUCTION

RIG-I-like receptors (RLRs) are ubiquitously expressed cytoplasmic pathogen recognition receptors. The RLR family of proteins are DExD/H box RNA helicases, and two of its members, namely retinoic acid-inducible gene-I (RIG-I) and melanoma differentiation-associated gene 5 (MDA5), specialize in detecting viral RNAs in infected cells (reviewed in (Kato et al., 2011)). Upon ligand recognition, RIG-I and MDA5 interact with a mitochondrion-anchored adaptor molecule, MAVS, which activates kinase complexes eventually leading to the transcription of type I interferons (IFN- α/β) and other proinflammatory cytokine genes (Kato et al., 2011).

RIG-I and MDA5 play differential roles in virus recognition. RIG-I recognizes most single-stranded (ss) RNA viruses investigated to date, including all minus-strand RNA [(-)RNA] viruses (e.g., influenza virus, Sendai virus and vesicular stomatitis virus) and some plus-strand RNA [(+) RNA] viruses (e.g., hepatitis C virus and Japanese encephalitis virus) (Kato et al., 2011). MDA5 recognizes some other (+)RNA viruses, namely encephalomyocarditis virus (EMCV) (Gitlin et al., 2006; Kato et al., 2006), Theiler's murine encephalomyelitis virus (TMEV) (Pichlmair et al., 2009), coxsackievirus B3 (CVB3) (Wang et al., 2010) – all of which are members of the Picornavirus family – and mouse norovirus (McCartney et al., 2008). Other ssRNA viruses, such as dengue virus, West Nile virus, mouse hepatitis virus, and several paramyxoviruses are recognized by both RIG-I and MDA5 (Kato et al., 2011). Recognition of a double-stranded (ds) RNA virus, reovirus, has also been shown to involve both of these RLRs (Kato et al., 2008).

The differential recognition of viruses by RIG-I and MDA5 has been attributed to their distinct preferences for RNA ligands. RIG-I can be activated by 5'-triphosphate (ppp)-containing RNAs as well as short (< 2 kbp) dsRNAs (Kato et al., 2011). The ligand specificity of RIG-I provides an explanation for how it differentiates viral RNAs from cellular RNAs. Many RNA viruses carry genomes that contain 5'ppp or produce 5'ppp-containing RNAs during their replication cycle in the cytoplasm of infected cells, whereas cytoplasmic cellular RNAs generally lack 5'ppp. The ligands of MDA5 are as yet poorly defined. MDA5 is activated by transfection of a long (> 2 kbp), synthetic dsRNA analogue of artificial sequence, namely polyinosinic:polycytidylic (poly(I:C)). Additionally, transfection-based experiments showed that the L segments of the reovirus genome (~3.9 kbp dsRNAs) induce an IFN- β response that is partially dependent on MDA5 (Kato et al., 2006). Based on these findings, it is believed that MDA5 recognizes long dsRNAs, which would be intrinsically "non-self". However, little is known about the identities and characteristics of physiological ligands of MDA5 in infected cells.

Many (+)RNA viruses, including picornaviruses, produce dsRNAs during infection. *Picornaviridae* is a large, highly diverse family of human and animal viruses, including many pathogens of great medical and/or economical significance. The picornavirus genome is a 7.5–8.0 kb ssRNA molecule that harbors a single open reading frame flanked by structured 5' and 3' non-translated regions and a poly(A) tail at the 3' end. The 5' terminus contains a small (20-24 aa) viral peptide, VPg, linked via an unusual tyrosine-RNA phosphodiester bond. Upon virus entry and uncoating, the virion RNA (vRNA) is released into the cytoplasm where it is directly translated. Viral RNA templates used for protein synthesis no longer contain VPg due to the activity of a yet unknown cellular enzyme (further referred to as unlinkase) (Rozovics et al., 2011). The viral polyprotein is proteolytically processed to release the viral proteins that engage in genomic RNA replication.

During this complex process several species of viral RNAs with unique features are generated (Fig. 2A). First, the viral genomic ssRNA is transcribed into a complementary (-)RNA by the virally encoded RNA-dependent RNA polymerase using VPg as primer, yielding a 7.5 kbp dsRNA named the replicative form (RF). The (-)RNA is subsequently used as a template for VPg-primed synthesis of large amounts of new (+)RNAs, which are identical to vRNA. Newly synthesized (+)RNAs either enter a new cycle of translation and RNA replication or are encapsidated to form new virion particles. During the process of (+)RNA synthesis, a partially ds replicative intermediate (RI) – consisting of multiple incomplete (+)RNAs undergoing active transcription along the full-length (-)RNA – is formed.

It is generally assumed that viral dsRNAs produced in cells infected with picornaviruses, as well as other (+)RNA viruses, activate MDA5. However, experimental evidence supporting such a hypothesis is lacking. In this study, we sought to identify physiological ligand(s) of MDA5 by studying the recognition of distinct picornavirus RNA species in transfected cells as well as during infection. Here, we identify for the first time a naturally occurring RNA from infected cells, the picornavirus RF, as a potent and specific activator of MDA5 during infection.

RESULTS

MDA5 recognizes viruses from various picornavirus genera

The picornavirus family contains hundreds of highly diverse members that are subcategorized in 12 genera. Based on the observation that MDA5 recognizes EMCV and TMEV, both members of the *Cardiovirus* genus, and CVB3, an enterovirus (Kato et al., 2011), it is generally assumed that all picornaviruses are recognized by MDA5, but experimental proof for this is lacking. Here, we set out to investigate the role of RLRs in the recognition of representative picornaviruses from various genera using wildtype (wt) and RIG-I^{-/-}, MDA5^{-/-} or MAVS^{-/-} mouse embryonic fibroblasts (MEFs). To bypass the requirement for specific entry receptors, we introduced vRNAs into the cytoplasm by transfection rather than infection. Fig. 1A shows IFN-β responses in wt and knock-out MEFs triggered by transfection of vRNA of wt mengovirus (a strain of EMCV) or infection of a mutant mengovirus (mengo-Zn). This virus generates high levels of IFN-β because its IFN antagonist has been compromised (Hato et al., 2007). Both methods resulted in a MDA5- and MAVS-dependent, but RIG-I-independent, IFN-β induction, demonstrating the suitability of the transfection method to identify the RLR(s) responsible for detecting picornaviruses.

Using this vRNA transfection assay, we studied recognition of members of three human *Enterovirus* species. In addition, we included Saffold virus (a recently identified human cardiovirus), human parechovirus (*Parechovirus* genus), and equine rhinitis A virus (a member of the Aphthovirus genus that also includes foot-and-mouth disease virus). Infectious viruses were produced upon transfection of all vRNAs, indicating efficient RNA replication in MEFs (data not shown). Replication of all viruses induced an MDA5- and MAVS-dependent, but RIG-I-independent, IFN-β response (Fig. 1B-C). These data provide experimental evidence that a broad spectrum of picornaviruses is indeed recognized by MDA5.

Two other cellular proteins, namely PKR and RNaseL, have also been implicated in recognition of some viruses (Kato et al., 2011). However, we found no difference in IFN-α/β responses to

mengo-Zn in cells deficient in RNaseL or PKR (Fig. S1), arguing against a major role of these proteins in detecting picornavirus RNA (see **Extended Results**).

Enrichment of ssRNA and dsRNA fractions from picornavirus-infected cells

To gain more insight into the identity of the RNA species detected by MDA5 in picornavirus-infected cells, we separately enriched for ssRNAs and dsRNAs by LiCl differential precipitation from mock- and CVB3-infected HeLa cells (Fig. 2B). The ssRNA pool of infected cells contained one additional RNA species of the same electrophoretic mobility as purified CVB3 vRNA (Fig. 2C), suggesting that it represents viral genomic ssRNA. Although partially ds, the viral RI is known to precipitate by 2M LiCl (Richards et al., 1984), the same condition used here to prepare ssRNA fractions. However, the amount of RI is most likely too low to be detected on gel. The dsRNA pool of CVB3-infected cells contained an RNA species of approximately 7.5 kbp that was absent in the dsRNA pool of mock-infected cells (Fig. 2B). Both the viral ssRNA and dsRNA bands were absent in HeLa cells infected with CVB3 in the presence of GuHCl (Fig. 2B), a well-known inhibitor of enterovirus (-)RNA synthesis (Barton and Flanagan, 1997) (Fig. 2D & S2), demonstrating that these RNAs were of viral origin.

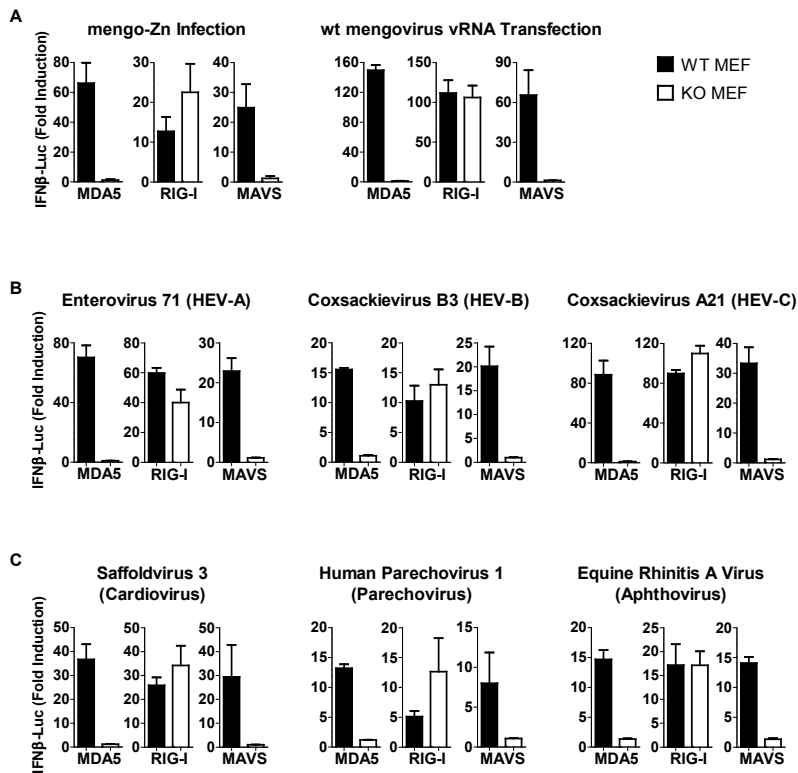


Figure 1. MDA5 recognizes picornaviruses across various genera. (A) MEFs of indicated genotypes were either infected with mengo-Zn (MOI 50) or transfected with virion RNA (vRNA) from wt mengovirus. IFN- β promoter activation at 8 h.p.t. was determined by an IFN- β -luciferase reporter assay. (B) MEFs of indicated genotypes were transfected with vRNAs from three human enteroviruses (HEVs), namely enterovirus 71, coxsackievirus B3 or coxsackievirus A21, a close relative to poliovirus. IFN- β promoter activation at 8 h.p.t. was determined by IFN reporter assay. (C) Same assay as B using vRNAs from Saffold virus 3, human parechovirus 1 and equine rhinitis A virus. Data presented as Mean \pm SD. See also Figure S1.

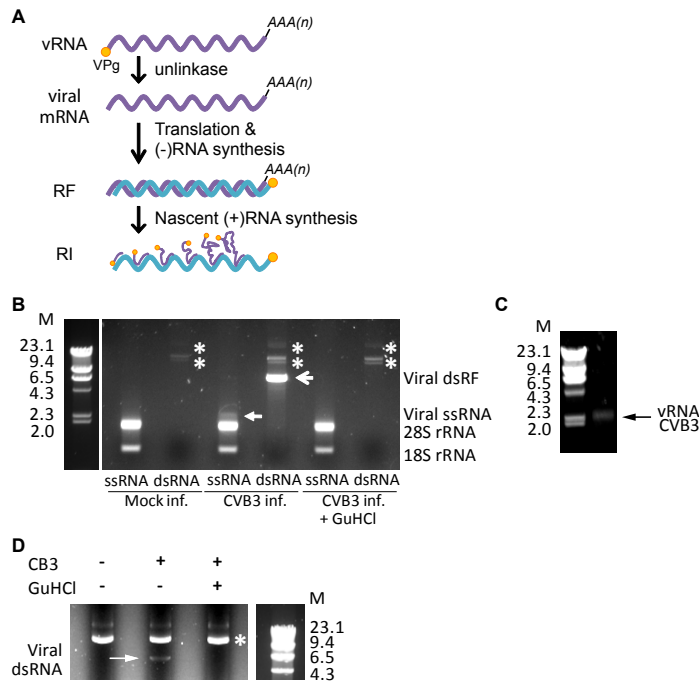


Figure 2. Enrichment of ssRNA and dsRNA fractions of CVB3-infected cells. (A) Viral RNA species produced during picornavirus infection. RF, replicative form. RI, replication intermediate. Purple line, (+)RNA. Blue line, (-)RNA. Orange circle, VPg. (B) HeLa cells were infected with CVB3 in the absence or presence of replication inhibitor GuHCl (2 mM) for 5 h and total RNA was extracted. ssRNA and dsRNA fractions were separated by LiCl differential precipitation and examined on agarose gel. Note that the ssRNA fraction was diluted 400-fold relative to the dsRNA fraction to load comparable amounts of RNAs. M, dsDNA marker with indicated size in kbp. Closed arrow, viral ssRNA. Arrow head, viral dsRNA. Asterisk, unknown bands. (C) vRNA purified from pelleted virus particles was visualized on agarose gel next to the same DNA marker as used in A. (D) HeLa cells were infected with CVB3 (MOI 100) in the absence or presence of GuHCl (2 mM) for 2.5 h and the dsRNA fraction was purified from total RNA extract by LiCl precipitation and examined on gel. M, dsDNA marker. Arrow, viral dsRNA. Asterisk, unknown bands. See also Figure S2.

The picornavirus 7.5 kbp RF is a potent MDA5 ligand upon transfection

The dsRNA fraction from CVB3-infected cells (Fig. 2B) was transfected into MEFs and IFN- β mRNA levels were measured at 2 hours post transfection (h.p.t.), a time point preceding RNA replication (Fig. S2), thereby excluding the possible role of other, newly produced viral RNA species. The dsRNA fraction triggered a MDA5- and MAVS-dependent IFN- β response (Fig. 3A). We next set out to identify the IFN-stimulatory RNA species in this fraction. In the dsRNA fractions, we observed two bands on gel; an infection-specific, 7.5 kbp species, and a larger fragment that was present in both mock- and CVB3-infected samples. To determine the nature of the higher band, we treated the dsRNA fractions with nucleases specific for ssRNA (RNase A), dsRNA (RNase III) and DNA. The non-specific larger band was completely digested upon DNase treatment, indicating that it was DNA (Fig. 3B). The 7.5 kbp CVB3 RF was specifically digested by RNase III, confirming that this is a dsRNA molecule (Fig. 3B).

Next we examined the ability of purified CVB3 RF to activate MDA5. When gel extracted and transfected into MEFs, the RF, but not the DNA molecule, induced high levels of IFN- β transcription in an MDA5- and MAVS-specific manner (Fig. 3C). Similar experiments were

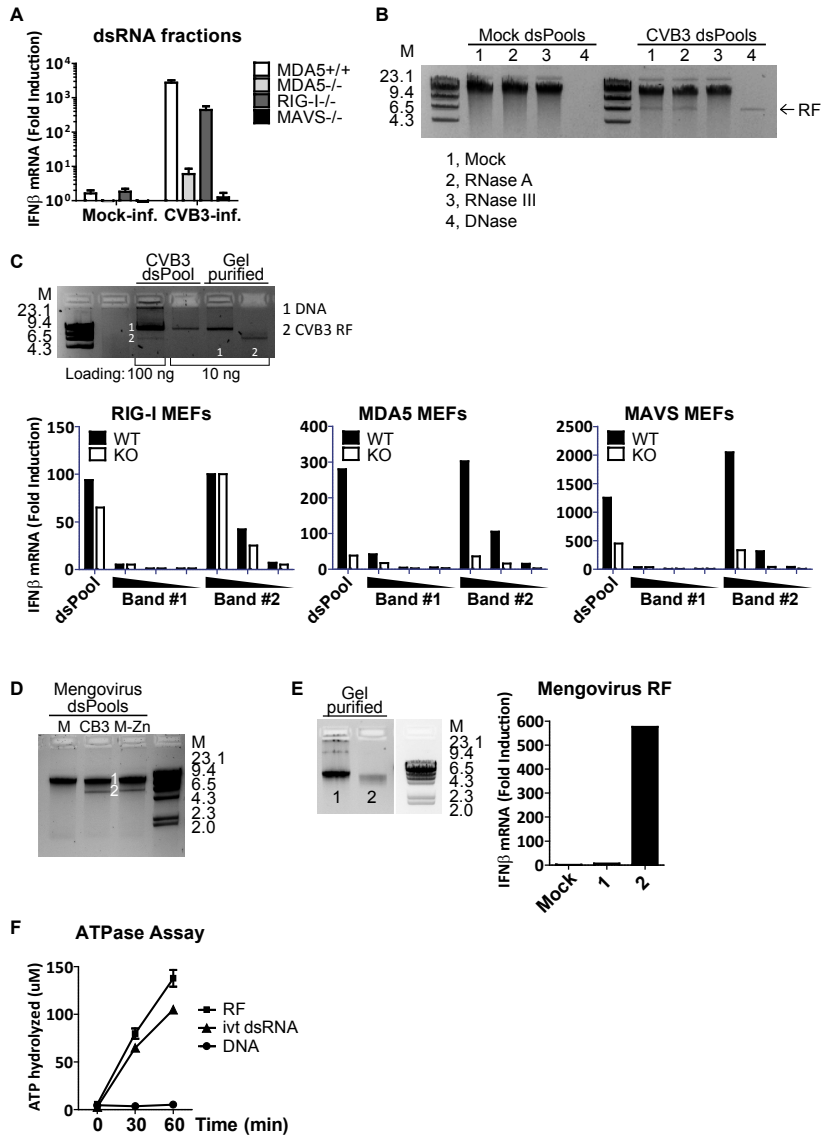


Figure 3. Picornavirus RF is a potent MDA5 agonist. (A) dsRNA fractions from mock- or CVB3-infected HeLa cells were transfected into MEFs of indicated genotypes, and IFN-β mRNA level at 2 h.p.t. was measured by RT-qPCR. Data presented as Mean ± SD. (B) dsRNA fractions (dsPool) of mock- and CVB3-infected cells were treated with 10 ng/μl RNase A, 10 mU RNase III or 10 mU DNase I at 37°C for 15 min, and analyzed on agarose gel. (C) DNA and RF bands observed in CVB3 dsRNA fraction were gel purified and analyzed on agarose gel. CVB3 dsRNA fraction (10 ng per well in 24-well format), and the gel purified RNAs (10, 2 or 0.4 ng/well) were transfected into wt, RIG-I^{-/-}, MDA5^{-/-} or MAVS^{-/-} MEFs in the presence of CHX (10 μg/ml). IFN-β mRNA induction was determined by RT-qPCR at 8 h.p.t.. (D) dsRNA fractions of mock-, CVB3- or mengovirus-infected cells were analyzed on agarose gel. (E) DNA and RF bands from mengovirus dsRNA fraction were gel purified and transfected into RIG-I^{-/-} MEFs in the presence of CHX (10 μg/ml). IFN-β response at 8 h.p.t. was measured by RT-qPCR. (F) Gel purified RF and DNA bands from CVB3 dsRNA fraction, as well as an in vitro transcribed dsRNA of CVB3 sequence (ivt dsRNA) (0.3 μg/ml) were incubated with recombinant MDA5 (0.3 μM) at 37°C in the presence of 2 mM ATP, and free Pi was measured using Green Reagent at 0, 30 and 60 minutes after reaction was started. M, dsDNA marker with indicated size in kbp. Bands number 1 and 2 on gel corresponds to the samples used in RNA transfection. Data presented as Mean ± SD.

performed with nucleic acids extracted from cells infected with mengovirus. The dsRNA fraction from mengovirus-infected cells appeared indistinguishable on gel from that from CVB3-infected cells (Fig. 3D), and the gel purified mengovirus RF also proved to be a potent MDA5 agonist (Fig. 3E). These data show that the RF of prototype members of at least two genera of picornaviruses can specifically and potently induce an MDA5-dependent IFN- α/β response.

To investigate whether the RF can directly activate MDA5, we performed *in vitro* ATPase assays where recombinant MDA5 was incubated with gel purified RF or the non-specific DNA band in the presence of ATP. ATP hydrolysis was followed at different time points by measuring free phosphate. CVB3 RF induced high levels of MDA5 ATPase activity – hydrolyzing nearly 150 μ M ATP in 60 min – while the DNA band did not induce any ATP hydrolysis during this time period (Fig. 3F). These results are in line with our transfection data (Fig. 3C & 3E) and confirm that RF can be directly recognized by MDA5 and potently induce its activation.

Picornavirus ssRNAs do not activate MDA5

We also tested the ssRNA fraction from infected cells (Fig. 2B) for its IFN- β -stimulatory activity. To our surprise, transfection of this fraction also led to an MDA5- and MAVS-dependent IFN- β response (Fig. 4A). However, subsequent nuclease digestion experiment revealed that the IFN- β -stimulatory activity is sensitive to RNase III (dsRNA-specific) treatment, but not RNase A (ssRNA-specific) (Fig. 4B-C). Indeed, after removal of rRNAs – the most abundant RNA species present in the ssRNA fractions – we observed a RNA species on gel that is specifically present in infected cells and has the same electrophoretic mobility as the RF band found in the dsRNA fraction from infected cells (Fig. S3A). These results suggest that residue amounts of RF is still present in our ssRNA fraction preparations, and the RF, but not viral ssRNAs, are responsible for the observed IFN- β induction upon transfection of this fraction. In line with this conclusion, we found that VPg-containing vRNA (Fig. 4D-E), VPg-unlinked viral mRNAs (Fig. 4E), and *in vitro* transcribed ssRNAs of viral sequence (Fig. S3B-C) all failed to induce any IFN- β response when purified and transfected into cells.

The viral RI is also reported to segregate in the ssRNA fraction using the LiCl precipitation method (Richards et al., 1984). To study the effect of RI on IFN- α/β induction without complications from RF, we attempted to remove the remaining RF from CVB3 ssRNA fraction by repeating the 2M LiCl precipitation procedure. However, even after two additional rounds of precipitation we did not observe significant loss of RF from the CVB3 ssRNA fraction, nor did we observe a reduced IFN- β response upon transfection (data not shown). Hence, we were unable to determine whether RI also exerts IFN-inducing activity.

Formation of viral RF, but not RI, is required for IFN- β induction in infected cells

Our results indicated that the picornavirus RF, and possibly also the RI, is a potent MDA5 activator when delivered into the cytoplasm by lipid-based transfection. However, the amount of RF/RI and their accessibility to MDA5 may differ greatly from the situation in infected cells, where viral RNA is covered with replication enzymes and localized in virus-induced, membrane-associated replication organelles (Belov and van Kuppeveld, 2012). Therefore, we set out to dissect the IFN-stimulatory abilities of different viral RNAs produced in cells infected with mengo-Zn, which induces strong IFN- β responses.

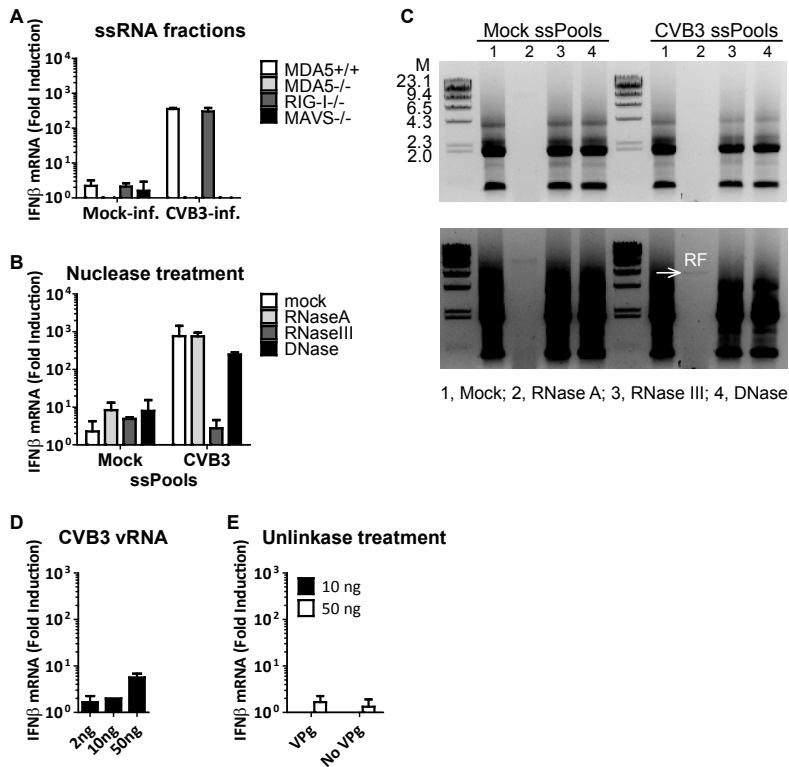


Figure 4. ssRNAs from CVB3-infected cells do not activate MDA5. (A) ssRNA (left) and dsRNA (right) fractions from mock- or CVB3-infected HeLa cells were transfected into MEFs of indicated genotypes, and IFN- β mRNA level at 2 h.p.t. was measured by RT-qPCR. Data presented as Mean \pm SD. (B) ssRNA fractions (ssPools) of mock- and CVB3-infected cells were treated with 10 ng/ μ l RNase A, 10 mU RNase III or 10 mU DNase I at 37°C for 15 min. Resulting RNA samples equivalent to 500 ng starting material were transfected into approximately 200,000 MAVS^{+/+} MEFs and IFN- β mRNA induction was determined by RT-qPCR at 8 h.p.t.. Data presented as Mean \pm SD. (C) The same samples as in B were analyzed on agarose gel. (D) CVB3 vRNA was isolated from pelleted viral particles. Indicated amounts of vRNA were transfected into RIG-I^{-/-} MEFs in the presence of CHX (10 μ g/ml), and IFN- β mRNA induction was determined by RT-qPCR at 8 h.p.t.. Data presented as Mean \pm SD. (E) Indicated amounts of mock-treated or uninkase-treated poliovirus vRNAs were transfected into RIG-I^{-/-} MEFs in the presence of CHX (10 μ g/ml). Total RNA was extracted at 8 h.p.t. and IFN- β mRNA induction was determined by RT-qPCR. Data presented as Mean \pm SD. See also Figure S3.

We first generated a comprehensive profile of the kinetics of viral RNA replication as well as host IFN- β response to Mengo-Zn in HeLa cells by measuring viral RNA and IFN- β mRNA levels by RT-qPCR every hour up till 10 h.p.i. (Fig. 5A). Viral RNA level remained at input levels in the first three hours of infection, then rapidly increased (i.e., active viral RNA replication) to reach a maximum at 6 h.p.i., and stabilized at this level through 10 h.p.i.. The host IFN- β response showed a slight delay as IFN- β mRNA levels in infected cells remained at background levels through the first six hours, then started to increase from 7 h.p.i., and reached their maximum at 8-9 h.p.i..

To study the separate contribution of viral ssRNA and dsRNA in inducing IFN- α/β response during infection we employed inhibitors of mengovirus replication, CHX and dipyrindamole (DIP) (Fig. 5B), which affect viral replication at different stages. CHX prevents protein synthesis and thereby RNA replication. DIP has little effect on (-)RNA synthesis but strongly inhibits (+)

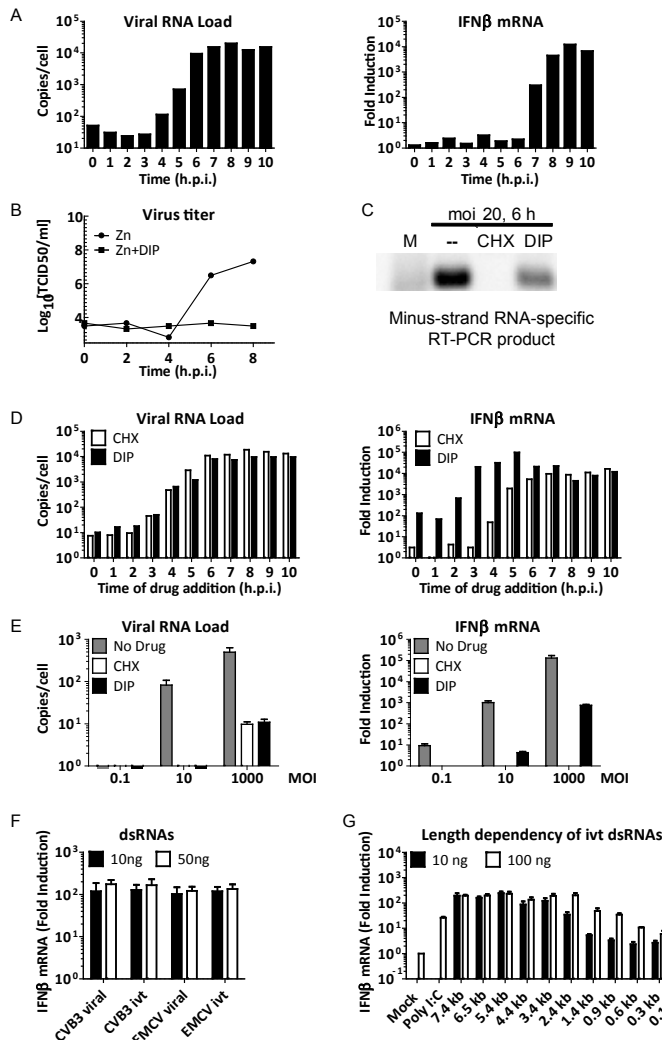


Figure 5. Viral RNA recognition in infected cells and characterization of determinant for MDA5 activation in RF. (A) HeLa cells were infected with mengo-Zn (MOI 10) and samples were taken every hour p.i.. Total RNA was extracted and viral RNA and host IFN-β mRNA levels were assayed by RT-qPCR. (B) Cells were infected with mengo-Zn in the absence or presence of DIP (100 μM). Production of infectious particles was determined by end-point titration on BHK-21 cells. (C) HeLa cells were mock-infected or infected with mengo-Zn (MOI 20) in the absence or presence of CHX (10 μg/ml) or DIP (100 μM) and total RNA was extracted at 6 h.p.i. dsRNA fraction was purified by LiCl precipitation and subjected to RT-PCR using primers specific to viral (-) RNA. (D) HeLa cells were infected with mengo-Zn at MOI 10. CHX (10 μg/ml) or DIP (100 μM) was added to infected cells either at time of infection or at indicated times p.i.. All samples were harvested at 12 h.p.i.. Total RNA was extracted and viral RNA and host IFN-β mRNA levels were analyzed by RT-qPCR. (E) HeLa cells were infected with mengo-Zn at indicated MOI's in the absence or presence of CHX (10 μg/ml) or DIP (100 μM). Total RNA was extracted at 10 h.p.i. and viral RNA and host IFN-β mRNA levels were measured by RT-qPCR. (F) RFs of CVB3 and mengovirus as well as in vitro transcribed dsRNAs of viral sequences were transfected into RIG-I^{-/-} MEFs in the presence of CHX (10 μg/ml) at indicated amounts per well in 24-well format. IFN-β mRNA levels were determined at 8 h.p.t. by RT-qPCR. (G) poly(I:C) or

in vitro transcribed dsRNAs of indicated length were transfected into RIG-I^{-/-} MEFs in the presence of CHX (10 μg/ml) at indicated amounts. IFN-β mRNA levels were determined at 8 h.p.t. by RT-qPCR. Data presented as Mean ± SD. See also Figure S4 & S5.

RNA synthesis in cell-free extract (Fata-Hartley and Palmenberg, 2005). Indeed, (-)RNAs were detected in cells infected in the presence of DIP, but not CHX, using a strand-specific PCR (Fig. 5C). The finding that the signal obtained from DIP-treated cells was lower than that from no drug-treated cells likely reflects a reduced amount of (-)RNA as DIP only allows (-)RNA synthesis from incoming genomic (+)RNA, whereas in the absence of DIP newly synthesized (+)RNAs can enter a new round of RNA replication, and therefore lead to the production of more RF.

To determine the IFN-β response to different viral RNA species formed in infected cells, we used DIP and CHX in a time-of-drug-addition experiment. HeLa cells were infected with Mengo-Zn, and DIP or CHX was added to cells at the indicated times (Fig. 5D). Cells were incubated until 12 h.p.i., harvested, and viral RNA and IFN-β mRNA levels were determined by RT-qPCR.

As shown in Fig. 5D, both DIP and CHX were effective in inhibiting viral RNA replication when added at early stages (0-2 h.p.i.) of infection. Later addition of the drugs resulted in partial, and eventually loss, of effect on RNA replication.

Under conditions where CHX and DIP completely inhibited viral RNA replication (i.e., added at 0-2 h.p.i., Fig. 5D), no IFN- β induction was detected in CHX-treated cells whereas a 100-fold, MDA5-dependent (Fig. S4) induction of IFN- β mRNA level was observed in DIP-treated cells. Additionally, when CHX or DIP was added at 3 h.p.i., a maximal IFN- β response was observed in DIP-treated cells, but virtually no IFN- β was induced in the CHX-treated cells (Fig. 5D). Analysis of viral RNA levels indicate that only a few new (+)RNAs had been made as addition of either CHX or DIP at this time point led to only a slight increase in viral RNA copy number at 12 h.p.i.. These newly synthesized (+)RNAs could serve as template to make additional RFs in the DIP-treated cells, but not in the CHX-treated cells, and result in the increase of IFN- β induction observed at 3 h.p.i.. It is theoretically possible that the observed differences in IFN- β levels in CHX- and DIP-treated cells were due to non-specific blockade or stimulation of the RLR signaling pathway by CHX or DIP, respectively. However, this is unlikely since these drugs had no such effects on poly(I:C)-induced IFN- β responses (Fig. S5).

In the experiment described above, the incoming vRNA alone (i.e., in the presence of CHX) induced no IFN- β response. To exclude that the amount of incoming vRNA at the used MOI was too low to induce a detectable IFN- β mRNA upregulation, we increased the infection dose from MOI 10 to 1000. This resulted in increased levels of IFN- β in no drug- and DIP-treated samples, but in CHX-treated cells the IFN- β level remained undetectable (Fig. 5E). This result clearly shows that the incoming vRNA, even when present at very high quantities, does not activate MDA5. Taken together, our results demonstrate that (-)RNA synthesis (i.e., formation of RF), but not (+)RNA synthesis (i.e., formation of RI), is required for achieving high levels of IFN- α/β induction.

Termini- and length-dependency of MDA5 activation by long dsRNAs

We next investigated whether the termini of picornavirus RF are important for MDA5 activation. The viral RF contains a VPg peptide at the 5' end of the (-)RNA, but not at the 5' end of the (+) RNA because of the activity of the unlinking enzyme. Furthermore, the RF contains a large unpaired poly(A) tail at the 3' end of the (+)RNA (van Ooij et al., 2006). To investigate whether these features are important for MDA5 activation, we produced CVB3 and mengovirus dsRNAs with 5'ppp and perfectly paired termini by *in vitro* transcription (ivt dsRNA) and compared them with viral RF purified from infected cells for their ability to activate MDA5. Strikingly, all dsRNAs triggered a similar IFN- β response both upon transfection into RIG-I^{-/-} MEFs (Fig. 5F). Additionally, CVB3 ivt dsRNA activated MDA5 to a similar extent as CVB3 RF in our *in vitro* ATPase assay (Fig. 3F). Thus, the recognition of long dsRNAs by MDA5 is likely independent of the termini of the RNA molecule.

Lastly, we investigated whether MDA5 activation by long dsRNAs is length dependent as proposed by Kato et al, who showed that only long poly(I:C) molecules (> 2kb) are efficiently recognized by MDA5 (Kato et al., 2008). To this end we generated ivt dsRNAs of various length (0.1 – 7.4 kbp) and determined IFN- β activation levels by RT-qPCR upon transfection of different amounts of these fragments. At relatively low quantities (10 ng), ivt dsRNAs shorter than 2.4

kbp induced only low levels of IFN- β mRNA. However, when larger amounts of dsRNA (100 ng) were transfected, smaller dsRNAs were also able to trigger an IFN- β response (Fig. 5G), indicating that there may not be a strict length cut-off value for MDA5 ligands.

DISCUSSION

Since the initial discovery of RLRs, significant progress has been made in identifying ligands for RIG-I, but the identity and molecular characteristics of viral MDA5 ligands remain largely unknown. Based on transfection experiments using poly(I:C), MDA5 is believed to recognize long dsRNAs. However, viral ssRNAs should not be excluded since base-paired regions in ssRNAs, as those in the picornavirus genomic RNA, could potentially be sufficient for MDA5 recognition. Furthermore, a virally encoded peptide, VPg, is covalently attached to the 5' terminus of picornavirus RNAs via a unique tyrosine-RNA bond, providing a potential "non-self" signature at the 5' end. Bearing this information in mind, we followed an unbiased approach to determine the IFN-stimulatory activities of different viral RNA species produced in picornavirus-infected cells.

The viral dsRNA, RF, has been assumed to be the MDA5 ligand produced by picornaviruses based on the fact that all known activators of MDA5 are dsRNAs (mimics). Here we provide experimental evidence that purified picornavirus RF not only can induce an MDA5-dependent IFN- α/β response upon transfection, but that it also directly binds to, and activates MDA5 *in vitro*. Viral ssRNAs, on the other hand, proved poor MDA5 stimuli. Neither vRNA (VPg-containing) nor viral mRNA (VPg-lacking) induced an IFN- β response when transfected into cells. This is in line with the observation that the full-length EMCV RNA failed to activate MDA5 ATPase activity *in vitro* (Peisley et al., 2011). Although we could not test IFN-stimulatory activity of purified RI, this molecule does not seem to play a crucial role in inducing IFN- α/β as treatment of the CVB3 ssRNA fraction with RNase A did not affect its ability to induce IFN- α/β . This observation also speaks against the hypothesis that other (viral) ssRNAs – which might have been produced by the action of cellular RNases like RNaseL – may be recognized by MDA5.

Collectively, our transfection experiments clearly identify the RF as an MDA5 agonist. Previously, Pichlmair and colleagues identified two virus-induced RNA species in their total RNA extract from EMCV-infected cells – one dsRNA of approximately 12 kbp and one high-molecular-weight RNA (HMW-RNA) that consisted of both ssRNAs and dsRNAs (Pichlmair et al., 2009). The HMW-RNA, but not the 12 kbp dsRNA, was found to be IFN- α/β -stimulatory upon transfection. We never observed either of these RNAs in our total RNA extracts or the fractionated RNA preparations. The identity of the HMW-RNA and the IFN-stimulatory element(s) within their mixed RNA population remains unclear.

Although transfection may serve a convenient method to study aspects of MDA5 ligand recognition, it may not faithfully recapitulate physiological conditions for several reasons. First, transfection delivers large amounts of viral RNA directly into the cytoplasm at once. This is different from the RNA release process during infectious entry as well as the gradual accumulation of viral RNAs during virus replication. Second, purified, and therefore "naked" RNAs are transfected into cells whereas viral RNAs are heavily coated with viral and host

factors during infection. Third, (+)RNA viruses induce the formation of membranous replication organelles, which may restrict access of MDA5 to replication intermediates such as RF and RI. To gain insight into MDA5 activation in a more physiologically relevant situation, we studied MDA5 activation in infected cells. Our data show that the incoming genomic ssRNA alone cannot induce any detectable IFN- β response even when large amounts were delivered by high MOI infection. When (-)RNA synthesis (i.e., formation of RF) was permitted but (+)RNA synthesis (i.e., formation of RI) was inhibited, a significant up-regulation of IFN- β mRNA was observed. These data further support the idea that picornavirus RF is the essential MDA5 agonist in the course of infection. Of note, a much higher IFN- β response was observed when RNA replication was allowed to proceed fully (i.e., in the absence of inhibitor). Although this finding may be interpreted as that RIs also activate MDA5, this increase can be attributed, at least partly, to the increased amount of RF produced from newly synthesized (+)RNAs that enter new rounds of RNA replication.

Recently, Züst et al suggested that MDA5 may also recognize RNA molecules with a “non-self” 5' termini, as a mutant coronavirus deficient in fully capping its mRNAs activated MDA5 in infected cells (Züst et al., 2011). Since picornavirus RF harbors distinctive termini we investigated whether this terminal composition of the RF is essential for MDA5 activation. Changing the physiological terminal groups of RF into 5'ppp and fully complemented 3' end did not change its ability to induce IFN- β upregulation. Other features such as secondary structures are common requirements for ligand recognition; however, the picornavirus RF is not known to contain distinct higher structures. Thus, it is likely that the long ds nature of the RF, and not its unique termini, renders this RNA a potent MDA5 activator.

We also investigated the length dependency of MDA5 ligand recognition as it has been suggested that only dsRNAs longer than 2 kbp can induce MDA5 activation (Kato et al., 2008). We tested dsRNAs of viral sequence *in vitro* that span a wide range of sizes (0.1 – 7.4 kbp), and found that although longer dsRNAs activate MDA5 more efficiently when provided at equal mass, short dsRNAs could also induce some levels of MDA5 activation when present at large quantities. These data suggest that MDA5 may not require its substrate to be longer than a strict cut-off size. In line with this, others have demonstrated efficient activation of MDA5 ATPase activity by dsRNAs as short as 112 bp (Peisley et al., 2011). Authors of this paper also showed that MDA5 ATPase activity, which is triggered by ligand binding, induces disassembly of MDA5 from the RNA ligand, the rate of which is inversely related to the length of the bound RNA molecule (Peisley et al., 2011). This provides some molecular explanation why longer dsRNAs are more efficient in activating MDA5 than shorter ones.

While this paper was in preparation, another study reported that enterovirus dsRNAs, but not ssRNAs, can activate MDA5-dependent IFN- β responses upon transfection (Triantafilou et al., 2012). Also shown in this study is co-localization of MDA5 with dsRNA in enterovirus-infected cells. Though not providing evidence of direct binding or functional activation, these data nicely show that MDA5 and viral dsRNA can be found in physical vicinity, and therefore, support our results that the RF can activate MDA5 in infected cells.

Collectively, our data suggest that the 7.5 kbp RF of picornaviruses is a highly potent MDA5 activator and is directly recognized by MDA5. Moreover, this study shows that manipulating

specific steps of virus replication is a powerful approach to study recognition of specific viral RNA species by RLRs under physiological conditions.

EXPERIMENTAL PROCEDURES

Cells, viruses, infectious cDNA clones and reagents. MEFs and HeLa cells were maintained in DMEM supplemented with 10% FBS and cyproxin (1 mg/ml). Viruses are described in Supplemental information. Infectious cDNA clones p53CB3/T7 (Wessels et al., 2005) and pM16.1 (Hato et al., 2007) were used to produce *in vitro* transcribed RNAs with CVB3 or mengovirus sequences, respectively. CHX and DIP were purchased from Sigma-Aldrich, and RNase A, RNase III and DNase I from Ambion.

Isolation of viral RNA from virions. Cells were infected with virus and grown until cytopathic effect was complete. This lysate was subjected to 3 freeze-thaw cycles, cleared and centrifuged at 25,000 rpm for 6 h in an SW28 rotor at 4°C. The virus pellet was suspended in either TRIzol reagent (Invitrogen) or the lysis buffer of GenElute™ mammalian total RNA Miniprep Kit (Sigma-Aldrich), and RNA was isolated according to the manufacturer's instructions.

Isolation of ssRNA and dsRNA fractions from control and infected cells. Total RNA was isolated using Trizol (Invitrogen) according to manufacturer's protocol. LiCl was added to the total RNA extract to an end concentration of 2 M. This was incubated at 4°C for 2-16 hours and ssRNAs were precipitated by centrifugation at 16,000 x g for 30 min at 4°C. The supernatant was subjected to ethanol precipitate in the presence of 0.8 M LiCl to precipitate dsRNAs. RNA pellets were washed with 75 % ethanol, air dried, and dissolved in RNase-free water.

IFN Reporter assays and Real-time, quantitative PCR analysis were carried out as described previously (Hato et al., 2007).

Preparation of full length IVT RNAs. ssRNAs and dsRNAs were transcribed using Riboprobe® *in vitro* transcription systems (Promega) and Replicator™ RNAi Kit (Finnzyme), respectively, following the manufacturer's instructions. RNAs were treated with DNaseI and purified prior to transfection.

Generation of partially purified VPg unlinkease, Isolation of ³⁵S-methionine labeled vRNA and *in vitro* unlinking reactions were conducted as described previously (Rozovics et al., 2011).

***In vitro* MDA5 ATPase assay** was performed as described previously (Peisley et al., 2011).

Ribosomal RNA removal was performed using Ribo-Zero™ rRNA Removal Kit (Human.Mouse.Rat) (Epicentre RZH1046) according to manufacturer's protocol.

Additional Information. More detailed descriptions of experimental procedures and materials are provided in Extended Experimental Procedures.

SUPPLEMENTAL INFORMATION

Supplemental Information includes Extended Results and Discussion, Extended Experimental Procedures, and five figures and can be found with this article online at <http://dx.doi.org/10.1016/j.celrep.2012.10.005>.

LICENSING INFORMATION

This is an open-access article distributed under the terms of the Creative Commons Attribution-NonCommercial-No Derivative Works License, which permits non-commercial use, distribution, and reproduction in any medium, provided the original author and source are credited.

2

ACKNOWLEDGMENTS

We wish to thank Drs. Shizuo Akira and James Chen for the gifts of MEFs, Thomas Michiels and Robert Silverman for the gift of HeLa-M cells, and Toby Tuthill and Dave Rowlands for the gift of ERAV. S.H. and Q.F. are supported by Mosaic grants (NWO-017.002.025 and NWO-017.006.043, respectively), M.L. by a Rubicon grant (NWO-825.11.022), and F.K. by an ECHO grant (NWO-CW-700.59.007), all from the Netherlands Organisation for Scientific Research (NWO). B.L.S. is a Senior Fellow of the American Asthma Foundation.

SUPPLEMENTAL INFORMATION

EXTENDED RESULTS AND DISCUSSION

RNaseL and PKR are not essential for recognition of picornaviruses.

Our data showed that picornavirus-induced IFN- β response is dependent on MDA5, but not RIG-I (Fig. 1B-C). Two other cellular proteins, namely RNaseL and PKR, have also been implicated in virus recognition (Kato et al., 2011). RNaseL has been suggested to process RNAs to generate ligands for RIG-I (Malathi et al., 2010) and MDA5 (Luthra et al., 2011), while PKR has been implicated in IFN- α/β protein synthesis in response to a number of RNA viruses (Carpentier et al., 2007; Nallagatla et al., 2011). To investigate whether RNaseL and/or PKR also play a role in IFN- α/β induction in response to picornaviruses, we infected wt cells or cells deficient in RNaseL or PKR with mengo-Zn virus and examined their abilities to induce IFN- β transcription. Instead of RNaseL^{-/-} MEFs we made use of a commonly used RNase L-deficient cell line, HeLa M (Dong et al., 2001; Xiang et al., 2003). These cells express virtually no RNaseL (Fig. S1A) and no RNaseL activity, as demonstrated by rRNA degradation, was detectable in HeLa M cells after transfection of poly(I:C) or 2',5'-oligoadenylates (Data not shown). Neither deficient cell line showed any major defect in triggering IFN- β gene transcription upon infection as compared to their wt control cells (Fig. S1B-C), arguing against significant involvement of PKR or RNaseL in detecting picornavirus RNA.

The lack of a role of PKR in picornavirus recognition seems to be at odds with a previous report of reduced IFN- α/β protein levels in TMEV-infected astrocytes in the absence of PKR (Carpentier

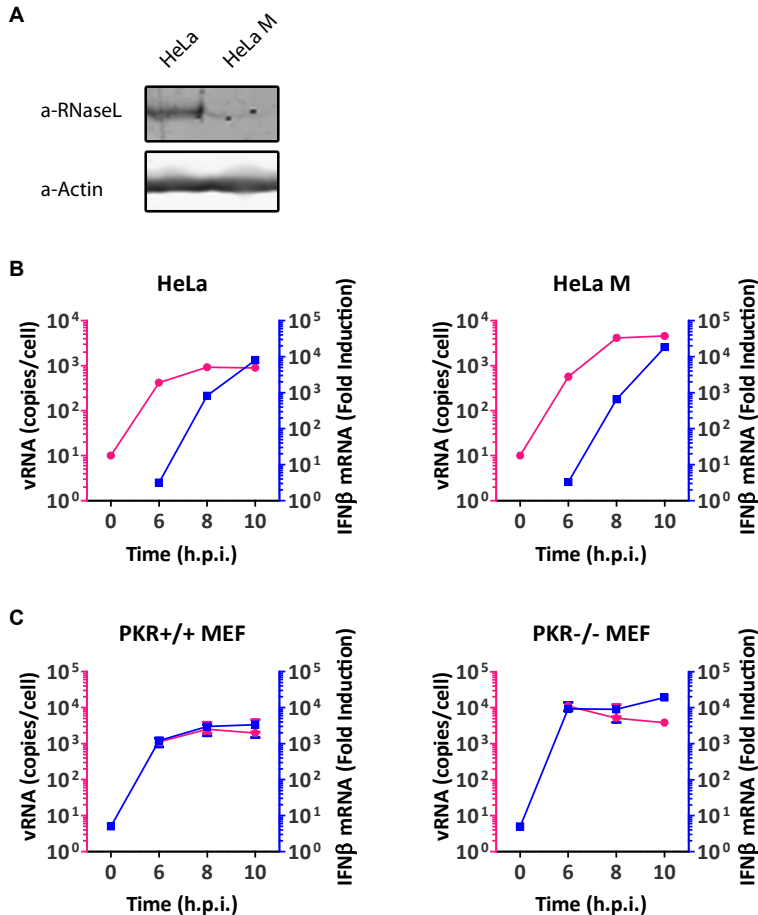


Figure S1. Picornavirus RF-induced IFN-β up-regulation is independent of RNaseL, Related to Figure 1. (A) Lysates of HeLa and HeLa-M cells were subjected to immunoblotting with RNaseL-specific antibody. Actin was taken as loading control. (B) HeLa and HeLa-M cells were infected with mengo-Zn (MOI 50) and viral RNA and host IFN-β mRNA levels in total RNA extracts at indicated hours post infection (h.p.i.) were determined by RT-qPCR. (C) Same experiment as B was performed with wt or PKR^{-/-} MEFs.

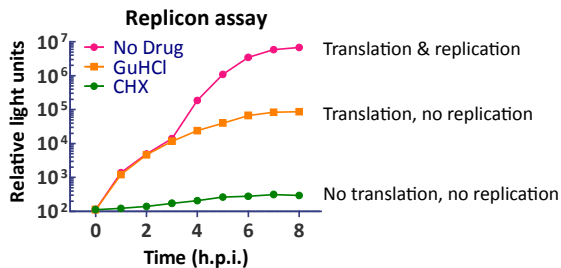


Figure S2. Effect of translation and RNA replication inhibitors, Related to Figure 2. Wt MEFs were transfected with CVB3 replicon RNA (p53CB3-LUC), which contains the CVB3 cDNA in which the capsid-coding region is replaced by the firefly luciferase gene (Wessels et al., 2005), and incubated in the absence or presence of GuHCl (2 mM) or CHX (10 μg/ml). Cells were collected every hour and the luciferase activity in the lysates was measured using a luminescent detector.

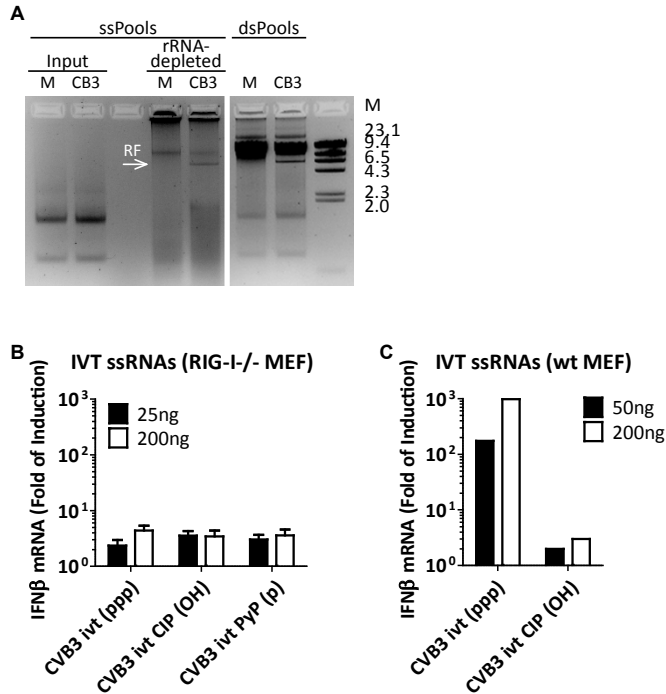


Figure S3. Picornavirus ssRNAs do not exert IFN- β -stimulatory activity, Related to Figure 4. (A) ssRNA fractions (ssPools) of mock- and CVB3-infected cells were subjected to rRNA removal. The input (2 %) and resulting materials were analyzed by agarose gel electrophoresis. The dsRNA fractions were loaded in parallel as a comparison. (B) In vitro transcribed ssRNA was prepared from CVB3 cDNA clone (CVB3 ivt) and treated with either calf intestinal alkaline phosphatase (CIP), which removes all three phosphate groups from the 5' end of the RNA, or 5' polyphosphatase (PyP), which removes the beta- and gamma- phosphate groups. Remaining 5' groups of these RNAs are indicated in brackets. RIG-I^{-/-} MEFs were transfected with indicated amounts of these CVB3 IVT RNAs in the presence of CHX (10 μ g/ml), and IFN- β induction was measured at 8 h.p.t. by RT-qPCR. Data presented as Mean \pm SD. (C) Mock- and CIP-treated CVB3 IVT RNAs as on the left were transfected into wt MEFs in the presence of CHX (10 μ g/ml), and IFN- β induction at 8 h.p.t. was measured by RT-qPCR. The 5'ppp-containing RNA, but not the 5'OH-containing RNA, induced high levels of IFN- β , confirming the quality of the in vitro transcribed RNAs produced and the efficiency of the CIP treatment.

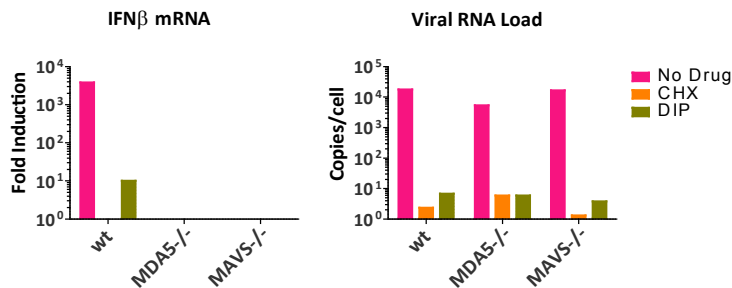


Figure S4. Mengo-Zn infection induces a MDA5-dependent IFN- α/β response in MEFs, Related to Figure 5. (A) MEFs derived from RIG-I^{-/-}, MDA5- or MAVS-deficient mice were infected with mengo-Zn at a MOI of 10 in the presence or absence of DIP (100 μ M) or CHX (10 μ g/ml). Total RNA was isolated at 10 .p.i. and IFN- β mRNA levels were determined by RT-qPCR.

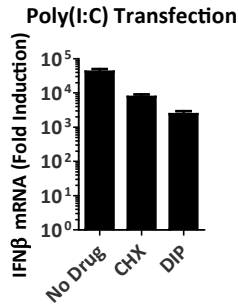


Figure S5. Poly(I:C)-induced IFN- β mRNA up-regulation in the absence or presence of CHX and DIP, Related to Figure 5. HeLa cells were transfected with 0.5 μ g/ml poly(I:C) in the presence or absence of CHX (10 μ g/ml) or DIP (100 μ M). IFN- β mRNA levels were determined at 10 h.p.t. by RT-qPCR. Both CHX and DIP treatments resulted in a reduced IFN- β mRNA induction in response to poly(I:C). Importantly, these results show that the difference in IFN- β induction we observed in CHX- and DIP-treated samples in Fig. 5D-E could not have been artifacts caused by these inhibitors themselves. Data presented as Mean \pm SD.

et al., 2007). This apparent discrepancy can be explained by the recently identified role of PKR in controlling IFN- α/β responses at the post-transcriptional level by regulating the integrity of the poly(A) tail of IFN- α/β mRNA (Schulz et al., 2010). Together with our data that the level of IFN- β mRNA is unaffected in picornavirus-infected PKR^{-/-} MEFs, it seems that PKR does not participate in the initial detection of picornavirus RNA in MEFs.

EXTENDED EXPERIMENTAL PROCEDURES

Cells. HeLa-M cells were provided by Prof. Robert Silvermann (Lerner Research Institute, Cleveland, USA) through Thomas Michiels (Université de Louvain, Belgium). RIG-I^{-/-}, RIG-I^{-/-}, MDA5^{+/+} and MDA5^{-/-} MEFs were provided by Prof. S. Akira (Osaka University, Japan), MAVS^{+/+} and MAVS^{-/-} MEFs were provided by Z.J. Chen (University of Texas, Dallas, USA), and PKR^{+/+} and PKR^{-/-} MEFs (Abraham et al., 1999) were provided by Prof. John Bell (Ottawa Regional Cancer Center, Ontario, Canada) through Thomas Michiels.

Viruses. Both wt mengovirus and mengo-Zn were obtained by transfection of *in vitro* RNA transcripts of infectious cDNA clone based on pM16.1, which contains a copy of mengovirus with a shortened poly C tract (Zoll et al., 1996). Coxsackievirus B3 (CVB3, strain Nancy) was obtained by transfection of *in vitro* RNA transcripts of p53CB3/T7, an infectious clone that contains a full-length cDNA of CVB3 (Wessels et al., 2005). Saffold virus 3 (SAFV3, strain NL2007) and human parechovirus type 1 (HPeV, strain 755532) have been described previously (Zoll et al., 2009a; Zoll et al., 2009b). Enterovirus 71 (EV71, strain Br-Cr) and Coxsackievirus A21 (CVA21, strain Kuykendall) were obtained from the National Institute for Public Health and the Environment (RIVM, Bilthoven, the Netherlands). Equine rhinitis A virus (ERAV, strain NM11/67) was a kind gift from T. Tuthill and D. Rowlands (University of Leeds, United Kingdom). Mengoviruses were propagated on BHK-21 cells. CVB3, ERAV, EV71 were propagated on BGM cells. CVA21 and SAFV3 were propagated on HeLa cells. HPeV1 was propagated on Vero cells. Virus titers were determined by endpoint titration as described previously (van Kuppeveld et al., 1995).

IFN Reporter assays. 1 × 10⁵ HeLa cells were transfected with 200 ng of pIFN- β -luc (Fitzgerald et al., 2003) and 50 ng pRL-TK (Promega; an internal control that constitutively expresses Renilla luciferase) using Fugene-6 (Roche). Cells were incubated for 24 h and were either mock treated, infected with virus, or transfected with RNA using lipofectamine™ 2000 (Invitrogen™) according to the manufacturer's instructions. Luciferase activity was measured at the indicated time points

using the Dual-luciferase Reporter assay system (Promega) according to the manufacturer's instructions. Firefly luciferase values were divided by Renilla luciferase values to normalize for transfection efficiency and are shown as fold induction over mock.

Real-time, quantitative PCR (RT-qPCR) analysis. 2×10^5 cells were transfected with indicated amounts of RNA using lipofectamine™ 2000 (Invitrogen™) according to the manufacturer's instructions. At the indicated time points, total cellular RNA was harvested using GenElute™ mammalian total RNA miniprep Kit (Sigma-Aldrich) according to the manufacturer's instructions. RNA was treated with DNase I (Invitrogen) prior to reverse transcription, which was performed using TaqMan® reverse transcription reagents kit (Applied Biosystems) according to the manufacturer's instructions. Quantitative analysis of gene expression was performed using quantitative PCR, using LightCycler® 480 SYBR® Green I master mix (Roche). Reactions were carried out by a LightCycler® 480 (Roche) and primary data analysis was done with the provided software. The following primers were used. Murine IFN- β forward (fw) and reverse (rv) primers: 5'-CAGCTCCAAGAAAGGACGAAC-3' and 5'-GGCAGTGTAACCTTCTGCAT-3', respectively. Primer sequences were acquired from the Primerbank (Wang and Seed, 2003) (Primerbank ID 6754304a1). Murine HPRT fw and rv primers: 5'-GTAATGATCAGTCAACGGGGAC-3' and 5'-CCAGCAAGCTTGCAACCTTAACCA-3', respectively. Human IFN- β fw and rv primers: 5'-ATGACCAACAAGTGTCTCCTCC-3' and 5'-GCTCATGGAAAGAGCTGTAGTG-3', respectively. Human Actin fw and rv primers: 5'-CCTTCTGGGCATGGAGTCCTG-3' and 5'-GGAGCAATGATCTTGATCTTC-3', respectively.

Preparation of full length IVT RNAs. The *in vitro* transcribed CVB3 RNA was generated by using cDNA clones p53CB3/T7 (Wessels et al., 2005) or pRibCB3/T7 (van Ooij et al., 2006) as templates. Uncapped, *in vitro* transcribed RNAs from linearized plasmids were synthesized using Riboprobe® *in vitro* transcription systems (Promega) following the manufacturer's instructions. Clean-up reactions were performed using TRIzol reagent (Invitrogen) or GenElute™ mammalian total RNA miniprep Kit (Sigma-Aldrich) according to manufacturer's instructions. RNAs were treated with DNase I (Invitrogen) and again cleaned up. RNA integrity was checked on agarose gel. To produce IVT dsRNAs of CVB3 and mengovirus the full-length genomes were amplified by PCR using primers with flanking T7 and Phi6 promoter sites and the cDNA clones p53CB3/T7 and pM16.1 as templates, respectively. dsRNAs were *in vitro* transcribed using Replicator™ RNAi Kit (Finnzyme) according to manufacturer's instructions.

Generation of partially purified VPg unlinkease. Approximately 70 ml of packed HeLa cells were homogenized by cryogenic grinding (Retsch) then solubilized in TDE buffer (10 mM Tris-HCl, pH 7.5, 5 mM DTT, 1 mM EDTA). The homogenate was centrifuged at 70,000 x g for 1 h and the supernatant was subjected to ammonium sulfate fractionation followed by successive chromatography on Q-Sepharose (Pharmacia Biotech), Heparin-Sepharose (GE Healthcare), SP-Sepharose (GE Healthcare), Sephacryl S200 (GE Healthcare), and Mono Q (Amersham) to generate partially purified unlinkease. To generate VPg-depleted ssRNA, 5 μ l of partially purified unlinkease or buffer was incubated with 0.4 pmol of vRNA in a 20 μ l reaction volume containing PDGM buffer (20 mM phosphate buffer, pH 7.0, 5 mM DTT, 10% glycerol, 2 mM MgCl₂) for 30 minutes at 30°C. To assay for the removal of VPg from vRNA, parallel reactions were spiked with 700 CPM ³⁵S-methionine labeled vRNA and quantified as described in (Rozovics et al., 2011).

Isolation of ³⁵S-methionine labeled vRNA. A mutant poliovirus carrying a VPg that can be radioactively labeled with [³⁵S]methionine and the method for isolating ³⁵S-methionine labeled vRNA have been described previously (Rozovics et al., 2011). Briefly, 1 mCi of ³⁵S-methionine was added to HeLa cells in suspension culture following poliovirus W1-VPg31 infection and methionine starvation for three hours at 37°C. At six hours post infection, the infected cells were pelleted and subjected to five cycles of freezing and thawing in RSB*MgCl₂ buffer (10 mM NaCl, 10 mM Tris-HCl, pH 7.5, 1.5 mM MgCl₂) to release the virions. The virions in the supernatant were pelleted by centrifugation at 29,700 rpm for 3.5 h in a Ti 70.1 rotor at 24°C. The pellet was resuspended in 0.1 buffer (0.1 M NaCl, 10 mM Tris-HCl, pH 7.5, 5 mM EDTA, 0.5% SDS) and then applied to a 15-30% sucrose gradient (5 mM EDTA, 0.1 M NaCl, 10 mM Tris-HCl, pH 7.5, 0.5% SDS) and centrifuged at 27,700 rpm for 2.5 h in an SW41 at 24°C. Fractions containing ³⁵S-methionine labeled virions were identified by scintillation counting, pooled and then subjected to two cycles of phenol/chloroform extraction and ethanol precipitation. The final volume of ³⁵S-methionine labeled vRNA was adjusted to 700 cpm/μl (~0.04 pmol/μl).

In vitro MDA5 ATPase assay. Recombinant MDA5 protein was purified as previously described (Peisley et al., 2011). Following a 3 minute pre-incubation of 0.3 μM MDA5 with 0.3 μg/mL nucleic acid in 20 mM Hepes, pH 7.5, 0.1 M NaCl, 1 mM MgCl₂ at 37°C the reaction was initiated by addition of 2 mM ATP. Aliquots were withdrawn at time 0, 30 and 60 minutes, and were quenched with 50 mM EDTA. The amount of ATP hydrolysed was determined by measuring released phosphate using BIOMOL Green Reagent (Enzo), which was added to the quenched reaction at a ratio of 9:1. OD₆₅₀ was measured using a Synergy2 plate reader (BioTek).

REFERENCES

- Abraham, N., Stojdl, D.F., Duncan, P.I., Me´ thot, N., Ishii, T., Dube, M., Vanderhyden, B.C., Atkins, H.L., Gray, D.A., McBurney, M.W., et al. (1999). Characterization of transgenic mice with targeted disruption of the catalytic domain of the double-stranded RNA-dependent protein kinase, PKR. *J. Biol. Chem.* 274, 5953–5962.
- Barton, D.J., and Flanagan, J.B. (1997). Synchronous replication of poliovirus RNA: initiation of negative-strand RNA synthesis requires the guanidineinhibited activity of protein 2C. *J. Virol.* 71, 8482–8489.
- Belov, G.A., and van Kuppeveld, F.J.M. (2012). (+)RNA viruses rewire cellular pathways to build replication organelles. *Curr. Opin. Virol.* 2, 740-747
- Carpentier, P.A., Williams, B.R., and Miller, S.D. (2007). Distinct roles of protein kinase R and toll-like receptor 3 in the activation of astrocytes by viral stimuli. *Glia* 55, 239–252.
- Dong, B., Niwa, M., Walter, P., and Silverman, R.H. (2001). Basis for regulated RNA cleavage by functional analysis of RNase L and Ire1p. *RNA* 7, 361–373.
- Fata-Hartley, C.L., and Palmenberg, A.C. (2005). Dipyridamole reversibly inhibits mengovirus RNA replication. *J. Virol.* 79, 11062–11070.
- Fitzgerald, K.A., McWhirter, S.M., Faia, K.L., Rowe, D.C., Latz, E., Golenbock, D.T., Coyle, A.J., Liao, S.M., and Maniatis, T. (2003). IKKepsilon and TBK1 are essential components of the IRF3 signaling pathway. *Nat. Immunol.* 4, 491–496.

Gitlin, L., Barchet, W., Gilfillan, S., Cella, M., Beutler, B., Flavell, R.A., Diamond, M.S., and Colonna, M. (2006). Essential role of mda-5 in type I IFN responses to polyriboinosinic:polyribocytidylic acid and encephalomyocarditis picornavirus. *Proc. Natl. Acad. Sci. USA* 103, 8459–8464.

Hato, S.V., Ricour, C., Schulte, B.M., Lanke, K.H., de Bruijini, M., Zoll, J., Melchers, W.J., Michiels, T., and van Kuppeveld, F.J. (2007). The mengovirus leader protein blocks interferon-alpha/beta gene transcription and inhibits activation of interferon regulatory factor 3. *Cell. Microbiol.* 9, 2921–2930.

Kato, H., Takeuchi, O., Sato, S., Yoneyama, M., Yamamoto, M., Matsui, K., Uematsu, S., Jung, A., Kawai, T., Ishii, K.J., et al. (2006). Differential roles of MDA5 and RIG-I helicases in the recognition of RNA viruses. *Nature* 441, 101–105.

Kato, H., Takeuchi, O., Mikamo-Satoh, E., Hirai, R., Kawai, T., Matsushita, K., Hiiragi, A., Dermody, T.S., Fujita, T., and Akira, S. (2008). Length-dependent recognition of double-stranded ribonucleic acids by retinoic acid-inducible gene-I and melanoma differentiation-associated gene 5. *J. Exp. Med.* 205, 1601–1610.

Kato, H., Takahashi, K., and Fujita, T. (2011). RIG-I-like receptors: cytoplasmic sensors for non-self RNA. *Immunol. Rev.* 243, 91–98.

Luthra, P., Sun, D., Silverman, R.H., and He, B. (2011). Activation of IFN- β expression by a viral mRNA through RNase L and MDA5. *Proc. Natl. Acad. Sci. USA* 108, 2118–2123.

Malathi, K., Saito, T., Crochet, N., Barton, D.J., Gale, M., Jr., and Silverman, R.H. (2010). RNase L releases a small RNA from HCV RNA that refolds into a potent PAMP. *RNA* 16, 2108–2119.

McCartney, S.A., Thackray, L.B., Gitlin, L., Gilfillan, S., Virgin, H.W., and Colonna, M. (2008). MDA-5 recognition of a murine norovirus. *PLoS Pathog.* 4, e1000108.

Nallagatla, S.R., Toroney, R., and Bevilacqua, P.C. (2011). Regulation of innate immunity through RNA structure and the protein kinase PKR. *Curr. Opin. Struct. Biol.* 21, 119–127.

Peisley, A., Lin, C., Wu, B., Orme-Johnson, M., Liu, M., Walz, T., and Hur, S. (2011). Cooperative assembly and dynamic disassembly of MDA5 filaments for viral dsRNA recognition. *Proc. Natl. Acad. Sci. USA* 108, 21010–21015.

Pichlmair, A., Schulz, O., Tan, C.P., Rehwinkel, J., Kato, H., Takeuchi, O., Akira, S., Way, M., Schiavo, G., and Reis e Sousa, C. (2009). Activation of MDA5 requires higher-order RNA structures generated during virus infection. *J. Virol.* 83, 10761–10769.

Richards, O.C., Martin, S.C., Jense, H.G., and Ehrenfeld, E. (1984). Structure of poliovirus replicative intermediate RNA. Electron microscope analysis of RNA cross-linked in vivo with psoralen derivative. *J. Mol. Biol.* 173, 325–340.

Rozovics, J.M., Virgen-Slane, R., and Semler, B.L. (2011). Engineered picornavirus VPg-RNA substrates: analysis of a tyrosyl-RNA phosphodiesterase activity. *PLoS ONE* 6, e16559.

Schulz, O., Pichlmair, A., Rehwinkel, J., Rogers, N.C., Scheuner, D., Kato, H., Takeuchi, O., Akira, S., Kaufman, R.J., and Reis e Sousa, C. (2010). Protein kinase R contributes to immunity against specific viruses by regulating interferon mRNA integrity. *Cell Host Microbe* 7, 354–361.

Triantafyllou, K., Vakakis, E., Kar, S., Richer, E., Evans, G.L., and Triantafyllou, M. (2012). Visualisation of direct interaction of MDA5 and the dsRNA replicative intermediate form of positive strand

- RNA viruses. *J. Cell Sci.* Published online July 13, 2012. <http://dx.doi.org/10.1242/jcs.103887>.
- van Kuppeveld, F.J., Galama, J.M., Zoll, J., and Melchers, W.J. (1995). Genetic analysis of a hydrophobic domain of coxsackie B3 virus protein 2B: a moderate degree of hydrophobicity is required for a cis-acting function in viral RNA synthesis. *J. Virol.* 69, 7782–7790.
- van Ooij, M.J., Polacek, C., Glaudemans, D.H., Kuijpers, J., van Kuppeveld, F.J., Andino, R., Agol, V.I., and Melchers, W.J. (2006). Polyadenylation of genomic RNA and initiation of antigenomic RNA in a positive-strand RNA virus are controlled by the same cis-element. *Nucleic Acids Res.* 34, 2953–2965.
- van Ooij, M.J., Vogt, D.A., Paul, A., Castro, C., Kuijpers, J., van Kuppeveld, F.J., Cameron, C.E., Wimmer, E., Andino, R., and Melchers, W.J. (2006). Structural and functional characterization of the coxsackievirus B3 CRE(2C): role of CRE(2C) in negative- and positive-strand RNA synthesis. *J. Gen. Virol.* 87, 103–113.
- Wang, J.P., Cerny, A., Asher, D.R., Kurt-Jones, E.A., Bronson, R.T., and Finberg, R.W. (2010). MDA5 and MAVS mediate type I interferon responses to coxsackie B virus. *J. Virol.* 84, 254–260.
- Wang, X., and Seed, B. (2003). A PCR primer bank for quantitative gene expression analysis. *Nucleic Acids Res.* 31, e154.
- Wessels, E., Duijsings, D., Notebaart, R.A., Melchers, W.J., and van Kuppeveld, F.J. (2005). A proline-rich region in the coxsackievirus 3A protein is required for the protein to inhibit endoplasmic reticulum-to-golgi transport. *J. Virol.* 79, 5163–5173.
- Xiang, Y., Wang, Z., Murakami, J., Plummer, S., Klein, E.A., Carpten, J.D., Trent, J.M., Isaacs, W.B., Casey, G., and Silverman, R.H. (2003). Effects of RNase L mutations associated with prostate cancer on apoptosis induced by 2',5'-oligoadenylates. *Cancer Res.* 63, 6795–6801.
- Zoll, J., Galama, J.M., van Kuppeveld, F.J., and Melchers, W.J. (1996). Mengovirus leader is involved in the inhibition of host cell protein synthesis. *J. Virol.* 70, 4948–4952.
- Zoll, J., Erkens Hulshof, S., Lanke, K., Verduyn Lunel, F., Melchers, W.J., Schoondermark-van de Ven, E., Roivainen, M., Galama, J.M., and van Kuppeveld, F.J. (2009a). Saffold virus, a human Theiler's-like cardiovirus, is ubiquitous and causes infection early in life. *PLoS Pathog.* 5, e1000416.
- Zoll, J., Galama, J.M., and van Kuppeveld, F.J. (2009b). Identification of potential recombination breakpoints in human parechoviruses. *J. Virol.* 83, 3379–3383.
- Zust, R., Cervantes-Barragan, L., Habjan, M., Maier, R., Neuman, B.W., Ziebuhr, J., Szretter, K.J., Baker, S.C., Barchet, W., Diamond, M.S., et al. (2011). Ribose 20-O-methylation provides a molecular signature for the distinction of self and non-self mRNA dependent on the RNA sensor Mda5. *Nat. Immunol.* 12, 137–143.

Chapter 3

Coxsackievirus Cloverleaf RNA Containing a 5' Triphosphate Triggers an Antiviral Response via RIG-I Activation

Qian Feng¹, Martijn A. Langereis¹, David Olagnier²,
Cindy Chiang², Roel van de Winkel³, Peter van Essen³,
Jan Zoll³, John Hiscott², Frank J. M. van Kuppeveld¹

¹Virology Division, Department of Infectious Diseases and Immunology,
Faculty of Veterinary Medicine, University of Utrecht, Utrecht, The Netherlands.

²Division of Infectious Diseases, Vaccine and Gene Therapy Institute of Florida, Port Saint Lucie,
Florida, United States of America.

³Department of Medical Microbiology, Radboud University Nijmegen Medical Centre,
Nijmegen, The Netherlands.

PLoS ONE. 2014. 9(4): e95927

ABSTRACT

Upon viral infections, pattern recognition receptors (PRRs) recognize pathogen-associated molecular patterns (PAMPs) and stimulate an antiviral state associated with the production of type I interferons (IFNs) and inflammatory markers. Type I IFNs play crucial roles in innate antiviral responses by inducing expression of interferon-stimulated genes and by activating components of the adaptive immune system. Although pegylated IFNs have been used to treat hepatitis B and C virus infections for decades, they exert substantial side effects that limit their use. Current efforts are directed toward the use of PRR agonists as an alternative approach to elicit host antiviral responses in a manner similar to that achieved in a natural infection. RIG-I is a cytosolic PRR that recognizes 5' triphosphate (5'ppp)-containing RNA ligands. Due to its ubiquitous expression profile, induction of the RIG-I pathway provides a promising platform for the development of novel antiviral agents and vaccine adjuvants. In this study, we investigated whether structured RNA elements in the genome of coxsackievirus B3 (CVB3), a picornavirus that is recognized by MDA5 during infection, could activate RIG-I when supplied with 5'ppp. We show here that a 5'ppp-containing cloverleaf (CL) RNA structure is a potent RIG-I inducer that elicits an extensive antiviral response that includes induction of classical interferon-stimulated genes, as well as type III IFNs and proinflammatory cytokines and chemokines. In addition, we show that prophylactic treatment with CVB3 CL provides protection against various viral infections including dengue virus, vesicular stomatitis virus and enterovirus 71, demonstrating the antiviral efficacy of this RNA ligand.

INTRODUCTION

Pathogen recognition is a key step in the initiation of the host antiviral innate immune response. Specialized pattern recognition receptors (PRRs) such as Toll-like receptors (TLRs) and RIG-I-like receptors (RLRs) detect evolutionarily conserved structures known as pathogen-associated molecular patterns (PAMPs) and initiate an antiviral response. TLRs detect various PAMPs commonly found in both bacteria and viruses, such as lipopolysaccharides (LPS), and non-methylated CpG-containing DNAs (reviewed in [1]). Although TLRs are highly important in pathogen recognition, these receptors are mostly found at the cell surface and/or endosomes in specialized cell types (e.g. dendritic cells and macrophages). RLRs are cytosolic sensors present in virtually all nucleated cells, and thereby sense intracellular pathogens at the site of infection [2]. RIG-I, a well-studied RLR, specializes in recognizing dsRNAs containing 5' triphosphate (5'ppp) groups (reviewed in [3]). Upon ligand engagement, RIG-I interacts with the mitochondrial adaptor molecule MAVS (also called IPS-1), which, in turn, interacts with TANK-binding kinase 1 (TBK1) and I κ B kinase (IKK) complexes, leading to the activation of IRF3 and NF- κ B, respectively. These transcription factors then activate transcription of type I interferons (IFNs) and many pro-inflammatory cytokine genes [2].

Type I IFNs play essential roles in combating viral infections by inducing expression of hundreds of interferon-stimulated genes (ISGs), which together establish an antiviral state in cells [2]. In addition, type I IFNs can activate components of the adaptive immune system such as natural killer cells and dendritic cells, and thereby orchestrate the emergence of the adaptive antiviral response [4,5]. The efficacy of type I IFNs against viral infections has not only been shown at the molecular level in the laboratory but has also been demonstrated in the clinic, where pegylated IFN- α has been used extensively as a therapeutic to treat infections of hepatitis B and C viruses [6,7]. However, clinical efficacy is accompanied by severe side effects such as nausea, hematological toxicity and depression [8], symptoms that lower the quality of life of recipients and also hamper adherence.

Recently, major efforts have been directed to the use of PRR agonists as antiviral agents. A TLR9 agonist, CpG oligodeoxynucleotides, was shown to prevent coxsackievirus B3 (CVB3)-induced myocarditis [9]. Pretreatment with polyinosinic:polycytidylic acid (poly(I:C)), a dsRNA mimic and ligand of TLR3 and RLRs, suppressed Hendra virus infection [10]. Recently, RNA ligands of RIG-I have also been reported to be highly immune stimulatory: a short, 5'ppp-containing RNA derived from the 3' UTR of foot-and-mouth disease virus was shown to be an efficient type I IFNs inducer that protected against challenge viral infections [11]; two 5'ppp-containing RNA hairpins, both of which effectively activated the RIG-I signaling pathway, were shown to elicit protective antiviral immunity [12,13]. Employing a systems analysis approach, Goulet et al. demonstrated that a VSV hairpin induced an extensive, broad spectrum of RIG-I responsive genes compared to the profile of interferon stimulated genes (ISGs) induced by recombinant type I IFNs, thus providing a more complete and balanced immune activation [13]. Together, these results indicate that RIG-I agonist may be promising candidates as antiviral agents.

From *in vitro* studies, it is known that RIG-I activation requires short double-stranded RNAs containing an intact 5'ppp group [14,15]. A number of viral RNA species have been reported to activate RIG-I, including the well-known panhandle RNA structures of many negative-strand

RNA viruses [2]. In addition, 5'ppp-containing *in vitro* transcripts of the Epstein–Barr virus (EBV)-encoded small RNAs (EBERs) [16], the Leader transcript of measles virus [17], and the polyU/UC tract from the 3' UTR of hepatitis C virus (HCV) genome [18] have also been shown to activate RIG-I. Remarkably, the secondary structures of these RNA elements vary considerably – the panhandle RNAs are hairpin-shaped, containing a short double-stranded stem and a relatively large single-stranded loop [19], whereas the EBERs form more complex structures involving multiple stems with bulges and loops [20]; and the polyU/UC tract of HCV is, in fact, believed to be a linear stretch of RNA [18]. These data indicate that the recognition of RNA structures by RIG-I is perhaps more complex than currently understood.

Picornaviruses do not produce 5'ppp-containing RNA species during infection, and are known to activate MDA5, but not RIG-I, through its double-stranded replication intermediate [21]. However, picornavirus genomic RNA contains several well-studied, stable RNA structures that could potentially serve as potent RIG-I ligands when artificially provided with 5' ppp moiety. In this study, we investigated whether any of these structured RNA elements, when provided with 5'ppp by *in vitro* transcription, would activate RIG-I signaling and the antiviral response. We demonstrate that a coxsackievirus B3 (CVB3) cloverleaf containing a 5'ppp moiety stimulated the RIG-I pathway, but other RNA stem-loop structures of similar lengths only poorly activated RIG-I, demonstrating the complexity and specificity of ligand recognition by this receptor. These results contribute to the identification and characterization of RIG-I ligands as potential antiviral agents.

RESULTS

T7 transcripts of the first 1000 nt of CVB3 sequence activates RIG-I.

Picornavirus genomic RNA contains several structured elements including the cloverleaf structure (CL) at the extreme 5' terminus, the stem-loop structures within the viral internal ribosomal entry site (IRES), the cis-acting RNA element (CRE) and additional stem-loop structures within the 3' UTR (Fig. 1A). To investigate whether any of these RNA elements in the CVB3 genomic RNA could stimulate RIG-I, we produced *in vitro* transcribed RNAs (ivtRNAs) corresponding to 2 kb fragments of the CVB3 genomic sequence with 1 kb overlaps, and investigated their individual abilities to activate RIG-I by an IFN reporter assay. Quality and concentrations of these transcripts were confirmed by gel electrophoresis prior to transfection (data not shown). Upon transfection in wt mouse embryonic fibroblasts (MEFs), ivtRNA corresponding to nucleotide (nt) 1-2000 of CVB3 genome (CVB3 1-2000) induced significantly higher levels of IFN- β promoter activation than all other segments of the genomic RNA (Fig. 1B). When RNA transfection was carried out in RIG-I^{-/-} MEFs none of the RNA fragments induced any significant IFN- β activation (Fig. 1C), demonstrating that the responses observed in Fig. 1B were indeed dependent on RIG-I.

To further refine the RNA element that activates RIG-I, shorter, 1 kb, 5'ppp-containing RNA fragments of CVB3 genomic sequence were generated, and their RIG-I-stimulatory activities were measured upon transfection into MEF cells. To demonstrate the contribution of cytoplasmic RNA sensors RIG-I and MDA5, transfections were performed in wt MEFs, as well as RIG-I^{-/-}, MDA5^{-/-} and IPS-1^{-/-} MEFs. All wt MEFs showed similar patterns of IFN- β induction, and

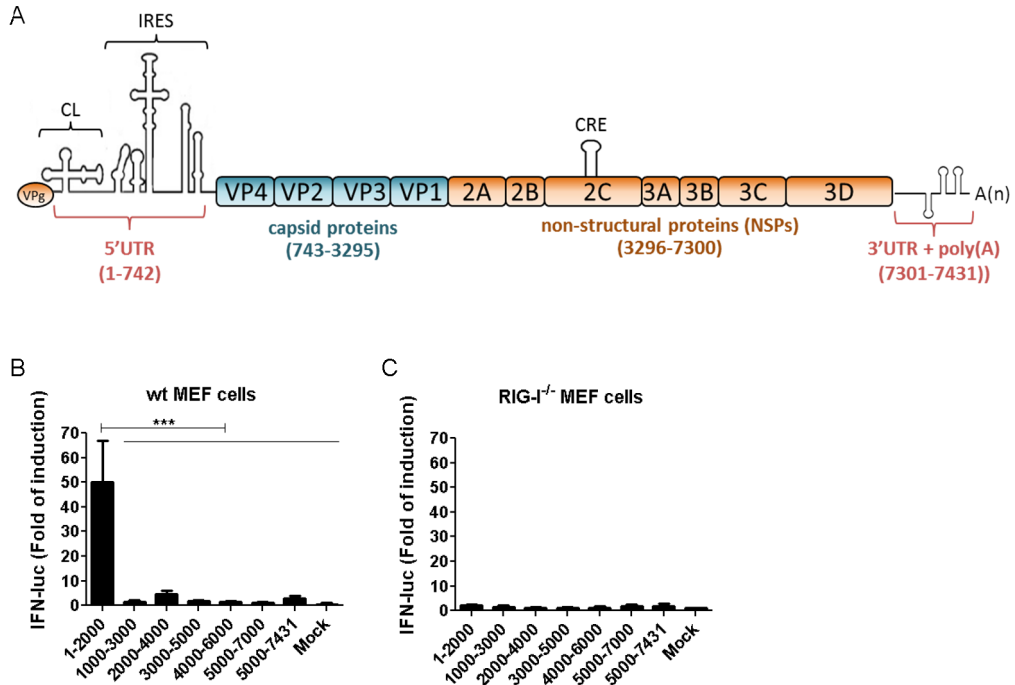


Figure 1. In vitro transcribed RNAs of the first 2 kb of CVB3 genome activates RIG-I. (A) Schematic representation of known RNA structures in CVB3 genomic RNA. CL, cloverleaf. IRES, internal ribosomal entry site. CRE, *cis*-acting RNA element. Numbers refer to nucleotide positions in the viral genomic RNA. (B, C) In vitro transcribed (ivt) RNAs with sequences corresponding to the indicated positions of CVB3 genomic RNA were transfected into WT (B) or RIG-I^{-/-} (C) MEFs. IFN-β luciferase reporter assay was carried out 8 hours post transfection (hr.p.t.). Data presented as mean ± SD.

the first 1 kb (CVB3 1-1000) was the most potent IFN-β inducer amongst all fragments tested (Fig. 2A, 2C and 2E). The positive signals were completely abolished in RIG-I^{-/-} and IPS-1^{-/-} MEFs (Figs. 2D, 2F) but not in MDA5^{-/-} MEFs (Fig. 2B), indicating that RNA activity was mediated by the RIG-I/IPS-1 signaling pathway.

To confirm that the first 1 kb of CVB3 sequence is truly the RNA element recognized by RIG-I, ivtRNAs of different lengths were produced, with or without the first 1000 nts of the genomic sequence and assayed their abilities to activate RIG-I. Upon transfection of all fragments including the first 1 kb and spanning 1 – 7 kb in total, we observed efficient activation of the IFN-β promoter (Fig. 2G). However, when RNAs of the same length, but lacking the first 1 kb sequence, were transfected into cells, only background levels of IFN-β promoter activity were observed (Fig. 2G). These results clearly demonstrate the importance of the first 1 kb of CVB3 genomic sequence in activating RIG-I.

5'ppp-containing CVB3 cloverleaf (CL) structure is a potent RIG-I ligand.

In addition to the 5'ppp moiety present in all RNA fragments tested so far, RIG-I also requires double-stranded regions for recognition [3]. The first 1 kb of CVB3 genome contains the large (nt 1-742) and highly structured 5' UTR (Fig. 1A), comprised of several stem-loop structures (further referred to as Domains I through VII), which were based on M-fold predictions as well

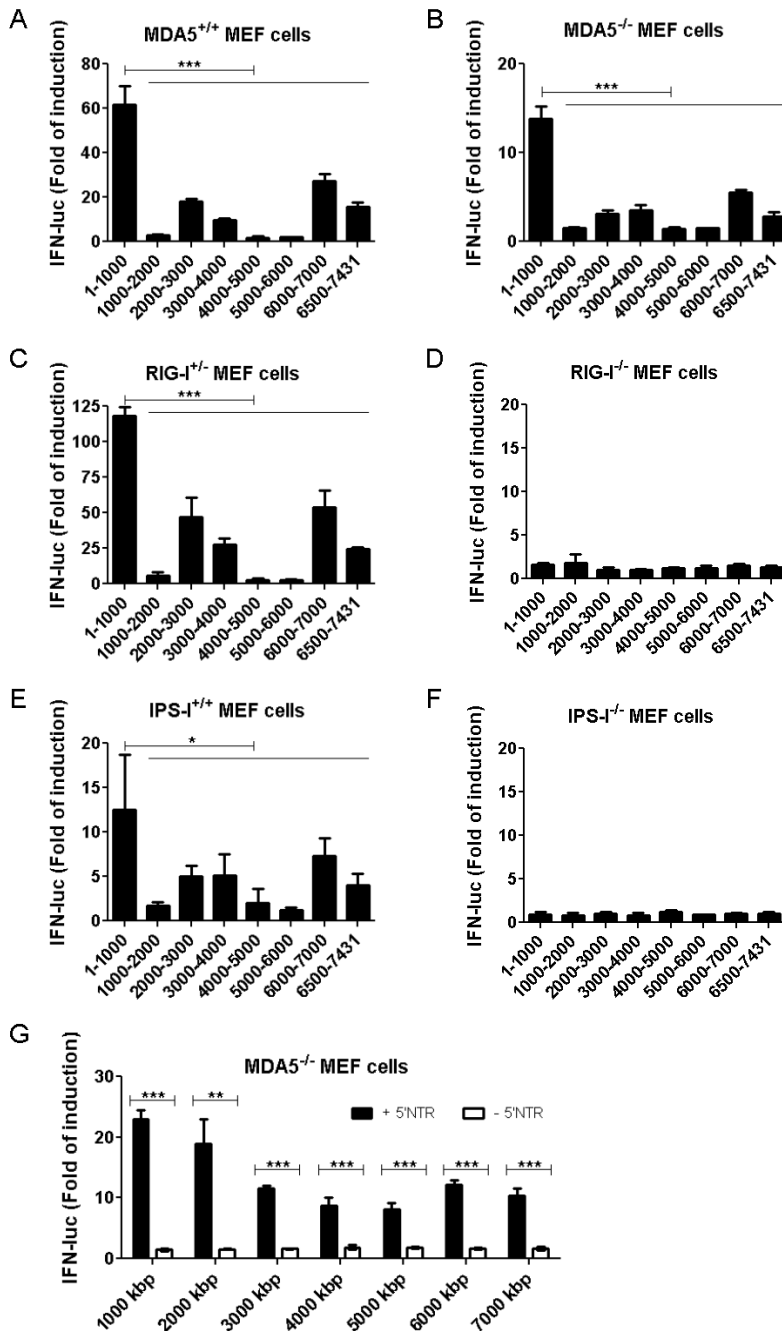


Figure 2. ivtRNA of the first 1 kb of CVB3 genome activates RIG-I. ivtRNAs with sequences corresponding to the indicated positions of CVB3 genomic RNA were transfected into MEFs from MDA5^{-/-} (B), RIG-I^{-/-} (D), IPS-I^{-/-} (F) mice or their WT litter controls (A, C, E). IFN-β luciferase reporter assay was carried out 8 hr.p.t.. Data presented as mean ± standard deviation (SD). (G) ivtRNAs with sequences corresponding to the indicated positions of CVB3 genomic RNA were transfected into WT or RIG-I^{-/-} MEFs. IFN-β luciferase reporter assay was carried out 8 hr.p.t.. Data presented as mean ± SD.

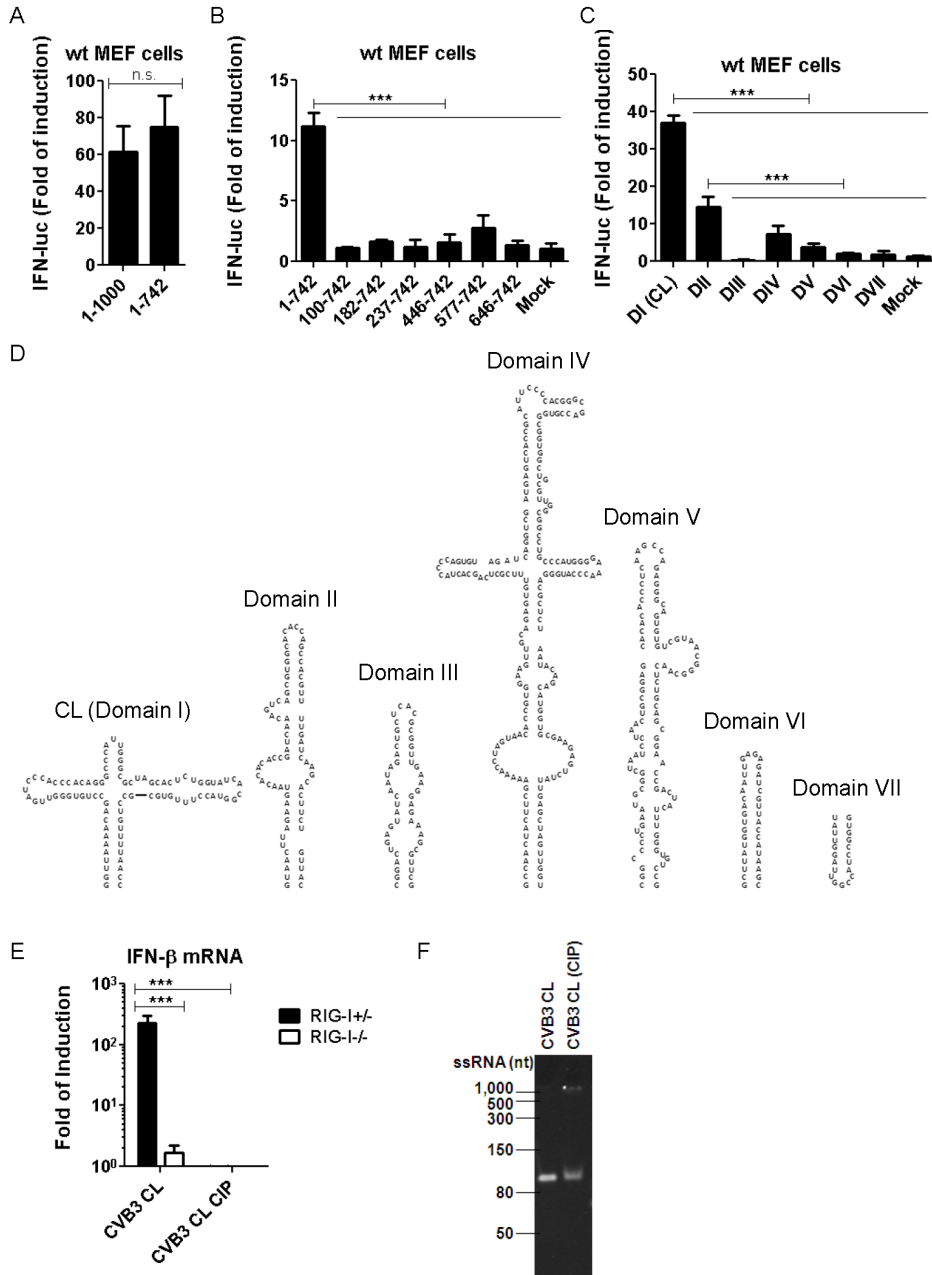


Figure 3. CVB3 Cloverleaf is a potent RIG-I agonist and protects against subsequent EV71 infection. (A, B) *in vitro* RNAs with sequences corresponding to the indicated positions of CVB3 genomic RNA were transfected into WT MEFs. IFN-β luciferase reporter assay was carried out 8 hr.p.t.. Data presented as mean ± SD. (C) *in vitro* RNAs of individual domains in CVB3 5' UTR were transfected into WT MEFs. IFN-β luciferase reporter assay was carried out 8 hr.p.t.. Data presented as mean ± SD. (D) Schematic representation of RNA ligands used in C. (E) CVB3 CL was mock-treated or treated with calf intestinal phosphatase (CIP), and transfected into RIG-I^{+/+} or RIG-I^{-/-} MEFs. IFN-β mRNA levels were determined at 8 hr.p.t.. Data presented as mean ± SD. (F) RNAs used in E were analyzed on an 8 M Urea / 8 % Acrylamide gel, and visualized with SYBR Gold staining. RNA fragments were transfected at equimolar amounts in each experiment.

as extensive RNA probing experiments (reviewed in [22]). These RNA elements are essential for viral translation and RNA replication, and therefore, are structurally highly stable and conserved among related viruses [23]. To test our hypothesis that the 5' UTR is the main RIG-I-stimulating RNA sequence within the first 1 kb of CVB3 sequence, we generated an ivtRNA containing only nt 1-742 (5' UTR) of CVB3 and compared its ability to activate RIG-I with that of nt 1-1000. Equimolar amounts of RNAs were transfected because RIG-I is known to bind to the termini of RNA ligands (i.e. in a 1:1 RIG-I:RNA molecular ratio). Under these conditions, nt 1-742 induced IFN- β promoter activation to the same extent as nt 1-1000 (Fig. 3A), suggesting that the 5' UTR sequence is the main RNA element that is recognized by RIG-I. This recognition is dependent on the 5'ppp since treatment of 5' UTR with polyphosphatase, which yields 5' monophosphate, or calf intestinal phosphatase, which yields 5' OH group, completely abolished IFN- β induction (data not shown).

To further refine the RNA region with the highest potency of RIG-I stimulation, we truncated the 5' UTR sequence from the 5' terminus, one stem-loop at a time, transfected equimolar amounts of the resulting RNAs, and measured IFN- β response by reporter assay. Surprisingly, loss of the first 100 nt of the 5' UTR, which corresponds to the CL structure, almost completely abolished the IFN-stimulatory activity of the RNAs (Fig. 3B), strongly implicating the CL as a potent RIG-I ligand. In line with this observation, when ivtRNAs corresponding to each individual domain within the 5' UTR (Fig. 3D) were transfected into cells, CL induced the highest level of IFN- β activation (Fig. 3C).

Having established that the CL is a potent IFN- β inducer, we set out to confirm that this response is truly dependent on RIG-I. To this end we transfected RIG-I^{+/-} and RIG-I^{-/-} MEFs with CL and determined IFN- β mRNA upregulation levels by RT-qPCR. In addition, we also treated the CL RNA with Calf Intestinal Phosphatase (CIP), which digests the 5'ppp moiety that is required for ssRNAs to activate RIG-I, and studied the resulting RNA to activation IFN- β response in RIG-I^{+/-} and RIG-I^{-/-} MEFs. As shown in Fig. 3E, the CL RNA induced high levels of IFN- β activation in RIG-I^{+/-}, but not RIG-I^{-/-} MEFs, and CIP treatment completely abolished the observed IFN- β response. To assess whether CL-induced RIG-I activation is due to copy-back species, which have been described as byproducts of T7 polymerase-produced RNAs [14,24], we analyzed this RNA (before and after phosphatase treatment) on a denaturing gel. As shown in Fig. 3F, only a single RNA species was present in our RNA preparations, which corresponded to the expected size of CL. This result also excludes that the lack of RIG-I activation by the phosphatase-treated CL is due to degradation of this RNA during treatment. Together, these results clearly identify CL as a potent RIG-I ligand.

CVB3 CL induces potent IFN- α/β and ISG induction.

We next sought to compare the antiviral activity of the CVB3 CL to that of the recently described short hairpin RNA derived from VSV UTR sequences (Fig. 4A) that was identified as a potent RIG-I agonist [13]. To confirm the lack of copy-back species in the VSV hairpin preparation we also analyzed this RNA on denaturing gel. As shown in Fig. 4A, both CVB3 CL and the VSV hairpin migrated as single RNA bands of their expected sizes. In comparison, a dsRNA control yielded two bands on denaturing gel. Next, we transfected varying amounts of CL or VSV hairpin RNA into A549 cells, and analyzed the phosphorylation status of IRF3 at Serine 396, a marker of early activation and prerequisite to RIG-I-mediated type I IFN induction. As shown by immunoblotting

using an antibody specifically against S396 phosphorylated IRF3, both VSV hairpin and CVB3 CL led to equal levels of IRF3 activation (Fig. 4B). We also assayed expression of several IFN-stimulated genes (ISGs) including STAT1, RIG-I and ISG56 by immunoblotting, and found that the induction profiles of all these proteins were identical upon transfection of equal amounts of VSV hairpin or CVB3 CL (Fig. 4B). Furthermore, profiles of IFN- β (Fig. 4C) as well as ISG56 (Fig. 4G) mRNA induction upon transfection of these two RNA ligands were also similar. We also compared the RIG-I-stimulatory activities of CVB3 CL and VSV hairpin with a 5'ppp-containing dsRNA of comparable size (100 bp), which is also known to activate RIG-I [15,25]. All three RNA species induced similar levels of RIG-I-mediated IFN- β activation (Fig. S1).

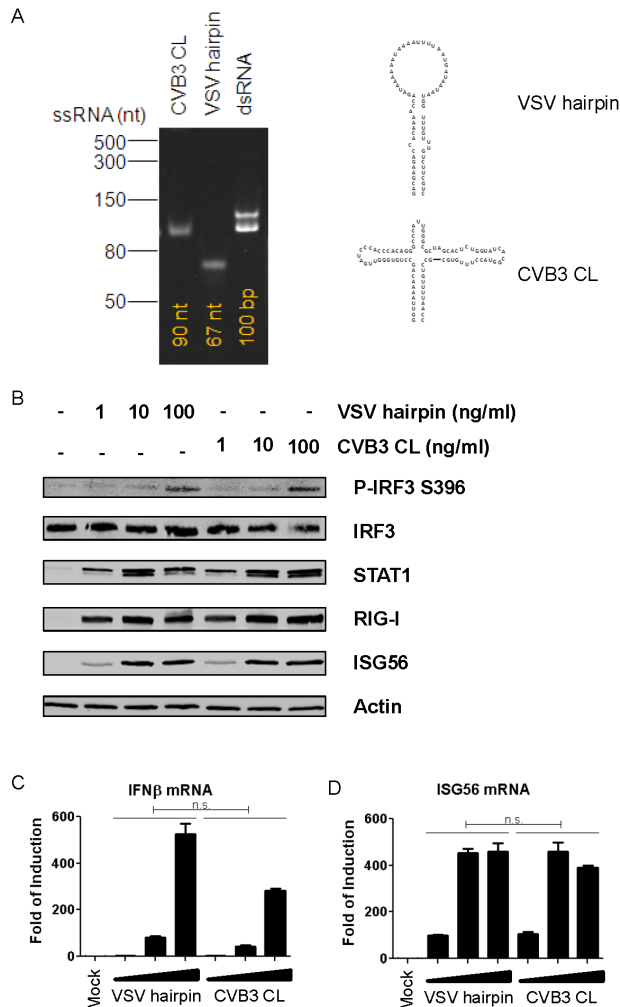


Figure 4. CVB3 CL activates IFN and ISG as efficiently as published ligand. (A) CVB3 CL (with and without CIP treatment), VSV hairpin and a short dsRNA control of 100 bp) were analyzed on an 8 M Urea / 8 % Acrylamide gel, and visualized with SYBR Gold staining. (B) A549 cells were transfected with indicated amounts of VSV short hairpin RNA or CVB3 CL RNA. Cells were lysed at 24 hr.p.t. and subjected SDS-PAGE analysis followed by immunoblotting using antibodies against the indicated proteins. (C, D) A549 cells were transfected with 0.1, 1 or 10 ng/ml of VSV short hairpin RNA or CVB3 CL RNA and incubated for 24 hrs. Total RNA was isolated and subjected to qRT-PCR analysis using primers specific for IFN β or ISG56 mRNAs. Data presented as mean \pm SD.

CVB3 CL induces a broad-spectrum antiviral response.

By employing the BioMark large-scale qRT-PCR analysis platform, we also analyzed the cytokine and chemokine induction profile of CVB3 CL as compared to that of VSV hairpin. As shown in Fig. 5, the gene induction profiles by these two RNA ligands were nearly identical for all genes analyzed. In addition to classical ISGs such as CCL5 (RANTES), IFIT1/2, and IFITM1/2, we also observed induction of type III IFNs (IL-28 α , IL-28 β , and IL-29). In addition, proinflammatory cytokines and chemokines including TNF- α , IL-1 α / β and IL-6 were also efficiently unregulated.

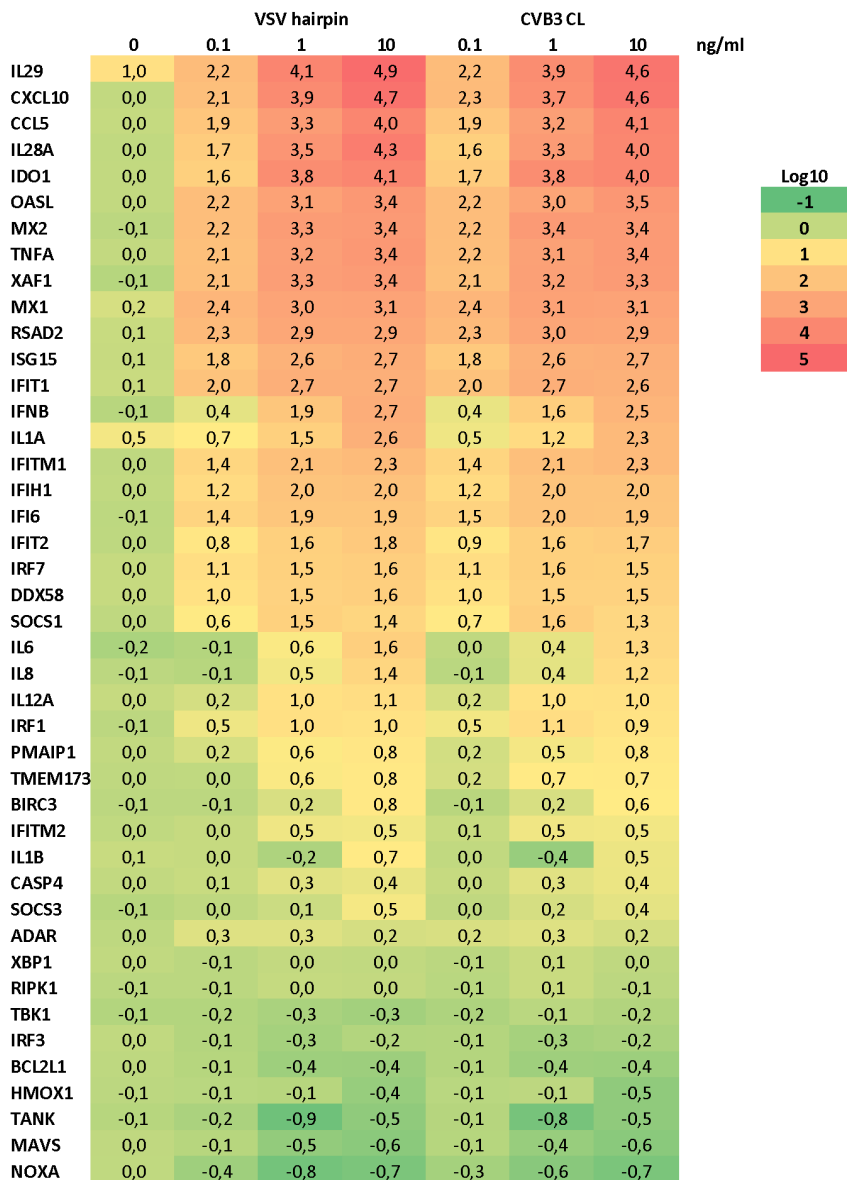


Figure 5. Gene induction profiles of CVB3 CL and VSV hairpin. A549 cells were transfected with indicated concentrations of CVB3 CL or VSV hairpin for 24 hrs. Total RNA was isolated and subjected to qRT-PCR analysis using the BioMark system. Data presented as fold of induction in log10 scale as compared to mock-treated sample.

Two inhibitors of IFN signaling, SOCS1 and 3 were also induced upon transfection of CVB3 CL and VSV hairpin, indicating that the negative feedback regulation of type I IFNs was also activated. These results demonstrate that CVB3 CL activates the RIG-I pathway as potently as VSV hairpin, an established RIG-I ligand with a classical panhandle structure.

CVB3 CL treatment protects cells against challenge virus infections

To further confirm the potency of CVB3 CL in triggering antiviral immunity, we performed infections with dengue virus (DENV) and VSV, in cells pre-treated with varying concentrations of CVB3 CL or VSV hairpin. As shown in Fig. 6, both RNAs provided protection against both viruses (Fig. 6A, B) at concentrations of 1 ng/ml and higher. This antiviral effect was not due to cytotoxicity since no significant change in cell viability was observed for either ligand at concentrations of up to 100 ng/ml (data not shown). Together, these data convincingly demonstrate that CVB3 CL is a potent immune stimulator and can effectively induce an antiviral response in transfected cells.

Not all 5'ppp stem-loop structures induced a RIG-I-mediated type I IFN response (Fig. 3C), and we next asked whether the observations with the IFN-β reporter assay were consistent with the antiviral protection. To this end, HeLa cells were transfected with various amounts of CL or Domain III, infected with enterovirus 71 (EV71) 20h later, and virus titers at 8 hours post infection were determined by end-point titration. In mock-treated as well as lipid alone-treated cells, EV71 infection led to high levels of virus replication (Fig. 6C). Introduction of CL at 100 ng reduced virus titer by approximately 100 fold, and this protective effect was reduced with decreasing amounts of CL transfected (Fig. 6C). Domain III did not protect cells against EV71 infection even at the highest dose used (Fig. 6C), consistent with the earlier observation that this RNA was a poor inducer of IFN-β promoter activity (Fig. 3C).

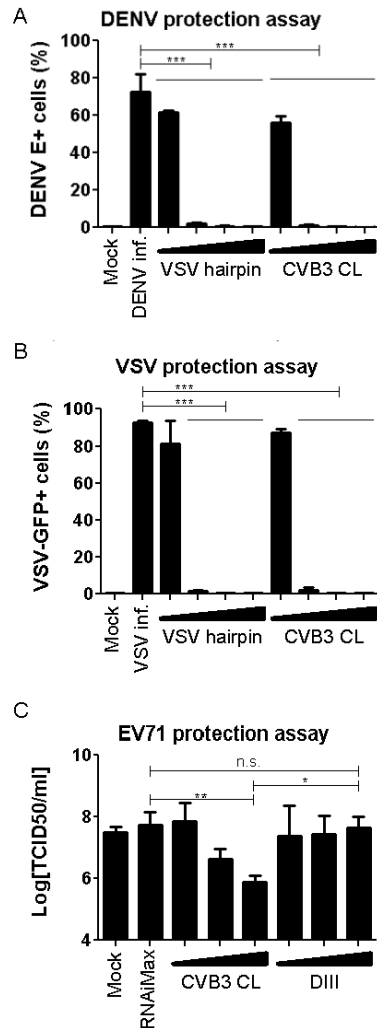


Figure 6. CVB3 CL protects cells against DENV and VSV infections. (A) A549 cells transfected with 0.1, 1, 10 or 100 ng/ml RNA constructs for 18hrs prior to DENV challenge at MOI of 0.5. Cells were fixed 24 hrs after infection and stained with an antibody against the viral envelop (E) protein. DENV E⁺ cells were quantified and presented as percentage of the total population. Data plotted as mean ± SD. (B) A549 cells were transfected with 0.1, 1, 10 or 100 ng/ml RNA constructs for 18 hrs prior to VSV-GFP challenge at MOI of 1. GFP-positive cells were quantified at 24 hrs post infection and presented as percentage of the total population. Data plotted as mean ± SD. (C) HeLa cells were transfected with 1, 10 or 100 ng cloverleaf (CL) or Domain III (DIII) and incubated for 16 hr. They were then infected with enterovirus (EV) 71 at an MOI of 0.05 for 8 hrs. Virus titers were determined by end point titration on HeLa cells. Data shown as mean ± SD.

DISCUSSION

PRR ligands are currently being investigated as potential antiviral agents. In this study, we examined several small, structured RNAs derived from CVB3 sequence in their RIG-I-stimulatory activities. Although none of these RNA ligands are natural PAMPs during CVB3 infection, the CL structure, when produced *in vitro* as a 5'ppp-carrying RNA, proved a highly potent RIG-I ligand. Upon transfection, CVB3 CL induces expression of type I IFNs and type III IFNs, as well as many proinflammatory cytokines and chemokines. This ligand protected cells against various viral infections including EV71, DENV and VSV – completely unrelated viruses that exploit different host factors and pathways for replication.

Another RIG-I agonist, a short hairpin derived from VSV genome, was previously characterized as a potent immune stimulator, capable of inducing ISG expression, similar to recombinant type I IFNs, but also pro-inflammatory cytokines such as TNF- α , IL-1 α/β , IL-6, and CXCL10 as a result of NF- κ B activation. We compared the potency of this ligand and our CVB3 CL in both immune stimulation as well as functional antiviral efficacy. Both ligands induced ISG and cytokine responses to similar extents at the RNA and protein levels. Consistent with this observation, both ligands fully protected cells against DENV and VSV infections at the same concentration. Moreover, the VSV hairpin was shown to protect mice against lethal influenza virus infection [13]. Although not tested in this study, the fact that a large number of cytokine and chemokine genes were induced to nearly identical extents by CVB3 CL and VSV hairpin suggests that CVB3 CL may also elicit protective antiviral immunity *in vivo*. Altogether, our data demonstrate the reliability of utilizing RIG-I pathway activation as a means of immune stimulation.

To date, most established RIG-I ligands, such as the panhandle structure of negative-strand RNA viruses and 5'ppp RNAs derived from Sendai virus and VSV, all adopt a hairpin structure. In comparison, our CVB3 CL adopts a rather unique structure, forming in total 4 short stems, one of which contains a 3-nt bulge, and 3 small loops. Interestingly, three other 5'ppp-containing RNA molecules tested in this study - Domains III, VI and VII - completely failed to activate RIG-I. These RNAs are all predicted to form hairpin structures, and contain 5'ppp on blunt ends, making them appear typical RIG-I ligands. Although Domains III, VI and VII are smaller (54, 36 and 21 nt, respectively) than CVB3 CL (90 nt), they are still larger than some of the established synthetic RIG-I ligands (reviewed in [3]), and Domain III (54 nt) is, in fact, similar in size as the VSV hairpin tested in this study (67 nt). It has also been reported that the length of dsRNAs can play an important role in determining RIG-I activation strength [15]. However, both Domain IV and VI have comparable or slightly longer double-stranded stems than CVB3 CL, but did not induce as much IFN- β as did CL. Of course, we cannot rule out that some of these predicted structures do not fold into their predicted structures, and therefore, poorly activate RIG-I. It is currently difficult to pinpoint why Domains III, VI and VII were incapable of inducing any detectable RIG-I activation, although these results do suggest that ligand recognition by RIG-I may be more complex than currently understood. These observations imply that identification of potent antiviral RIG-I ligands may require additional fundamental investigation.

Known RIG-I ligands not only include 5'ppp-containing ssRNAs such as CVB3 CL and VSV hairpin, but also short 5'ppp-containing dsRNAs [14,15,25]. One may ask whether one type of RNA ligand is generally better than the other. We showed that a 100 bp 5'ppp dsRNA *in vitro*

transcript induced similar level of IFN- β response upon transfection as the CVB3 CL and the VSV hairpin RNAs, suggesting that both single-stranded and double-stranded ligands can be potent triggers of the RIG-I signaling pathway. Also conceptually, it may not be particularly beneficial to use single-stranded or double-stranded RIG-I ligands to activation this pathway. With respect to large scale production of RIG-I ligands (e.g. as a vaccine adjuvant or antiviral agent), chemical synthesis of the 5'ppp moiety is currently challenging. In this regard, dsRNA ligands may be favorable since it has been suggested 5'ppp is not essential for RIG-I activation by dsRNAs longer than 200 bp [15]. However, producing long dsRNAs in a unified form in large quantities may also pose a technical challenge. Research on exploiting RIG-I ligands as a means of clinical intervention (as vaccine adjuvants or antiviral agents) is still at its infancy. We know little about the *in vivo* safety profile, delivery efficiency and potency of single-stranded or double-stranded RIG-I ligands. Having a large repertoire of various RIG-I-activating RNA molecules (as well as those that fail to do so) may be very important to make better-informed decisions in the future.

Recombinant pegylated IFNs has been used as an antiviral therapy against hepatitis B and C virus infections with tremendous success, but with the price of prolonged severe side effects. Therefore, efforts have been focused on the use of ligands of TLRs and RLRs as inducers of antiviral immunity, because these agonists likely mimic the earliest immune recognition events of a natural antiviral response and induce a more extensive and balanced immune activation. Because of the ubiquitous expression profile of RIG-I, RNA agonists would be able to stimulate virtually any cell type, including those at the site of infection. The identification of a novel RIG-I agonist comprising the CVB3 cloverleaf will contribute to the development of RIG-I-based antiviral agents. The identification of RNA ligands that possess all the characteristics required for RIG-I induction - but fail to do so - further demonstrates that there is much to learn about the stimulation of the innate immune response by natural RNA ligands.

MATERIALS AND METHODS

***In vitro* synthesis of VSV hairpin and CVB3 ivtRNAs.** The sequence of 5'pppVSV hairpin RNA was derived from the 5' and 3' UTRs of the VSV genome as previously described (Schlee 2009 Immunity) and *in vitro* transcribed RNA was prepared as previously described (Goulet 2013 PLoS Pathogens). CVB3 ivtRNAs were produced by T7-driven *in vitro* transcription using PCR products amplified the CVB3 infectious clone p53CB3/T7 [26]. 5'pppRNAs were purified using Qiagen miRNA Mini Kit (Qiagen) or by precipitation. Integrity and concentration of purified RNA ligands were controlled by agarose gel electrophoresis prior to each transfection experiment.

Cells culture and transfection. MEFs [27–29] and HeLa [21] cells were maintained in DMEM supplemented with 10 % FCS and 100 U/ml penicillin-streptomycin, in a humidified incubator in the presence of 5 % CO₂. A549 [30] cells were grown in F12K medium (ATCC) supplemented with 10 % FBS and antibiotics. Lipofectamine RNAi Max (Invitrogen) was used for transfection of 5'pppRNAs according to the manufacturer's recommendations.

Viruses. Enterovirus 71 (strain BrCr) was produced on HeLa R19 cells and titers determined by cytopathic effect-based end-point titration. DENV (serotype 2 strain New Guinea C) was produced on C6/36 cells and purified by ultracentrifugation through a 20 % sucrose cushion.

DENV titers were determined by FACS upon E protein staining on Vero cells (ATCC). VSV-GFP bearing the methionine 51 deletion in the matrix protein was kindly provided by J. Bell (Ottawa Health Research Institute, CA). Virus stocks were grown on Vero cells, concentrated from cell-free supernatants by centrifugation at 15,000 rpm for 90 minutes at 4°C. Virus concentration was determined by plaque assay.

SDS-PAGE and immunoblotting analysis. 5'ppp-treated cells were lysed in RIPA buffer (50 mM Tris-Hcl PH 8, 1 % sodium deoxycholate, 1 % NP-40, 5 mM EDTA, 150 mM NaCl, 0.1 % sodium dodecyl sulfate) and cleared by centrifugation at 17,000 x g for 15 min at 4°C. Cleared lysates were subjected to SDS-PAGE analysis on 4-20 % acrylamide Mini-Protean® TGX precast gels (Biorad, Hercules, USA). Proteins were electrophoretically transferred to Immobilon®-PSQ PVDF membranes (Millipore, Billerica, USA) and then subjected to immunoblotting using indicated antibodies. Anti-pIRF3 Ser 396 and anti-RIG-I antibodies were purchased from EMD Millipore, anti-IRF3 from IBL, Japan, anti-IFIT1 from Thermo Fisher Scientific, anti pSTAT1 Tyr701 and anti-STAT1 from Cell Signaling, and anti-β-actin from Odyssey.

IFN-β luciferase reporter assay was performed as previously described [21]. Briefly, approximately 200,000 cells were transfected with 50 ng pTK-Rluc, which encodes renilla luciferase (Rluc) under the control of a constitutively active promotor, and 250 ng pIFN-β-luc, which codes for firefly luciferase (Fluc) under the control of the full IFN-β promoter. 24 hours later cells were transfected with the indicate amounts of RNA ligands and lysed 8 hrs post transfection (hr.p.t.) in 1 x passive lysis buffer (Promega). Luciferase activities were measured using Dual Luciferase System (Promega) according to manufacturer's protocols. Fluc signal was first normalized against Rluc signal, then against mock-transfected samples. Differences were analyzed using student t-tests or one-way ANOVA (Tukey's Multiple Comparison Test). Throughout: *, p<=0.05; **, p<=0.01; ***, p<=0.001.

Real-time quantitative PCR (RT-qPCR) was conducted as previously described [21].

Cell viability analysis. Cell surface expression of phosphatidylserine was measured using an APC-conjugated annexin V antibody, as recommended by the manufacturer (Biolegend). Briefly, specific annexin V binding was achieved by incubating A549 cells in Annexin-V binding buffer (Becton Dickinson) containing a saturating concentration of APC-annexin V antibody and 7-amino-actinomycin D (7-AAD) (Becton Dickinson) for 15 min in the dark. APC-annexin V and 7-AAD binding to the cells was analyzed by flow cytometry, as described previously using an LSRII flow cytometer and FACS Diva software.

Fluidigm BioMark™ assay. Total RNA and cDNA were prepared as described above. Intron-spanning PCR primers were designed using Roche's Universal Probe Library Assay Design Center (www.universalprobelibrary.com) and obtained from the Integrated DNA Technology company (Suppl. Table 1). cDNA along with the entire pool of primers were pre-amplified for 14 cycles using TaqMan® PreAmp Master Mix as recommended by manufacturer's protocol (Applied Biosystems). cDNA was treated with Exonuclease I (New England Biolabs). cDNA samples were prepared with 2X FastStart TaqMan® Probe Master (Roche), GE sample loading buffer (Fluidigm) and Taq Polymerase (Invitrogen). Assays were prepared with 2X assay loading reagent (Fluidigm, NY, USA), primers (IDT) and probes (Roche). Samples and assays were loaded

in their appropriate inlets on a 48.48 BioMark chip. The chip was run on the Biomark™ HD System (Fluidigm, San Francisco USA), which enabled quantitative measurement of up to 48 different mRNAs in 48 samples under identical reaction conditions. Runs contained 40 cycles. Raw Ct values were calculated by the real time PCR analysis software (Fluidigm) and software-designated failed reactions were discarded from analysis. All data are presented as a relative quantification with efficiency correction based on the relative expression of target gene versus the geomean of (GAPDH + Actin + β 2 microglobulin) as the invariant control. Fold of induction as compared to mock-treated sample was plotted on a \log_{10} scale and used to generate the heat map. Statistical analyses were performed as described above.

ACKNOWLEDGEMENTS

We wish to thank Dr Shizuo Akira for kindly providing RIG-I^{+/-}, RIG-I^{-/-}, MDA5^{+/-} and MDA5^{-/-} MEFs, and James Chen for IPS-1^{+/+} and IPS-1^{-/-} MEFs. We are also thankful to Dr J. Bell (Ottawa Health Research Institute, Canada) for providing VSV-GFP harboring the Met 51 deletion in the matrix protein.

SUPPORTING INFORMATION

Figure S1.

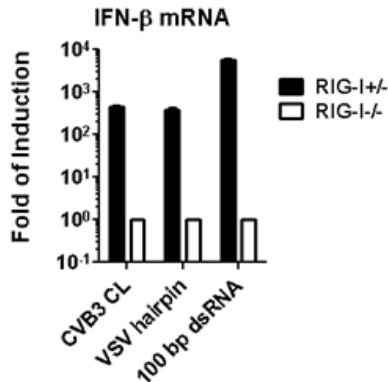


Figure S1. RNAs used in Fig. 4A were transfected into RIG-I^{+/-} or RIG-I^{-/-} MEF cells at equimolar amounts. Cells were harvested at 8 hrs post transfection. IFN- β mRNA level in total RNA isolates was measured by RT-qPCR.

Chapter 3

TABLE S1. List of primers and probes used for high throughput RT-q-PCR

Gene		Sequence (5' to 3')	Probe	Gene		Sequence (5' to 3')	Probe
ACTB	F	attgccaatgagcgggtc	11	IL8	F	agacagcagagcacacaagc	72
	R	tgaaggtagttcgtggatgc			R	tggtcctccgggtgt	
ADAR	F	ttcagaatcccaacaagg	39	IL12A	F	cactcccaaaacctgctgag	50
	R	ctggattccacagggtgt			R	tctctcagaagtgcgaaggta	
B2M	F	ttctggcctggaggctatc	42	IL28A	F	ccagttccgggctgtat	79
	R	tcaggaaattgacttccattc			R	agccaggggactcctttt	
BCL2L1	F	gctgagtaccggcatcc	10	IL29	F	cctgaggcttcccagggtg	75
	R	ttctgaaggagagaagaagattc			R	ccaggacctcagcgctca	
BIRC3	F	gactggcttgcctgtct	44	IRF1	F	gggctgtcagttgattctgg	57
	R	aagaagtcgtttcctcttgt			R	ctatggcacatgcctcaaaa	
CASP4	F	ttgctttctcttcaacg	80	IRF3	F	ctggaagcagcggctac	18
	R	gtgtgatgaagatagagcccatt			R	cgggaacatagcaccagt	
CCL5	F	tgcccacatcaaggagtatt	59	IRF7	F	gcagagccgtacctgtcac	23
	R	ttcgggtgacaagaagcga			R	gccttctgatcatgatgtcac	
CXCL10	F	gaaagcagttagaagaaaggt	34	ISG15	F	gcaaatcacttttccagta	23
	R	gacataactcctatgtagggaagtga			R	ccagcatctcaccgctcag	
DENV2	F	atcctctatggtacgcacaaa	5	MAVS	F	tgcagcaatggtatctcat	39
	R	ctccagattattgaagctgctatcc			R	aaatgattcagcgggagaaa	
DDX58	F	tgtggcaatgcatcaaaa	6	MX1	F	ttcagcactgatggccta	79
	R	gaagcactgtcactcttgc			R	aaagggatgtggctggagat	
GAPDH	F	agccacatcgctcagacac	60	MX2	F	cagacctgacctcattgacc	9
	R	gccaatacgaccaaatcc			R	tgatgagacctgatctgc	
HMOX-1	F	ggcagagggtagataagagg	15	NOXA1	F	gtggatttctgggcaag	5
	R	agctctcgaactcctcaaa			R	tcatggtctgctctgtg	
IDO1	F	cagcgtcttcagtgcttg	3	OASL	F	ttgctatgacaacagggagaac	78
	R	ggaggaactgagcagcatgt			R	ctgtcaagtggatgtctcgtg	
IFI6	F	aaccgtttactcgtctgt	40	PMAIP1	F	ggagatgctgggaagaag	11
	R	gggctccgtcactagacct			R	ccaaatctcctgagttgagtagc	
IFIH1	F	ggcaccatgggaagtgt	20	RIPK1	F	gtgtacaagggcccaact	25
	R	gatgatgatattctccctcca			R	cggctgtctcagctgtt	
IFIT1	F	gcctaatttacagcaacctga	50	RSAD2	F	tgctttgttaaggaagctg	39
	R	tcataatggataactccatgt			R	aggattctccccggctctg	
IFIT2	F	atataggtctctcagcattttgggt	35	SOCS1	F	cccctgtgtgtgagcag	36
	R	caaggaattcttattgttctcactca			R	gtaggagggtgcgagttcagg	
IFITM1	F	cacgcagaaaaccacctc	60	SOCS3	F	gacctgaagggaaacctcct	55
	R	tgttctcctgtgcatcttc			R	tgttttcggtgactgtcc	
IFITM2	F	tgaaccacattgtcaaacc	75	TANK	F	gaggaatgtctcaaaaggaagactg	80
	R	ctctccttgagcatctcgt			R	actataaaggatggagtaaatgacagg	
IFNA2	F	aatggcctgaccttgcct	49	TBK1	F	tgtttgcgagatgtgggtg	72
	R	cacagagcagcttgacttgc			R	ctccccataaacagcatga	
IFNB1	F	ctttgctattttcagacaagattca	20	TMEM173	F	cgctcattgcctaccag	79
	R	gccaggaggttctcaacaat			R	gctgccacagtaacctt	
IL1A	F	tgacgccctcaatcaaaagta	66	TNFA	F	gacaagcctgtagcccatgt	79
	R	tgactataagcaccatgtcaa			R	tctcagctccacgccatt	
IL1B	F	tacctgtcctcgtgttgaa	78	XAF1	F	cctgccatcctaatacaac	2
	R	tctttgggttaattttgggatct			R	tttcttttgatgaagctaacca	
IL6	F	caggagcccagctatgaact	7	XBP1	F	ggagtaagacagcgtctgg	37
	R	gaaggcagcagcacaac			R	cactggcctcactcattcc	

REFERENCES

1. Kato H, Takahasi K, Fujita T (2011) RIG-I-like receptors: cytoplasmic sensors for non-self RNA. *Immunol Rev* 243: 91–98.
2. Goubau D, Deddouche S, Reis E Sousa C (2013) Cytosolic sensing of viruses. *Immunity* 38: 855–869.
3. Schlee M (2013) Master sensors of pathogenic RNA - RIG-I like receptors. *Immunobiology* 218: 1322–1335.
4. Stackaruk ML, Lee AJ, Ashkar AA (2013) Type I interferon regulation of natural killer cell function in primary and secondary infections. *Expert Rev Vaccines* 12: 875–884.
5. Chen Y-L, Chen T-T, Pai L-M, Wesoly J, Bluysen HAR, et al. (2013) A type I IFN-Flt3 ligand axis augments plasmacytoid dendritic cell development from common lymphoid progenitors. *J Exp Med* 210: 2515–2522.
6. Ploss A, Dubuisson J (2012) New advances in the molecular biology of hepatitis C virus infection: towards the identification of new treatment targets. *Gut* 61 Suppl 1: i25–35.
7. Dogan UB, Golge N, Akin MS (2013) The comparison of the efficacy of pegylated interferon α -2a and α -2b in chronic hepatitis B patients. *Eur J Gastroenterol Hepatol* 25: 1312–1316.
8. Sleijfer S, Bannink M, Van Gool AR, Kruit WHJ, Stoter G (2005) Side effects of interferon-alpha therapy. *Pharm World Sci* 27: 423–431.
9. Zhao T, Wu X, Song D, Fang M, Guo S, et al. (2012) Effect of prophylactically applied CpG ODN on the development of myocarditis in mice infected with Coxsackievirus B3. *Int Immunopharmacol* 14: 665–673.
10. McCaskill JL, Marsh GA, Monaghan P, Wang L-F, Doran T, et al. (2013) Potent inhibition of Hendra virus infection via RNA interference and poly I:C immune activation. *PLoS One* 8: e64360.
11. Rodríguez-Pulido M, Borrego B, Sobrino F, Sáiz M (2011) RNA structural domains in noncoding regions of the foot-and-mouth disease virus genome trigger innate immunity in porcine cells and mice. *J Virol* 85: 6492–6501.
12. Martínez-Gil L, Goff PH, Hai R, García-Sastre A, Shaw ML, et al. (2013) A Sendai virus-derived RNA agonist of RIG-I as a virus vaccine adjuvant. *J Virol* 87: 1290–1300.
13. Goulet M-L, Olganier D, Xu Z, Paz S, Belgnaoui SM, et al. (2013) Systems Analysis of a RIG-I Agonist Inducing Broad Spectrum Inhibition of Virus Infectivity. *PLoS Pathog* 9: e1003298.
14. Schlee M, Roth A, Hornung V, Hagmann CA, Wimmenauer V, et al. (2009) Recognition of 5' triphosphate by RIG-I helicase requires short blunt double-stranded RNA as contained in panhandle of negative-strand virus. *Immunity* 31: 25–34.
15. Binder M, Eberle F, Seitz S, Mücke N, Hüber CM, et al. (2011) Molecular mechanism of signal perception and integration by the innate immune sensor retinoic acid-inducible gene-I (RIG-I). *J Biol Chem* 286: 27278–27287.
16. Samanta M, Iwakiri D, Kanda T, Imaizumi T, Takada K (2006) EB virus-encoded RNAs are

- recognized by RIG-I and activate signaling to induce type I IFN. *EMBO J* 25: 4207–4214.
17. Plumet S, Herschke F, Bourhis J-M, Valentin H, Longhi S, et al. (2007) Cytosolic 5'-triphosphate ended viral leader transcript of measles virus as activator of the RIG I-mediated interferon response. *PLoS One* 2: e279.
 18. Saito T, Owen DM, Jiang F, Marcotrigiano J, Gale Jr. M (2008) Innate immunity induced by composition-dependent RIG-I recognition of hepatitis C virus RNA. *Nature* 454: 523–527.
 19. Cheong HK, Cheong C, Choi BS (1996) Secondary structure of the panhandle RNA of influenza virus A studied by NMR spectroscopy. *Nucleic Acids Res* 24: 4197–4201.
 20. Glickman JN, Howe JG, Steitz JA (1988) Structural analyses of EBER1 and EBER2 ribonucleoprotein particles present in Epstein-Barr virus-infected cells. *J Virol* 62: 902–911.
 21. Feng Q, Hato S V., Langereis MA, Zoll J, Virgen-Slane R, et al. (2012) MDA5 detects the double-stranded RNA replicative form in picornavirus-infected cells. *Cell Rep* 2: 1187–1196.
 22. Wimmer E, Hellen CU, Cao X (1993) Genetics of poliovirus. *Annu Rev Genet* 27: 353–436.
 23. Witwer C, Rauscher S, Hofacker IL, Stadler PF (2001) Conserved RNA secondary structures in Picornaviridae genomes. *Nucleic Acids Res* 29: 5079–5089.
 24. Schmidt A, Schwerd T, Hamm W, Hellmuth JC, Cui S, et al. (2009) 5'-triphosphate RNA requires base-paired structures to activate antiviral signaling via RIG-I. *Proc Natl Acad Sci U S A* 106: 12067–12072.
 25. Hornung V, Ellegast J, Kim S, Brzózka K, Jung A, et al. (2006) 5'-Triphosphate RNA is the ligand for RIG-I. *Science* 314: 994–997.
 26. Klump WM, Bergmann I, Müller BC, Ameis D, Kandolf R (1990) Complete nucleotide sequence of infectious Coxsackievirus B3 cDNA: two initial 5' uridine residues are regained during plus-strand RNA synthesis. *J Virol* 64: 1573–1583.
 27. Kato H, Sato S, Yoneyama M, Yamamoto M, Uematsu S, et al. (2005) Cell type-specific involvement of RIG-I in antiviral response. *Immunity* 23: 19–28.
 28. Kato H, Takeuchi O, Sato S, Yoneyama M, Yamamoto M, et al. (2006) Differential roles of MDA5 and RIG-I helicases in the recognition of RNA viruses. *Nature* 441: 101–105.
 29. Kumar H, Kawai T, Kato H, Sato S, Takahashi K, et al. (2006) Essential role of IPS-1 in innate immune responses against RNA viruses. *J Exp Med* 203: 1795–1803.
 30. Olganier D, Scholte FEM, Chiang C, Albulescu IC, Nichols C, et al. (2014) Inhibition of dengue and chikungunya virus infection by RIG-I-mediated type I IFN-independent stimulation of the innate antiviral response. *J Virol* 88: 4180–4194.

Chapter 4

Enterovirus 2A^{pro} Targets MDA5 and MAVS in Infected Cells

Qian Feng¹, Martijn A. Langereis¹, Marie Lork², Mai Nguyen²,
Stanleyson V. Hato², Kjerstin Lanke², Luni Emdad³,
Praveen Bhoopathi³, Paul B. Fisher³, Richard E. Lloyd⁴,
Frank J. M. van Kuppeveld¹

¹Virology Division, Department of Infectious Diseases and Immunology,
Faculty of Veterinary Medicine, Utrecht University, Utrecht, The Netherlands.

²Department of Medical Microbiology, Radboud University Nijmegen Medical Centre,
Nijmegen, The Netherlands.

³Department of Human and Molecular Genetics, VCU Institute of Molecular Medicine,
VCU Massey Cancer Center, Virginia Commonwealth University,
School of Medicine, Richmond, Virginia, USA.

⁴Department of Molecular Virology and Microbiology,
Baylor College of Medicine, Houston, Texas, USA.

Journal of Virology. 2014. 88(6):3369-78

ABSTRACT

RIG-I-like receptors (RLRs) MDA5 and RIG-I are key players in the innate antiviral response. Upon recognition of viral RNA, they interact with MAVS, eventually inducing type I interferon production. The interferon induction pathway is commonly targeted by viruses. How enteroviruses suppress interferon production is incompletely understood. MDA5 has been suggested to undergo caspase- and proteasome-mediated degradation during poliovirus infection. Additionally, MAVS is reported to be cleaved during infection with coxsackievirus B3 (CVB3) by the CVB3 proteinase 3C^{pro}, whereas MAVS cleavage by enterovirus 71 has been attributed to 2A^{pro}. As yet, a detailed examination of the RLR pathway as a whole during any enterovirus infection is lacking. We performed a comprehensive analysis of crucial factors of the RLR pathway, including MDA5, RIG-I, LGP2, MAVS, TBK1, and IRF3, during infection of CVB3, a human enterovirus B (HEV-B) species member. We show that CVB3 inhibits the RLR pathway upstream of TBK1 activation, as demonstrated by limited phosphorylation of TBK1 and a lack of IRF3 phosphorylation. Furthermore, we show that MDA5, MAVS, and RIG-I all undergo proteolytic degradation in CVB3-infected cells through a caspase- and proteasome-independent manner. We convincingly show that MDA5 and MAVS cleavages are both mediated by CVB3 2A^{pro}, while RIG-I is cleaved by 3C^{pro}. Moreover, we show that proteinases 2A^{pro} and 3C^{pro} of poliovirus (HEV-C) and enterovirus 71 (HEV-A) exert the same functions. This study identifies a critical role of 2A^{pro} by cleaving MDA5 and MAVS and shows that enteroviruses use a common strategy to counteract the interferon response in infected cells.

IMPORTANCE

Human enteroviruses (HEVs) are important pathogens that cause a variety of diseases in humans, including poliomyelitis, hand, foot, and mouth disease, viral meningitis, cardiomyopathy, and more. Like many other viruses, enteroviruses target the host immune pathways to gain replication advantage. The MDA5/MAVS pathway is responsible for recognizing enterovirus infections in the host cell and leads to expression of type I interferons (IFN-I), crucial antiviral signaling molecules. Here we show that three species of HEVs all employ the viral proteinase 2A (2A^{pro}) to proteolytically target MDA5 and MAVS, leading to an efficient blockade upstream of IFN-I transcription. These observations suggest that MDA5/MAVS antagonization is an evolutionarily conserved and beneficial mechanism of enteroviruses. Understanding the molecular mechanisms of enterovirus immune evasion strategies will help to develop countermeasures to control infections with these viruses in the future.

INTRODUCTION

Type I interferons (IFNs; alpha/beta interferon [IFN- α/β]) are key players in the innate antiviral response against virus infections. Initially produced and secreted by infected cells, IFN- α/β can bind to the type I IFN receptor (IFNAR) in autocrine and paracrine manners, thereby initiating the JAK/STAT pathway. Activation of this pathway leads to the expression of hundreds of interferon-stimulated genes (ISGs), which together induce a so-called antiviral state that restricts virus replication (reviewed in reference 1). The initiation of the IFN- α/β response relies on specialized pathogen recognition receptors (PRRs) that recognize pathogen-associated molecular patterns (PAMPs), molecular motifs bearing non-self-signatures to the host cell. Some members of the Toll-like receptor (TLR) family, such as TLR3 and TLR7/8, are known to play crucial roles in virus recognition. TLRs are mostly expressed in macrophages, dendritic cells, and other immune cell types, where they detect PAMPs at the cell surface or in endosomes (2). Another family of PRRs is the RIG-I-like receptors, including RIG-I (3), MDA5 (4–6), and LGP2 (3, 7). These receptors are ubiquitously expressed and monitor the cytoplasm of virtually all nucleated cells. Upon activation by viral RNA, RIG-I and MDA5 interact with MAVS, an adaptor molecule localized at the outer membrane of mitochondria (8–11). MAVS then initiates signaling cascades via TANK-binding kinase 1 (TBK1) and I κ B kinase (IKK) complexes, leading to activation of IRF3 and NF- κ B, transcription factors required for transcription activation of IFN- α/β and other proinflammatory cytokine genes (2). RIG-I and MDA5 have nonredundant roles in detecting invading viruses. While RIG-I is crucial in detecting many negativestrand RNA viruses (e.g., vesicular stomatitis virus and influenza virus) and some flaviviruses (e.g., hepatitis C virus and Japanese encephalitis virus) (12–15), MDA5 is important for the recognition of members of the Picornavirus, Coronavirus, and Calicivirus families (16–18). The molecular motifs that activate RIG-I and MDA5 also vary. RIG-I is activated by 5'-triphosphate (5'ppp)-containing double-stranded RNAs (dsRNAs) as well as doublestranded regions within single-stranded RNA molecules, such as the panhandle structure formed by genomic RNAs of negativestrand RNA viruses (2, 19, 20). MDA5 requires long dsRNA duplexes for potent activation, as exemplified by the replicative form of picornaviruses (16, 21).

The *Picornaviridae* is a large family of nonenveloped, positivestrand RNA viruses. This family includes many important human and animal pathogens, and members of the *Enterovirus* genus are particularly important. Poliovirus (PV), the causative agent of poliomyelitis, is the subject of a multi-billion-dollar eradication campaign from the World Health Organization. Enterovirus 71 (EV71) continues to cause outbreaks of hand, foot, and mouth disease associated with neurological complications in Southeast Asia. Coxsackieviruses (CVs) and echoviruses are the leading causes of viral meningitis and cardiomyopathy. Rhinoviruses cause common colds and are frequently associated with asthma exacerbations and chronic obstructive pulmonary disease. Upon entry, the viral genome is immediately translated into a single polyprotein, which is proteolytically processed into mature peptides by viral proteinases 2A^{pro} and 3C^{pro}. These viral proteins then facilitate viral RNA replication and, eventually, production of progeny virion particles. Like most viruses, picornaviruses have evolved to actively suppress the host IFN- α/β response to gain a replication advantage. In fact, many reports have demonstrated that picornaviruses efficiently suppress IFN- α/β at the transcription level in cultured cells (16, 22, 23). However, the mechanism by which picornaviruses interfere with IFN- α/β induction is not completely understood.

Many studies have been performed to investigate how picornaviruses interfere with the RIG-I like receptor (RLR)-mediated IFN- α/β induction pathway. MDA5, the receptor responsible for recognizing picornavirus RNA, is reported to be degraded during infection of PV (24) and EV71 (25). MDA5 degradation was shown to be dependent on caspases and, in the case of PV, also proteasome activities (24). Surprisingly, other closely related enteroviruses, such as human rhinovirus 16 (HRV16) and echovirus 1, did not induce MDA5 degradation (24), suggesting that there may be variations among enteroviruses in their strategies to suppress IFN- α/β induction. Besides MDA5, RIG-I is also targeted by several enteroviruses, such as PV, echovirus, and HRV16 and -1A, most likely via their 3C^{pro}s (26), though it remains to be elucidated why these viruses would target an RNA sensor that does not participate in their recognition. In addition, the downstream adaptor molecule MAVS is targeted by several enteroviruses, including HRV1A (27), coxsackievirus B3 (CVB3) (23), and EV71 (28). However, different mechanisms regarding how these viruses accomplish MAVS inactivation have been proposed. MAVS is reported to be cleaved by 2A^{pro} during EV71 infection (28) and by 3C^{pro} during CVB3 infection (23), whereas both of these viral proteinases, as well as caspase 3, were implicated in HRV1A-induced MAVS cleavage (27). This diversity in MAVS inactivation mechanisms is rather uncommon for enteroviruses, as they often utilize the same strategies to target a particular host factor. For instance, eukaryotic initiation factor 4G (eIF4G) is cleaved by the 2A^{pro}s of various enteroviruses and rhinoviruses (29, 30), while G3BP is cleaved by the 3C^{pro} of PV (31) as well as by that of CVB3 (this study). Importantly, each of the studies focused on a single factor (MDA5, MAVS, or RIG-I) and used a different group of viruses. Hence, it is yet impossible to paint a complete picture of the IFN- α/β antagonization strategy of any individual virus, and it is challenging to conclude with confidence whether different enteroviruses truly employ diverse strategies to inactivate these host factors or whether the differences merely result from the use of different reagents and/or assays in different studies.

To gain a comprehensive overview of the fate of the important components of the RLR signaling pathway during enterovirus infection, we examined multiple factors along the signaling cascade during infection of a model virus, CVB3. We show that RIG-I is targeted by 3C^{pro} of CVB3, PV, and EV71, resulting in similar cleavage products previously reported for PV (26). Importantly, we report that cleavage of MDA5 occurs in a caspase- and proteasome-independent manner and relies on viral proteinase 2A^{pro}. Furthermore, in contrast to a previous report (23), we demonstrate that MAVS cleavage during CVB3 infection is also (primarily) mediated by 2A^{pro} and not 3C^{pro}. Moreover, we show that 2A^{pro}s from other enteroviruses, namely, PV and EV71, also target MDA5 and MAVS for cleavage, suggesting that enteroviruses likely share common strategies to target the RLR-mediated IFN- α/β induction pathway.

MATERIALS AND METHODS

Cells and viruses. HeLa R19 cells were maintained in Dulbecco modified Eagle medium supplemented with 10 % fetal calf serum and 100 U/ml penicillin-streptomycin in a humidified incubator in the presence of 5 % CO₂. Coxsackievirus B3, mengovirus, and a mengovirus which lost its IFN-suppressing activities due to substitutions in the Zn finger domain of the leader protein (mengo-Zn) have been described previously (16). M-2A(CVB3/PV/EV71) and M-3C(CVB3/PV/EV71) cDNAs were generated by cloning the 2A^{pro}- or 3C^{pro}-coding region of

the indicated viruses, respectively, upstream of the leader-coding region in the mengovirus infectious clone pM16.1. To ensure proper maturation of the 2A^{pro} or 3C^{pro} from the mengovirus polyprotein, we also added glutamine-glycine codons after the inserted sequences, to allow cleavage by mengovirus 3C^{pro} during polyprotein processing. Viruses were produced by directly transfecting *in vitro*-transcribed RNAs from the infectious clones of M-2A(CVB3/PV/EV71) and M-3C(CVB3/PV/EV71) in BHK-21 or HeLa R19 cells.

Plasmids. pcDNA3-FLAG-MAVS-HA was generated by inserting the hemagglutinin (HA) tag in pcDNA3-FLAG-MAVS, provided by Z. Chen (University of Texas Southwestern Medical Center, Texas). The Q148A mutation was generated by site-directed mutagenesis.

Reagents. Antibodies against MDA5 have been previously described (32). Antibodies against RIG-I were purchased from Abgent, MAVS was purchased from Alexis-Biochemicals, IRF3 was purchased from Santa Cruz Biotechnology, p-IRF3 (S396), TBK1, and phosphorylated TBK1 (p-TBK1; phosphorylation at S172) were purchased from Cell Signaling Technology, LGP2 was purchased from Abcam, actin and the FLAG tag were purchased from Sigma-Aldrich, eIF4G was purchased from Bethyl Laboratories, the HA tag was purchased from Covance, G3BP was purchased from BD Biosciences, and procyclic acidic repetitive protein (PARP) was purchased from Roche Applied Sciences. Q-VD-OPh (QVD) was purchased from BioVision, MG132 was purchased from Sigma-Aldrich, and staurosporine (STS) was purchased from Roche Applied Sciences. Recombinant CVB3 2A^{pro} has been previously described (33), and recombinant CVB3 3C^{pro} was a kind gift from Rolf Hilgenfeld (University of Lübeck, Lübeck, Germany).

Quantitative real-time PCR was performed as previously described (16).

Immunoblotting. Cells were lysed in TEN lysis buffer (40 mM Tris- HCl, 150 mM NaCl, 10 mM EDTA, 1 % NP-40), and lysate was cleared by centrifugation at 16,000 x g at 4°C for 5 min. Total protein concentrations were determined using Bio-Rad protein assay dye reagent concentrate according to the manufacturer's protocols. Lysates were subjected to SDS-PAGE and immunoblotting using the indicated antibodies. Native PAGE (for IRF3 dimerization assay) was performed as described previously (22).

***In vitro* cleavage with recombinant 2A^{pro} or 3C^{pro}.** Cells were resuspended in a 2 volume of the cell pellet of hypotonic buffer [20 mM HEPES, pH 7.4, 10 mM KCl, 1.5 mM Mg(CH₃COO)₂, 1 mM dithiothreitol (DTT)], incubated on ice for 10 min, and lysed by repeated passage through a thin needle at 4°C. A 0.1 volume of buffer A [200 mM HEPES, pH 7.4, 1.2 M KCH₃COO, 40 mM Mg(CH₃COO)₂, 50 mM DTT] was added to the cell lysate, and this was cleared by centrifugation at 2,500 x g for 5 min at 4°C. Unless indicated otherwise, 0.5 g 2A^{pro} or 0.75 g 3C^{pro} was incubated with 150 g lysate at room temperature overnight. The reaction was terminated by addition of Laemmli sample buffer and heat treatment at 95°C for 10 min.

RESULTS

CVB3 interrupts the RLR pathway upstream of TBK1 phosphorylation. It is known that picornaviruses induce little IFN- α/β response in infected cells (23, 28, 34). In cells infected with

wildtype (wt) CVB3 or mengovirus (a strain of encephalomyocarditis virus [EMCV] that was used as a control), little IFN- β mRNA was detected, and only at very late stages of infection (i.e., at 9 and 12 h postinfection [p.i.]) (Fig. 1A). In contrast, infection with a mutant mengovirus which lost its IFN-suppressing activities due to substitutions in the Zn finger domain of the leader protein (mengo-Zn) (22) already induced strong IFN- mRNA upregulation at 6 h p.i., and this further dramatically increased and eventually reached a plateau at 9 h p.i. (Fig. 1A). This increased IFN- α/β response induced by mengo-Zn was not due to differences in virus replication, as viral RNA accumulated with kinetics and at levels similar to those for wt mengovirus and CVB3 (Fig. 1B).

To gain a first insight into how the viruses interfere with IFN- α/β induction pathways, we first asked whether the key transcription factor required for IFN- α/β transcription activation, namely, IRF3, is activated in infected cells. HeLa R19 cells were infected with CVB3 and harvested at 6, 9, and 12 h p.i. Cell lysates were subjected to immunoblotting to determine the IRF3 expression level, as well as the activation status of IRF3, as indicated by phosphorylation at serine 396 and dimerization of this transcription factor. We also performed parallel experiments with mengovirus or mengo-Zn as negative and positive controls, respectively. Infection with mengo-Zn, but not wt mengovirus, induced efficient IRF3 phosphorylation and dimerization (Fig. 1C). CVB3 infection did not induce any detectable IRF3 phosphorylation or dimerization (Fig. 1C), consistent with the lack of a significant IFN- β mRNA induction (Fig. 1A). The absence of IRF3

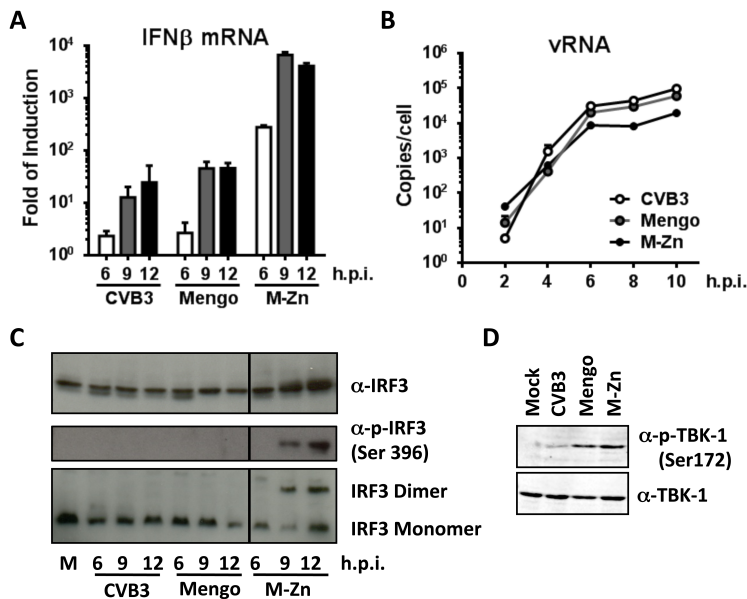


FIG. 1. CVB3 antagonizes the RLR pathway upstream of TBK1, while mengovirus does so downstream of TBK1 activation. HeLa R19 cells were mock infected or infected with CVB3, mengovirus (mengo), or mengo-Zn (M-Zn) at a multiplicity of infection of 50, and cells were harvested at the indicated times (h) p.i. Total RNA was isolated and subjected to reverse transcription-quantitative PCR analysis for IFN- β mRNA (A) and viral RNA (vRNA) (B). Data were first normalized against those for actin mRNA, and then the fold induction compared to that for the mock-infected sample was calculated and is presented as the mean \pm SD. (C) Infection was carried out as described for panel A, and cells were lysed at the indicated times (h) p.i. Lysates were then subjected to SDS-PAGE, followed by immunoblotting using the indicated antibodies. IRF3 dimerization analysis was carried out under native conditions. Lane M, mock infection. (D) Infection was carried out as described for panel A, and cells were lysed at 9 h p.i. Cell lysates were analyzed by SDS-PAGE, followed by immunoblotting using the indicated antibodies. Data are representative of those from at least 3 independent experiments.

activation was not due to changes in IRF3 expression levels, since these remained unchanged throughout the CVB3 (and mengovirus) infection (Fig. 1C). Our data clearly indicate that the IFN- α/β induction pathway is severely inhibited upstream of IRF3 phosphorylation during wt CVB3 infection.

It is well established that IRF3 phosphorylation relies on the activity of TBK1, which is itself activated by phosphorylation at serine 172 (35). We therefore asked whether TBK1 expression and/or activation is affected in CVB3-infected cells. Cells were infected with CVB3, wt mengovirus, and mengo-Zn for 9 h, and cell lysates were analyzed by immunoblotting using a polyclonal antibody against TBK1 and a monoclonal antibody against S172-phosphorylated TBK1. As shown in Fig. 1D, the basal level of TBK1 expression did not change during infection with any of the three viruses. As expected, S172 phosphorylation of TBK1 was readily detectable in mengo-Zn-infected cells. wt mengovirus infection also resulted in TBK1 phosphorylation to the same extent as mengo-Zn infection, but this was significantly reduced in CVB3-infected cells (Fig. 1D). These results indicate that CVB3 targets the RLR pathway upstream of TBK1 phosphorylation, while mengovirus does so between TBK1 activation and IRF3 phosphorylation.

CVB3 induces MDA5, MAVS, and RIG-I cleavage in infected cells. To further investigate where CVB3 interferes with the RLR pathway, we examined the crucial factors involved in this signaling cascade by immunoblotting during a course of infection. From 9 h p.i. onwards, we observed a decrease in the full-length MDA5 signal accompanied by the appearance of a smaller product of about 100 kDa (Fig. 2), suggesting that MDA5 is cleaved during CVB3 infection. Also, RIG-I and MAVS, but not TBK1 or LGP2, another member of the RLR family, were cleaved from 9 h p.i. (Fig. 2). RIG-I cleavage was accompanied by the appearance of a band at about 70 kDa, similar to the cleavage product observed in PVinfected cells (26). We also observed a putative cleavage product (37 kDa) of MAVS (Fig. 2) which was significantly smaller than the reported cleavage product (50 kDa) produced by CVB3 3C^{pro} (23), suggesting an alternative MAVS cleavage. None of these factors were cleaved during infection of mengovirus or mengo-Zn (Fig. 2), in agreement

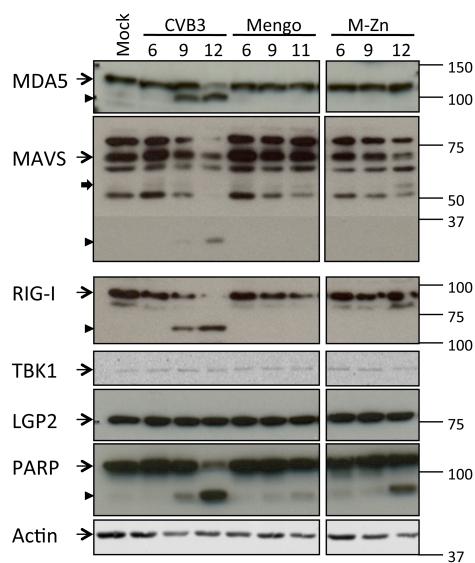


FIG. 2. Fate of multiple factors of the RLR signaling pathway during infection. HeLa R19 cells were mock infected or infected with CVB3, mengovirus (mengo), or mengo-Zn (M-Zn) at a multiplicity of infection of 50, and cells were lysed at the indicated times (h) p.i. Cell lysates were analyzed by SDS-PAGE, followed by immunoblotting using the indicated antibodies. Marker bands of the indicated size (in kDa) are indicated on the right side. Arrow with a narrow tail, full-length protein; arrowhead, putative cleavage products; arrow with a wide tail, known MAVS cleavage product from caspase-mediated cleavage. Data are representative of those from at least 3 independent experiments.

with our observation that the RLR pathway upstream of TBK1 phosphorylation remains intact in cells infected with these viruses (Fig. 1).

CVB3-induced MDA5, MAVS, and RIG-I cleavages are independent of caspase or proteasome activities. We noticed that the cleavage of RIG-I, MDA5, and MAVS in CVB3-infected cells coincided with PARP cleavage, resulting in an 89-kDa cleavage product (Fig. 2), the hallmark of apoptosis. It has been suggested that poliovirus and enterovirus 71 induce caspase-dependent MDA5 degradation (24, 25). Therefore, we asked whether caspases could be responsible for cleaving MDA5, MAVS, and/or RIG-I in CVB3-infected cells. To address this question, we chemically induced apoptosis in mock-infected cells using staurosporine (STS), a general kinase inhibitor. MDA5, MAVS, and RIG-I in mock- or STS-treated cells were analyzed by immunoblotting. STS induced potent caspase activation, as shown by PARP cleavage, as well as the appearance of the known caspase 3-mediated MAVS cleavage product of about 50 kDa (27). However, it did not lead to any detectable cleavage of MDA5, MAVS, or RIG-I like that observed in CVB3-infected cells (Fig. 3A), suggesting that caspases or the proteasome may not catalyze the infection-induced cleavage events reported here. To further demonstrate that MDA5 is not cleaved by caspases, we infected cells with CVB3 in the presence of a broad-spectrum caspase inhibitor, QVD-OPh (QVD). We also included a proteasome inhibitor, MG132, in a parallel experiment because efficient caspase activation like the one that we observed in CVB3-infected cells (Fig. 2) often leads to protein degradation via the proteasome system. QVD and MG132 both inhibited apoptosis, as demonstrated by significantly decreased PARP cleavage in treated cells (Fig. 3A). Under these conditions, CVB3 infection still induced MDA5, MAVS, and RIG-I cleavage to an extent similar to that in nontreated cells (Fig. 3A). Also, in an independent experiment where apoptosis was completely inhibited by QVD, efficient MDA5 cleavage induced by CVB3 infection was observed (Fig. 3B). Together with our STS data, these results indicate that the cleavage events of MDA5, MAVS, and RIG-I during CVB3 infection are not mediated by caspases or the proteasome.

Recombinant CVB3 proteinase 2A^{pro} induces MDA5 and MAVS cleavage, and 3C^{pro} induces RIG-I cleavage. Next, we asked whether the two viral proteinases 2A^{pro} and 3C^{pro} could be responsible for the cleavage events that we observed during CVB3 infection. Since these proteinases efficiently shut off host mRNA translation by cleaving eIF4G (29, 36, 37), their overexpression results in poor expression levels and severe cytotoxicity. Therefore, we chose to address this question using recombinant 2A^{pro} and 3C^{pro}. Native cell lysate was treated with recombinant 2A^{pro} or 3C^{pro} and subjected to immunoblotting analysis using antibodies against MDA5, MAVS, and RIG-I. To control for the activities of 2A^{pro} and 3C^{pro}, we also probed for eIF4G, which is known to be cleaved by 2A^{pro}- and 3C^{pro}-activated caspase 3 (29, 37, 38), and G3BP, which is cleaved by 3C^{pro} only (31). As clearly shown in Fig. 4, both proteinases were very active in our *in vitro* cleavage assay. Under these conditions, MDA5 and MAVS cleavages were observed in 2A^{pro}-treated samples, whereas RIG-I was cleaved in 3C^{pro}-treated lysate (Fig. 4). The cleavage products seen in the *in vitro* cleavage assay showed electrophoretic mobility identical to the mobility of the cleavage products from CVB3-infected cells (Fig. 4), demonstrating the relevance of our *in vitro* findings. In 3C^{pro}-treated samples, a putative MDA5 cleavage product of approximately 100 kDa was detected; however, this protein fragment was not consistently detected in *in vitro* cleavage assays with 3C^{pro}. More importantly, we never observed this cleavage product in CVB3-infected cells. These results suggest that the CVB3-induced cleavage of MDA5 and MAVS resulted from 2A^{pro} activity, whereas that of RIG-I resulted from 3C^{pro} activity.

As mentioned before, it has been reported that CVB3 3C^{pro} cleaves MAVS, resulting in an N-terminal cleavage product of 50 kDa, and a single amino acid substitution at position 148 (Q148A) was sufficient to prevent this cleavage (23). We also observed a 3C^{pro}-induced cleavage product of approximately 50 kDa when we prepared lysates from cells overexpressing a FLAG- and HA tagged MAVS protein (FLAG-MAVS-HA) (Fig. 5A). This cleavage product was also detectable using an antibody against the N-terminal FLAG tag but not one against the C-terminal HA tag, confirming that it is an N-terminal fragment of MAVS. When the reported cleavage-resistant mutant (Q148A) was overexpressed, the 3C^{pro}-mediated cleavage was no

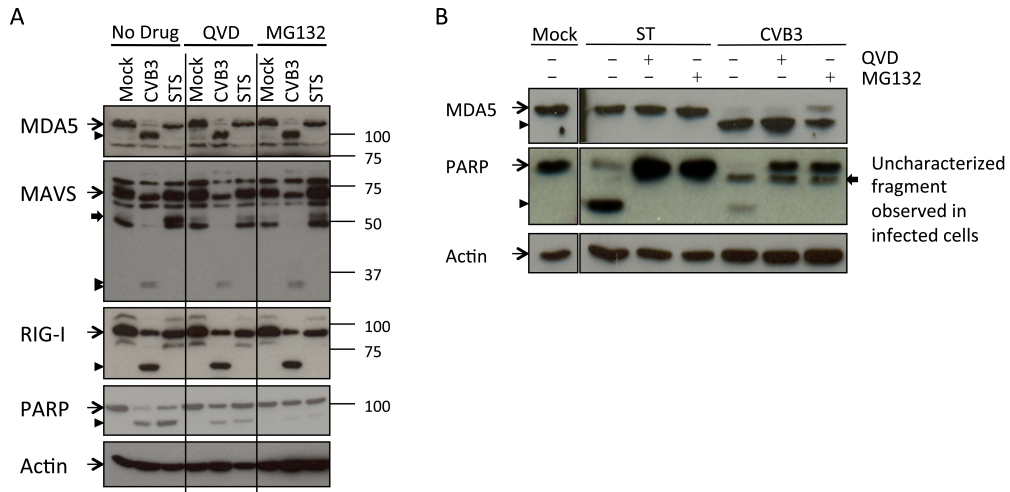


FIG. 3. Caspases and proteasomal proteases are not responsible for CVB3-induced MDA5, MAVS, or RIG-I cleavage. (A) HeLa R19 cells were mock infected, infected with CVB3 at a multiplicity of infection of 50 for 9 h, or treated with 2 μ M staurosporine (STS) for 6 h in the presence or absence of 10 μ M QVD or 10 μ M MG132. Cells were lysed, and the indicated proteins were analyzed by SDS-PAGE, followed by immunoblotting. Arrow with a narrow tail, full-length protein; arrowhead, putative cleavage products; arrow with a wide tail, known MAVS cleavage product from caspase-mediated cleavage. Marker bands of the indicated size (in kDa) are indicated on the right side. (B) HeLa R19 cells were mock treated, infected with CVB3 at a multiplicity of infection of 50 for 9 h, or treated with 2 μ M STS for 6 h in the presence or absence of 10 μ M QVD or 10 μ M MG132. Cells were lysed, and MDA5, PARP, and actin were analyzed by SDS-PAGE, followed by immunoblotting. Arrow with a narrow tail, full-length protein; arrowhead, putative cleavage products; arrow with a wide tail, additional PARP-derived fragment that was observed in CVB3-infected but not STS-treated cells and that persisted throughout CVB3 infection. Data are representative of those from at least 5 experiments.

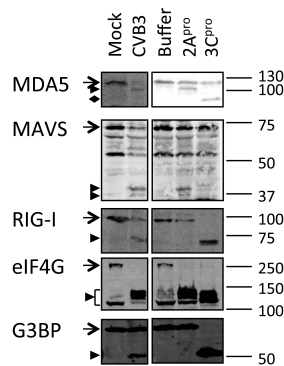


FIG. 4. Recombinant CVB3 2A^{pro} cleaves MDA5 and MAVS, while 3C^{pro} cleaves RIG-I. A native lysate of HeLa R19 cells was treated with recombinant CVB3 2A^{pro} or 3C^{pro} at room temperature overnight. The reaction mixtures were subjected to SDS-PAGE, followed by immunoblotting using antibodies against the indicated proteins. As controls, lysates from mock- and CVB3-infected (multiplicity of infection, 50; 8 h) cells were also included. Arrow, full-length protein; arrowhead, putative cleavage products; filled diamond, product obtained by cleavage of MDA5 by 3C^{pro} that is not seen in CVB3-infected cells. Marker bands of the indicated size (in kDa) are indicated on the right side. Data are representative of those from at least 3 experiments.

longer detectable (Fig. 5B), indicating that it is likely the same cleavage product reported by Mukherjee et al. (23). However, we did not observe this cleavage fragment from endogenous MAVS during CVB3 infection (Fig. 2 to 4), even when using the same antibody used in the previously published study (23) (data not shown).

The 2A^{pro}-mediated cleavage was readily detectable from both overexpressed MAVS (Fig. 5) and endogenous MAVS (Fig. 2 to 4), releasing two cleavage products (approximately 30 and 40 kDa) (Fig. 5). Using antibodies against tags at either terminus of overexpressed MAVS, we saw that the smaller cleavage product represented an N-terminal fragment, whereas the larger product was a C-terminal fragment (Fig. 5). These data suggest that MAVS is primarily cleaved by 2A^{pro} in CVB3-infected cells.

2A^{pro} mediates cleavage of MDA5 and MAVS, while 3C^{pro} cleaves RIG-I in infected cells. We further pursued experiments to confirm these results in the context of an infection. As 2A^{pro} and 3C^{pro} are both essential for CVB3 polyprotein processing, deletion mutations of these proteinases are lethal. Instead, we took advantage of the fact that wt mengovirus does not induce cleavage of RIG-I, MDA5, or MAVS (Fig. 2). By inserting CVB3 2A^{pro} or 3C^{pro} in front of the leader-coding region (i.e., at the extreme 5' terminus of the polyprotein-coding region) in the mengovirus genome, we could study the role of the CVB3 proteinases in the cleavage events during a normal picornavirus infection. These viruses, named M-2A(CVB3) and M-3C(CVB3), were used to infect cells, and RIG-I, MDA5, and MAVS cleavages were examined by immunoblotting. As shown before, wt mengovirus infection did not induce any changes in the integrity of these factors, whereas M-2A(CVB3) induced MDA5 and MAVS cleavage, and M-3C(CVB3) induced RIG-I cleavage (Fig. 6A). The cleavage products observed in M-2A(CVB3)- and M-3C(CVB3)-infected

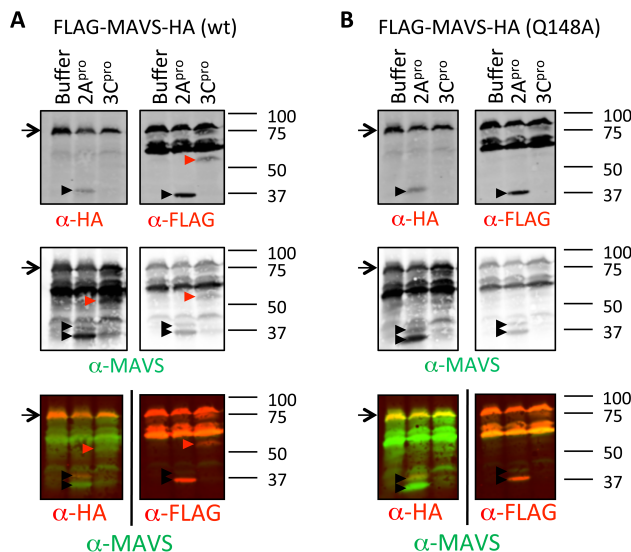


FIG. 5. Both 2A^{pro} and 3C^{pro} of CVB3 can cleave MAVS, but at different sites. Plasmids carrying FLAG-MAVS-HA (A) or FLAG-MAVS-HA (Q148A) (B) were transfected into cells and lysed 24 h later under native conditions. The native lysates were treated with recombinant 2A^{pro} or 3C^{pro} at room temperature overnight and analyzed by SDS-PAGE and immunoblotting using the indicated antibodies. Arrow, full-length protein; arrowhead, putative cleavage product. Marker bands of the indicated size (in kDa) are indicated on the right side of each panel. Data are representative of those from at least 2 experiments.

cells were exactly the same as those seen in CVB3-infected cells (Fig. 6A). We observed an additional band at about 90 kDa with the anti-RIG-I antibody in M-2A(CVB3)-infected cells (Fig. 6A). We never observed a cleavage product of this electrophoretic mobility in wt CVB3-infected cells, and this 90-kDa band was also absent in M-2A(CVB3)-infected cells in other experiments (Fig. 6B). As additional controls to confirm that the cleavages were the result of the proteinase activities of 2A^{pro} and 3C^{pro}, we also produced mutant mengoviruses carrying the catalytically inactive forms of 2A^{pro} (2A-C109A) and 3C^{pro} (3C-C147A). Infection with these viruses did not lead to cleavage of targets of 2A^{pro} or 3C^{pro} (Fig. 6B). These results, combined with our *in vitro* cleavage data, convincingly show that CVB3 induces MDA5 and MAVS cleavage via 2A^{pro} activity and RIG-I cleavage via 3C^{pro} activity.

Other enteroviruses also target MDA5 and MAVS by their 2A^{pro}s and RIG-I by their 3C^{pro}s.

We further asked whether the cleavage events that we observed here were unique to CVB3, a human enterovirus B (HEV-B) member, or are common to other enterovirus species as well. To this end, we produced mengoviruses carrying 2A^{pro} or 3C^{pro} from enterovirus 71 (EV71) and poliovirus (PV), belonging to HEV-A and HEV-C, respectively. Infections with these mutant viruses revealed that the 2A^{pro}s and 3C^{pro}s from both viruses induced MDA5 and RIG-I cleavage, respectively (Fig. 7A). The cleavage products found with these viruses were identical to the corresponding cleavage products observed in CVB3-infected cells (Fig. 6A). M-2A(EV71) and M-2A(PV) infections also induced MAVS cleavage, though M-2A(PV) infection resulted in a less prominent MAVS cleavage and a MAVS cleavage product pattern slightly different from that of CVB3 infection. The larger cleavage product (40 kDa) seemed to be identical to that from M-2A(CVB3)- and M-2A(EV71)-infected cells, but the smaller product (35 kDa) had a slower electrophoretic mobility than that from CVB3-infected cells (30 kDa) (Fig. 7A).

To investigate whether these cleavages also occur during a normal infection of enteroviruses, we infected cells with EV71 (strain BrCr) and analyzed MDA5, MAVS, and RIG-I by immunoblotting. Infection with EV71 induced the cleavage of all three factors similar to that seen in CVB3-infected cells (Fig. 7B). Together with data from the M-2A viruses, our results suggest that cleavage of RIG-I, MDA5, and MAVS may be a common phenomenon among enteroviruses.

DISCUSSION

The RLR signaling pathway is a crucial part of the innate antiviral response. Consequently, this pathway is targeted by numerous viruses from various families, including picornaviruses. However, our knowledge on how picornaviruses interfere with this pathway remains somewhat fragmented, since the reported studies each used a different panel of viruses and focused on only one factor of the pathway at a time. Here we performed the first comprehensive analysis of key factors of the RLR signaling pathway during enterovirus infections. Our data suggest that enteroviruses utilize their 2A^{pro}s to target MDA5 and MAVS and their 3C^{pro}s to cleave RIG-I. Consistent with these results, several studies have reported that IRF3 activation is severely inhibited during enterovirus infection (Fig. 1C) (23, 25, 27). Thus, cleavage of upstream factors of the RLR pathway is likely an evolutionarily conserved and advantageous mechanism to suppress IFN type I gene transcription. Meanwhile, it is worth noting that RLR pathway antagonization may not be the only evasion mechanism of enteroviruses. It is known that enteroviruses induce

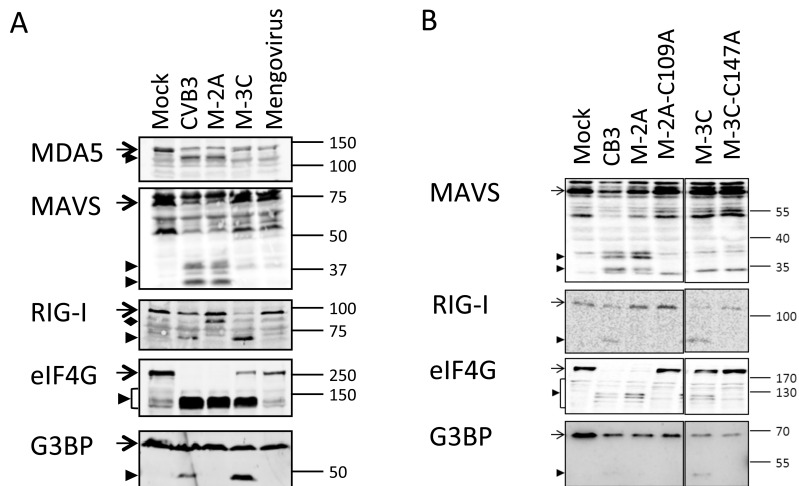


FIG. 6. MDA5, MAVS, and RIG-I cleavage in the context of an infection. (A) HeLa R19 cells were mock infected or infected with CVB3, mengovirus expressing CVB3 2A^{pro} or 3C^{pro} (M-2A and M-3C, respectively), or wt mengovirus at a multiplicity of infection of 50 for 8 h. Cells were lysed, and the indicated proteins were analyzed by SDS-PAGE, followed by immunoblotting. Arrow, full-length protein; arrowhead, putative cleavage products; filled diamond, product obtained by cleavage RIG-I by 2A^{pro} that is not seen in CVB3-infected cells. (B) HeLa R19 cells were mock infected or infected with CVB3, M-2A(CVB3), M-3C(CVB3), M-2A-C109A(CVB3), or M-3C-C147A(CVB3) at a multiplicity of infection of 50 for 8 h. Cells were lysed, and the indicated proteins were analyzed by SDS-PAGE followed by immunoblotting. Arrow, full-length protein; arrowhead, putative cleavage products. Marker bands of the indicated size (in kDa) are indicated on the right side of each panel. Data are representative of those from at least 3 experiments.

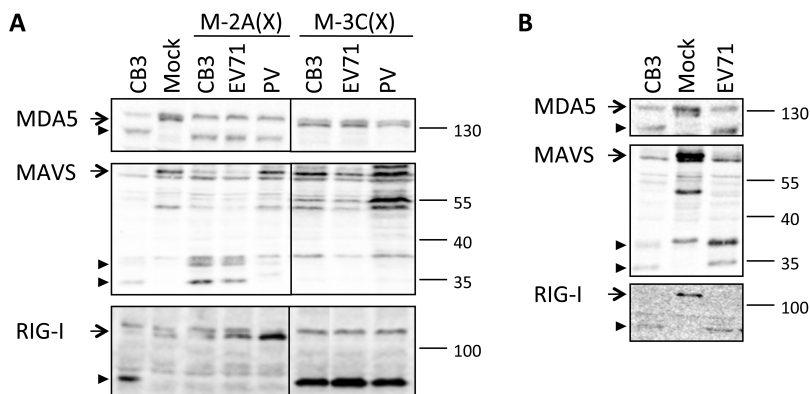


FIG. 7. MDA5, MAVS, and RIG-I cleavage by other enteroviruses. (A) HeLa R19 cells were mock infected or infected with CVB3, M-2A(CVB3), M-2A(EV71), M-2A(PV), M-3C(CVB3), M-3C(EV71), or M-3C(PV) at a multiplicity of infection of 50 for 8 h. Cell lysates were analyzed by SDS-PAGE, followed by immunoblotting using antibodies against the indicated proteins. (B) HeLa R19 cells were mock infected or infected with CVB3 or EV71 at a multiplicity of infection of 50 for 8 h. Cells lysates were analyzed as described for panel A. Arrow, full-length protein; arrowhead, putative cleavage product. Marker bands of the indicated size (in kDa) are indicated on the right side of each panel. Data are representative of those from at least 2 experiments.

a shutoff of host mRNA transcription and translation, which likely further limits the production of, among other factors, virus-induced cytokines, such as IFNs. To what extent the host shutoff contributes to suppressing IFN production is difficult to investigate, since enterovirus-induced host shutoff is also mediated by 2A^{pro} and 3C^{pro} (38–40), the same proteinases that cleave factors of the RLR-mediated IFN induction pathway, making it difficult to separately investigate the role of these phenomena.

MDA5, the receptor responsible for sensing picornavirus infection (16, 21), is cleaved during infection of CVB3 and EV71. Using recombinant CVB3 2A^{pro} and our M-2A viruses carrying 2A^{pro} of CVB3, EV71, or PV, we demonstrate that this cleavage can be mediated by all these 2A^{pro}s, indicating that this may be a common strategy by which enteroviruses inactivate MDA5. This seems to contradict previous reports that PV and EV71 induce caspase-mediated (and, in the case of PV, also proteasome-mediated) MDA5 degradation. However, in those studies, cells were first transfected with either poly(I:C) (24) or viral RNA (25) in order to upregulate MDA5 expression to a detectable level before infections were carried out. Pretreatments with these triggers induce IFN- α/β production, which, in turn, upregulates expression of interferon-stimulated genes, including MDA5. It is important to realize that IFN- α/β itself is known to potentiate cells to virus-induced apoptosis (41). Therefore, it is likely that in IFN- α/β primed virus-infected cells, MDA5 is degraded in a caspase-dependent manner. In this study, we investigated the fate of endogenous MDA5 during enterovirus infection of naive cells. We show convincingly that MDA5 cleavage during infection is not attributed to caspases or the proteasome but is attributed to the viral proteinase 2A^{pro}.

We also set out to identify the 2A^{pro} cleavage site in MDA5 by infecting cells overexpressing MDA5 mutants carrying substitutions at potential 2A^{pro} recognition sites. However, infection following protein overexpression proved to be very inefficient in our hands (i.e., viruses preferably infect nontransfected cells) (data not shown). Another approach to test potential cleavage-resistant MDA5 mutants was to use lysates from cells overexpressing tagged MDA5 mutants in our *in vitro* cleavage assay. However, under conditions where we did observe cleavage of endogenous MDA5 or MAVS or overexpressed MAVS (e.g., in the Q148A mutant), we did not find any cleavage product of the overexpressed MDA5 (as detected by antibodies against terminal epitope tags) (data not shown). In addition, no cleavage of recombinant MDA5 purified from mammalian cells was observed (data not shown). It eludes us why overexpressed MDA5 was so poorly cleaved by recombinant 2A^{pro}, and unfortunately, it did not allow us to further investigate and identify the 2A^{pro} cleavage site in MDA5.

In addition to MDA5, the downstream adaptor molecule MAVS was also cleaved in a 2A^{pro}-dependent manner during enterovirus infection. CVB3 and EV71 induced identical MAVS cleavage products. These products were also reasonably similar to what was previously observed when *in vitro*-translated MAVS was treated with CVB3 2A^{pro} (27), further supporting our conclusion that this is a 2A^{pro}-mediated cleavage. PV 2A^{pro} also led to MAVS cleavage, suggesting a similar cleavage mechanism, though the cleavage products were slightly different from those induced by CVB3. While this paper was in preparation, it was shown in another study that EV71 2A^{pro} cleaves MAVS at three distinct positions, namely, Q209, Q251, and Q265, leading to the production of two cleavage products of 30 to 40 kDa (28). We show here that both CVB3 and EV71 induce identical MAVS cleavage patterns, yielding two cleavage products

similar in size to those reported in that study, leading us to conclude that CVB3 2A^{pro} likely also cleaves MAVS at these positions. Furthermore, 2A^{pro} of PV also targeted MAVS, though the size of one of the cleavage products was slightly different from that observed in CVB3- or EV71-infected cells. It is not at odds with the finding that 2A^{pro}s from different enteroviruses cleave the same target protein at various positions. It has previously been shown that 2A^{pro}s of human rhinoviruses cleave nucleoporins at different sites, most likely due to sequence diversity in 2A^{pro} (42). Moreover, caspase-mediated MAVS cleavage has been suggested for HRV1A (27). We did not observe the caspase-mediated MAVS cleavage product during CVB3 infection in HeLa R19 cells or cells of other human cell lines, such as HeLa Kyoto and Huh7 (data not shown). Together, our data show that the 2A^{pro}s from three different enterovirus species all target not only MDA5 but also MAVS during infection. The evolutionary conservation of these activities suggests that this is probably highly advantageous for enterovirus replication.

Although RIG-I is dispensable in sensing picornaviruses (16), it has been reported to be cleaved during infection of a few enteroviruses, such as PV, echovirus, and HRV16, mostly likely via their 3C^{pro}s. Here we provide data that two additional enteroviruses, namely, CVB3 and EV71, also cleave RIG-I via their 3C^{pro}s. Unlike the various 2A^{pro} cleavage sites in MAVS, the yet unidentified site in RIG-I cleaved by 3C^{pro} seems to be well conserved across this panel of different enteroviruses, each yielding a putative cleavage product of approximately 70 kDa (26).

Cleavage of RIG-I, MDA5, and MAVS does not appear to be common to all picornaviruses. In this study, we also examined the fate of factors involved in the RLR pathway during infection with mengovirus, a species of EMCV of the *Cardiovirus* genus. We show that MDA5, MAVS, RIG-I, LGP2, and TBK1 all remained intact in cells infected with either wt mengovirus, which effectively suppresses the IFN- α/β response, or mengo-Zn, which induces high levels of IFN- α/β . Furthermore, equal levels of TBK1 activation were observed in cells infected with both wt mengovirus and mengo-Zn, indicating that factors upstream of TBK1 are not targeted by mengovirus. These results may seem to contradict earlier reports that MDA5 and RIG-I are also cleaved in mengovirus-infected cells (24). However, MDA5 cleavage was observed only in cells pretreated with poly(I:C) (24), which, as mentioned before, potentiates cells for virus-induced apoptosis and likely results in caspase-mediated MDA5 cleavage. In agreement with our observation that MDA5 is not cleaved in mengovirus-infected cells, MDA5 also remained intact during EMCV infection without poly(I:C) pretreatment in an independent study (43). Two reports have shown that RIG-I, which is dispensable for EMCV RNA recognition (16), is targeted by EMCV. Barral et al. reported that RIG-I is cleaved in EMCV-infected cells and implicated 3C^{pro} as the responsible proteinase since the cleavage product (of approximately 70 kDa) was similar to the cleavage product released by 3C^{pro} of PV (26). Another study showed a gradual decrease of RIG-I during EMCV infection which could be prevented by a caspase inhibitor, indicating that this is caspase-mediated degradation of RIG-I (43). These authors also demonstrated that recombinant EMCV 3C^{pro} can cleave RIG-I *in vitro*, resulting in a putative cleavage product of approximately 50 kDa. However, this RIG-I fragment was not observed during a normal EMCV infection (43), suggesting that it may be an artifact of *in vitro* study, similar to the MDA5 cleavage that we observed with CVB3 3C^{pro} in our own *in vitro* cleavage experiments.

The exact mechanism that EMCV uses to suppress the IFN- α/β response remains to be clarified. As indicated above, this blockade likely lies between TBK1 activation and IRF3 phosphorylation.

It is known that TBK1 must form a complex with other kinases, such as the noncanonical I κ B kinase IKK-epsilon, in order to phosphorylate its substrate, IRF3 (44–46). The assembly of a functional TBK1 complex requires not only phosphorylation of TBK1 at serine 172 but also other posttranslational modifications of IKK-epsilon and the assistance of scaffold proteins, such as NAP1 and SINTBAD (47). It is possible that mengovirus interferes with the correct assembly of the TBK1 complex to terminate the signal transduction. Alternatively, IFN- α/β shutdown may be a secondary effect of the so-called nuclear-cytoplasmic trafficking disorder that is induced by mengovirus leader protein (48). This causes an unregulated cargo transport between the nucleus and cytoplasm and possibly interferes with IRF3 activation, since this transcription factor must shuttle between these two compartments. Intriguingly, the same mutations in the leader protein (e.g., those in the Zn finger domain) simultaneously inactivate its activities in both IFN- α/β suppression (16, 22, 34) and the induction of the nuclear-cytoplasmic trafficking disorder (48), suggesting that there may be a link between these two phenomena. Future research is called upon to investigate the exact mechanism of IFN antagonization by mengovirus.

In short, our data show that several enteroviruses target MDA5, MAVS, and RIG-I in infected cells and that all do so via the same mechanisms (i.e., 2A^{pro} targeting MDA5 and MAVS and 3C^{pro} targeting RIG-I). These cleavage events likely account for the lack of an IFN- α/β response in enterovirus-infected cells. Our data that TBK1 phosphorylations and, thus, activation are inhibited in CVB3-infected cells indicate that the pathway is shut down upstream of TBK1. The fact that the RLR pathway is targeted at multiple steps during infection makes it technically challenging to demonstrate the biological consequence of these cleavage events. One would have to simultaneously reconstitute a minimum of three factors, MDA5, MAVS, and RIG-I, to, it is hoped, study the effect of an intact RLR signaling pathway on virus replication. Additionally, enteroviruses may also employ additional mechanisms to ensure effective IFN- α/β suppression. For instance, enterovirus 2A^{pro} is also known to cause nuclear-cytoplasmic trafficking disorder (49), possibly interfering with IRF3 activation, and, thereby, further ensure a total shut off of the IFN- α/β response in infected cells. Although a clear contribution of these phenomena to IFN- α/β inhibition remains to be established, this study provides important new insights into the potential roles of enterovirus proteinases in suppressing the RLR-mediated antiviral pathway.

ACKNOWLEDGMENTS

We acknowledge Rolf Hilgenfeld (University of Lübeck) for the kind gift of recombinant CVB3 3C^{pro}. Q.F. and S.V.H. are supported by Mosaic grants (NWO-017.006.043 and NWO-017.002.025, respectively), M.A.L. is supported by a Rubicon grant (NWO-825.11.022), and F.J.M.V.K. is supported by an ECHO grant (NWO-CW-700.59.007), all from the Netherlands Organization for Scientific Research (NWO). P.B.F. was funded by NIH/NCI grant R01 CA097318 and the VCU MCC. P.B.F. holds the Thelma Newmeyer Corman Chair in Cancer Research in the MCC.

REFERENCES

1. Stark GR, Darnell JEJ. 2012. The JAK-STAT pathway at twenty. *Immunity* 36:503–514. <http://dx.doi.org/10.1016/j.immuni.2012.03.013>.

2. Goubau D, Deddouche S, Reis E, Sousa C. 2013. Cytosolic sensing of viruses. *Immunity* 38:855–869. <http://dx.doi.org/10.1016/j.immuni.2013.05.007>.
3. Yoneyama M, Kikuchi M, Natsukawa T, Shinobu N, Imaizumi T, Miyagishi M, Taira K, Akira S, Fujita T. 2004. The RNA helicase RIG-I has an essential function in double-stranded RNA-induced innate antiviral responses. *Nat. Immunol.* 5:730–737. <http://dx.doi.org/10.1038/ni1087>.
4. Kang D, Gopalkrishnan RV, Wu Q, Jankowsky E, Pyle AM, Fisher PB. 2002. mda-5: an interferon-inducible putative RNA helicase with doublestranded RNA-dependent ATPase activity and melanoma growthsuppressive properties. *Proc. Natl. Acad. Sci. U. S. A.* 99:637–642. <http://dx.doi.org/10.1073/pnas.022637199>.
5. Kang D-C, Gopalkrishnan RV, Lin L, Randolph A, Valerie K, Pestka S, Fisher PB. 2004. Expression analysis and genomic characterization of human melanoma differentiation associated gene-5, mda-5: a novel type I interferon-responsive apoptosis-inducing gene. *Oncogene* 23:1789–1800. <http://dx.doi.org/10.1038/sj.onc.1207300>.
6. Andrejeva J, Childs KS, Young DF, Carlos TS, Stock N, Goodbourn S, Randall RE. 2004. The V proteins of paramyxoviruses bind the IFN inducible RNA helicase, mda-5, and inhibit its activation of the IFN-beta promoter. *Proc. Natl. Acad. Sci. U. S. A.* 101:17264–17269. <http://dx.doi.org/10.1073/pnas.0407639101>.
7. Yoneyama M, Kikuchi M, Matsumoto K, Imaizumi T, Miyagishi M, Taira K, Foy E, Loo YM, Gale M, Jr, Akira S, Yonehara S, Kato A, Fujita T. 2005. Shared and unique functions of the DExD/H-box helicases RIG-I, MDA5, and LGP2 in antiviral innate immunity. *J. Immunol.* 175: 2851–2858. <http://www.jimmunol.org/content/175/5/2851.full.pdf>.
8. Seth RB, Sun L, Ea C-KK, Chen ZJ. 2005. Identification and characterization of MAVS, a mitochondrial antiviral signaling protein that activates NF-kappaB and IRF 3. *Cell* 122:669–682. <http://dx.doi.org/10.1016/j.cell.2005.08.012>.
9. Xu LG, Wang YY, Han KJ, Li LY, Zhai Z, Shu HB. 2005. VISA is an adapter protein required for virus-triggered IFN-beta signaling. *Mol. Cell* 19:727–740. <http://dx.doi.org/10.1016/j.molcel.2005.08.014>.
10. Kawai T, Takahashi K, Sato S, Coban C, Kumar H, Kato H, Ishii KJ, Takeuchi O, Akira S. 2005. IPS-1, an adaptor triggering RIG-I- and Mda5-mediated type I interferon induction. *Nat. Immunol.* 6:981–988. <http://dx.doi.org/10.1038/ni1243>.
11. Meylan E, Curran J, Hofmann K, Moradpour D, Binder M, Bartenschlager R, Tschopp J. 2005. Cardif is an adaptor protein in the RIG-I antiviral pathway and is targeted by hepatitis C virus. *Nature* 437:1167–1172. <http://dx.doi.org/10.1038/nature04193>.
12. Baum A, Sachidanandam R, García-Sastre A. 2010. Preference of RIG-I for short viralRNAmolecules in infected cells revealed by next-generation sequencing. *Proc. Natl. Acad. Sci. U. S. A.* 107:16303–16308. <http://dx.doi.org/10.1073/pnas.1005077107>.
13. Chang T-H, Liao C-L, Lin Y-L. 2006. Flavivirus induces interferon-beta gene expression through a pathway involving RIG-I-dependent IRF-3 and PI3K-dependent NF-kappaB activation. *Microbes Infect.* 8:157–171. <http://dx.doi.org/10.1016/j.micinf.2005.06.014>.
14. Plumet S, Herschke F, Bourhis J-M, Valentin H, Longhi S, Gerlier D. 2007. Cytosolic 5'-triphosphate ended viral leader transcript of measles virus as activator of the RIG I-mediated

- interferon response. PLoS One 2:e279. <http://dx.doi.org/10.1371/journal.pone.0000279>.
15. Malathi K, Saito T, Crochet N, Barton DJ, Gale M, Jr, Silverman RH. 2010. RNase L releases a small RNA from HCV RNA that refolds into a potent PAMP. RNA 16:2108–2119. <http://dx.doi.org/10.1261/rna.2244210>.
16. Feng Q, Hato SV, Langereis MA, Zoll J, Virgen-Slane R, Peisley A, Hur S, Semler BL, van Rij RP, van Kuppeveld FJM. 2012. MDA5 detects the double-stranded RNA replicative form in picornavirus-infected cells. Cell Rep. 2:1187–1196. <http://dx.doi.org/10.1016/j.celrep.2012.10.005>.
17. McCartney SA, Thackray LB, Gitlin L, Gilfillan S, Virgin HW, Colonna M. 2008. MDA-5 recognition of a murine norovirus. PLoS Pathog. 4:e1000108. <http://dx.doi.org/10.1371/journal.ppat.1000108>.
18. Roth-Cross JK, Bender SJ, Weiss SR. 2008. Murine coronavirus mouse hepatitis virus is recognized by MDA5 and induces type I interferon in brain macrophages/microglia. J. Virol. 82:9829–9838. <http://dx.doi.org/10.1128/JVI.01199-08>.
19. Hornung V, Ellegast J, Kim S, Brzózka K, Jung A, Kato H, Poeck H, Akira S, Conzelmann K-KK, Schlee M, Endres S, Hartmann G. 2006. 5'-Triphosphate RNA is the ligand for RIG-I. Science 314:994–997. <http://dx.doi.org/10.1126/science.1132505>.
20. Schlee M, Roth A, Hornung V, Hagmann CA, Wimmenauer V, Barchet W, Coch C, Janke M, Mihailovic A, Wardle G, Juraneck S, Kato H, Kawai T, Poeck H, Fitzgerald KA, Takeuchi O, Akira S, Tuschl T, Latz E, Ludwig J, Hartmann G. 2009. Recognition of 5= triphosphate by RIG-I helicase requires short blunt double-stranded RNA as contained in panhandle of negative-strand virus. Immunity 31:25–34. <http://dx.doi.org/10.1016/j.immuni.2009.05.008>.
21. Triantafyllou K, Vakakis E, Kar S, Richer E, Evans GL, Triantafyllou M. 2012. Visualisation of direct interaction of MDA5 and the dsRNA replicative intermediate form of positive strand RNA viruses. J. Cell Sci. 125: 4761–4769. <http://dx.doi.org/10.1242/jcs.103887>.
22. Hato SV, Ricour C, Schulte BM, Lanke KH, de Bruijini M, Zoll J, Melchers WJ, Michiels T, van Kuppeveld FJ. 2007. The mengovirus leader protein blocks interferon-alpha/beta gene transcription and inhibits activation of interferon regulatory factor 3. Cell. Microbiol. 9:2921–2930. <http://dx.doi.org/10.1111/j.1462-5822.2007.01006.x>.
23. Mukherjee A, Morosky SA, Delorme-Axford E, Dybdahl-Sissoko N, Oberste MS, Wang T, Coyne CB. 2011. The coxsackievirus B 3C protease cleaves MAVS and TRIF to attenuate host type I interferon and apoptotic signaling. PLoS Pathog. 7:e1001311. <http://dx.doi.org/10.1371/journal.ppat.1001311>.
24. Barral PM, Morrison JM, Drahos J, Gupta P, Sarkar D, Fisher PB, Racaniello VR. 2007. MDA-5 is cleaved in poliovirus-infected cells. J. Virol. 81:3677–3684. <http://dx.doi.org/10.1128/JVI.01360-06>.
25. Kuo R-L, Kao L-T, Lin S-J, Wang RY-L, Shih S-R. 2013. MDA5 plays a crucial role in enterovirus 71 RNA-mediated IRF3 activation. PLoS One 8:e63431. <http://dx.doi.org/10.1371/journal.pone.0063431>.
26. Barral PM, Sarkar D, Fisher PB, Racaniello VR. 2009. RIG-I is cleaved during picornavirus infection. Virology 391:171–176. <http://dx.doi.org/10.1016/j.virol.2009.06.045>.

27. Drahos J, Racaniello VR. 2009. Cleavage of IPS-1 in cells infected with human rhinovirus. *J. Virol.* 83:11581–11587. <http://dx.doi.org/10.1128/JVI.01490-09>.
28. Wang B, Xi X, Lei X, Zhang X, Cui S, Wang J, Jin Q, Zhao Z. 2013. Enterovirus 71 protease 2Apro targets MAVS to inhibit anti-viral type I interferon responses. *PLoS Pathog.* 9:e1003231. <http://dx.doi.org/10.1371/journal.ppat.1003231>.
29. Liebig HD, Ziegler E, Yan R, Hartmuth K, Klump H, Kowalski H, Blaas D, Sommergruber W, Frasel L, Lamphear B. 1993. Purification of two picornaviral 2A proteinases: interaction with eIF-4 gamma and influence on *in vitro* translation. *Biochemistry* 32:7581–7588. <http://dx.doi.org/10.1021/bi00080a033>.
30. Sommergruber W, Ahorn H, Klump H, Seipelt J, Zoephel A, Fessl F, Krystek E, Blaas D, Kuechler E, Liebig HD. 1994. 2A proteinases of coxsackie- and rhinovirus cleave peptides derived from eIF-4 gamma via a common recognition motif. *Virology* 198:741–745. <http://dx.doi.org/10.1006/viro.1994.1089>.
31. White JP, Cardenas AM, Marissen WE, Lloyd RE. 2007. Inhibition of cytoplasmic mRNA stress granule formation by a viral proteinase. *Cell Host Microbe* 2:295–305. <http://dx.doi.org/10.1016/j.chom.2007.08.006>.
32. Barral PM, Sarkar D, Su Z, Barber GN, DeSalle R, Racaniello VR, Fisher PB. 2009. Functions of the cytoplasmic RNA sensors RIG-I and MDA-5: key regulators of innate immunity. *Pharmacol. Ther.* 124:219–234. <http://dx.doi.org/10.1016/j.pharmthera.2009.06.012>.
33. Kuyumcu-Martinez NM, Joachims M, Lloyd RE. 2002. Efficient cleavage of ribosome-associated poly(A)-binding protein by enterovirus 3C protease. *J. Virol.* 76:2062–2074. <http://dx.doi.org/10.1128/jvi.76.5.2062-2074.2002>.
34. Zoll J, Melchers WJG, Galama JMD, van Kuppeveld FJM. 2002. The mengovirus leader protein suppresses alpha/beta interferon production by inhibition of the iron/ferritin-mediated activation of NF-kB. *J. Virol.* 76:9664–9672. <http://dx.doi.org/10.1128/JVI.76.19.9664-9672.2002>.
35. Zhao W. 2013. Negative regulation of TBK1-mediated antiviral immunity. *FEBS Lett.* 587:542–548. <http://dx.doi.org/10.1016/j.febslet.2013.01.052>.
36. Chau DHW, Yuan J, Zhang H, Cheung P, Lim T, Liu Z, Sall A, Yang D. 2007. Coxsackievirus B3 proteases 2A and 3C induce apoptotic cell death through mitochondrial injury and cleavage of eIF4GI but not DAP5/p97/NAT1. *Apoptosis* 12:513–524. <http://dx.doi.org/10.1007/s10495-006-0013-0>.
37. Zhang B, Morace G, Gauss-Müller V, Kusov Y. 2007. Poly(A) binding protein, C-terminally truncated by the hepatitis A virus proteinase 3C, inhibits viral translation. *Nucleic Acids Res.* 35:5975–5984. <http://dx.doi.org/10.1093/nar/gkm645>.
38. Marissen WE, Lloyd RE. 1998. Eukaryotic translation initiation factor 4G is targeted for proteolytic cleavage by caspase 3 during inhibition of translation in apoptotic cells. *Mol. Cell. Biol.* 18:7565–7574.
39. Joachims M, Van Breugel PC, Lloyd RE. 1999. Cleavage of poly(A)-binding protein by

- enterovirus proteases concurrent with inhibition of translation in vitro. *J. Virol.* 73:718–727.
40. Yalamanchili P, Harris K, Wimmer E, Dasgupta A. 1996. Inhibition of basal transcription by poliovirus: a virus-encoded protease (3C_{pro}) inhibits formation of TBP-TATA box complex in vitro. *J. Virol.* 70:2922–2929.
41. Balachandran S, Roberts PC, Kipperman T, Bhalla KN, Compans RW, Archer DR, Barber GN. 2000. Alpha/beta interferons potentiate virus-induced apoptosis through activation of the FADD/caspase-8 death signaling pathway. *J. Virol.* 74:1513–1523. <http://dx.doi.org/10.1128/JVI.74.3.1513-1523.2000>.
42. Watters K, Palmenberg AC. 2011. Differential processing of nuclear pore complex proteins by rhinovirus 2A proteases from different species and serotypes. *J. Virol.* 85:10874–10883. <http://dx.doi.org/10.1128/JVI.00718-11>.
43. Papon L, Oteiza A, Imaizumi T, Kato H, Brocchi E, Lawson TG, Akira S, Mechetti N. 2009. The viral RNA recognition sensor RIG-I is degraded during encephalomyocarditis virus (EMCV) infection. *Virology* 393:311–318. <http://dx.doi.org/10.1016/j.virol.2009.08.009>.
44. Hemmi H, Takeuchi O, Sato S, Yamamoto M, Kaisho T, Sanjo H, Kawai T, Hoshino K, Takeda K, Akira S. 2004. The roles of two I B kinase-related kinases in lipopolysaccharide and double stranded RNA signaling and viral infection. *J. Exp. Med.* 199:1641–1650. <http://dx.doi.org/10.1084/jem.20040520>.
45. Fitzgerald KA, McWhirter SM, Faia KL, Rowe DC, Latz E, Golenbock DT, Coyle AJ, Liao S-MM, Maniatis T. 2003. IKKepsilon and TBK1 are essential components of the IRF3 signaling pathway. *Nat. Immunol.* 4:491–496. <http://dx.doi.org/10.1038/ni921>.
46. Sharma S, ten Oever BR, Grandvaux N, Zhou G-P, Lin R, Hiscott J. 2003. Triggering the interferon antiviral response through an IKK-related pathway. *Science* 300:1148–1151. <http://dx.doi.org/10.1126/science.1081315>.
47. Chau T-L, Gioia R, Gatot J-S, Patrascu F, Carpentier I, Chapelle J-P, O’Neill L, Beyaert R, Piette J, Chariot A. 2008. Are the IKKs and IKK-related kinases TBK1 and IKK-epsilon similarly activated? *Trends Biochem. Sci.* 33:171–180. <http://dx.doi.org/10.1016/j.tibs.2008.01.002>.
48. Lidsky PV, Hato S, Bardina MV, Aminev AG, Palmenberg AC, Sheval EV, Polyakov VY, van Kuppeveld FJ, Agol VI. 2006. Nucleocytoplasmic traffic disorder induced by cardioviruses. *J. Virol.* 80:2705–2717. <http://dx.doi.org/10.1128/JVI.80.6.2705-2717.2006>.
49. Belov G, Lidsky P, Mikitas O, Egger D, Lukyanov K, Bienz K, Agol V. 2004. Bidirectional increase in permeability of nuclear envelope upon poliovirus infection and accompanying alterations of nuclear pores. *J. Virol.* 78:10166–10177. <http://dx.doi.org/10.1128/JVI.78.18.10166-10177.2004>.

Chapter 5

MDA5 Localizes to Stress Granules, but This Localization Is Not Required for the Induction of Type I Interferon

Martijn A. Langereis, Qian Feng, Frank J. van Kuppeveld

Department of Medical Microbiology, Radboud University Nijmegen Medical Centre,
Nijmegen Centre for Molecular Life Sciences & Nijmegen Institute for Infection,
Inflammation and Immunology, Nijmegen, The Netherlands.
Virology Division, Department of Infectious Diseases and Immunology, Faculty of Veterinary
Medicine, Utrecht University, Utrecht, The Netherlands.

Journal of Virology. 2013. 87(11):6314-25.

ABSTRACT

Virus infection can initiate a type I interferon (IFN- α/β) response via activation of the cytosolic RNA sensors retinoic acid-inducible gene-I (RIG-I) and melanoma differentiation-associated gene 5 (MDA5). Furthermore, it can activate kinases that phosphorylate eukaryotic translation initiation factor 2 α (eIF2 α), which leads to inhibition of (viral) protein translation and formation of stress granules (SG). Most viruses have evolved mechanisms to suppress these cellular responses. Here, we show that a mutant mengovirus expressing an inactive leader (L) protein, which we have previously shown to be unable to suppress IFN- α/β , triggered SG formation in a protein kinase R (PKR)-dependent manner. Furthermore, we show that infection of cells that are defective in SG formation yielded higher viral RNA levels, suggesting that SG formation acts as an antiviral defense mechanism. Since the induction of both IFN- α/β and SG is suppressed by mengovirus L, we set out to investigate a potential link between these pathways. We observed that MDA5, the intracellular RNA sensor that recognizes picornaviruses, localized to SG. However, activation of the MDA5 signaling pathway did not trigger and was not required for SG formation. Moreover, cells that were unable to form SG - by protein kinase R (PKR) depletion, using cells expressing a nonphosphorylatable eIF2 α protein, or by drug treatment that inhibits SG formation - displayed a normal IFN- α/β response. Thus, although MDA5 localizes to SG, this localization seems to be dispensable for induction of the IFN- α/β pathway.

INTRODUCTION

Every nucleated cell in our bodies is equipped with a number of complex systems to guard against invading pathogens. The initial step of this protection is the recognition of the invaders by specialized sensors, the so-called pattern recognition receptors (PRRs). These specialized sensors detect certain pathogen-associated molecular patterns (PAMPs) that are “non-self” to the cell. Recognition of viral PAMPs by PRRs activates downstream signaling pathways and the production of effector proteins to combat viral infection. The RIG-I-like receptors (RLRs) are a group of cytoplasmic PRRs that belong to the DExD/H-box RNA helicase family and recognize non-self RNA motifs. This RLR family encompasses retinoic acid-inducible gene-I (RIG-I), melanoma differentiation-associated gene 5 (MDA5), and laboratory of genetics and physiology 2 (LGP2). RIG-I recognizes RNA containing 5'-triphosphate (1) as well as relatively small (2.0-kb) doublestranded RNA (dsRNA) or base-paired RNA molecules (2, 3). MDA5 recognizes long (2.0-kb) dsRNA by a mechanism that is still poorly understood (4, 5). Recognition of these PAMPs by RIG-I or MDA5 leads to ubiquitin-induced oligomerization (6) and the interaction with and subsequent aggregation of mitochondrial antiviral signaling protein (MAVS) on mitochondria (7). MAVS acts as a signaling hub that results in activation of the I κ B kinase epsilon (IKK- ϵ) and TANK-binding kinase 1 (TBK1) complex as well as the I κ B kinase beta (IKK- β) complex. These kinase complexes phosphorylate transcription factors IRF3 and NF- κ B, respectively, resulting in the transcription of type I interferon (IFN- α/β) genes and other proinflammatory cytokines (8). The production and secretion of IFN- α/β play a key role in the implementation of an antiviral state that restricts virus replication in infected cells as well as in neighboring cells.

Another cellular defense mechanism that limits virus replication is the stress response pathway (for two excellent reviews, see references 9 and 10). Cells react to several types of stress by phosphorylating eukaryotic translation initiation factor 2 α (eIF2 α) at serine 51, thereby rendering eIF2 α inactive and halting cap-dependent translation (11). The stalled translation preinitiation mRNA complexes — together with aggregated prion-like T-cell-restricted intracellular antigen 1 (TIA1), TIA1-related protein (TIAR), Ras-GAP SH3 domain binding protein (G3BP), and several other proteins — form the cytoplasmic stress granules (SG) (12). Four kinases are known to phosphorylate eIF2 α upon encountering different forms of cellular stress. Heme-regulated eIF2 α kinase (HRI) is predominantly expressed in erythroid cells and is activated when heme concentrations decline (13). General control nonrepressed 2 (GCN2) is a ubiquitously expressed kinase that halts protein translation in amino acid-starved cells (14). Cytosolic protein kinase R (PKR) and PKR-like endoplasmic reticulum (ER)-localized eIF2 α kinase (PERK) phosphorylate eIF2 α upon recognition of non-self RNA (15, 16) and under conditions of ER stress (17), respectively. The latter two kinases are frequently activated during virus infection. Vaccinia virus, orthoreovirus, respiratory syncytial virus, rotavirus, murine cytomegalovirus, and reovirus all activate a cellular stress response via PKR, while several coronaviruses, vesicular stomatitis virus, Epstein-Barr virus, and human cytomegalovirus activate PERK (9, 10). In cells infected with Sindbis virus, SG are formed in a GCN2-dependent manner (18).

For some viruses, it has been reported that SG induction is associated with increased virus replication (19, 20). Recently, the group of Bartenschlager showed that hepatitis C virus induces a dynamic assembly/disassembly of SG, which correlated with the PKR-mediated phosphorylation and protein phosphatase 1-mediated dephosphorylation of eIF2 α (21). This

oscillation prevents cell death caused by prolonged translational shutoff and thereby allows chronic infection of cells. In most cases, however, the formation of SG has a negative effect on virus fitness (10). Several mechanisms have been proposed to explain how SG formation limits virus replication. Induction of the stress pathway results in the inhibition of cap-dependent translation and thereby also viral protein synthesis. Additionally, viral mRNA transcripts that are translated in a cap-independent manner can be constrained in these granules and as a result can exclude them from translation (22). Apart from viral RNA, cellular factors essential for viral RNA translation and replication can also be trapped in SG (23, 24). Therefore, many viruses have evolved mechanisms to counteract SG formation.

The family *Picornaviridae* consists of a large number of small RNA viruses. They possess a single-stranded genome of positive polarity with a length of 7.5 to 8.5 kb. The viral genome has a single open reading frame that codes for a large polyprotein, which is processed by viral proteases into the structural and nonstructural proteins. During viral RNA replication, a fully complementary dsRNA product is synthesized that has recently been identified as the ligand that activates MDA5 (25). Members of the genera *Enterovirus*, represented by important human pathogens such as poliovirus, coxsackieviruses (CV), and rhinoviruses, circumvent this induction of IFN- α/β by degrading MDA5 via the proteasome degradation pathway and by cleaving downstream signaling proteins by viral proteases 2A^{pro} and 3C^{pro} (26). Additionally, poliovirus actively reverses the formation of SG by cleaving the essential component G3BP (27).

Viruses that belong to the *Cardiovirus* genus, such as Theiler's murine encephalomyelitis virus (TMEV), encephalomyocarditis virus (EMCV), and the recently identified human-tropic Saffold virus (SAFV), also efficiently suppress IFN- α/β induction (28–31). The cardiovirus leader (L) protein plays a major role in antagonizing the IFN- α/β induction. In addition, L modulates nucleocytoplasmic trafficking and suppresses apoptosis (32). Mutations in L equally affect these different activities, suggesting that they are linked. However, the mechanism of action of L remains to be established.

Interestingly, a recent report showed that TMEV L also represses the formation of SG (23). Strikingly, nonstructural protein 1 (NS1) of influenza A virus, a well-known IFN- α/β antagonist (33), was also recently shown to inhibit SG formation (34). The observation that two independent viral IFN- α/β antagonists also block formation of SG suggests that a link between these two antiviral pathways may exist.

Here, we present a comprehensive analysis of SG induction upon infection of cells with mengovirus, a strain of EMCV. We show that a mutant mengovirus with a compromised L, but not wild-type (wt) virus, induces SG formation in a PKR-dependent manner. Moreover, we demonstrate that MDA5 is recruited to SG in cells infected with mutant mengovirus as well as by other stress stimuli. The importance of MDA5 localization to these SG for induction of IFN- α/β is investigated in detail.

MATERIALS AND METHODS

Chemical inhibitors and RNA ligands. Emetine, cycloheximide, and puromycin were purchased

at Sigma-Aldrich and used at a final concentration of 10 µg/ml (emetine and cycloheximide) and 20 µg/ml (puromycin). The PKR inhibitor (PKRi) was purchased at Merck-Millipore and used at a final concentration of 10 µM. Poly(I:C) was purchased from GE Healthcare. Triphosphate-containing RNA (pppRNA) was produced by runoff RNA transcription using a T7 RiboMAX kit (Promega) from a 250-bp PCR product template encoding the 5' end of the coxsackievirus B3 (CVB3) genome containing a T7 promoter sequence.

Cells and viruses. RIG-I wild-type (RIG-I^{wt}), RIG-I knockout (RIG-I^{KO}), MDA5^{wt}, and MDA5^{KO} mouse embryonic fibroblasts (MEFs) were provided by S. Akira (2). The MAVS^{wt} and MAVS^{KO} MEFs were provided by Z. J. Chen (35). PKR^{wt} and PKR^{KO} MEFs were provided by J. Bell (36) through T. Michiels. The PERK^{wt}, PERK^{KO}, GCN2^{wt}, and GCN2^{KO} MEFs were provided by D. Ron (37, 38), and eIF2α S^{51S} and eIF2α S^{51A} MEFs were provided by R. J. Kaufman (39) through C. A. de Haan. MEFs and HeLa, BGM, and BHK-21 cells were maintained in Dulbecco's modified Eagle's medium supplemented with 10 % fetal calf serum (FCS) and ciproxin (1 mg/ml). Mengovirus and a mengovirus Zn-finger domain mutant (mengo-Zn) (28) were propagated on BHK-21 cells. Coxsackievirus B3 strain Nancy (40) was propagated on BGM cells.

Plasmids. The expression plasmid encoding the RIG-I caspase recruitment domain (CARD) was described previously (41). Plasmid encoding green fluorescent protein (GFP)-tagged MAVS was constructed by PCR amplification of the GFP gene using primers flanked by NheI (Fw; 5'-GCTAGCGCCGCCACCATGGTGAGCAAGG-3') and NotI (Rv; 5'-GCGGCCGCCCTTGTACAGCTCGTCCATG-3') restriction sites (underlined). The PCR product was cloned into NheI-NotI-digested pcDNA4/V5-His-A vector, resulting in the pcDNA-GFP vector. The gene encoding the human MAVS was PCR amplified using primers flanked by NotI (Fw 5'-GCGGCCGCATGCCGTTTGCTGAAGACAAG-3') and XhoI (Rv 5'-CTCGAGCTAGTGCAGACGCCGCCGTAC-3') restriction sites and cloned into the NotI-XhoI-digested pcDNA-GFP vector, yielding the pcDNA-GFP-MAVS expression plasmid.

Single-step growth curve. Confluent monolayers of HeLa cells were infected with the different picornaviruses (multiplicity of infection [MOI] 10), and RNA was harvested at 2 h intervals until 10 h postinfection (h.p.i.). Total RNA was isolated using a GenElute mammalian total RNA miniprep kit (Sigma-Aldrich) according to the manufacturer's instructions. Isolated RNA was used to determine IFN-β and viral RNA levels using real-time quantitative reverse transcription-PCR (RT-qPCR). Cells grown on glass coverslips were infected simultaneously, fixed at the indicated time points, and used for an immunofluorescence assay.

RT-qPCR. Total cellular RNA from confluent monolayers of a 24-well cluster (2 x 10⁵ cells) was isolated using a GenElute mammalian total RNA miniprep kit (Sigma-Aldrich) according to the manufacturer's instructions. Isolated RNA was DNase I treated (Invitrogen) prior to reverse transcription using a TaqMan reverse transcription reagent kit (Applied Biosystems) with random hexamer primers according to the manufacturer's instructions. Quantitative analysis of mRNA levels was performed using a LightCycler 480 system (Roche).

Immunofluorescence assay. Cells on glass coverslips were washed once with phosphate-buffered saline (PBS) and fixed with paraformaldehyde (4 %)-PBS for 15 min. Cells were permeabilized with PBS-0.2 % Triton X-100, washed three times with washing buffer (PBS-0.1 % Tween 20), and

incubated with blocking buffer (PBS–0.1 % Tween 20–2 % bovine serum albumin) for 1 h. Cell monolayers were incubated for 1 h with primary antibody rabbit- α -MDA5 (Barral et al. [42]) (1:200), goat- α -MDA5 (Imgenex) (1:25), mouse- α -G3BP (BD) (1:1,000), rabbit- α -TIA1 (Santa-Cruz) (1:50), mouse- α -dsRNA (J2) (English & Scientific Consulting) (1:1,000), goat- α -eIF3 (Santa-Cruz) (1:100), rabbit- α -Sam68 (Santa-Cruz) (1:100), mouse- α -PKR (BD) (1:100), or rabbit- α -Flag (Sigma) (1:200) and then for 30 min with goat- α -rabbit-Alexa 488 (Invitrogen) (1:100), goat- α -mouse-Alexa 594 (Invitrogen) (1:100), or donkey- α -goat-Alexa 594 (Invitrogen) (1:100) and Hoechst-33258 (1:2,000) diluted in blocking buffer. Between and after the incubations, the cell monolayers were washed, thrice each time, with washing buffer. Finally, the cells were washed once with distilled water and coverslips were mounted on glass slides in Mowiol (Polysciences). Cells were examined by standard fluorescence microscopy (Leica DMR) or confocal microscopy (Leica SPE-II).

Stress induction. HeLa and MEF cells were grown on coverslips in 24-well clusters, and confluent monolayers were treated with 0.5 mM arsenic acid for 30 min (oxidative stress), exposed to heat shock by incubation for 30 min in a water bath of 46°C (ER stress), treated with 0.1 mM MG132 for 4 h at 37°C (amino acid deprivation), or treated with 2 μ M thapsigargin for 1 h at 37°C (ER stress). Formation of stress granules was determined using an immunofluorescence assay.

siRNA knockdown. PKR mRNA knockdown in HeLa cells was performed by reverse transfection of 20 pmol small interfering RNA (siRNA) duplex per well (5'-GCAGGGAGUAGUACUUAAAUA[dT] [dT]-3' and 5'-UAUUUAAGUACUACUCCUGC[dT][dT]-3', where the last two nucleotides in each sequence are deoxyribonucleotides [dT]) using Lipofectamine RNAiMAX and Opti-MEM (Invitrogen) in a 24-well cluster. Briefly, PKR siRNA duplex or scrambled siRNA (Qiagen) was diluted in 100 μ l Opti-MEM, 1 μ l Lipofectamine RNAiMAX was added, and the reaction mixture was incubated 25 min in a 24-well cluster. HeLa cells were diluted in FCS-supplemented medium (without antibiotics), 5 x 10⁴ cells in 0.5 ml medium was added per well, and the reaction mixture was incubated 48 h at 37°C. Following the siRNA transfection, cells were used for RNA transfection or mengo-Zn infection. Knockdown efficiency was determined by RT-qPCR, immunofluorescence assay, and Western blot analysis.

Western blot analysis. For Western blot analysis of PKR, poly(ADP-ribose) polymerase (PARP), and LC3 expression, HeLa cells transfected with either scrambled siRNAs or siRNAs directed against PKR were suspended in ice-cold cell lysis buffer (20 mM Tris-HCl [pH 8.0], 100 mM NaCl, 0.5 % Triton X-100, 1 mM EDTA) and incubated 30 min on ice. Cell debris was pelleted for 15 min at 15,000 x g, and the protein concentration of the supernatant was determined by a Bradford protein assay (Bio-Rad) according to the manufacturer's instructions. Proteins (50 μ g cell lysate) were separated using reducing sodium dodecyl sulfate-polyacrylamide gel electrophoresis (SDS-PAGE) and transferred to nitrocellulose membranes by semidry electrophoretic transfer. Membranes were washed once with washing buffer (PBS–0.1 % Tween 20) and incubated 1 h in blocking buffer (PBS–0.1 % Tween 20–5 % nonfat milk). Membranes were successively incubated for 1 h with primary antibody mouse- α -PKR (BD) (1:1,000), rabbit- α -PARP (Roche) (1:5,000), rabbit- α -LC3 (Novus Biologicals) (1:3,000), or mouse- α -actin (Sigma-Aldrich) (1:20,000) and then for 30 min with goat- α -mouse-IRDye680 (Li-COR) (1:15,000) or goat- α -rabbit-IRDye800 (Li-COR) (1:15,000) diluted in blocking buffer. Between and after the incubations, the membranes were washed, thrice each time, with washing buffer. Finally, membranes were washed once with PBS and scanned using an Odyssey Imager (Li-COR).

TCID₅₀ assay. Infected HeLa and MEF cells were freeze-thawed three times. Cells were pelleted using high-speed centrifugation, and supernatants were used for endpoint dilution. HeLa cells in 96-well clusters were infected with 3-fold serial dilutions of the cleared supernatants, and 50 % tissue culture infective dose (TCID₅₀) values were calculated 2 days after infection.

PKRi treatment of HeLa and MEF cells. HeLa and MEF cells were grown in 24-well clusters and infected with mengo-Zn (MOI 10) for 1 h. Following infection, medium was replaced by 0.5 ml fresh medium or medium supplemented with 10 μM PKR inhibitor (PKRi). Total RNA was isolated 6 h postinfection and used to determine intracellular viral RNA levels by RT-qPCR. Cells grown on glass coverslips were simultaneously infected and PKRi treated and used for an immunofluorescence assay.

Recombinant IFN treatment. HeLa and MEF cells were grown on coverslips and either mock treated or incubated with recombinant human IFN-2α (Roferon-A; Roche) (500 U/ml) and mouse IFN-α/β (Sigma) (500 U/ml), respectively, for 24 h. Cells were paraformaldehyde fixed and used for an immunofluorescence assay. Simultaneously, RNA was isolated and used to determine PKR and MDA5 levels by RT-qPCR.

RIG-I CARD and GFP-MAVS overexpression. Activation of the RLR pathway was achieved by overexpression of the Flag-tagged CARD of RIG-I or GFP-tagged MAVS. Confluent monolayers of HeLa cells were transfected with 800 ng plasmid DNA using Lipofectamine 2000 (Invitrogen) according to the manufacturer's instructions. Briefly, plasmid DNA was diluted in 50 μl Opti-MEM, 2 μl Lipofectamine 2000–50 μl Opti-MEM was added, and the reaction mixture was incubated 25 min and added to confluent monolayers grown in 24-well clusters. At 24 h posttransfection, the total RNA was isolated and used to determine IFN-α/β levels by RT-qPCR. Cells grown on glass coverslips were simultaneously transfected and used for an immunofluorescence assay.

RNA ligand transfection. For transfection of MDA5 and RIG-I ligands, cells were grown in 24-well clusters in 0.4 ml medium. Confluent monolayers were transfected with either 100 ng pppRNA or poly(I:C) using Lipofectamine 2000 (Invitrogen) according to the manufacturer's instructions. Briefly, RNA ligand was diluted in 50 μl Opti-MEM, 1 μl Lipofectamine 2000–50 μl Opti-MEM was added, and the reaction mixture was incubated 25 min and added to the cells. Total RNA was isolated and used to determine IFN-α/β levels by RT-qPCR. Cells grown on glass coverslips were simultaneously transfected and used for an immunofluorescence assay.

Drug treatment. HeLa cells were grown in 24-well clusters. Prior to RNA ligand transfection, the medium was replaced by 0.4 ml medium supplemented with 12.5 μg/ml emetine or cycloheximide or 25 μg/ml puromycin. Cells were mock, pppRNA, or poly(I:C) transfected as described before. Total RNA was isolated and used to determine IFN-α/β levels by RT-qPCR. Cells grown on glass coverslips were simultaneously transfected and used for an immunofluorescence assay.

RESULTS

SG formation in picornavirus-infected cells. It was recently shown that TMEV L represses the formation of SG and also that the L proteins of mengovirus and SAFV are endowed with this function when introduced in TMEV in place of its L (23). Consistent with this observation, we

found that a mutant mengovirus in which the Zn-finger domain of L is disrupted (mengo-Zn) (28) induced clear cytoplasmic aggregates of G3BP, a hallmark of SG (Fig. 1A). In contrast, wild-type mengovirus (mengo-wt) failed to induce SG. This was not due to differences in replication kinetics, as indicated by similar levels of dsRNA (Fig. 1B) and intracellular viral RNA (Fig. 1E). SG formation by mengo-Zn differed from that by coxsackievirus B3 (CVB3), an enterovirus. This enterovirus induced small G3BP-containing granules early in infection which gradually decreased in size later in infection (Fig. 1A). A similar observation has been made in cells infected with poliovirus, another enterovirus (27, 43).

It has been proposed that virus infection leads to the formation of a unique SG—marked by presence of Src-associated protein in mitosis of 68 kDa (Sam68) (22, 44)—that is distinct from the SG induced by other stimuli. Nevertheless, although mengo-Zn clearly induced granular localization of G3BP (Fig. 1A) and TIA1 (Fig. 1C), we were unable to detect Sam68 in these virus-induced SG (Fig. 1D). Sam68 was also absent in SG induced by an L mutant TMEV (23), suggesting that this protein is not recruited to SG in cardiovascular-infected cells. The kinetics of SG induction correlates flawlessly with the transcription of IFN- α/β mRNA (Fig. 1A and F). While CVB3 and mengo-wt efficiently repressed IFN- α/β induction (31, 45), mengo-Zn that lacks L's IFN- α/β antagonizing activity (28) induced high levels of IFN- α/β mRNA (Fig. 1F).

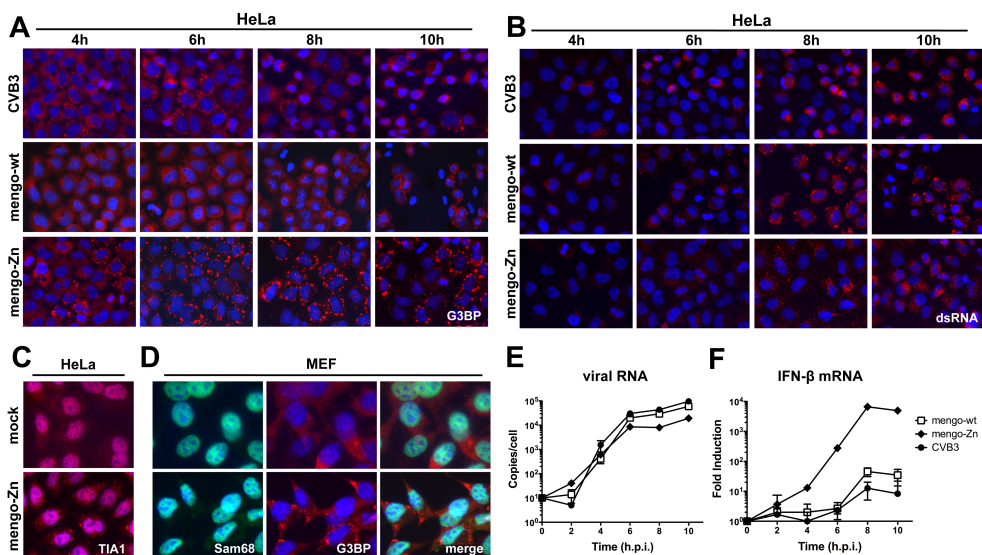


FIG. 1. Induction of the IFN- α/β pathway and SG formation by picornavirus infection. (A and B) Immunofluorescence images of HeLa cells infected with coxsackievirus B3 (CVB3), mengovirus (mengo-wt), and mengovirus with a Zn-finger domain mutation in L (mengo-Zn) (MOI = 10). Cells were fixed at indicated time points and for G3BP (A) or dsRNA (B). Nuclei were stained using Hoechst-33258. (C) Immunofluorescence images of either mock-treated or mengo-Zn-infected (MOI = 10) HeLa cells. Cells were fixed 6 h.p.i. and stained using an antibody against TIA1. Nuclei were stained with Hoechst-33258. (D) Immunofluorescence images of mock-treated or mengo-Zn-infected (MOI = 10) MEF cells. Cells were stained using antibodies against G3BP (red) and SAM68 (green). Nuclei were stained with Hoechst-33258. TIA1 and G3BP form cytoplasmic aggregates upon mengo-Zn infection, while Sam68 maintains its nuclear localization. (E and F) In the same experiment as described for panel A, total RNA from infected cells was isolated and used for RT-qPCR analysis of intracellular viral RNA levels (E) and induction of IFN- β mRNA (F). Data are presented as the means \pm standard deviations (SD) of the results of triplicate experiments.

Mengovirus-induced SG formation is PKR dependent and represses viral RNA replication. The induction of cellular stress by virus infection is often mediated by the activation of PERK, GCN2, and/or PKR (9, 10, 18). Activation of these kinases leads to phosphorylation of eIF2 α that, in turn, induces SG formation. The identity of the kinase that is activated by mengo-Zn, or any other picornavirus, is as yet unknown. To investigate this, we used mouse embryonic fibroblasts (MEFs) with a specific disruption of the PERK, GCN2, or PKR gene (these cells are referred to here as knockout [KO] MEFs). To confirm that the KO MEFs used were behaving properly, they were subjected to stress inducers that are known to specifically activate each of these kinases. As expected, the PERK KO cells, but not the wt cells, failed to form SG upon treatment with thapsigargin (38) (Fig. 2A). Likewise, the GCN2 KO cells showed no SG induction upon MG132 treatment (46) (Fig. 2B). However, both PERK and GCN2 KO cells were still able to form SG upon mengo-Zn infection (Fig. 3A). In contrast, PKR KO cells (36) failed to induce cytoplasmic granules upon mengo-Zn infection (Fig. 3A). The prerequisite of PKR activation for mengo-Zn-induced SG was confirmed in HeLa cells in which PKR expression was depleted by siRNAs (Fig. 3B and C). Of note, the absence of SG in cells lacking PKR was not due to an intrinsic defect in the stress response pathway since they were still able to form SG upon exposure to other stress stimuli (Fig. 2C and D). These data strongly suggest that mengo-Zn infection induces SG in a PKR-dependent manner.

To investigate the effect of stress pathway activation on viral RNA replication, intracellular viral RNA levels were determined in HeLa and MEF cells that lacked PKR expression and thus SG formation (Fig. 3A and B). In both cell types, mengo-Zn replicated to higher yields (2-to-3-fold

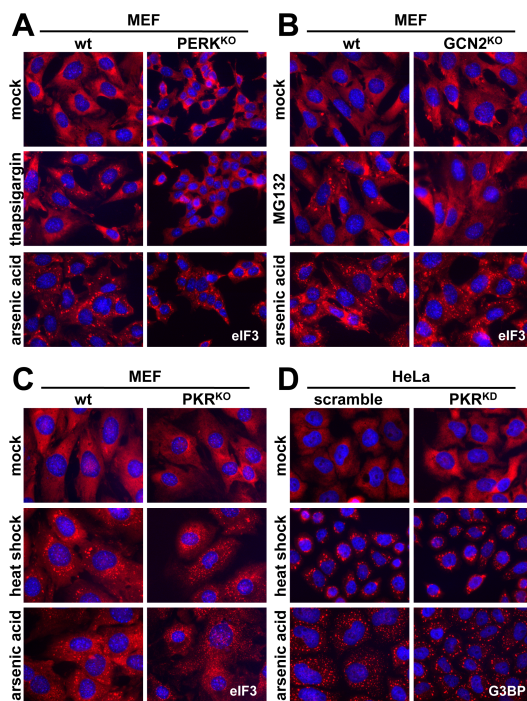


FIG. 2. Integrity of cells lacking PERK, GCN2, or PKR expression.

(A to C) Immunofluorescence images of MEFs from mice deficient in PERK (PERK KO) (A), GCN2 (GCN2 KO) (B), or PKR (PKR KO) (C) and their litter controls (wt) that were either mock treated or treated with MG132, thapsigargin, heat shock, or arsenic acid. Cells were stained for eIF3, and nuclei were stained with Hoechst-33258. Note that PERK KO cells failed to form SG upon thapsigargin treatment (PERK-mediated stress induction), while GCN2 KO cells failed to form SG upon MG132 treatment (GCN2-mediated stress induction). (D) Immunofluorescence analysis of HeLa cells transfected with scrambled siRNA (scramble) or PKR siRNA (PKR KD) and subsequently mock treated or treated with heat shock or arsenic acid. Cells were stained using an antibody against G3BP, and nuclei were stained with Hoechst-33258.

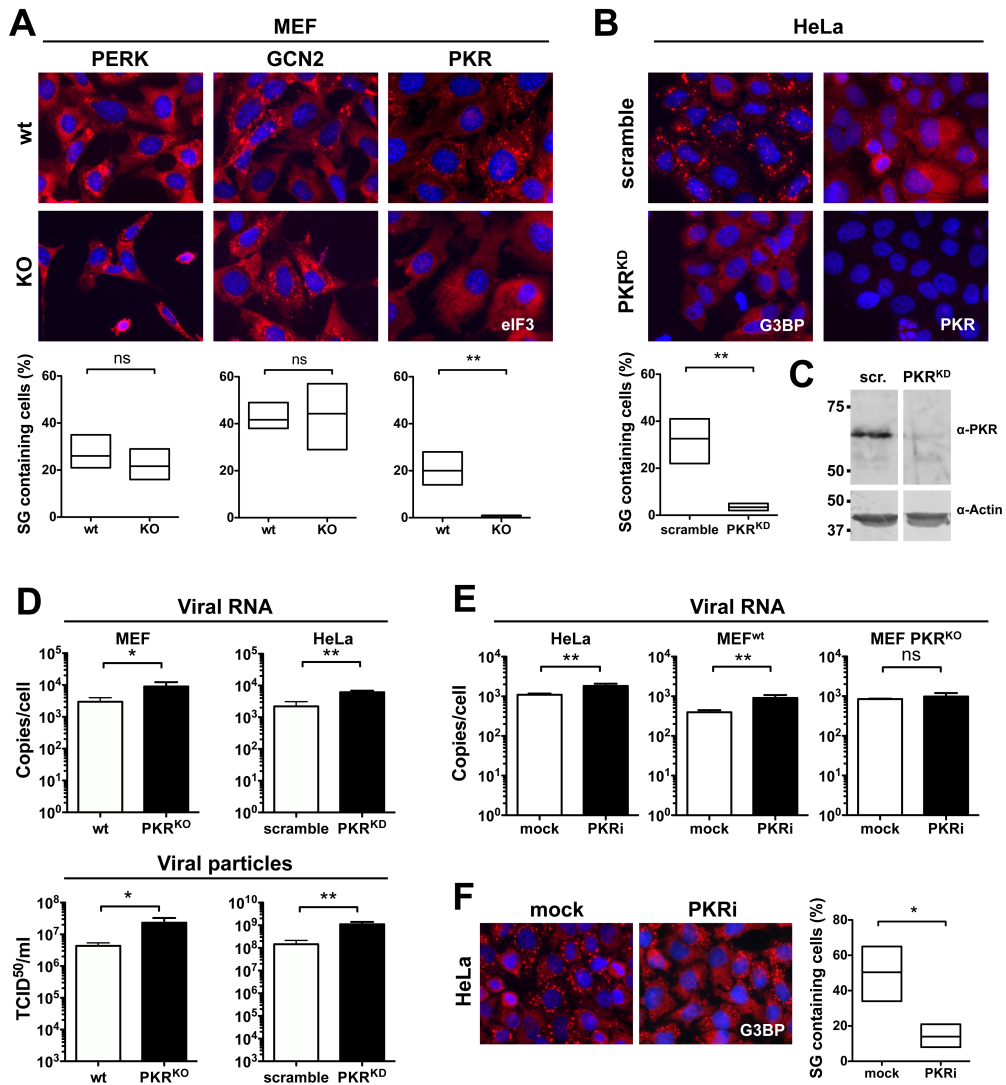


FIG. 3. Mengo-Zn induces SG in a PKR-dependent manner. (A) Immunofluorescence images of knockout (KO) MEFs and cells of their litter control (wt) infected with mengo-Zn (MOI = 10). Cells were fixed at 6 h postinfection (h.p.i.) and stained for eIF3. Nuclei were stained with Hoechst-33258. Cells containing SG were counted, and the results are shown in the graphs. While MEFs deficient in GCN2 and PERK expression showed SG formation, MEFs deficient in PKR expression were devoid of SG formation. (B) Immunofluorescence images of scrambled siRNA (scramble)- or PKR siRNA (PKR KD)-transfected HeLa cells infected with mengo-Zn (MOI = 10). Cells were fixed at 6 h.p.i. and stained for G3BP or PKR. Nuclei were stained with Hoechst-33258. Cells containing SG were counted, and the results are shown in the graph. (C) Lysates of scrambled siRNA (scr.)- and PKR siRNA (PKR KD)-transfected HeLa cells were made in parallel and analyzed for expression of PKR by Western blotting using an antibody against PKR. Additionally, detection of β -actin expression was used as a loading control. (D) MEFs from PKR-deficient mice (PKRKO) and cells of their litter control (wt) and HeLa cells transfected with scrambled siRNA (scramble) or PKR siRNA (PKR KD) were infected with mengo-Zn (MOI = 10). Total RNA was isolated at 8 h.p.i. and used for RT-qPCR to determine intracellular viral RNA levels (Viral RNA). Additionally, viral particle formation was determined using endpoint dilution and TCID₅₀ values are shown. Data are presented as the means \pm SD of the results of triplicate experiments analyzed using an unpaired t test (* and **, significant differences at $P < 0.05$ and $P < 0.01$, respectively). (E) HeLa cells, PKR knockout MEFs (MEF PKR KO), and cells

increase in intracellular viral RNA level) than their litter controls (Fig. 3D). This difference in intracellular viral RNA levels reflects the difference in infectious particles as determined by endpoint dilutions (Fig. 3D). Additionally, mengo-Zn replicated to 2-fold-higher levels in HeLa and MEF cells treated with a PKR inhibitor (PKRi; Fig. 3E) that reduced SG formation (Fig. 3F). This increase was not due to an off-target effect of the drug, since viral RNA replication was unaffected in PKR KO MEFs (Fig. 3E).

Importantly, mengovirus infection induces also the autophagy and apoptosis pathways (47, 48). We investigated whether virus-induced activation of the stress pathway and the consequent formation of SG influenced activation of the apoptosis or autophagy pathway in virus-infected HeLa cells in which PKR was depleted by siRNAs. Inhibition of the stress pathway had no effect on PARP cleavage (a hallmark of apoptosis) or LC3 lipidation (a hallmark of autophagy) in either wt- or mengo-Zn-infected cells (Fig. 4).

Together, our results suggest that the PKR-mediated activation of the stress response pathway acts as an antiviral response that limits virus replication, although the impact on virus titers is relatively small.

MDA5 is recruited to SG under conditions of cellular stress. In our studies aimed at elucidation of the potential link between the stress pathway and IFN- α/β pathway, we focused on MDA5, as this receptor plays a key role in activating the IFN- α/β response upon picornavirus infection (25, 49). MDA5 has a cytosolic localization in naive cells (50). However, the distribution of MDA5 upon virus infection is largely unknown. Therefore, we investigated the localization of MDA5 in picornavirus-infected cells using immunofluorescence microscopy. In both CVB3- and mengo wt-infected cells, MDA5 maintained its cytosolic localization (Fig. 5A). Surprisingly, infection with mengo-Zn resulted in granular localization of MDA5 (Fig. 5A), which was confirmed by another assay using MDA5-specific antibody (data not shown). The MDA5 granules were distinct from the smaller dsRNA-containing puncta that most likely represent the replication complexes (Fig. 5A and B). Hence, we considered that MDA5 might localize to SG. Indeed, MDA5 was demonstrated to colocalize with G3BP in both mengo-Zn-infected HeLa and MEF cells (Fig. 5C) and also with TIA1 in mengo-Zn-infected HeLa cells (data not shown). Taken together, these data show that MDA5 migrates to SG upon mengo-Zn infection.

To investigate whether MDA5 is recruited to SG only during virus-induced stress or whether it is also recruited under non-viral stress conditions, we activated the cellular stress response by the use of different stimuli. In Fig. 5D, it is shown that MDA5 also localizes to SG under conditions of ER stress induced by heat shock and oxidative stress induced by arsenic acid treatment. It is noteworthy that MDA5 was detected in all SG induced by any kind of stress, which suggests that MDA5 is a general component of SG. Importantly, neither treatment resulted in the activation of MDA5 and the downstream IFN- α/β pathway (data not shown). Therefore, we conclude that MDA5 localizes to SG upon the induction of cellular stress and that the localization is independent of its activation.

of their litter control (MEF wt) were incubated in the presence or absence of PKR inhibitor (PKRi) and subsequently infected with mengo-Zn (MOI = 10). Intracellular viral RNA levels were determined by RT-qPCR. Data are presented as the means \pm SD of the results of triplicate experiments analyzed using an unpaired t test (ns, no significant difference; **, significant difference at $P < 0.01$). (F) In the same experiment, HeLa cells were fixed and stained for G3BP. Nuclei were stained with Hoechst-33258. Cells containing SG were counted, and results are shown in the graph.

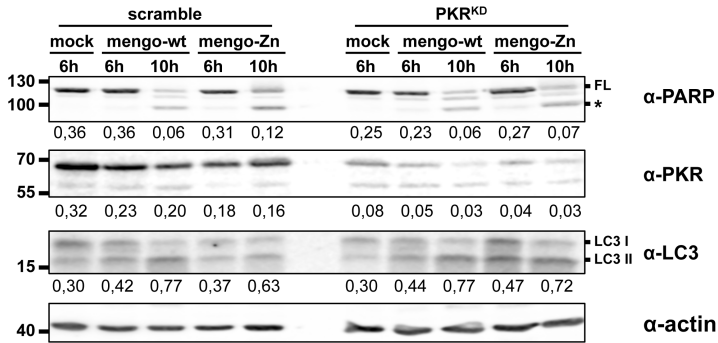


FIG. 4. Inhibition of the stress response had no effect on the apoptosis or autophagy pathways. Lysates of scrambled siRNA (scramble)- and PKR siRNA (PKR KD)-transfected HeLa cells infected with mengo-wt or mengo-Zn (MOI = 10) were analyzed for expression of PARP, PKR, LC3, and actin by Western blotting. PKR knockdown, which prevents SG formation, had no effect on the induction of apoptosis as detected by the degradation of full-length (FL) PARP into the smaller cleavage product (indicated by the asterisk). Additionally, lack of SG formation had no effect on the activation of the autophagy pathway as determined by the conversion of LC3 I into LC3 II.

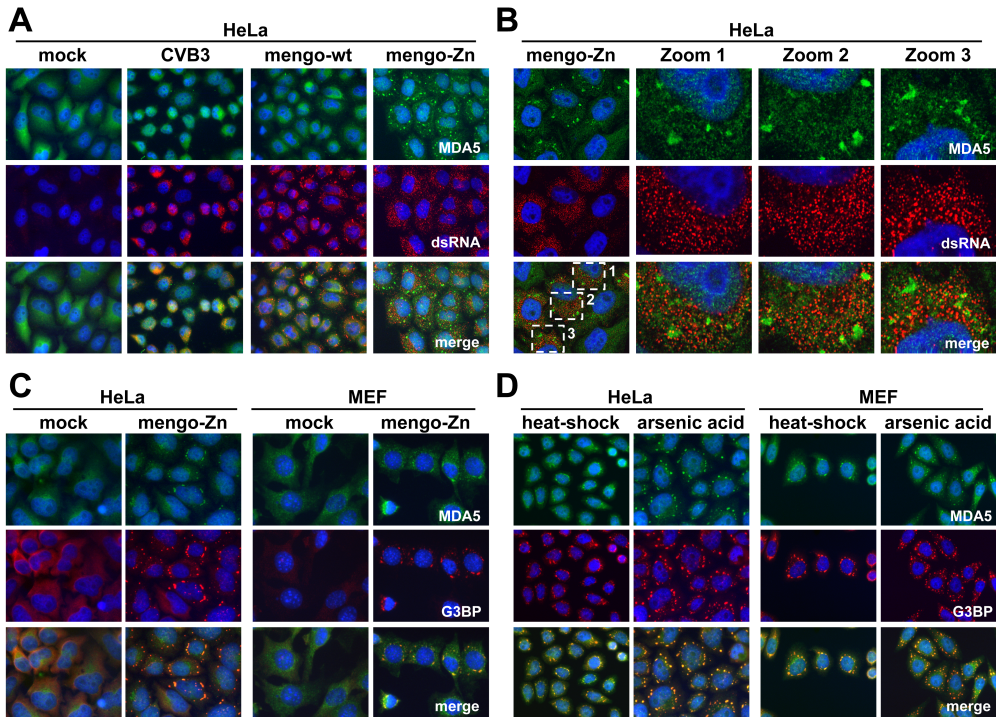


FIG. 5. MDA5 is recruited to SG upon stress induction. (A) Immunofluorescence images of mock-treated and picornavirus-infected HeLa cells (MOI = 10). Cells were fixed at 6 h.p.i. and stained with an antibody developed by Barral et al. (42) against MDA5 (and was used to stain for MDA5 unless stated otherwise) (green) and dsRNA (red). Nuclei were stained with Hoechst-33258. (B) Confocal microscopy analysis of mengo-Zn-infected HeLa cells (MOI = 10) stained for MDA5 and dsRNA as described for panel A. Single-cell magnified images clearly showed that dsRNA does not colocalize with the MDA5 granules. (C) Immunofluorescence images of mock-treated and mengo-Zn-infected HeLa and MEF cells (MOI = 10). Cells were fixed at 6 h.p.i. and stained for G3BP (red) and MDA5 (green). Nuclei were stained with Hoechst-33258. (D) Immunofluorescence images of heat shock- or arsenic acid-treated HeLa and MEF cells. Cells were fixed after treatment and stained as described for panel C.

Activation of the RLR pathway does not induce and is not needed for SG formation. The observation that SG are formed only in cells infected with a virus deficient in suppressing IFN- α/β (Fig. 1) suggested a possible link between the stress pathway and the IFN- α/β pathway. To investigate whether secreted IFN- α/β might induce a cellular stress response, HeLa and MEF cells were treated with recombinant human IFN-2 α and mouse IFN- α/β , respectively. Although the transcription of interferon-stimulated genes (MDA5 and PKR) was induced (data not shown), neither of the cell types showed formation of SG upon IFN treatment (Fig. 6A).

Alternatively, the activation of the RLR pathway rather than downstream responses of IFN- α/β could one way or another be involved in SG formation. To test this possibility, we overexpressed the caspase recruitment domain (CARD) of RIG-I or its downstream interacting partner MAVS, both of which have been reported to trigger phosphorylation of IRF3 and transcription of IFN- α/β mRNA upon ectopic expression (41). Cells overexpressing RIG-I CARD or MAVS were devoid of SG (Fig. 6B), although clear induction of IFN- β mRNA was observed (Fig. 6C). Thus, activation of the RLR pathway and subsequent induction of IFN- α/β gene transcription also do not induce SG formation.

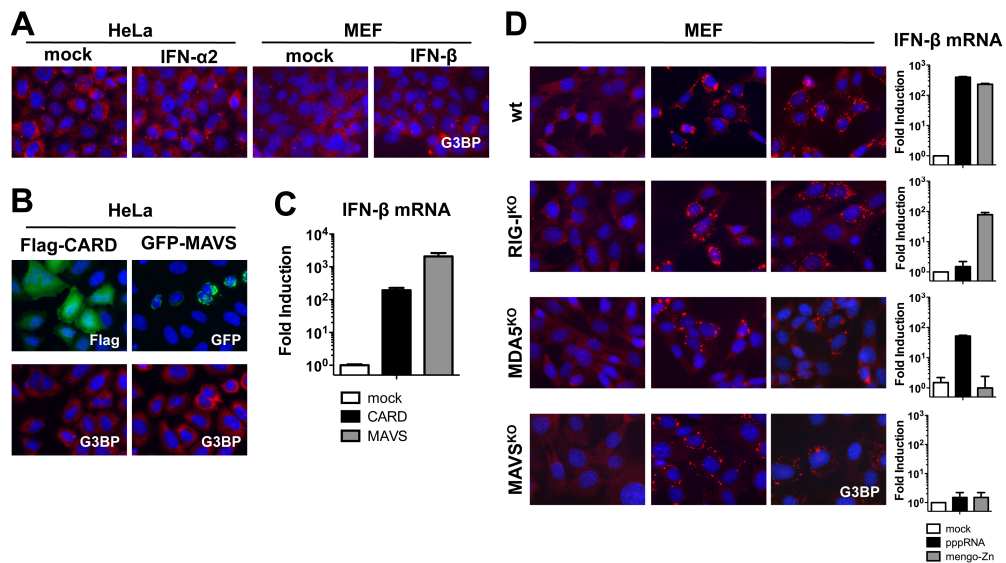


FIG. 6. Activation of the RLR pathway does not lead to SG formation. (A) Immunofluorescence images of mock- and recombinant IFN-treated HeLa and MEF cells. Cells were fixed 24 h post-treatment and stained for G3BP. Nuclei were stained with Hoechst-33258. (B) Plasmids encoding the Flag-CARD of RIG-I or GFP-MAVS were transfected in HeLa cells. Cells were fixed 24 h posttransfection and stained for Flag (green) and G3BP (red). Nuclei were stained with Hoechst-33258. (C) In the same experiment, total RNA was isolated from plasmid-transfected cells and used for RT-qPCR analysis of IFN- β mRNA levels. Data are presented as the means \pm SD of the results of triplicate experiments. (D) Immunofluorescence images of MEFs from mice deficient in RIG-I (RIG-I KO), MDA5 (MDA5 KO), or MAVS (MAVS KO) expression and wild-type control cells (wt) were mock transfected, transfected with pppRNA ligand, or infected with mengo-Zn (MOI = 10). Cells were fixed 6 h post-infection or -transfection and stained for G3BP. Nuclei were stained with Hoechst-33258. In the same experiment, total RNA was isolated from infected and transfected MEFs and used for RT-qPCR analysis of IFN- β mRNA levels (right panels). Data are presented as the means \pm SD of the results of triplicate experiments. Note that cells that lacked IFN- β mRNA induction still formed SG via activation of PKR.

To rule out the possibility that activation of the RLR pathway is required for SG formation, we activated PKR by mengo-Zn infection and transfection of a triphosphate-containing RNA ligand (pppRNA) in MEFs lacking MDA5, RIG-I, or MAVS. SG formation was observed in all cells (Fig. 6D). This observation shows that mengovirus RNA and pppRNA efficiently induce SG in the absence of RLR pathway activation.

Collectively, these data indicate that activation of the stress pathway and formation of SG do not rely on the integrity or activation of the RLR pathway.

Localization of MDA5 to SG is not required for IFN- α/β induction. Finally, we considered the possibility that localization of MDA5 to SG is important for ligand recognition and IFN- α/β induction. To investigate this, we measured IFN- α/β responses in cells that are unable to form SG by three different approaches.

First, we transfected pppRNA and poly(I:C)—a synthetic dsRNA ligand that activates MDA5 (49)—in HeLa and MEF cells that were deficient in PKR expression. In contrast to wild-type cells, PKR-deficient cells failed to show SG formation upon RNA ligand transfection (Fig. 7A). Yet transcription of IFN- β mRNA was efficiently induced by RNA ligand transfection in cells lacking SG formation (Fig. 7B). In HeLa cells where PKR expression was reduced by siRNA knockdown, a small reduction in IFN- β mRNA induction was observed upon mengo-Zn infection; however, this was not observed in MEFs lacking PKR expression (Fig. 7B).

To investigate the involvement of SG formation in cells expressing normal levels of PKR, we next treated HeLa cells with drugs that stall protein translation and in some cases also repress the assembly of SG. Puromycin is a known inhibitor of protein translation that causes disassembly of the ribosome complex, thereby making the mRNA available for the incorporation into SG (51). In contrast, emetine and cycloheximide are compounds that fix complete ribosomes on mRNA transcripts, which results also in a halt in protein translation but prevents the formation of SG (52). Accordingly, transfection of pppRNA and poly(I:C) into cells treated with puromycin resulted in SG formation, while cells treated with emetine and cycloheximide were devoid of SG (Fig. 7C). Still, transfection of RNA ligands in cells that were unable to form SG displayed induction of the IFN- α/β pathway similar to that seen with mock-treated cells (Fig. 7D).

Last, we also used MEFs expressing the nonphosphorylatable eIF2 α S⁵¹A protein (39). These cells are deficient in the formation of SG upon arsenic acid and heat shock treatment (data not shown) and also during mengo-Zn infection or RNA ligand transfection (Fig. 7E). Although these cells were unable to form SG, both mengo-Zn infection and transfection of RNA ligands potently induced IFN- β mRNA transcription (Fig. 7F).

In conclusion, three lines of evidence show that SG formation, and thus MDA5 localization to these granular structures, is dispensable for triggering IFN- α/β responses.

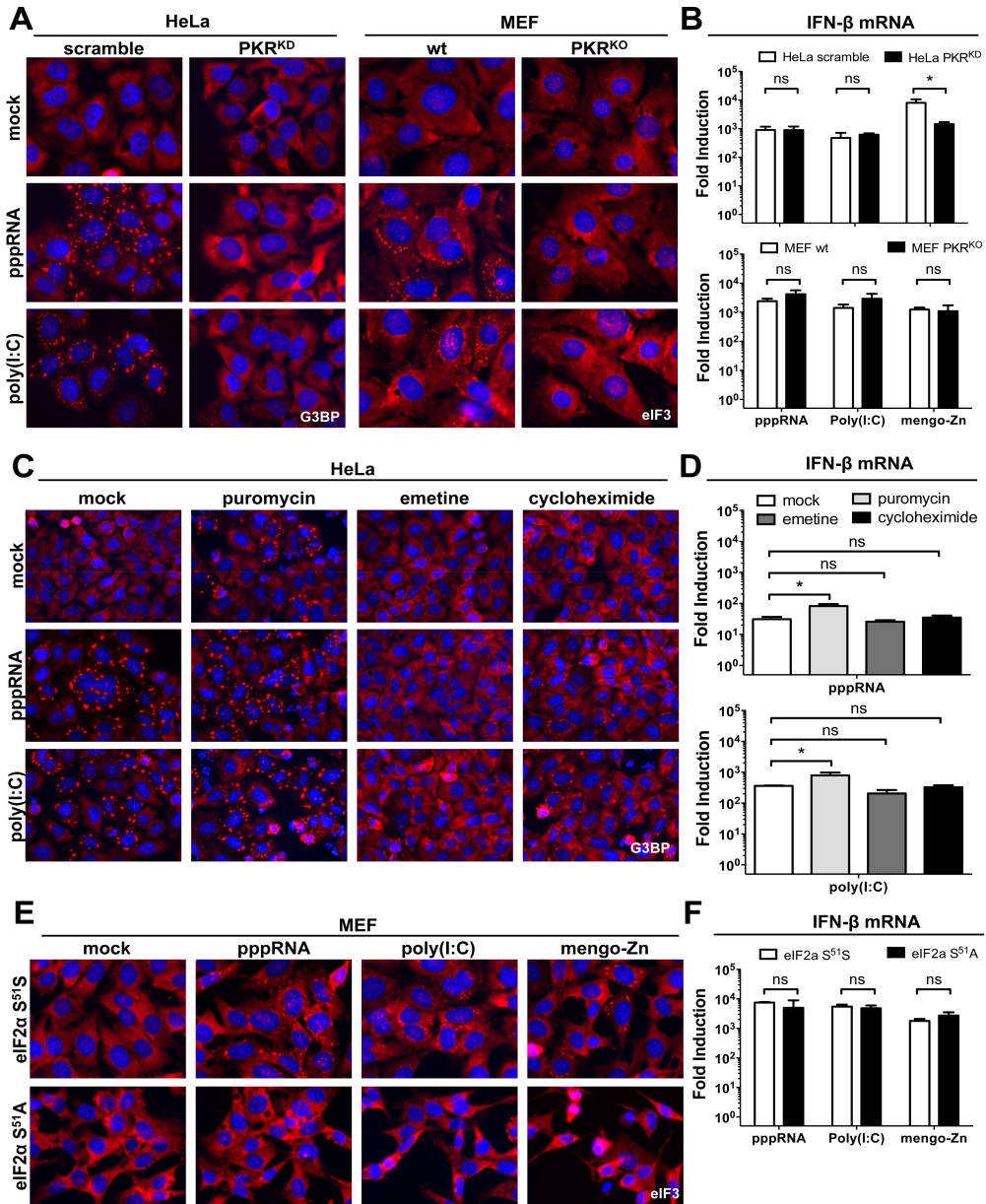


FIG 7. SG formation is not required for ligand recognition and IFN-β mRNA induction. (A) HeLa cells transfected with scrambled siRNA (scramble) or PKR siRNA (PKR KD) and MEFs from PKR-deficient mice (PKR KO) and cells of their litter control (wt) were transfected with pppRNA and poly(I:C) ligands. Cells were fixed at 6 h.p.i. and analyzed by immunofluorescence. HeLa cells were stained for G3BP and MEF cells for eIF3. Nuclei were stained with Hoechst-33258. (B) In the same experiment, total RNA from transfected HeLa cells (top) and MEF cells (bottom) was isolated and used for RT-qPCR analysis of IFN-β mRNA levels. Additionally, RT-qPCR analysis of IFN-β mRNA levels from mengo-Zn-infected HeLa and MEF cells is presented. Data are presented as the means ± SD of the results of triplicate experiments analyzed using an unpaired t test (ns, no significant difference; *, significant difference at $P < 0.05$). (C) Immunofluorescence images of mock- and RNA ligand-transfected HeLa cells in the presence or absence of puromycin, cycloheximide, or emetine. Cells were fixed 6 h posttransfection and stained for G3BP, and nuclei were stained with Hoechst-33258.

DISCUSSION

Virus infection triggers several antiviral responses that limit virus replication. To counteract these responses, viruses express dedicated proteins that antagonize these antiviral pathways. Previously, we showed that a mutant mengovirus with a disabled L protein was unable to repress the induction of IFN- α/β (28). Here, we show that the same mutant mengovirus activates the stress response pathway via PKR, resulting in SG formation. Furthermore, we show that infection of cells that are unable to form SG resulted in an increase, albeit modest, in intracellular viral RNA levels. Previously, it was shown that SG formation slightly repressed viral RNA replication of poliovirus, another picornavirus (43). Thus, our observation lends support to the idea that SG formation acts as an intrinsic antiviral mechanism against (picorna) virus infection by repressing viral RNA replication.

Our data demonstrate that a single viral protein, L, antagonizes the induction of the IFN- α/β pathway as well as the antiviral stress pathway. Interestingly, the NS1 protein of influenza A virus, a well-known IFN antagonist, was recently also recognized to suppress the stress response pathway (34). Although these evolutionarily conserved systems are believed to act strictly autonomously, accumulating evidence suggests that some antiviral mechanisms have coevolved and are intertwined. For instance, components of the autophagy pathway seem also to be involved in dampening the induction of the IFN- α/β pathway (53, 54). Moreover, ligand binding by some Toll-like receptors (TLR) stimulates the activation of the autophagy pathway (55, 56).

The finding that single viral proteins of two unrelated viruses can repress the induction of both IFN- α/β and the stress pathways suggested a possible link between these two antiviral systems. In our pursuit for this connection, we found that MDA5, the sensor for picornavirus RNA, displayed a granular distribution in cells infected with mengo-Zn but not in cells infected with CVB3 or mengo-wt. The MDA5-containing granules colocalized with G3BP and TIA-1, suggesting that MDA5 localizes to SG in mengo-Zn-infected cells. SG are storage places for preinitiated mRNA complexes, which are formed under cellular stress conditions (12). One possible explanation of why MDA5 would relocate to SG upon viral infection is that these RNA-rich granules also serve as a ligand recognition platform for MDA5. Recently, it was found that MDA5 specifically recognizes the dsRNA replication intermediate in picornavirus-infected cells (25). Therefore, we hypothesized that the dsRNA ligand could be trapped in SG and thereby could be attracting MDA5 to these structures. However, using confocal microscopy analysis we showed that the SG were devoid of dsRNA. Previously, the single-stranded genomic RNAs of TMEV and poliovirus were also found to be absent from SG (23, 44). These data argue that it is unlikely that SG act as sites for viral RNA recognition in picornavirus-infected cells.

(D) In the same experiment, total RNA from pppRNA (top)- and poly(I:C) (bottom)-transfected HeLa cells was isolated and used for RT-qPCR analysis of IFN- β mRNA levels. Data are presented as the means \pm SD of the results of triplicate experiments analyzed using an unpaired t test (ns, no significant difference; *, significant difference at $P < 0.05$). (E) Immunofluorescence images of MEFs from mice expressing a non-phosphorylatable eIF2 α protein (MEF eIF2 α S⁵¹A) and cells of their litter control (MEF eIF2 α S⁵¹S) that were mock treated, transfected with RNA ligands, or infected with mengo-Zn (MOI = 10). Cells were fixed at 6 h post-infection or -transfection and stained for eIF3. Nuclei were stained with Hoechst-33258. (F) In the same experiment, total RNA was isolated and used for RT-qPCR analysis of IFN- β mRNA levels. Data are presented as the means \pm SD of the results of triplicate experiments analyzed using an unpaired t test (ns, no significant difference).

To better understand the physiological relevance of the MDA5 localization in SG, we determined IFN- α/β induction in cells that were deficient in SG formation. We showed that infection with mengo-Zn and transfection of non-self RNA ligands such as poly(I:C) and pppRNA (i.e., a specific RIG-I ligand) induced high levels of IFN- β mRNA in PKR KO MEFs and PKR knockdown HeLa cells. Additionally, cycloheximide and emetine treatment of HeLa cells, which represses SG formation, did not affect the IFN- β mRNA induction by pppRNA and poly(I:C) transfection. Furthermore, MEFs that are incapable of forming SG by an eIF2 α S⁵¹A mutation showed levels of induction of the IFN- α/β pathway upon mengo-Zn infection and transfection of pppRNA and poly(I:C) similar to those seen with wild-type MEFs. These data strongly suggest that SG formation is dispensable for the induction of the IFN- α/β pathway. This is in agreement with data from studies by Sen et al. and Clavarino et al., who showed efficient induction of IFN- β mRNA transcription by poly(I:C) transfection in PKR KO MEFs as well as in MEFs that are incapable of forming SG due to the eIF2 α S⁵¹A mutation (57, 58). Moreover, a recent report by Schulz et al. showed that EMCV infection resulted in comparable levels of IFN- β mRNA in wild-type and PKR KO MEFs (59). Collectively, these data strongly suggest that SG formation is not needed for efficient induction of the IFN- α/β pathway via RLR activation.

While this paper was in preparation, a study by Onomoto et al. reported the localization of RLRs to SG in cells infected with influenza A virus lacking the NS1 gene (IAV-NS1) (60). In that paper, the authors suggested that SG fulfill an essential role in activation of the IFN- α/β pathway by functioning as sites of RNA recognition. The authors showed that IAV-NS1 induced SG in a PKR-dependent manner and that the viral ssRNA colocalized with RIG-I, the known sensor of IAV, and SG markers TIAR, eIF3, and G3BP. They also demonstrated that siRNA knockdown of G3BP reduced the amount of IAV-NS1-induced SG by 3-fold and reported a 5-fold reduction in IFN- β mRNA transcription. Additionally, an almost 10-fold reduction of IFN- β mRNA transcription was observed in IAV-NS1-infected PKR KO MEFs compared to control cells whereas a complete lack of IFN- α/β pathway activation was observed in PKR KO MEFs upon transfection of IAV ssRNA and poly(I:C).

The differences between our data and those of Onomoto et al. might be explained by comparing the sources of the PKR KO MEFs. Onomoto et al. used MEFs derived from mice with a disruption in exons 2 and 3, including the initiating methionine, of the PKR gene (61). This results in the expression of a truncated PKR lacking the N-terminal dsRNA-binding domain region (62). In contrast, we used MEFs derived from mice with a disruption of the PKR kinase domain in exon 12 (36). This disruption results in the expression of a PKR protein lacking a part of the kinase domain and thus kinase activity (62). Importantly, apart from inducing the stress pathway, PKR is also involved in activating I κ B kinase beta (IKK- β), which occurs independently of PKR's kinase activity (63, 64). Activation of IKK- β is essential for the induction of the NF- κ B pathway and, thereby, transcription of IFN- α/β mRNA (65). Thus, expression of a N-terminally truncated PKR may negatively influence the induction of the IFN- α/β pathway as a consequence of the inability to activate IKK- β . Indeed, in a comparative study by Iordanov et al., a reduction in IFN- α/β mRNA transcription was observed in MEFs expressing N-terminally truncated PKR but not in MEFs expressing PKR lacking kinase activity due to disruption of the kinase domain (66). Therefore, results obtained with MEFs expressing the N-terminally truncated PKR should be evaluated with caution. Importantly, we used not only MEFs expressing PKR lacking kinase activity but also several other cell systems and approaches to prevent SG formation, all of which indicated that SG are dispensable for efficient induction of the IFN- α/β pathway.

The issue remains why MDA5 localizes to SG upon mengo-Zn infection. Our observation that MDA5 also localized to SG under nonviral stress conditions, such as heat shock and arsenic acid treatment, strongly suggests that MDA5 is recruited to SG independently of its function as a PRR. Similar to the observations concerning MDA5, other members of the DExD/H-box RNA helicase family such as RHAU, DDX1, DDX3, and DDX6 were also shown to reside in SG under stress conditions (reviewed in reference 12). Therefore, it might be that the RNA screening function of MDA5, which includes also binding to nonviral RNA (4, 5), results in its SG association under stress conditions, but this requires further investigation.

ACKNOWLEDGMENTS

We thank S. Akira, Z. J. Chen, J. Bell, R. J. Kaufman, T. Michiels, and C. A. de Haan for the kind gift of MEFs. M.A.L. is supported by a Rubicon grant, and Q.F. is supported by a Mosaic grant from the Netherlands Organization for Scientific Research (NWO) (NWO-825.11.022 and NWO-017.006.043, respectively).

REFERENCES

1. Hornung V, Ellegast J, Kim S, Brzozka K, Jung A, Kato H, Poeck H, Akira S, Conzelmann KK, Schlee M, Endres S, Hartmann G. 2006. 5'-Triphosphate RNA is the ligand for RIG-I. *Science* 314:994–997.
2. Kato H, Takeuchi O, Mikamo-Satoh E, Hirai R, Kawai T, Matsushita K, Hiiragi A, Dermody TS, Fujita T, Akira S. 2008. Length-dependent recognition of double-stranded ribonucleic acids by retinoic acid-inducible gene-I and melanoma differentiation-associated gene 5. *J. Exp. Med.* 205:1601–1610.
3. Schmidt A, Schwerd T, Hamm W, Hellmuth JC, Cui S, Wenzel M, Hoffmann FS, Michallet MC, Besch R, Hopfner KP, Endres S, Rothenfusser S. 2009. 5'-Triphosphate RNA requires base-paired structures to activate antiviral signaling via RIG-I. *Proc. Natl. Acad. Sci. U. S. A.* 106:12067–12072.
4. Berke IC, Modis Y. 2012. MDA5 cooperatively forms dimers and ATP-sensitive filaments upon binding double-stranded RNA. *EMBO J.* 31:1714–1726.
5. Peisley A, Lin C, Wu B, Orme-Johnson M, Liu M, Walz T, Hur S. 2011. Cooperative assembly and dynamic disassembly of MDA5 filaments for viral dsRNA recognition. *Proc. Natl. Acad. Sci. U. S. A.* 108:21010–21015.
6. Jiang X, Kinch LN, Brautigam CA, Chen X, Du F, Grishin NV, Chen ZJ. 2012. Ubiquitin-induced oligomerization of the RNA sensors RIG-I and MDA5 activates antiviral innate immune response. *Immunity* 36:959–973.
7. Hou F, Sun L, Zheng H, Skaug B, Jiang QX, Chen ZJ. 2011. MAVS forms functional prion-like aggregates to activate and propagate antiviral innate immune response. *Cell* 146:448–461.
8. Seth RB, Sun L, Ea CK, Chen ZJ. 2005. Identification and characterization of MAVS, a mitochondrial antiviral signaling protein that activates NF- κ B and IRF 3. *Cell* 122:669–682.
9. Beckham CJ, Parker R. 2008. P bodies, stress granules, and viral life cycles. *Cell Host Microbe*

3:206–212.

10. White JP, Lloyd RE. 2012. Regulation of stress granules in virus systems. *Trends Microbiol.* 20:175–183.

11. Dever TE. 2002. Gene-specific regulation by general translation factors. *Cell* 108:545–556.

12. Buchan JR, Parker R. 2009. Eukaryotic stress granules: the ins and outs of translation. *Mol. Cell* 36:932–941.

13. Han AP, Yu C, Lu L, Fujiwara Y, Browne C, Chin G, Fleming M, Leboulch P, Orkin SH, Chen JJ. 2001. Heme-regulated eIF2alpha kinase (HRI) is required for translational regulation and survival of erythroid precursors in iron deficiency. *EMBO J.* 20:6909–6918.

14. Dever TE, Feng L, Wek RC, Cigan AM, Donahue TF, Hinnebusch AG. 1992. Phosphorylation of initiation factor 2 alpha by protein kinase GCN2 mediates gene-specific translational control of GCN4 in yeast. *Cell* 68:585–596.

15. Farrell PJ, Balkow K, Hunt T, Jackson RJ, Trachsel H. 1977. Phosphorylation of initiation factor eIF-2 and the control of reticulocyte protein synthesis. *Cell* 11:187–200.

16. Nallagatla SR, Hwang J, Toroney R, Zheng X, Cameron CE, Bevilacqua PC. 2007. 5'-Triphosphate-dependent activation of PKR by RNAs with short stem-loops. *Science* 318:1455–1458.

17. Harding HP, Zhang Y, Ron D. 1999. Protein translation and folding are coupled by an endoplasmic-reticulum-resident kinase. *Nature* 397:271–274.

18. Berlanga JJ, Ventoso I, Harding HP, Deng J, Ron D, Sonenberg N, Carrasco L, de Haro C. 2006. Antiviral effect of the mammalian translation initiation factor 2alpha kinase GCN2 against RNA viruses. *EMBO J.* 25:1730–1740.

19. Lindquist ME, Lifland AW, Utley TJ, Santangelo PJ, Crowe JE, Jr. 2010. Respiratory syncytial virus induces host RNA stress granules to facilitate viral replication. *J. Virol.* 84:12274–12284.

20. Raaben M, Groot Koerkamp MJ, Rottier PJ, de Haan CA. 2007. Mouse hepatitis coronavirus replication induces host translational shutoff and mRNA decay, with concomitant formation of stress granules and processing bodies. *Cell Microbiol.* 9:2218–2229.

21. Ruggieri A, Dazert E, Metz P, Hofmann S, Bergeest JP, Mazur J, Bankhead P, Hiet MS, Kallis S, Alvisi G, Samuel CE, Lohmann V, Kaderali L, Rohr K, Frese M, Stoecklin G, Bartenschlager R. 2012. Dynamic oscillation of translation and stress granule formation mark the cellular response to virus infection. *Cell Host Microbe* 12:71–85.

22. Henao-Mejia J, Liu Y, Park IW, Zhang J, Sanford J, He JJ. 2009. Suppression of HIV-1 Nef translation by Sam68 mutant-induced stress granules and nef mRNA sequestration. *Mol. Cell* 33:87–96.

23. Borghese F, Michiels T. 2011. The leader protein of cardioviruses inhibits stress granule assembly. *J. Virol.* 85:9614–9622.

24. Fujimura K, Kano F, Murata M. 2008. Identification of PCBP2, a facilitator of IRES-mediated translation, as a novel constituent of stress granules and processing bodies. *RNA* 14:425–431.

25. Feng Q, Hato SV, Langereis MA, Zoll J, Virgen-Slane R, Peisley A, Hur S, Semler BL, van Rij RP, van Kuppeveld F. 2012. MDA5 detects the double-stranded RNA replicative form in picornavirus-

infected cells. *Cell Rep.* 2:1187–1196.

26. Barral PM, Sarkar D, Su ZZ, Barber GN, DeSalle R, Racaniello VR, Fisher PB. 2009. Functions of the cytoplasmic RNA sensors RIG-I and MDA-5: key regulators of innate immunity. *Pharmacol. Ther.* 124:219–234.

27. White JP, Lloyd RE. 2011. Poliovirus unlinks TIA1 aggregation and mRNA stress granule formation. *J. Virol.* 85:12442–12454.

28. Hato SV, Ricour C, Schulte BM, Lanke KH, de Bruijini M, Zoll J, Melchers WJ, Michiels T, van Kuppeveld FJ. 2007. The mengovirus leader protein blocks interferon-alpha/beta gene transcription and inhibits activation of interferon regulatory factor 3. *Cell Microbiol.* 9:2921–2930.

29. Ricour C, Delhaye S, Hato SV, Olenyik TD, Michel B, van Kuppeveld FJ, Gustin KE, Michiels T. 2009. Inhibition of mRNA export and dimerization of interferon regulatory factor 3 by Theiler's virus leader protein. *J. Gen. Virol.* 90:177–186.

30. van Pesch V, van Eyll O, Michiels T. 2001. The leader protein of Theiler's virus inhibits immediate-early alpha/beta interferon production. *J. Virol.* 75:7811–7817.

31. Zoll J, Melchers WJ, Galama JM, van Kuppeveld FJ. 2002. The mengovirus leader protein suppresses alpha/beta interferon production by inhibition of the iron/ferritin-mediated activation of NF-kappa B. *J. Virol.* 76:9664–9672.

32. Agol VI, Gmyl AP. 2010. Viral security proteins: counteracting host defences. *Nat. Rev. Microbiol.* 8:867–878.

33. Wang X, Li M, Zheng H, Muster T, Palese P, Beg AA, Garcia-Sastre A. 2000. Influenza A virus NS1 protein prevents activation of NF-kappaB and induction of alpha/beta interferon. *J. Virol.* 74:11566–11573.

34. Khapersky DA, Hatchette TF, McCormick C. 2012. Influenza A virus inhibits cytoplasmic stress granule formation. *FASEB J.* 26:1629–1639.

35. Bhoj VG, Sun Q, Bhoj EJ, Somers C, Chen X, Torres JP, Mejias A, Gomez AM, Jafri H, Ramilo O, Chen ZJ. 2008. MAVS and MyD88 are essential for innate immunity but not cytotoxic T lymphocyte response against respiratory syncytial virus. *Proc. Natl. Acad. Sci. U. S. A.* 105:14046–14051.

36. Abraham N, Stojdl DF, Duncan PI, Methot N, Ishii T, Dube M, Vanderhyden BC, Atkins HL, Gray DA, McBurney MW, Koromilas AE, Brown EG, Sonenberg N, Bell JC. 1999. Characterization of transgenic mice with targeted disruption of the catalytic domain of the doublestranded RNA-dependent protein kinase, PKR. *J. Biol. Chem.* 274:5953–5962.

37. Harding HP, Novoa I, Zhang Y, Zeng H, Wek R, Schapira M, Ron D. 2000. Regulated translation initiation controls stress-induced gene expression in mammalian cells. *Mol. Cell* 6:1099–1108.

38. Harding HP, Zhang Y, Bertolotti A, Zeng H, Ron D. 2000. Perk is essential for translational regulation and cell survival during the unfolded protein response. *Mol. Cell* 5:897–904.

39. Scheuner D, Song B, McEwen E, Liu C, Laybutt R, Gillespie P, Saunders T, Bonner-Weir S, Kaufman RJ. 2001. Translational control is required for the unfolded protein response and in vivo glucose homeostasis. *Mol. Cell* 7:1165–1176.

40. Wessels E, Duijsings D, Notebaart RA, Melchers WJ, van Kuppeveld FJ. 2005. A proline-rich region in the coxsackievirus 3A protein is required for the protein to inhibit endoplasmic reticulum-to-golgi transport. *J. Virol.* 79:5163–5173.
41. Yoneyama M, Kikuchi M, Matsumoto K, Imaizumi T, Miyagishi M, Taira K, Foy E, Loo YM, Gale M, Jr, Akira S, Yonehara S, Kato A, Fujita T. 2005. Shared and unique functions of the DExD/H-box helicases RIG-I, MDA5, and LGP2 in antiviral innate immunity. *J. Immunol.* 175:2851–2858.
42. Barral PM, Morrison JM, Drahos J, Gupta P, Sarkar D, Fisher PB, Racaniello VR. 2007. MDA-5 is cleaved in poliovirus-infected cells. *J. Virol.* 81:3677–3684.
43. White JP, Cardenas AM, Marissen WE, Lloyd RE. 2007. Inhibition of cytoplasmic mRNA stress granule formation by a viral proteinase. *Cell Host Microbe* 2:295–305.
44. Piotrowska J, Hansen SJ, Park N, Jamka K, Sarnow P, Gustin KE. 2010. Stable formation of compositionally unique stress granules in virusinfected cells. *J. Virol.* 84:3654–3665.
45. Mukherjee A, Morosky SA, Delorme-Axford E, Dybdahl-Sissoko N, Oberste MS, Wang T, Coyne CB. 2011. The coxsackievirus B 3C protease cleaves MAVS and TRIF to attenuate host type I interferon and apoptotic signaling. *PLoS Pathog.* 7:e1001311. doi:10.1371/journal.ppat.1001311.
46. Mazroui R, Di Marco S, Kaufman RJ, Gallouzi IE. 2007. Inhibition of the ubiquitin-proteasome system induces stress granule formation. *Mol. Biol. Cell* 18:2603–2618.
47. Romanova LI, Lidsky PV, Kolesnikova MS, Fominykh KV, Gmyl AP, Sheval EV, Hato SV, van Kuppeveld FJ, Agol VI. 2009. Antiapoptotic activity of the cardiovirus leader protein, a viral “security” protein. *J. Virol.* 83:7273–7284.
48. Zhang Y, Li Z, Ge X, Guo X, Yang H. 2011. Autophagy promotes the replication of encephalomyocarditis virus in host cells. *Autophagy* 7:613–628.
49. Kato H, Takeuchi O, Sato S, Yoneyama M, Yamamoto M, Matsui K, Uematsu S, Jung A, Kawai T, Ishii KJ, Yamaguchi O, Otsu K, Tsujimura T, Koh CS, Reis e Sousa C, Matsuura Y, Fujita T, Akira S. 2006. Differential roles of MDA5 and RIG-I helicases in the recognition of RNA viruses. *Nature* 441:101–105.
50. Kang DC, Gopalkrishnan RV, Wu Q, Jankowsky E, Pyle AM, Fisher PB. 2002. mda-5: an interferon-inducible putative RNA helicase with doublestranded RNA-dependent ATPase activity and melanoma growthsuppressive properties. *Proc. Natl. Acad. Sci. U. S. A.* 99:637–642.
51. Kedersha N, Cho MR, Li W, Yacono PW, Chen S, Gilks N, Golan DE, Anderson P. 2000. Dynamic shuttling of TIA-1 accompanies the recruitment of mRNA to mammalian stress granules. *J. Cell Biol.* 151:1257–1268.
52. Kedersha N, Chen S, Gilks N, Li W, Miller IJ, Stahl J, Anderson P. 2002. Evidence that ternary complex (eIF2-GTP-tRNA(i)(Met))-deficient preinitiation complexes are core constituents of mammalian stress granules. *Mol. Biol. Cell* 13:195–210.
53. Jounai N, Takeshita F, Kobiyama K, Sawano A, Miyawaki A, Xin KQ, Ishii KJ, Kawai T, Akira S, Suzuki K, Okuda K. 2007. The Atg5 Atg12 conjugate associates with innate antiviral immune responses. *Proc. Natl. Acad. Sci. U. S. A.* 104:14050–14055.
54. Lei Y, Wen H, Yu Y, Taxman DJ, Zhang L, Widman DG, Swanson KV, Wen KW, Damania B,

Moore CB, Giguere PM, Siderovski DP, Hiscott J, Razani B, Semenkovich CF, Chen X, Ting JP. 2012. The mitochondrial proteins NLRX1 and TUFM form a complex that regulates type I interferon and autophagy. *Immunity* 36:933–946.

55. Delgado MA, Elmaoued RA, Davis AS, Kyei G, Deretic V. 2008. Toll-like receptors control autophagy. *EMBO J.* 27:1110–1121.

56. Sanjuan MA, Dillon CP, Tait SW, Moshiah S, Dorsey F, Connell S, Komatsu M, Tanaka K, Cleveland JL, Withoff S, Green DR. 2007. Toll-like receptor signalling in macrophages links the autophagy pathway to phagocytosis. *Nature* 450:1253–1257.

57. Clavarino G, Claudio N, Couderc T, Dalet A, Judith D, Camosseto V, Schmidt EK, Wenger T, Lecuit M, Gatti E, Pierre P. 2012. Induction of GADD34 is necessary for dsRNA-dependent interferon-beta production and participates in the control of Chikungunya virus infection. *PLoS Pathog.* 8:e1002708. doi:10.1371/journal.ppat.1002708.

58. Sen A, Pruijssers AJ, Dermody TS, Garcia-Sastre A, Greenberg HB. 2011. The early interferon response to rotavirus is regulated byPKRand depends on MAVS/IPS-1, RIG-I, MDA-5, and IRF3. *J. Virol.* 85:3717–3732.

59. Schulz O, Pichlmair A, Rehwinkel J, Rogers NC, Scheuner D, Kato H, Takeuchi O, Akira S, Kaufman RJ, Reis e Sousa C. 2010. Protein kinase R contributes to immunity against specific viruses by regulating interferon mRNA integrity. *Cell Host Microbe* 7:354–361.

60. Onomoto K, Jogi M, Yoo JS, Narita R, Morimoto S, Takemura A, Sambhara S, Kawaguchi A, Osari S, Nagata K, Matsumiya T, Namiki H, Yoneyama M, Fujita T. 2012. Critical role of an antiviral stress granule containing RIG-I and PKR in viral detection and innate immunity. *PLoS One* 7:e43031. doi:10.1371/journal.pone.0043031.

61. Yang YL, Reis LF, Pavlovic J, Aguzzi A, Schafer R, Kumar A, Williams BR, Aguet M, Weissmann C. 1995. Deficient signaling in mice devoid of doublestranded RNA-dependent protein kinase. *EMBO J.* 14:6095–6106.

62. Baltzis D, Li S, Koromilas AE. 2002. Functional characterization of pkr gene products expressed in cells from mice with a targeted deletion of the N terminus or C terminus domain of PKR. *J. Biol. Chem.* 277:38364–38372.

63. Bonnet MC, Daurat C, Ottone C, Meurs EF. 2006. The N-terminus of PKR is responsible for the activation of the NF-kappaB signaling pathway by interacting with the IKK complex. *Cell Signal.* 18:1865–1875.

64. Bonnet MC, Weil R, Dam E, Hovanessian AG, Meurs EF. 2000. PKR stimulates NF-kappaB irrespective of its kinase function by interacting with the IkappaB kinase complex. *Mol. Cell. Biol.* 20:4532–4542.

65. Chu WM, Ostertag D, Li ZW, Chang L, Chen Y, Hu Y, Williams B, Perrault J, Karin M. 1999. JNK2 and IKKbeta are required for activating the innate response to viral infection. *Immunity* 11:721–731.

66. Iordanov MS, Wong J, Bell JC, Magun BE. 2001. Activation of NFkappaB by double-stranded RNA (dsRNA) in the absence of protein kinase R and RNase L demonstrates the existence of two separate dsRNA triggered antiviral programs. *Mol. Cell. Biol.* 21:61–72.

Chapter 6

Summary and General Discussion

Part of this chapter will be included in a review article:
Qian Feng, Martijn A. Langereis, Frank J.M. van Kuppeveld.
2014. Cytokine and Growth Factor Reviews.
Submitted upon invitation.

Picornaviruses are a large family of important human and animal pathogens including poliovirus (PV), coxsackievirus (CV), human rhinovirus (HRV), enterovirus 71 (EV71), encephalomyocarditisvirus (EMCV), hepatitis A virus (HAV) and foot-and-mouth disease virus (FMDV). The interaction between picornaviruses and the innate antiviral response is incompletely understood. Upon viral infections, cells are able to recognize invading viral pathogens and mount antiviral responses to limit their replication and spread. RIG-I and MDA5 are crucial intracellular RNA sensors that stimulate IFN- α/β induction upon viral RNA recognition. IFN- α/β are extremely potent antiviral molecular messengers that prime cells to reach an antiviral state by inducing the expression of hundreds of IFN-stimulated genes (ISGs). While RIG-I responds to many negative-strand RNA viruses and a couple of flaviviruses, MDA5 is crucial for sensing several positive-strand RNA viruses, among which picornaviruses. The MDA5-mediated antiviral response forms a significant component in controlling picornavirus infections, as mice deficient in MDA5 or MAVS, the downstream adaptor molecule, have been shown to exhibit increased susceptibility to various picornaviruses including CVB3, HRV and EMCV (1–3).

During picornavirus RNA replication, several viral RNA species are generated, all bearing “non-self” features that can be potentially recognized by cellular sensors including MDA5. Which of these picornavirus RNAs can activate MDA5, and more importantly, which of these are actually recognized by MDA5 under physiological conditions (i.e. in infected cells) was unclear. Furthermore, since IFN- α/β exert such potent antiviral activities, many viruses including picornaviruses actively interfere with the IFN- α/β system. How picornaviruses interact with the RLR-mediated IFN- α/β induction pathway had been studied by several groups, using different viruses and studying one factor at a time. The results of these studies were fragmented and sometimes contradictory. Thus, no common evasion strategies had emerged for any specific group of picornaviruses. Moreover, the cellular stress response has been recently suggested to have antiviral effects for some viruses. The interaction between picornaviruses and the stress pathway are just starting to be understood.

This thesis focuses on deepening our knowledge on the recognition of picornaviruses by the RLRs as well as the viral strategies to evade innate antiviral responses. Two important genera of picornaviruses, namely *Enterovirus* and *Cardiovirus*, are studied in this thesis using two model viruses, CVB3 and EMCV (strain mengovirus), respectively.

SUMMARY OF MAIN FINDINGS

As mentioned before, the natural ligand of MDA5 in picornavirus-infected cells was unknown. In **Chapter 2**, we first systematically examined the role of different picornavirus RNA species in activating MDA5 by transfection studies, then provided the first glimpse of picornaviral RNA recognition during a normal infection. By separating ssRNA and dsRNA fractions from CVB3- or mengovirus-infected cells, and by digestion with RNases specific for ssRNAs or dsRNAs, we demonstrated that a dsRNA-specific RNase-sensitive RNA species was able to activate MDA5 upon transfection. This conclusion was supported by experiments using purified viral RNA species. RF purified from infected cells potently activated MDA5. In contrast, viral ssRNAs, including the VPg-containing virion RNA as well as the VPg-lacking viral mRNAs did not induce any IFN- α/β response in transfected cells. We further demonstrated that RF can directly

activate MDA5, without additional factor(s), in an *in vitro* assay. Importantly, using inhibitors of different steps of virus replication, we showed that negative-strand RNA synthesis, the step that generates the RF, is a prerequisite for IFN- β mRNA production in mengovirus-infected cells.

Chapter 3 describes the use of a small, artificial 5' triphosphate (5'ppp)-containing RNA transcript, as a highly potent antiviral agent via RIG-I activation. The sequence of this RNA molecule is derived from the cloverleaf (CL) structure found in the 5' UTR of CVB3 genomic RNA. Transfection of this RNA ligand induced production of IFN- α/β , type III interferons, as well as proinflammatory cytokines and chemokines. Cells pretreated with CVB3 CL RNA were protected against challenge viral infections including dengue virus, vasicular stomatitis virus (VSV) as well as EV71.

As sophisticated as our antiviral responses are, viruses are masters at circumventing these reactions and navigating the hostile environment in the host. In **Chapter 4** and **5** we describe the evasion strategies of CVB3 and other enteroviruses as well as mengovirus with respect to two important antiviral systems of the cell – the RLR-mediated IFN- α/β induction pathway, and the stress response. In **Chapter 5** we also explore a possible interaction between these two cellular antiviral pathways themselves.

In **Chapter 4** we show that both CVB3 and mengovirus effectively suppress IRF3 phosphorylation. In CVB3-infected cells, TBK1 phosphorylation, which is required for its activity to phosphorylate and activate IRF3, is severely inhibited, indicating that the blockade of the RLR signaling pathway lies upstream, or at the level of, TBK1 activation. Mengovirus, on the other hand, induced significant levels of TBK1 phosphorylation. Thus, the IFN- α/β induction pathway is inhibited at a step between TBK1 activation and IRF3 phosphorylation. We further showed that MDA5, MAVS and RIG-I were cleaved during CVB3 infection, but remained intact in mengovirus-infected cells. Unlike previously published for a number of enteroviruses (4), CVB3-induced MDA5 cleavage was not due to caspase or proteasome activities. Using recombinant 2A^{pro} and 3C^{pro} of CVB3, we demonstrated that the same cleavage patterns of MDA5 and MAVS could be reproduced by treatment with 2A^{pro}, whereas that of RIG-I by 3C^{pro}. We then studied the effect of 2A^{pro} and 3C^{pro} of various enterovirus species in an infection context by inserting the coding region of individual enterovirus proteinases into the genome of mengovirus. Using these recombinant mengoviruses, we showed that MDA5 and MAVS are both targeted by 2A^{pro} of a number of enteroviruses representing species *Enterovirus A* (EV71), *B* (CVB3) and *C* (PV). Cleavage of RIG-I, on the other hand, relied on the 3C^{pro} activities of these viruses.

Besides interfering with the RLR pathway, we show in **Chapter 5** that both CVB3 and mengovirus also interfere with the formation of SGs in infected cells. In the case of mengovirus, SG inhibition was attributed to the activity of the viral L protein. Infection of a recombinant virus carrying a mutant L (L^{mut}) led to formation of large numbers of SGs, the formation of which was dependent on the activity of PKR. SG formation negatively affected virus replication, albeit moderately, which was likely independent of the RLR-mediated IFN- α/β response. Interestingly, MDA5 localizes to SGs upon L^{mut} mengovirus infection, heat shock as well as oxidative stress. However, this localization did not appear essential for SG formation, nor was it important for mengovirus RNA recognition. The exact underlying antiviral mechanism of SGs during picornavirus infection remains to be elucidated.

GENERAL DISCUSSION

I. Picornavirus recognition by the RIG-I-like receptors (RLRs)

What is the viral PAMP(s) that activates MDA5 in picornavirus-infected cells?

MDA5 is a crucial receptor for mounting IFN- α/β response against several viruses. Although much research has been conducted using *in vitro* assays, our knowledge on natural MDA5 activation in infected cells is still extremely scarce. A picornavirus RNA replication intermediates, namely the RF, was able to induce MDA5 activation when transfected into cells in its purified form (**Chapter 2**). Using inhibitors of different steps of viral RNA replication, we showed that RF formation is absolutely required to activate MDA5 during a picornavirus infection (**Chapter 2**). Another replication intermediate of enteroviruses, the RI, was also shown to activate MDA5 upon transfection (5), but whether this molecule truly contributes to MDA5 activation during an infection remains to be investigated. Recent findings indicate that MDA5 activation involves formation of filamentous MDA5 oligomers along the length of dsRNAs (6–9), and the stability of the MDA5 filaments is shown to be directly related to the length of the RNA ligand (6). In other words, the longer the dsRNA, the more stable the MDA5 filament, and (presumably) the more efficient the MAVS activation. While dsRNAs as short as 112 bp have been successfully used to induce recombinant MDA5 activation in *in vitro* studies, transfection studies in cultured cells suggest that longer dsRNAs may be necessary to induce MDA5-mediated IFN- α/β response (10). Unlike the RF, which is a RNA duplex of 7-8 kbp, the RI is a primarily ssRNA molecule, containing many protruding single-stranded ends – incomplete positive-strand RNAs undergoing active transcription, with double-stranded regions (11). In addition, RI (and RF) is most likely coated with numerous host and viral factors that support RNA replication during infection. Whether there are sufficient free MDA5 binding sites on the double-stranded regions of RI to allow efficient MAVS activation remains to be demonstrated.

Role of LGP2 and possible additional RNA PAMPs for picornavirus-induced MDA5 activation

It was previously reported that wt EMCV-induced IFN- α/β is not only dependent on MDA5 but also LGP2 (12), the RLR that lacks the ability to signal to MAVS but retains RNA binding activity. In line with this finding, Deddouche and colleagues recently revealed that LGP2-associated RNAs isolated from EMCV-infected cells exert MDA5-stimulatory activity upon transfection of naive cells (13). Deep-sequencing analysis of the RNA pool that co-immunoprecipitated (IP) with LGP2 upon EMCV infection revealed a clear enrichment for a small (~ 170 nt) region in the viral negative-strand RNA, complementary to the L-encoding region. Remarkably, when this small L antisense RNA was produced by *in vitro* transcription and transfected into cells, it led to MDA5 activation. The complementary sequence (L sense RNA), on the other hand, failed to activate MDA5 upon transfection, suggesting that the sequence may be of importance in this case. Several questions arise in view of these recent findings.

L Antisense RNA or RF?

The instinctively urgent question is whether the recent report contradicts the finding that the RF is an important MDA5 ligand during picornavirus infection. Not likely. A recombinant EMCV carrying deletions in the L-encoding region (Δ L), and thereby could not produce the 170 nt L

antisense RNA during infection, nonetheless induced IFN- α/β response, albeit to a lesser extent than another recombinant virus that also lacks the functional L protein due to point mutations but can produce the L antisense RNA (13). In addition, similar Δ L mutants of cardioviruses have been widely used as IFN-stimulating viruses in many studies (14–16). Together, these results clearly indicate that other IFN-stimulatory viral PAMPs are produced during EMCV infection, quite possibly the RF, and perhaps also the RI. Furthermore, not all picornavirus genomes contain a RNA fragment that shares significant sequence similarity with the L RNA found in EMCV. Whether viruses from other genera also produce small, LGP2-associated, MDA5-stimulating RNAs is to be further investigated. Nonetheless, for EMCV, the 170 nt L antisense RNA may represent an important viral PAMP that contributes to IFN- α/β activation during infection.

Small antisense L RNA or the whole minus-strand RNA?

Secondly, it is important to investigate whether the 170 nt L antisense RNA is produced as a specific entity during EMCV infection, or it merely represents the most stable fragment of a larger trunk of, or even the full-length, negative-strand RNA during the isolation procedure. Northern blotting analysis failed to detect this RNA species in total RNA preparation from EMCV-infected cells (13). However, given the difference in sensitivity between Northern blotting and deep-sequencing, this does not necessarily disprove the existence of this small RNA. RNase L has been reported to generate small RNAs from host and viral RNAs, which can then activate RIG-I and MDA5 (17–19). However, there is no evidence of involvement of RNase L in this case since no enrichment of any host sequence was found after LGP2 IP. Moreover, ribosomal RNAs also remained intact during EMCV infection ((13) and **Chapter 2**). This is also supported by our data that no significant difference in IFN- α/β response against mengo-Zn infection was observed in RNase L KO cells as compared to wt cells (**Chapter 2**). It remains to be clarified whether and, if so, how this small viral negative-sense RNA is produced during EMCV infection.

LGP2-MDA5 interaction in the context of picornavirus infection

LGP2 has long been thought to play regulatory roles on RIG-I and MDA5. A previous study reported that LGP2 was required for EMCV-induced MDA5 activation (12), however no mechanistic explanation was provided. Deddouche et al showed that the small L antisense RNA co-precipitated with LGP2, and not MDA5, but induced an MDA5-dependent IFN- α/β response upon transfection (13). This led the authors to hypothesize that perhaps LGP2 first binds to this small RNA, and then recruits MDA5 molecules and facilitates its interaction with MAVS. This model is supported by subtle differences in the interactions between LGP2 and MDA5 with their respective RNA ligands. Although both receptors primarily bind dsRNAs, LGP2 seems to display higher affinity to dsRNAs than MDA5 (20, 21). In addition, although LGP2 dimerization and oligomerization seem to require dsRNAs of 30-40 bp (22), it has been shown to bind to shorter dsRNAs (some as short as 8 bp) or even single-stranded *in vitro* transcripts with predicted base-paired regions (20, 23, 24). MDA5, on the other hand, requires long dsRNAs to become activated (10, 25, 26). The 170 nt EMCV L antisense RNA is predicted to form base-paired regions, and was indeed sensitive to both ssRNA- and dsRNA-specific RNases (13). It is possible that LGP2 binds to the structured regions within this small RNA, and then stimulates MDA5 activation. LGP2 and MDA5 can interact with each other, though this seems to depend on the presence of dsRNAs (27). It remains to be clarified whether the base-paired regions in the L antisense RNA are sufficient to facilitate such LGP2/MDA5 complex formation, or LGP2 induces MDA5 activation via a yet unknown mechanism.

It is also intriguing to ask whether picornavirus RF-mediated MDA5 activation also requires, or can be enhanced by, LGP2. Our data that purified RF is able to activate recombinant MDA5 *in vitro* (**Chapter 2**) indicates that MDA5 can be directly activated by this RNA. However, as mentioned above, RF is very likely associated with multiple host and viral factors in infected cells. It is to be investigated whether MDA5 is able to form long filaments on the RF during active virus replication. Examining IFN- α/β response in LGP2 KO cells versus wt cells upon Δ L EMCV infection, which does not produce the L antisense RNA, should shed some light on this issue. It will also be interesting to investigate whether LGP2 and MDA5 can intrinsically collaborate and form filamentous heterooligomers on long dsRNAs.

Future perspectives – picornavirus RNA recognition by RLRs

As mentioned above, our understanding of MDA5 activation during natural viral infections is limited. We provided a first glimpse on MDA5 activation during picornavirus infection, namely that the negative-strand RNA synthesis is required (**Chapter 2**), but much is still to be learned about MDA5 activation during virus infections in general. What RNA(s) are directly bound by MDA5? What is the minimum length of MDA5 filaments that can activate MAVS in cells? Is LGP2 a positive regulator of MDA5 in general, or is it only needed for specific (types of) RNA ligands? IP-based approaches have been successfully used to identify RIG-I- and LGP2-associated RNAs from virus-infected cells (13, 28), however, no such data has been published, to date, for MDA5. Authors of the recent report on the L antisense RNA indicated that MDA5 IP had been performed but consistently failed to yield immune-stimulatory RNAs (13). Although *in vitro* studies of RNA binding by recombinant MDA5 have been reported, they seem to indicate that MDA5 has relative weak affinity for dsRNAs as compared to RIG-I and LGP2 (20, 21). Also, if MDA5 is only able to form short filaments on viral ligands in infected cells (because RNAs are partially covered by other factors), these filaments will quickly disassemble (26), making it more difficult to isolate. These observations may explain why MDA5 IP from infected cells, where the concentrations of both MDA5 and available viral ligands cannot compare to those used in *in vitro* assays, could be problematic. While IP remains to be a valuable tool to study MDA5-RNA interactions in cells, super-resolution microscopy studies can also provide valuable insights. Lots of advances have been made in protein and RNA tagging and labeling in the recent years. For instance, the CRISPR/Cas9 genome editing system makes it technically approachable to add tags to endogenous proteins (29). Click-based labeling methods have been used to label *de novo* synthesized viral RNAs (30). And new techniques such as Multiply Labeled Tetravalent RNA Imaging Probe (MTIRP) have been used to label single-molecule RNAs in live cells (31). Combinations of these tools may provide powerful methods to study MDA5/RNA, MDA5/LGP2 interactions in the context of an ongoing infection.

Furthermore, these methods will also reveal where in an infected cell MDA5 gains access to viral dsRNA. As explained in **Chapter 1**, picornavirus RNA replication occurs at densely packed membranous structures, the replication organelles (ROs), and viral proteins and RNAs, including the RF, are presumably concentrated at these sites. Whether MDA5 (and LGP2) specifically locate to these structures to detect viral RNA products, or small amounts of viral RNA ligands leak from the ROs into the cytosol where they are detected by MDA5 remains to be elucidated. Recently, it was shown by immunofluorescence staining that dsRNA (as visualized by an antibody that recognizes RNA duplexes longer than 40 bp) colocalizes with MDA5, but not RIG-I, at what

appears to be punctate structures in the cytoplasm of picornavirus-infected cells (5). It remains to be investigated where these MDA5/dsRNA punctae localize with respect to the ROs (e.g. as stained by a viral protein). Electron microscopy studies have been extremely helpful to visualize these replication structures. Together with immunostaining for dsRNA and MDA5 this could help to clarify where MDA5 activation occurs in infected cells.

II. Use of pattern recognition receptor (PRR) ligands as immune modulatory agents

Research on PRRs have not only deepened our understanding on virus recognition, but have also led to a new approach exploiting these PRR pathways for immune modulatory purposes such as the development of vaccine adjuvants, antiviral agents and even anti-cancer therapeutics (32–38). PRR ligands induce IFN- α/β production, and thereby, the expression of the classical ISGs and activation of the innate and adaptive immune system. Additionally, PRR pathways also lead to NF- κ B activation and consequently the production of many proinflammatory cytokines and chemokines, all important players of the antiviral system. It is also thought that by using PRR ligands one activates the immune system in a similar manner as during an infection, possibly leading to more balanced immune activation (38).

In comparison to Toll-like receptor (TLR) ligands, RLR ligands can potentially activate IFN- α/β and cytokine production in virtually all nucleated cells (at the site of administration) due to the ubiquitous expression of the receptors. Between RIG-I and MDA5, there may not be a theoretical advantage to activate one or the other. However, small RIG-I ligands, such as the VSV hairpin or the CVB3 CL RNA (**Chapter 3**), may prove more economical to produce (in a unified form) than the long dsRNAs that activate MDA5. Smaller RNA molecules may also have more desirable pharmacological kinetics since they are likely more stable, and can be more efficiently delivered. One current technical challenge in producing small RIG-I ligands is perhaps the production of 5'ppp moiety at the termini of RNAs under GMP (Good Manufacturing Practices) and GLP (Good Laboratory Practice) conditions. But research in the field of synthetic chemistry are currently underway to hopefully resolve this issue in the near future (39, 40).

Of course, to activate intracellular receptors such as the RLRs, one must combine the RNA ligand with a delivery reagent. Many lipid- or non-lipid-based *in vivo* delivery reagents are currently available for animal use (42, 43). Additionally, virosomes – artificial virus membrane envelopes – have been shown to utilize viral proteins that are integrated at the surface to deliver its contents in the cytoplasm of target cells (reviewed in (44)). These reagents make intracellular delivery of RLR ligands technically feasible. Some virosomes and other forms of liposomes with surface modifications can even specifically target the liver for delivery (reviewed in (45, 46)), presenting opportunities to use these RLR ligands as therapeutics to treat liver infections such as hepatitis B and C, for which systematic interferon therapy has been used, at the price of severe and prolonged side effects. However, much research is required to study the combination of RLR ligands with delivery reagents/systems, and the safety profile for repeated (as in the case of vaccine adjuvant) and prolonged (as in the case of chronic hepatitis infection treatment) administration.

III. Strategies of picornaviruses to evade the IFN- α/β system

IFN- α/β is a powerful antiviral system, such that most viruses actively suppress the induction and/or signaling of IFN- α/β to gain replication advantage. IFN- α/β antagonization is so crucial to viruses that many of them interfere with multiple steps of the IFN- α/β system (47–52). It comes as no surprise that also picornaviruses have developed various strategies to interfere with the IFN- α/β antiviral response. A few established picornavirus-induced modifications to the host cell have been proposed as potential IFN- α/β antagonization mechanisms. As mentioned in **Chapter 1**, members of both *Enterovirus* and *Cardiovirus* genera inhibit host cell cap-dependent translation (53), which have been thought to also inhibit cytokine production. In addition, enteroviruses-induced secretory pathway inhibition (54–57) has also been shown to reduce the secretion of IFN- α/β and other cytokines (58), though only little amounts of these proteins are produced during enterovirus infections due to upstream blockades. Although these events may also contribute to limiting host antiviral responses, we and others showed that little IFN- α/β mRNAs can be detected during enterovirus and cardiovirus infections (**Chapter 4, 5** and (5, 59–62)), implicating that the actual blockade lies upstream, or at the level of, IFN- α/β transcription.

Enteroviral strategies to restrict IFN- α/β transcription

Enterovirus infections trigger little, if any, IRF3 activation (59–61). In **Chapter 4**, we showed that in CVB3-infected cells, TBK1 phosphorylation, a prerequisite for its activity to phosphorylate downstream substrates including IRF3, was only marginally observed, indicating inactivation of the pathway upstream of TBK1 activation. Concurrently, both MDA5 and its downstream interaction partner MAVS are cleaved by 2A^{pro} of different enterovirus species, providing a probable explanation for the lack of activation of downstream signaling molecules. In addition, these results also suggest that various species of enteroviruses very likely employ a unified mechanism to interfere with the RLR-mediated IFN- α/β induction pathway.

MAVS inactivation seems to be a common viral countermeasure to restrict IFN- α/β response. For instance, both HAV and hepatitis C virus (HCV) target MAVS for proteolytic cleavage by viral proteinases during infection (63, 64), and Hepatitis B virus promotes ubiquitination and subsequent proteasomal degradation of this adaptor molecule (65). Interestingly, since MAVS is localized primarily to mitochondria, viral proteinases that target MAVS must also localize to (the vicinity of) these specific sites to carry out their tasks. The HAV proteinase responsible for MAVS cleavage (i.e. 3C^{pro}) must be present in its precursor 3ABC form to induce MAVS cleavage, and a transmembrane domain within the 3A protein was shown to be necessary to localize this precursor to the mitochondria (63). The HCV proteinase, NS3/4A, encounters and cleaves MAVS at the mitochondria-associated membrane (MAM) (66), a mitochondria-ER contact site (reviewed in (67)). These results raise an interesting question – where does enterovirus 2A^{pro} encounter MAVS in infected cells? To date, there is no evidence that 2A^{pro} localizes to the mitochondria (or any other specific organelle of the cell) during infection. Is it also recruited to the mitochondria or MAM via interactions with other (host or viral) proteins? Alternatively, do enterovirus ROs, where 2A is produced, “naturally” have contact sites with mitochondria? These questions call for future research focused on subcellular localizations of 2A^{pro}, MAVS and their interaction partners during the course of an infection.

Besides MDA5 and MAVS cleavage, enterovirus-induced IFN- α/β transcription suppression may also partly result from virus-induced disturbance of macromolecule trafficking between the nucleus and the cytoplasm, a phenomenon often referred to as nucleo-cytoplasmic trafficking (NCT) disorder. Nucleoporins (Nups), proteins that form the nuclear pore complex and regulate protein and mRNA trafficking through the nuclear pore, are cleaved in enterovirus-infected cells, leading to a bidirectional loss of selectivity of the pore (68–74). In healthy cells, IRF3 shuttles between the cytoplasm and the nucleus. Upon activation (i.e. phosphorylation) by TBK1, which is a cytoplasmic protein, IRF3 dimerizes and translocates to the nucleus to activate IFN- α/β transcription. It is possible that the shuttling of IRF3 is important for its interaction with TBK1, and the NCT disorder prevents IRF3 phosphorylation by interfering with its shuttling and localization (as discussed in more detail in the section **Cardiovirus evasion strategies – the role of Leader**).

Do picornaviruses hide from cellular immune sensors?

It has also been suggested that virus-induced ROs, which is common to all positive-strand RNA viruses, may inhibit or delay the initial viral RNA recognition by receptors by shielding viral RNAs. While this remains a possible contributing factor for enteroviruses, other evidence suggests that ROs unlikely completely prevent viral RNA recognition by cellular sensors. Dengue virus and West Nile virus both induce formations of membranous structures during replication, but have both been shown to activate RIG-I as well as MDA5 (75–77), suggesting that these RLRs do gain access to viral RNA PAMPs in the presence of virus-induced ROs. Furthermore, the observation that both MDA5 and MAVS are cleaved by a variety of enteroviruses suggests that antagonization of this pathway has likely been selected for during virus evolution, implying that the pathway is, to some degree, turned on during infection.

The role of 3C^{pro} in IFN- α/β antagonization

Enterovirus 3C^{pro} is known to cause virus-induced transcription shutoff. Studying 3C proteinase-dead mutant in the context of natural enterovirus infections is nearly impossible since this protein is essential for viral polyprotein processing. Instead, we recently studied the role of 3C^{pro} in the context of infection of a recombinant EMCV carrying an defective L, which can induce production of large amounts of IFN- α/β mRNA during infection (14, 78, 79). Insertion of enterovirus 3C^{pro} to these recombinant L mutant EMCVs did not impair EMCV-induced IFN- β mRNA induction (Langereis, Feng, et al, unpublished results), suggesting that 3C^{pro}-mediated events such as transcription shutoff (80–82) may be less important in IFN- α/β transcription suppression. In line with this finding, array studies performed in enterovirus-infected cells have shown upregulation of large numbers of gene transcripts (83). In addition, transcription of ISGs and NF- κ B-driven genes have been reported to proceed during PV-induced transcription shutoff (84, 85). These data all point to an incomplete transcription shutoff during enterovirus infection. Another 3C^{pro}-dependent event is the intriguing cleavage of RIG-I by enteroviruses (**Chapter 4**). It is not surprising that RIG-I targeting does not contribute to IFN- α/β antagonization by enteroviruses since it is, to our best knowledge, not involved in detecting picornavirus RNAs. But is it a coincidence that 3C^{pro} of three species of enterovirus all target this factor for cleavage? Not likely. In fact, it has been proposed that RIG-I may be able to directly stimulate STAT1 activation in an IFN- α/β -independent fashion, and thereby activate ISG expression (86), suggesting that enteroviruses may cleave RIG-I in order to prevent an augmentation of ISG expression via the STAT1 pathway.

The important role of 2A^{pro}

Picornaviruses have a very small genome, encoding merely 7 mature non-structural proteins (NSPs) in the case of enteroviruses. Strikingly, one of the enterovirus NSPs, namely 2A^{pro}, is responsible for the cleavage of MDA5, MAVS, as well as Nups, making it a strong candidate for IFN- α/β antagonist. Recently, we also studied the ability of enterovirus 2A^{pro} to counteract IFN- α/β response in the context of the EMCV (L mutant) infection. Unlike 3C^{pro}, insertion of enterovirus 2A^{pro} almost completely abolished the EMCV-triggered IFN- α/β transcription activation (Langereis, Feng, et al, unpublished results), confirming a prominent role of 2A^{pro} in IFN- α/β antagonization.

It remains to be clarified which of the activities of 2A^{pro} serve(s) as the primary IFN- α/β suppression mechanism during enterovirus infections. As mentioned above, 2A^{pro} antagonizes the RLR signaling pathway by cleaving MDA5 and MAVS. In addition, it induces NCT disorder by cleaving several Nups, possibly negatively affecting IRF3 activation. With respect to the timing of these events, NCT disorder can be observed rather early during infection (i.e. before the exponential phase of viral RNA accumulation, data not shown). The cleavages of MDA5 and MAVS, on the other hand, were not detectable until after viral RNA level had reached its plateau under the conditions used (**Chapter 4**), urging one to ask whether these events are simply too late to possibly benefit virus replication. To answer this question, one must consider the microenvironment where virus replication takes place. It is quite possible that 2A^{pro} already actively engage in cleaving MDA5 and/or MAVS at early stage of infection, but only does so in the vicinity of viral RNA replication where the ligands of MDA5 are produced. Such local cleavage of a small number of MDA5 and/or MAVS molecules would not be detectable when analyzing whole cytoplasmic lysates by immunoblotting. To demonstrate the consequence of each 2A^{pro}-mediated event, one must study these events in isolation. Unfortunately, our current knowledge on 2A recognition site does not allow us to generate mutants that are specifically deficient in recognizing a given target protein. Alternatively, one could produce cleavage-resistant mutants of each or combinations of target(s) (e.g. MDA5 and MAVS) and study the effects of their expression on virus replication. Of note, overexpression of MDA5 and MAVS by themselves are known to induce IFN- α/β activation without additional triggers (64, 87, 88). Therefore, the expression levels of these proteins must be kept as similar to their endogenous levels as possible during these experiments. As mentioned above, the recently established CRISPR/Cas9 system allows genomic gene editing, i.e. introducing mutations in endogenous genes, providing an plausible system to study 2A^{pro} cleavage-resistant factors (such as MDA5, MAVS and Nups) in picornavirus replication.

Cardiovirus evasion strategies – the role of Leader

As mentioned above, cardioviruses also efficiently inhibit IFN- α/β transcription activation. Members from both species of cardiovirus (e.g. EMCV and TMEV) trigger little, if any, IFN- β mRNA production in infected cells (**Chapter 4** and **5**) (62)). In this case, the cardiovirus IFN- α/β antagonist is well established, namely the L protein, as evidenced by the observation that L mutants induce high levels of IFN- β mRNA production in infected cells (**Chapter 2** and **4**) (62)). However, the exactly mechanism underlying the IFN- α/β -suppressing activity of L is incompletely understood.

In cells infected with mengovirus the RLR-mediated IFN- α/β induction pathway upstream of TBK1 activation seems functional – both MDA5 and MAVS remain intact; and TBK1 phosphorylation, which is required for its activity to phosphorylate IRF3, can be detected as prominently in cells infected with the wt virus as with an IFN-inducing L mutant virus (**Chapter 4**). However, no IRF3 phosphorylation was observed in wt mengovirus-infected cells (**Chapter 4**), pinpointing the target of viral antagonization to a step between TBK1 activation and IRF3 phosphorylation. A couple of plausible underlying mechanisms are discussed below.

TBK1 complex formation

TBK1 is a kinase that has recently emerged as an important signaling component of many innate immune pathways including the RLR-mediated IFN- α/β pathway (reviewed in (89)). Its mode of activation is just beginning to be understood. The current model (89–91) suggests that TBK1 activation requires local concentration of TBK1 molecules to allow autophosphorylation *in trans* (89–91). This is achieved by scaffold proteins such as TANK, NAP1 and Sintbad that recruit TBK1 to specific signaling complexes. These scaffold proteins have been shown to have differential interaction partners and were suggested to exhibit different subcellular localization patterns, and thereby regulate TBK1 activation (92). It is currently unclear how exactly the upstream signals are relayed to the correct scaffold protein of choice, and whether these scaffold proteins also directly participate in selecting downstream substrates of TBK1. It is possible that L interferes with the interaction between TBK1 and the scaffold proteins, and thereby prevents efficient IRF3 activation by TBK1.

Interestingly, preliminary results suggest that mengovirus L protein may exhibit deubiquitinating (DUB) activity, as infection of an L mutant virus resulted in higher levels of globular protein ubiquitination than observed with wt virus infection (Feng et al, unpublished results). Ubiquitination of TBK1 has been shown to be important for its activation, possibly by participating in the complex formation (93, 94). DUB activity is certainly not an uncommon mechanism of viral evasion. Both the FMDV L^{pro} as well as the arterivirus papain-like protease 2 suppress IFN- α/β response via their DUB activities (95, 96). In fact, the FMDV L^{pro} has been shown to deubiquitinate, among others, TBK1 (95). Future research is required to establish (or disprove) a cause-effective relationship between DUB activity of L and failure of activated TBK1 to phosphorylate IRF3.

Nucleo-cytoplasmic trafficking disorder

Like enteroviruses, cardioviruses also induce disregulated NCT. In this case, the NCT disorder is not caused by 2A-mediated Nup cleavage, but the activities of the viral protein L (97, 98). Two known activities of L are thought to participate in inducing NCT disorder. L forms a tight complex with small GTPase Ran in the nucleus, and thereby disrupts the RanGDP/GTP gradient across the nuclear pore, which is crucial for nuclear import and export regulation (99). L also induces hyperphosphorylation of several Nups (100, 101) within their phenylalanine-glycine (FG)-containing repeats, which form the physical barriers of the nuclear pore and provide important docking sites for transport receptors (102–104). Hyperphosphorylation within these domains are proposed to physically interfere with interaction with cargo transporters (100). Recently, L mutants that can no longer bind Ran also failed to induce Nup68 phosphorylation (105), suggesting that these L-induced events may be linked, and may together be responsible for inducing the NCT disorder.

Disregulated NCT can negatively affect IRF3 distribution, and thereby its activation. As mentioned above, IRF3 normally shuttles between the nucleus and the cytoplasm, but shows predominantly cytoplasmic localization. Upon viral infection, IRF3 must be phosphorylated by TBK1 in the cytoplasm, then dimerize and translocate to the nucleus where it is retained by association with the nuclear factor CBP/p300 and activates target gene transcription (reviewed in (106)). It has been shown that during TMEV infection, a significant portion of IRF3 is found in the nucleus though there is little IRF3 phosphorylation (98, 107), suggesting a defect in regulated IRF3 shuttling. As mentioned above, TBK1 activation appears to be regulated on the level of subcellular localization, and it is possible that active IRF3 shuttling is required for proper interaction with TBK1. In fact, TANK, the scaffold protein that is required for RLR-mediated IRF3 activation, has been suggested to exhibit perinuclear localization (92), positioning it in the vicinity of the nuclear pores. In agreement with the hypothesis that the NCT disorder (partly) leads to IFN- α/β transcription inhibition, a small compound that delayed wt mengovirus-induced NCT disorder also led to moderately increased IFN- α/β mRNA response in infected cells (Baggen, Feng, et al. unpublished results).

IV. SGs as an antiviral mechanism during picornavirus infection

Besides shutting down the RLR-mediated IFN- α/β induction pathway, both enteroviruses and cardioviruses also repress SG formation. In CVB3-infected cells, SGs are observed early during infection, but disappear as infection advances (**Chapter 5**). Similar observations have been reported for PV (108), suggesting that this may be a common phenomenon induced by enteroviruses. Both CVB3- and PV-induced SG repression has been attributed to G3BP1 cleavage by the viral proteinase 3C^{pro} (108, 109). In the case of cardioviruses, the viral protein L of both EMCV and TMEV is responsible for suppressing SG formation, as infections with L mutants induced large amounts of SGs whereas the wt viruses did not (**Chapter 5** and (110)). Interestingly, a recent study reported cleavage of (exogenously expressed) G3BP1 during EMCV, which could be reproduced by overexpression of EMCV 3C^{pro} (111), imposing a potential role of EMCV 3C^{pro} in SG suppression. However, no data on the fate of endogenous G3BP1 during EMCV infection was provided. These results contradict previous findings that cardioviruses carrying mutations in the L protein, which still express active 3C^{pro}, could induce massive SG formation (**Chapter 5** and (110)). We also did not observe cleavage (or down-regulation) of endogenous G3BP1 during mengovirus (a strain of EMCV) infection (**Chapter 4**). It is currently unclear what causes this discrepancy concerning cardiovirus strategies to suppress SGs.

The antiviral mechanism of SGs

For both enteroviruses and cardioviruses, SG formation appeared to be disadvantageous for virus replication, albeit only to moderate levels. Artificial induction of SGs during enterovirus and cardiovirus infections led to reduced virus replication (108, 109, 111). Accordingly, SG inhibition during EMCV (L mutant) infection resulted in increased virus replication levels (**Chapter 5**). Although the reduction in virus replication upon SG manipulation are generally small, SG-mediated antiviral response seems to be a common phenomenon and applicable to many other viruses (112). Underlying mechanisms of the antiviral activity of SGs are still being sought out. Since the primary function of SGs is to halt translation and temporarily store

performed mRNA/protein complexes (112, 113), it has been suggested that also viral translation is inhibited in the presence of SGs. Indeed, in influenza virus-infected cells, SG formation has been associated with reduced viral protein accumulation levels (114). During enterovirus infections, artificial induction of SGs reduced viral translation at early times of infection, but this effect was overcome by the virus as infection progressed and more 3C^{pro}-mediated G3BP1 cleavage was observed (115). The initial SG-mediated translation inhibition is unlikely due to sequestering of viral mRNAs at these structures since viral ssRNAs, which includes viral mRNAs, were not detected at SGs during enterovirus infections (116). It remains to be demonstrated whether the sequestration of translation initiation factors at SGs is the primary cause of SG-mediated inhibition of viral translation.

An emerging view is that the stress pathway may be intimately linked to the innate immune responses (112), which could explain the antiviral activities of SGs. This hypothesis is also supported by the observation that two unrelated recombinant viruses (influenza Δ NS1 and cardiovirus L mutants) are deficient in both IFN- α/β antagonization and SG suppression (**Chapter 5**, (110, 114)). A possible connection is that SG formation may be a necessary component of the RLR-mediated IFN- α/β induction pathway, and thereby, exerts its antiviral functions. However, this did not seem to be the case since RLR pathway activation by various triggers did not lead to different levels of IFN- α/β induction in the presence or absence of SGs (**Chapter 5**). A recent report suggested that SGs may provide a physical platform in the initial RNA recognition process, and show antiviral activities. In influenza virus-infected cells, both RIG-I and viral RNA PAMP were found at SGs, and their localization was important for virus-induced IFN- α/β response (117). We also investigated whether a similar scenario would apply to mengovirus RNA recognition by MDA5. Although MDA5 was found at mengovirus (L mutant)-induced SGs, no viral dsRNAs, the ligands of MDA5, were detected at these granules (**Chapter 5** and (110)), making it unlikely that MDA5 utilizes these SGs as (primary) RNA recognition sites during infection of this virus. Exactly how SGs negatively affect cardiovirus replication remains to be established.

The relationship between the stress pathway and the IFN- α/β -based antiviral response

As mentioned above, we did not find evidence that SG formation is necessary for RLR-mediated IFN- α/β induction. Another possible link between these two cellular pathways is that SG formation may be an effector of IFN- α/β signaling and participate, together with ISGs, in establishing an antiviral state. However, this also did not appear to be the case since IFN- α/β treatment by itself did not lead to SG formation. Neither were SGs consistently observed upon activation of the RLR pathway (**Chapter 5**). Although options explored so far have not yielded a plausible mechanism, SG formation and IFN- α/β induction are associated during some viral infections, suggesting a coupling between these phenotypes. Perhaps the link lies within the protein content of SGs? G3BP2, a closely related protein to G3BP1 (an important structural component of SGs), was implicated in regulating NF- κ B localization, and thereby activity (118). NF- κ B is normally retained in the cytoplasm via interaction with I κ B (inhibitor of NF- κ B). Upon upstream pathway activation, I κ B releases NF- κ B, which then translocates to the nucleus to activate target gene transcription. G3BP2, which localizes to the cytoplasm, was found to interact with both I κ B and I κ B/NF- κ B complex (118). These observations led the authors to speculate that G3BP2 may finely regulate NF- κ B activation by binding to either the free or NF- κ B-bound form of I κ B. Interestingly, G3BP2 has also been recently reported to participate in SG formation (119), making this a possible connection between the two cellular antiviral pathways.

V. Concluding remarks

The interaction between an invading virus and the host antiviral immune responses is extremely intricate and complex. In this thesis, we investigated the process of picornavirus RNA recognition by MDA5, as well as how these viruses counteract the MDA5-mediated innate antiviral pathway. We provided the first experimental evidence on MDA5 activation by a natural viral ligand under physiological conditions. We also demonstrated a central role of enterovirus 2A^{pro} in the antagonization of the MDA5-mediated IFN- α / β induction pathway during infections of these viruses. Meanwhile, we also provided new insights into the IFN- α / β -suppressing mechanism of cardiovirus L, pinpointing it to a step between TBK1 phosphorylation and IRF3 activation. Furthermore, we presented data on the antiviral activity of SG formation, as well as the interaction between the cellular stress pathway and the RLR signaling pathway. Lastly, but not leastly, we showed using an artificial small RNA ligand that RLR pathway activation may present an opportunity for antiviral therapeutic interventions. These new insights may be valuable to future development of vaccines and antiviral therapies against the large family of picornaviruses.

REFERENCES

1. McCartney SA, Vermi W, Lonardi S, Rossini C, Otero K, Calderon B, Gilfillan S, Diamond MS, Unanue ER, Colonna M. 2011. RNA sensor-induced type I IFN prevents diabetes caused by a β cell-tropic virus in mice. *J. Clin. Invest.* 121:1497–507.
2. Wang Q, Miller DJ, Bowman ER, Nagarkar DR, Schneider D, Zhao Y, Linn MJ, Goldsmith AM, Bentley JK, Sajjan US, Hershenson MB. 2011. MDA5 and TLR3 initiate pro-inflammatory signaling pathways leading to rhinovirus-induced airways inflammation and hyperresponsiveness. *PLoS Pathog.* 7:e1002070.
3. Wang JP, Cerny A, Asher DR, Kurt-Jones EA, Bronson RT, Finberg RW. 2010. MDA5 and MAVS mediate type I interferon responses to coxsackie B virus. *J. Virol.* 84:254–260.
4. Barral PM, Morrison JM, Drahos J, Gupta P, Sarkar D, Fisher PB, Racaniello VR. 2007. MDA-5 is cleaved in poliovirus-infected cells. *J. Virol.* 81:3677–84.
5. Triantafilou K, Vakakis E, Kar S, Richer E, Evans GL, Triantafilou M. 2012. Visualisation of direct interaction of MDA5 and the dsRNA replicative intermediate form of positive strand RNA viruses. *J. Cell Sci.* 125:4761–9.
6. Peisley A, Lin C, Wu B, Orme-Johnson M, Liu M, Walz T, Hur S. 2011. Cooperative assembly and dynamic disassembly of MDA5 filaments for viral dsRNA recognition. *Proc. Natl. Acad. Sci. U. S. A.* 108:21010–5.
7. Berke IC, Modis Y. 2012. MDA5 cooperatively forms dimers and ATP-sensitive filaments upon binding double-stranded RNA. *EMBO J.* 31:1714–1726.
8. Berke IC, Yu X, Modis Y, Egelman EH. 2012. MDA5 assembles into a polar helical filament on dsRNA. *Proc. Natl. Acad. Sci. U. S. A.* 109:18437–41.
9. Wu B, Peisley A, Richards C, Yao H, Zeng X, Lin C, Chu F, Walz T, Hur S. 2013. Structural basis for dsRNA recognition, filament formation, and antiviral signal activation by MDA5. *Cell* 152:276–

89.

10. Kato H, Takeuchi O, Mikamo-Satoh E, Hirai R, Kawai T, Matsushita K, Hiiragi A, Dermody TS, Fujita T, Akira S. 2008. Length-dependent recognition of double-stranded ribonucleic acids by retinoic acid-inducible gene-I and melanoma differentiation-associated gene 5. *J. Exp. Med.* 205:1601–10.

11. Richards OC, Martin SC, Jense HG, Ehrenfeld E. 1984. Structure of poliovirus replicative intermediate RNA. Electron microscope analysis of RNA cross-linked in vivo with psoralen derivative. *J. Mol. Biol.* 173:325–340.

12. Satoh T, Kato H, Kumagai Y, Yoneyama M, Sato S, Matsushita K, Tsujimura T, Fujita T, Akira S, Takeuchi O. 2010. LGP2 is a positive regulator of RIG-I- and MDA5-mediated antiviral responses. *Proc. Natl. Acad. Sci. U. S. A.* 107:1512–1517.

13. Deddouche S, Goubau D, Rehwinkel J, Chakravarty P, Begum S, Maillard P V., Borg A, Matthews N, Feng Q, van Kuppeveld FJM, Reis e Sousa C. 2014. Identification of an LGP2-associated MDA5 agonist in picornavirus infected cells. *eLife.* 3:e01535.

14. Hato S V, Ricour C, Schulte BM, Lanke KH, de Bruijn M, Zoll J, Melchers WJ, Michiels T, van Kuppeveld FJ. 2007. The mengovirus leader protein blocks interferon-alpha/beta gene transcription and inhibits activation of interferon regulatory factor 3. *Cell Microbiol.* 9:2921–2930.

15. Zoll J, Melchers WJG, Galama JMD, Kuppeveld FJM Van. 2002. The mengovirus leader protein suppresses alpha/beta interferon production by inhibition of the iron/ferritin-mediated activation of NF-kappa B. *J. Virol.* 76:9664–9672.

16. Stavrou S, Feng Z, Lemon SM, Roos RP. 2010. Different strains of Theiler's murine encephalomyelitis virus antagonize different sites in the type I interferon pathway. *J. Virol.* 84:9181–9.

17. Luthra P, Sun D, Silverman RH, He B. 2011. Activation of IFN-beta expression by a viral mRNA through RNase L and MDA5. *Proc. Natl. Acad. Sci. U. S. A.* 108:2118–2123.

18. Malathi K, Saito T, Crochet N, Barton DJ, Gale Jr. M, Silverman RH. 2010. RNase L releases a small RNA from HCV RNA that refolds into a potent PAMP. *RNA* 16:2108–2119.

19. Malathi K, Dong B, Gale Jr. M, Silverman RH. 2007. Small self-RNA generated by RNase L amplifies antiviral innate immunity. *Nature* 448:816–819.

20. Takahasi K, Kumeta H, Tsuduki N, Narita R, Shigemoto T, Hirai R, Yoneyama M, Horiuchi M, Ogura K, Fujita T, Inagaki F. 2009. Solution structures of cytosolic RNA sensor MDA5 and LGP2 C-terminal domains: identification of the RNA recognition loop in RIG-I-like receptors. *J. Biol. Chem.* 284:17465–17474.

21. Yoneyama M, Kikuchi M, Matsumoto K, Imaizumi T, Miyagishi M, Taira K, Foy E, Loo YM, Gale Jr. M, Akira S, Yonehara S, Kato A, Fujita T. 2005. Shared and unique functions of the DExD/H-box helicases RIG-I, MDA5, and LGP2 in antiviral innate immunity. *J. Immunol.* 175:2851–2858.

22. Murali A, Li X, Ranjith-Kumar CT, Bhardwaj K, Holzenburg A, Li P, Kao CC. 2008. Structure and function of LGP2, a DEX(D/H) helicase that regulates the innate immunity response. *J. Biol. Chem.* 283:15825–33.

23. Li X, Ranjith-Kumar CT, Brooks MT, Dharmiah S, Herr AB, Kao C, Li P. 2009. The RIG-I-like receptor LGP2 recognizes the termini of double-stranded RNA. *J. Biol. Chem.* 284:13881–91.
24. Saito T, Hirai R, Loo Y-M, Owen D, Johnson CL, Sinha SC, Akira S, Fujita T, Gale M. 2007. Regulation of innate antiviral defenses through a shared repressor domain in RIG-I and LGP2. *Proc. Natl. Acad. Sci. U. S. A.* 104:582–7.
25. Hornung V, Ellegast J, Kim S, Brzozka K, Jung A, Kato H, Poeck H, Akira S, Conzelmann KK, Schlee M, Endres S, Hartmann G. 2006. 5'-Triphosphate RNA is the ligand for RIG-I. *Science* (80-). 314:994–997.
26. Peisley A, Lin C, Wu B, Orme-Johnson M, Liu M, Walz T, Hur S. 2011. Cooperative assembly and dynamic disassembly of MDA5 filaments for viral dsRNA recognition. *Proc. Natl. Acad. Sci. U. S. A.* 108:21010–21015.
27. Childs KS, Randall RE, Goodbourn S. 2013. LGP2 plays a critical role in sensitizing mda-5 to activation by double-stranded RNA. *PLoS One* 8:e64202.
28. Baum A, Sachidanandam R, García-Sastre A. 2010. Preference of RIG-I for short viral RNA molecules in infected cells revealed by next-generation sequencing. *Proc. Natl. Acad. Sci. U. S. A.* 107:16303–8.
29. Yang H, Wang H, Shivalila CS, Cheng AW, Shi L, Jaenisch R. 2013. One-Step Generation of Mice Carrying Reporter and Conditional Alleles by CRISPR/Cas-Mediated Genome Engineering. *Cell* 154:1370–1379.
30. Hagemeyer MC, Vonk AM, Monastyrska I, Rottier PJM, de Haan CA. 2012. Visualizing coronavirus RNA synthesis in time by using click chemistry. *J. Virol.* 86:5808–16.
31. Santangelo PJ, Lifland AW, Curt P, Sasaki Y, Bassell GJ, Lindquist ME, Crowe JE. 2009. Single molecule-sensitive probes for imaging RNA in live cells. *Nat. Methods* 6:347–9.
32. Oosterhoff D, Heusinkveld M, Loughheed SM, Kosten I, Lindstedt M, Bruijns SCM, van Es T, van Kooyk Y, van der Burg SH, de Gruijl TD. 2013. Intradermal delivery of TLR agonists in a human explant skin model: preferential activation of migratory dendritic cells by polyribosinic-polyribocytidylic acid and peptidoglycans. *J. Immunol.* 190:3338–45.
33. Arsenault RJ, Kogut MH, He H. 2013. Combined CpG and poly I:C stimulation of monocytes results in unique signaling activation not observed with the individual ligands. *Cell. Signal.* 25:2246–54.
34. McCaskill JL, Marsh GA, Monaghan P, Wang L-F, Doran T, McMillan NAJ. 2013. Potent inhibition of Hendra virus infection via RNA interference and poly I:C immune activation. *PLoS One* 8:e64360.
35. Zhao T, Wu X, Song D, Fang M, Guo S, Zhang P, Wang L, Wang L, Yu Y. 2012. Effect of prophylactically applied CpG ODN on the development of myocarditis in mice infected with Coxsackievirus B3. *Int. Immunopharmacol.* 14:665–73.
36. Rodríguez-Pulido M, Borrego B, Sobrino F, Sáiz M. 2011. RNA structural domains in noncoding regions of the foot-and-mouth disease virus genome trigger innate immunity in porcine cells and mice. *J. Virol.* 85:6492–501.
37. Martínez-Gil L, Goff PH, Hai R, García-Sastre A, Shaw ML, Palese P. 2013. A Sendai virus-

- derived RNA agonist of RIG-I as a virus vaccine adjuvant. *J. Virol.* 87:1290–300.
38. Goulet M-L, Olganier D, Xu Z, Paz S, Belgnaoui SM, Lafferty EI, Janelle V, Arguello M, Paquet M, Ghneim K, Richards S, Smith A, Wilkinson P, Cameron M, Kalinke U, Qureshi S, Lamarre A, Haddad EK, Sekaly RP, Peri S, Balachandran S, Lin R, Hiscott J. 2013. Systems Analysis of a RIG-I Agonist Inducing Broad Spectrum Inhibition of Virus Infectivity. *PLoS Pathog.* 9:e1003298.
39. Zlatev I, Manoharan M, Vasseur J-J, Morvan F. 2012. Solid-phase chemical synthesis of 5'-triphosphate DNA, RNA, and chemically modified oligonucleotides. *Curr. Protoc. Nucleic Acid Chem.* Chapter 1:Unit1.28.
40. Caton-Williams J, Lin L, Smith M, Huang Z. 2011. Convenient synthesis of nucleoside 5'-triphosphates for RNA transcription. *Chem. Commun. (Camb).* 47:8142–4.
41. Crampton SP, Deane J a, Feigenbaum L, Bolland S. 2012. Ifih1 gene dose effect reveals MDA5-mediated chronic type I IFN gene signature, viral resistance, and accelerated autoimmunity. *J. Immunol.* 188:1451–9.
42. Thermo Scientific. TurboFect in vivo Transfection Reagent.
43. Life Technologies. Invivofectamine 2.0.
44. Saga K, Kaneda Y. 2013. Virosome Presents Multimodel Cancer Therapy without Viral Replication. *Biomed Res. Int.* 2013:764706.
45. Poelstra K, Prakash J, Beljaars L. 2012. Drug targeting to the diseased liver. *J. Control. Release* 161:188–97.
46. Ding B, Li T, Zhang J, Zhao L, Zhai G. 2012. Advances in liver-directed gene therapy for hepatocellular carcinoma by non-viral delivery systems. *Curr. Gene Ther.* 12:92–102.
47. Hale BG, Randall RE, Ortín J, Jackson D. 2008. The multifunctional NS1 protein of influenza A viruses. *J. Gen. Virol.* 89:2359–76.
48. Childs K, Stock N, Ross C, Andrejeva J, Hilton L, Skinner M, Randall R, Goodbourn S. 2007. mda-5, but not RIG-I, is a common target for paramyxovirus V proteins. *Virology* 359:190–200.
49. Childs K, Randall R, Goodbourn S. 2012. Paramyxovirus V proteins interact with the RNA Helicase LGP2 to inhibit RIG-I-dependent interferon induction. *J. Virol.* 86:3411–21.
50. Lu LL, Puri M, Horvath CM, Sen GC. 2008. Select paramyxoviral V proteins inhibit IRF3 activation by acting as alternative substrates for inhibitor of kappaB kinase epsilon (IKKe)/TBK1. *J. Biol. Chem.* 283:14269–76.
51. Schuhmann KM, Pfaller CK, Conzelmann K-K. 2011. The measles virus V protein binds to p65 (RelA) to suppress NF-kappaB activity. *J. Virol.* 85:3162–71.
52. Wohnsland A, Hofmann WP, Sarrazin C. 2007. Viral determinants of resistance to treatment in patients with hepatitis C. *Clin. Microbiol. Rev.* 20:23–38.
53. Chase AJ, Semler BL. 2012. Viral subversion of host functions for picornavirus translation and RNA replication. *Future Virol.* 7:179–191.
54. Belov G a, Altan-Bonnet N, Kovtunovych G, Jackson CL, Lippincott-Schwartz J, Ehrenfeld E. 2007. Hijacking components of the cellular secretory pathway for replication of poliovirus RNA.

J. Virol. 81:558–67.

55. Belov GA, Feng Q, Nikovics K, Jackson CL, Ehrenfeld E. 2008. A critical role of a cellular membrane traffic protein in poliovirus RNA replication. *PLoS Pathog.* 4:e1000216.

56. Wessels E, Duijsings D, Niu T-KK, Neumann S, Oorschot VM, de Lange F, Lanke KHW, Klumperman J, Henke A, Jackson CL, Melchers WJG, van Kuppeveld FJM. 2006. A viral protein that blocks Arf1-mediated COP-I assembly by inhibiting the guanine nucleotide exchange factor GBF1. *Dev. Cell* 11:191–201.

57. Doedens JR, Kirkegaard K. 1995. Inhibition of cellular protein secretion by poliovirus proteins 2B and 3A. *EMBO J.* 14:894–907.

58. Dodd DA, Giddings TH, Kirkegaard K. 2001. Poliovirus 3A protein limits interleukin-6 (IL-6), IL-8, and beta interferon secretion during viral infection. *J. Virol.* 75:8158–65.

59. Drahos J, Racaniello VR. 2009. Cleavage of IPS-1 in cells infected with human rhinovirus. *J. Virol.* 83:11581–7.

60. Kuo R-L, Kao L-T, Lin S-J, Wang RY-L, Shih S-R. 2013. MDA5 Plays a Crucial Role in Enterovirus 71 RNA-Mediated IRF3 Activation. *PLoS One* 8:e63431.

61. Mukherjee A, Morosky SA, Delorme-Axford E, Dybdahl-Sissoko N, Oberste MS, Wang T, Coyne CB. 2011. The coxsackievirus B 3C protease cleaves MAVS and TRIF to attenuate host type I interferon and apoptotic signaling. *PLoS Pathog.* 7:e1001311.

62. Van Pesch V, van Eyll O, Michiels T. 2001. The leader protein of Theiler's virus inhibits immediate-early alpha/beta interferon production. *J. Virol.* 75:7811–7.

63. Yang Y, Liang Y, Qu L, Chen Z, Yi M, Li K, Lemon SM. 2007. Disruption of innate immunity due to mitochondrial targeting of a picornaviral protease precursor. *Proc. Natl. Acad. Sci. U. S. A.* 104:7253–8.

64. Li X-D, Sun L, Seth RB, Pineda G, Chen ZJ. 2005. Hepatitis C virus protease NS3/4A cleaves mitochondrial antiviral signaling protein off the mitochondria to evade innate immunity. *Proc. Natl. Acad. Sci. U. S. A.* 102:17717–22.

65. Wei C, Ni C, Song T, Liu Y, Yang X, Zheng Z, Jia Y, Yuan Y, Guan K, Xu Y, Cheng X, Zhang Y, Yang X, Wang Y, Wen C, Wu Q, Shi W, Zhong H. 2010. The hepatitis B virus X protein disrupts innate immunity by downregulating mitochondrial antiviral signaling protein. *J. Immunol.* 185:1158–68.

66. Horner SM, Liu HM, Park HS, Briley J, Gale M. 2011. Mitochondrial-associated endoplasmic reticulum membranes (MAM) form innate immune synapses and are targeted by hepatitis C virus. *Proc. Natl. Acad. Sci. U. S. A.* 108:14590–5.

67. Lebieczynska M, Szabadkai G, Jones AWE, Duszynski J, Wieckowski MR. 2009. Interactions between the endoplasmic reticulum, mitochondria, plasma membrane and other subcellular organelles. *Int. J. Biochem. Cell Biol.* 41:1805–16.

68. Belov G, Lidsky P, Mikitas O, Egger D, Lukyanov K, Bienz K, Agol V. 2004. Bidirectional increase in permeability of nuclear envelope upon poliovirus infection and accompanying alterations of nuclear pores. *J. Virol.* 78:10166–10177.

69. Belov GA, Evstafieva AG, Rubtsov YP, Mikitas O V, Vartapetian AB, Agol VI. 2000. Early alteration of nucleocytoplasmic traffic induced by some RNA viruses. *Virology* 275:244–8.
70. Gustin KE, Sarnow P. 2001. Effects of poliovirus infection on nucleo-cytoplasmic trafficking and nuclear pore complex composition. *EMBO J.* 20:240–9.
71. Park N, Katikaneni P, Skern T, Gustin KE. 2008. Differential targeting of nuclear pore complex proteins in poliovirus-infected cells. *J. Virol.* 82:1647–55.
72. Gustin KE, Sarnow P. 2002. Inhibition of nuclear import and alteration of nuclear pore complex composition by rhinovirus. *J. Virol.* 76:8787–96.
73. Watters K, Palmenberg AC. 2011. Differential processing of nuclear pore complex proteins by rhinovirus 2A proteases from different species and serotypes. *J. Virol.* 85:10874–83.
74. Castelló A, Izquierdo JM, Welnowska E, Carrasco L. 2009. RNA nuclear export is blocked by poliovirus 2A protease and is concomitant with nucleoporin cleavage. *J. Cell Sci.* 122:3799–809.
75. Nasirudeen AMA, Wong HH, Thien P, Xu S, Lam K-P, Liu DX. 2011. RIG-I, MDA5 and TLR3 synergistically play an important role in restriction of dengue virus infection. *PLoS Negl. Trop. Dis.* 5:e926.
76. Fredericksen BL, Gale Jr. M. 2006. West Nile virus evades activation of interferon regulatory factor 3 through RIG-I-dependent and -independent pathways without antagonizing host defense signaling. *J. Virol.* 80:2913–2923.
77. Fredericksen BL, Keller BC, Fornek J, Katze MG, Gale Jr. M. 2008. Establishment and maintenance of the innate antiviral response to West Nile Virus involves both RIG-I and MDA5 signaling through IPS-1. *J. Virol.* 82:609–616.
78. Zoll J, Galama JM, van Kuppeveld FJ, Melchers WJ. 1996. Mengovirus leader is involved in the inhibition of host cell protein synthesis. *J. Virol.* 70:4948–4952.
79. Zoll J, Melchers WJG, Galama JMD, Kuppeveld FJM Van. 2002. The Mengovirus Leader Protein Suppresses Alpha/Beta Interferon Production by Inhibition of the Iron/Ferritin-Mediated Activation of NF-kappaB. *J. Virol.* 76:9664–9672.
80. Das S, Dasgupta a. 1993. Identification of the cleavage site and determinants required for poliovirus 3CPro-catalyzed cleavage of human TATA-binding transcription factor TBP. *J. Virol.* 67:3326–31.
81. Kundu P, Raychaudhuri S, Tsai W, Dasgupta A. 2005. Shutoff of RNA polymerase II transcription by poliovirus involves 3C protease-mediated cleavage of the TATA-binding protein at an alternative site: incomplete shutoff of transcription interferes with efficient viral replication. *J. Virol.* 79:9702–13.
82. Yalamanchili P, Datta U, Dasgupta A. 1997. Inhibition of host cell transcription by poliovirus: cleavage of transcription factor CREB by poliovirus-encoded protease 3Cpro. *J. Virol.* 71:1220–6.
83. Pietiäinen V, Huttunen P, Hyypiä T. 2000. Effects of echovirus 1 infection on cellular gene expression. *Virology* 276:243–50.
84. Doukas T, Sarnow P. 2011. Escape from transcriptional shutoff during poliovirus infection: NF-κB-responsive genes IκBa and A20. *J. Virol.* 85:10101–8.

85. Paulson M, Press C, Smith E, Tanese N, Levy DE. 2002. IFN-Stimulated transcription through a TBP-free acetyltransferase complex escapes viral shutoff. *Nat. Cell Biol.* 4:140–7.
86. Jiang L-J, Zhang N-N, Ding F, Li X-Y, Chen L, Zhang H-X, Zhang W, Chen S-J, Wang Z-G, Li J-M, Chen Z, Zhu J. 2011. RA-inducible gene-I induction augments STAT1 activation to inhibit leukemia cell proliferation. *Proc. Natl. Acad. Sci. U. S. A.* 108:1897–902.
87. Andrejeva J, Childs KS, Young DF, Carlos TS, Stock N, Goodbourn S, Randall RE. 2004. The V proteins of paramyxoviruses bind the IFN-inducible RNA helicase, mda-5, and inhibit its activation of the IFN-beta promoter. *Proc. Natl. Acad. Sci. U. S. A.* 101:17264–17269.
88. Seth RB, Sun L, Ea C-KK, Chen ZJ. 2005. Identification and characterization of MAVS, a mitochondrial antiviral signaling protein that activates NF-kappaB and IRF 3. *Cell* 122:669–682.
89. Helgason E, Phung QT, Dueber EC. 2013. Recent insights into the complexity of Tank-binding kinase 1 signaling networks: the emerging role of cellular localization in the activation and substrate specificity of TBK1. *FEBS Lett.* 587:1230–7.
90. Chau T-L, Gioia R, Gatot J-S, Patrascu F, Carpentier I, Chapelle J-P, O’Neill L, Beyaert R, Piette J, Chariot A. 2008. Are the IKKs and IKK-related kinases TBK1 and IKK-epsilon similarly activated? *Trends Biochem. Sci.* 33:171–80.
91. Ma X, Helgason E, Phung QT, Quan CL, Iyer RS, Lee MW, Bowman KK, Starovasnik MA, Dueber EC. 2012. Molecular basis of Tank-binding kinase 1 activation by transautophosphorylation. *Proc. Natl. Acad. Sci. U. S. A.* 109:9378–9383.
92. Goncalves A, Bürckstümmer T, Dixit E, Scheicher R, Górna MW, Karayel E, Sugar C, Stukalov A, Berg T, Kralovics R, Planyavsky M, Bennett KL, Colinge J, Superti-Furga G. 2011. Functional dissection of the TBK1 molecular network. *PLoS One* 6:e23971.
93. Tu D, Zhu Z, Zhou AY, Yun C, Lee K-E, Toms A V, Li Y, Dunn GP, Chan E, Thai T, Yang S, Ficarro SB, Marto JA, Jeon H, Hahn WC, Barbie DA, Eck MJ. 2013. Structure and ubiquitination-dependent activation of TANK-binding kinase 1. *Cell Rep.* 3:747–58.
94. Wang L, Li S, Dorf ME. 2012. NEMO binds ubiquitinated TANK-binding kinase 1 (TBK1) to regulate innate immune responses to RNA viruses. *PLoS One* 7:e43756.
95. Wang D, Fang L, Li P, Sun L, Fan J, Zhang Q, Luo R, Liu X, Li K, Chen H, Chen Z, Xiao S. 2011. The leader proteinase of foot-and-mouth disease virus negatively regulates the type I interferon pathway by acting as a viral deubiquitinase. *J. Virol.* 85:3758–66.
96. Van Kasteren PB, Bailey-Elkin BA, James TW, Ninaber DK, Beugeling C, Khajehpour M, Snijder EJ, Mark BL, Kikkert M. 2013. Deubiquitinase function of arterivirus papain-like protease 2 suppresses the innate immune response in infected host cells. *Proc. Natl. Acad. Sci. U. S. A.* 110:E838–47.
97. Lidsky P V, Hato S, Bardina M V, Aminev AG, Palmenberg AC, Sheval E V, Polyakov VY, van Kuppeveld FJ, Agol VI. 2006. Nucleocytoplasmic traffic disorder induced by cardioviruses. *J. Virol.* 80:2705–2717.
98. Delhay S, van Pesch V, Michiels T. 2004. The leader protein of Theiler’s virus interferes with nucleocytoplasmic trafficking of cellular proteins. *J. Virol.* 78:4357–62.
99. Porter FW, Bochkov YA, Albee AJ, Wiese C, Palmenberg AC. 2006. A picornavirus protein

interacts with Ran-GTPase and disrupts nucleocytoplasmic transport. *Proc. Natl. Acad. Sci. U. S. A.* 103:12417–22.

100. Porter FW, Brown B, Palmenberg AC. 2010. Nucleoporin phosphorylation triggered by the encephalomyocarditis virus leader protein is mediated by mitogen-activated protein kinases. *J. Virol.* 84:12538–12548.

101. Bardina M V, Lidsky P V, Sheval E V, Fominykh K V, van Kuppeveld FJM, Polyakov VY, Agol VI. 2009. Mengovirus-induced rearrangement of the nuclear pore complex: hijacking cellular phosphorylation machinery. *J. Virol.* 83:3150–61.

102. Tu L-C, Fu G, Zilman A, Musser SM. 2013. Large cargo transport by nuclear pores: implications for the spatial organization of FG-nucleoporins. *EMBO J.* 32:3220–30.

103. Fiserova J, Spink M, Richards SA, Saunter C, Goldberg MW. 2014. Entry into the nuclear pore complex is controlled by a cytoplasmic exclusion zone containing dynamic GLFG-repeat nucleoporin domains. *J. Cell Sci.* 127:124–36.

104. Wälde S, Kehlenbach RH. 2010. The Part and the Whole: functions of nucleoporins in nucleocytoplasmic transport. *Trends Cell Biol.* 20:461–9.

105. Bacot-Davis VR, Palmenberg AC. 2013. Encephalomyocarditis virus Leader protein hinge domain is responsible for interactions with Ran GTPase. *Virology* 443:177–185.

106. Reich NC. 2002. Nuclear/cytoplasmic localization of IRFs in response to viral infection or interferon stimulation. *J. Interferon Cytokine Res.* 22:103–9.

107. Stavrou S, Feng Z, Lemon SM, Roos RP. 2010. Different strains of Theiler's murine encephalomyelitis virus antagonize different sites in the type I interferon pathway. *J. Virol.* 84:9181–9.

108. White JP, Cardenas AM, Marissen WE, Lloyd RE. 2007. Inhibition of cytoplasmic mRNA stress granule formation by a viral proteinase. *Cell Host Microbe* 2:295–305.

109. Fung G, Ng CS, Zhang J, Shi J, Wong J, Piesik P, Han L, Chu F, Jagdeo J, Jan E, Fujita T, Luo H. 2013. Production of a Dominant-Negative Fragment Due to G3BP1 Cleavage Contributes to the Disruption of Mitochondria-Associated Protective Stress Granules during CVB3 Infection. *PLoS One* 8:e79546.

110. Borghese F, Michiels T. 2011. The leader protein of cardioviruses inhibits stress granule assembly. *J. Virol.* 85:9614–22.

111. Ng CS, Jogi M, Yoo J-S, Onomoto K, Koike S, Iwasaki T, Yoneyama M, Kato H, Fujita T. 2013. Encephalomyocarditis virus disrupts stress granules, the critical platform for triggering antiviral innate immune responses. *J. Virol.* 87:9511–22.

112. Reineke LC, Lloyd RE. 2013. Diversion of stress granules and P-bodies during viral infection. *Virology* 436:255–67.

113. White JP, Lloyd RE. 2012. Regulation of stress granules in virus systems. *Trends Microbiol.* 20:175–83.

114. Khapersky D a, Hatchette TF, McCormick C. 2012. Influenza A virus inhibits cytoplasmic stress granule formation. *FASEB J.* 26:1629–39.

Chapter 6

115. White JP, Reineke LC, Lloyd RE. 2011. Poliovirus switches to an eIF2-independent mode of translation during infection. *J. Virol.* 85:8884–93.
116. Piotrowska J, Hansen SJ, Park N, Jamka K, Sarnow P, Gustin KE. 2010. Stable formation of compositionally unique stress granules in virus-infected cells. *J. Virol.* 84:3654–65.
117. Onomoto K, Jogi M, Yoo J-S, Narita R, Morimoto S, Takemura A, Sambhara S, Kawaguchi A, Osari S, Nagata K, Matsumiya T, Namiki H, Yoneyama M, Fujita T. 2012. Critical role of an antiviral stress granule containing RIG-I and PKR in viral detection and innate immunity. *PLoS One* 7:e43031.
118. Prigent M, Barlat I, Langen H, Dargemont C. 2000. IkappaBalpha and IkappaBalpha /NF-kappa B complexes are retained in the cytoplasm through interaction with a novel partner, RasGAP SH3-binding protein 2. *J. Biol. Chem.* 275:36441–9.
119. Matsuki H, Takahashi M, Higuchi M, Makokha GN, Oie M, Fujii M. 2013. Both G3BP1 and G3BP2 contribute to stress granule formation. *Genes Cells* 18:135–46.

Chapter 7

Samenvattingen in het Nederlands en Chinees

Virus infecties komen heel vaak voor in ons leven, maar gelukkig hebben wij afweerreacties die ons beschermen tegen virussen. Een van de eerste antivirale afweerreacties is de type I interferon (IFN- α/β) respons. IFN- α/β zijn kleine moleculen die als alarmsignalen functioneren. Bijna alle celsoorten zijn in staat om IFN- α/β te maken wanneer ze geïnfecteerd worden door een virus. Vervolgens wordt het IFN- α/β door de cellen in de omgeving herkend, wat leidt tot een zogenaamde “antivirale” toestand in deze cellen waardoor ze beter tegen virussen bestand zijn. Om een IFN- α/β respons op het juiste moment te starten, moeten cellen wel een virus infectie kunnen herkennen en daar zijn gespecialiseerde sensoren voor aanwezig in de cel. RIG-I-like receptors (RLRs) zijn een familie van zulke sensoren, waartoe onder andere RIG-I en MDA5 behoren. Ze herkennen lichaamsvreemde RNA moleculen van pathogenen zoals virussen, en vervolgens induceren zij de productie van IFN- α/β via een aantal andere eiwitten zoals MAVS, TBK1 en IRF3.

Omdat het IFN- α/β systeem zo’n sterke antiviraal effect heeft, hebben vele virussen, zoals de picornavirussen, tijdens de co-evolutie met hun gastheren geleerd om dit systeem juist sterk te onderdrukken om infectie te kunnen bewerkstelligen. Picornavirussen zijn een grote familie van virussen, die verschillende ziekten in zowel mens als dier kunnen veroorzaken. Deze diverse virus familie bevat een grote aantal subgroepen (genera) en honderden verschillende virussen typen. Bekende leden van deze familie zijn bijvoorbeeld de verwekkers van kinderverlamming (poliovirus [PV]), hersenvliesontsteking (onder andere coxsackievirus [CV]), verkoudheid (human rhinovirus [HRV]), hepatitis A (hepatitis A virus) en mond-en-klauwzeer (foot-and-mouth disease virus [FMDV]) in dieren. De interactie tussen deze virussen en de IFN- α/β respons is nog grotendeels niet opgehelderd. Om dit te begrijpen is het belangrijk om diepgaand inzicht in de herkenning van picornavirale RNAs, en de virale ontwikkelingsmechanismen te verkrijgen.

Tijdens picornavirus infecties worden er een aantal virale RNA moleculen gemaakt die lichaamsvreemde karakteristieken dragen, wat meer gedetailleerd is beschreven in **Hoofdstuk 1**. Het virale RNA (vRNA) is een enkelstrengs RNA (ssRNA) van positieve polariteit, wat betekent dat het direct gebruikt worden om eiwitten te maken. Het vRNA draagt een klein viraal eiwit (VPg) aan zijn 5' eind. Tijdens infecties wordt VPg los geknipt van het RNA, wat leidt tot een enkelstrengs RNA met een 5' monofosfaat. Tijdens viraal RNA replicatie wordt de positieve RNA streng eerst gerepliceerd tot een negatiefstrengs RNA. Tijdens dit proces wordt tijdelijk een volledige dubbelstrengs RNA (dsRNA) product (Replicative Form, RF) gegenereerd. Daarna wordt het negatiefstrengs RNA gebruikt om een groot aantal nieuwe positiefstrengs RNAs te maken. In dit proces wordt een ander tussenliggend RNA product (Replicative Intermediate, RI) gemaakt, wat een primaire enkelstrengs RNA met dubbelstrengse gedeeltes is. Het was nog niet opgehelderd welke van deze picornavirale RNAs MDA5 kan activeren, en bovendien welk picornaviraal RNA door MDA5 wordt herkend in een natuurlijke omgeving, namelijk een geïnfecteerde cel. Het is wel bekend dat picornavirussen de IFN- α/β respons sterk kunnen onderdrukken, maar hoe ze dit precies volbrengen was onvolledig begrepen.

Naast de IFN- α/β respons, is de stress respons recentelijk ook geïmpliceerd belangrijk te zijn in antivirale reacties. Tijdens stress, bijvoorbeeld door hitte, kou, oxidatieve stress of een virus infectie, maken cellen zogenaamde “stress granules” (SG). Deze SGs zijn grote aggregaten in de cel die lichaamseigen RNA en eiwit moleculen als het ware vangen om ze tijdelijk te bewaren en translatie op te houden. Wanneer de stress weer verdwenen is, worden deze moleculen

weer vrijgegeven, waarna ze weer hun normale taken kunnen uitvoeren. Het is nog grotendeels onbekend wat voor rol deze stress respons speelt tijdens virus infecties.

In dit proefschrift wordt onze kennis over het herkennen van picornavirussen door de RLRs en de strategie van deze virussen om aangeboren antivirale responsen te remmen verder verdiept. Twee belangrijke genera (groepen) van picornavirussen, voornamelijk *Enterovirus* en *Cardiovirus*, werden bestudeerd met behulp van twee model virussen, te weten coxsackievirus groep B stam 3 (CVB3) en encephalomyocarditis virus (EMCV, stam mengovirus).

SAMENVATTING VAN BELANGRIJKSTE BEVINDINGEN

Het doel van **Hoofdstuk 2** was om het picornavirus RNA molecuul dat tijdens een infectie in de cel door MDA5 wordt herkend op te helderen. Om de verschillende picornavirale RNAs systematisch te bestuderen, begonnen we met het totale RNA extract van cellen geïnfecteerd met CVB3 of mengovirus. Vanuit dit extract (dat zowel virale als cellulaire RNAs bevatte) hebben we het ssRNAs en dsRNAs van elkaar gescheiden, waarna we ze apart van elkaar in cellen hebben gebracht door middel van transfectie om te bestuderen of ze IFN productie konden induceren. De dsRNA fractie, maar niet de ssRNA fractie, bleek MDA5 te kunnen activeren en daardoor IFN- β te induceren, wat suggereert dat de MDA5 ligand een dsRNA(s) is. Omdat de ssRNA en dsRNA fractie ook nog cellulaire RNA moleculen bevatte, hebben we deze fracties gezuiverd tot puur viraal ssRNA of dsRNA. Gezuiverd RF kon MDA5 krachtig activeren, terwijl de virale ssRNAs (zowel met en zonder VPg) geen IFN- α/β reactie induceerden. Verder hebben we ook aangetoond dat gezuiverd RF recombinant MDA5 direct activeerde zonder hulp van bijkomende factor(en). Tot slot hebben we als eerste ook de MDA5 activatie tijdens een picornavirus infectie bestudeerd. Met behulp van remmers van verschillende stappen van virusrepletie hebben we laten zien dat synthese van het negatiefstrengs RNA, de stap waarbij de RF wordt gemaakt, essentieel is om een IFN- β respons te induceren tijdens mengovirus infectie.

Hoofdstuk 3 beschrijft het gebruik van een kleine, artificiële 5'-trifosfaat bevattende RNA transcript als een zeer krachtige antiviraal middel via RIG-I activatie. De sequentie van het RNA molecuul is gebaseerd op een RNA structuur – de "cloverleaf" (CL) – in het genoom van CVB3. Transfectie van dit RNA molecuul induceerde productie van zowel type I en III IFNs alsmede pro-inflammatoire cytokines en chemokines. Behandeling met dit CL RNA beschermde de cellen tegen verschillende virusinfecties, waaronder dengue virus, vesicular stomatitis virus en enterovirus 71.

Zo geavanceerd als onze antivirale afweerreacties zijn, zijn virussen meesters in het omzeilen van deze reacties en het navigeren in de vijandige omgeving in de gastheer. In **Hoofdstuk 4** en **5** beschrijven we het ontwijkgingsmechanisme van enerzijds CVB3 en andere enterovirussen en anderzijds mengovirus met betrekking tot twee belangrijke antivirale systemen van de cel: de RLR-gemedieerde IFN- α/β inductie route en de stress respons. In **Hoofdstuk 5** hebben we verder de mogelijke interacties tussen deze twee cellulaire antivirale responsen zelf onderzocht.

Normaliter leidt activatie van RIG-I of MDA5 tot activatie van achtereenvolgens MAVS, TBK1 en IRF3. In **Hoofdstuk 4** bestudeerden we hoe enterovirussen en cardiovirussen de

RLR gemedieerde IFN- α/β inductie route onderdrukken. We laten zien dat zowel CVB3 als mengovirus de RLR signaleringcascade onderdrukken door IRF3 fosforylering effectief te remmen. TBK1 fosforylering, wat nodig is om IRF3 te fosforyleren en daarbij te activeren, is ook sterk geremd in CVB3 geïnfecteerde cellen. Dit gaf aan dat de CVB3 geïnduceerde blokkade van de RLR signalering pathway ofwel op het niveau van TBK1 activatie ligt ofwel eerder in de signaleringcascade. Mengovirus daarentegen induceerde sterke TBK1 fosforylering, maar toch geen IRF3 activatie, wat suggereert dat dit virus de IFN- α/β inductie route remde bij een stap tussen TBK1 fosforylering en IRF3 fosforylering. Daarnaast toonden we aan dat belangrijke factoren die tot TBK1 activatie leiden, waaronder MDA5, MAVS en RIG-I, geknipt werden tijdens CVB3 infectie, maar intact bleven tijdens mengovirus infectie. Resultaten uit eerder gepubliceerd studies met een aantal enterovirussen suggereerden dat MDA5 afgebroken werd door caspases en proteases uit het proteasoom. Onze studie met CVB3 laat echter zien dat MDA5 knipping werd bewerkstelligd door de virale protease 2A^{pro}. Met behulp van recombinant 2A^{pro} en 3C^{pro} van CVB3 toonden wij verder aan dat dezelfde afbraak patronen van MDA5 en MAVS gereproduceerd konden worden door behandeling met 2A^{pro}, terwijl die van RIG-I door 3C^{pro}. Om het effect van 2A^{pro} en 3C^{pro}, van zowel CVB3 evenals andere enterovirussen, in de context van een infectie te kunnen bestuderen, hebben we deze enterovirale proteasen in het genoom van mengovirus gezet. Door middel van deze recombinante mengovirussen hebben we laten zien dat MDA5 en MAVS beide werden geknipt door 2A^{pro} van enterovirussen van drie species, namelijk **Enterovirus A** (EV71), **B** (CVB3) en **C** (PV). In al deze gevallen werd het knippen van RIG-I gemedieerd door de 3C^{pro} van deze virussen.

Naast het interfereren met de RLR pathway, toonden we in **Hoofdstuk 5** aan dat zowel CVB3 als mengovirus ook de vorming van SGs onderdrukten tijdens infectie. Bij mengovirus werd SG remming toegeschreven aan de activiteit van het virale eiwit L. Infectie van een mutant virus met een inactief L leidde tot het ontstaan van grote aantallen SGs, waarvan de vorming afhankelijk was van de activiteit van PKR. SG formatie had een matig negatief effect op virus replicatie. Dit antivirale effect van SGs bleek onafhankelijk te zijn van de RLR gemedieerde IFN- α/β respons. Opmerkelijk was dat MDA5 ook op SGs aanwezig was tijdens L mutant mengovirus infectie, evenals tijdens andere stress behandelingen. Ondanks deze interessante observatie, was deze lokalisatie van MDA5 niet essentieel voor SG formatie, of MDA5 activatie door mengovirus RNAs. Het exacte onderliggende antivirale mechanisme van SGs tijdens picornavirus infecties moet nog worden opgehelderd.

In **Hoofdstuk 6** worden de bevindingen van dit promotieonderzoek in relatie tot de bestaande literatuur bediscussieerd. Daarnaast wordt ook beschreven hoe deze nieuwe inzichten een bijdrage kunnen leveren aan de toekomstige ontwikkeling van vaccins en antivirale therapieën tegen de grote familie van picornavirussen.

微小核糖核酸病毒是一个很大的病原家族, 包含了许多重要的人和动物病原, 比如脊髓灰质炎 (又称小儿麻痹症) 病毒, 柯萨基病毒, 人鼻病毒, 肠道病毒71, 甲型肝炎病毒, 脑心肌炎病毒, 和口蹄疫病毒. 我们对微小核糖核酸病毒与宿主的相互作用及宿主的先天抗病毒免疫机制至今尚不完全清楚. 当病毒感染细胞后, 细胞可以识别人侵的病原并通过提高宿主的抗病毒反应来抑制病毒的复制和扩散. RIG-I和MDA5是两个重要的细胞内核糖核酸感受器 (统称为RLRs), 它们能够识别病毒核糖核酸, 并通过一系列其他蛋白比如MAVS, TBK1和IRF3诱导一型干扰素的表达. 一型干扰素是非常有效的抗病毒分子信使, 它可以通过激活上百种干扰素刺激基因的表达, 从而诱导细胞达到抗病毒状态. RIG-I主要识别负链核糖核酸病毒和几种黄病毒 (正链, 比如丙肝病毒), 而MDA5在识别很多正链核糖核酸病毒中起着至关重要的作用, 其中就包括微小核糖核酸病毒. MDA5介导的抗病毒反应在控制微小核糖核酸病毒感染中起着重要作用. MDA5或MAVS缺陷型小鼠对很多微小核糖核酸病毒如柯萨基病毒, 人鼻病毒和脑心肌炎病毒感染的敏感性都有所增强.

微小核糖核酸病毒在核糖核酸复制过程中生产出了很多病毒的核糖核酸, 这其中有单链和双链核糖核酸, 并且它们都具有“非自我细胞的特征”. 这些特征能被细胞内的感受器比如MDA5所识别. 这些病毒的基因组核糖核酸是一个单链核糖核酸分子, 在它的5'端带有一个病毒小肽VPg. 在感染过程中, 这个VPg会被细胞酶从一些病毒基因组核糖核酸上切掉, 从而产生一种5'带有单磷酸的单链核糖核酸. 另外, 病毒复制过程中还会产生两种中间产物. 第一种叫做RF的中间产物是一个双链核糖核酸. 第二种叫做RI的是一个带有局部双链结构的单链核糖核酸. 在这些病毒核糖核酸中哪一种能够激活MDA5, 更重要的是, 又有哪些是真正在生理状态下 (在被感染细胞中) 能够被MDA5识别的, 我们在这个课题开始前并不太清楚. 此外, 由于一型干扰素发挥着如此有效的抗病毒作用, 很多病毒包括微小核糖核酸病毒均可以有效的抑制一型干扰素系统. 几个研究小组此前已经对微小核糖核酸病毒如何与RLR介导的一类干扰素产生的信号通路进行相互作用进行了初步研究, 但是这些研究结果很零散, 甚至有些结果互相矛盾. 因此, 还没有一个微小核糖核酸病毒通用的免疫逃避策略呈现出来.

除了一型干扰素系统, 应激反应近来也被指出可能有抗病毒效应. 在不利的自然界条件下, 比如过热, 过冷, 过氧化环境或病毒感染, 细胞会自己生产“应激颗粒”. 这些应激颗粒是大量核糖核酸和蛋白的聚集体. 细胞以这种方式暂时储存和保护这些分子. 当外界压力消失或病毒感染被控制后, 这些核糖核酸和蛋白分子会被再次释放, 并可以重新执行它们的正常功能. 对于这种细胞应激反应对微小核糖核酸病毒所起的抑制作用, 以及它和RLR介导的一类干扰素产生信号通路之间的相互作用的研究才刚刚起步.

本论文在于加深我们对RLR识别微小核糖核酸病毒核糖核酸的认识, 以及对病毒逃脱内源抗病毒反应策略的了解. 本研究利用了两个模型病毒来着重研究微小核糖核酸病毒中的两个种属, 分别为肠病毒属中的毒株柯萨基病毒B3(CVB3)和心病毒属中的毒株脑心肌炎病毒门戈病毒.

主要结果摘要

如前所述,小核糖核酸病毒感染细胞时,被感染细胞中MDA5的天然配体尚不知晓.在第二章中,我们首先通过转染实验系统地研究了不同小核糖核酸病毒的核糖核酸在激活MDA5中起的作用,然后通过正常的感染实验对小核糖核酸病毒核糖核酸在生理环境下的识别过程进行了初步探索.我们首先从柯萨基病毒B3或者门戈病毒感染的细胞中分离了单链核糖核酸和双链核糖核酸(两者各自包含细胞核糖核酸和病毒核糖核酸),并发现一类双链核糖核酸能够在转染试验中激活MDA5.这一结论后来又通过使用纯化的病毒核糖核酸(不再含有细胞核糖核酸)的实验得以证实.从感染细胞中纯化得到的双链核糖核酸RF能够有效地激活MDA5.相反,病毒的单链核糖核酸(包括包含VPg的病毒核糖核酸和缺少VPg的病毒核糖核酸)并未在转染的细胞中诱导一型干扰素反应.体外实验进一步证明,RF能够在没有其他因子辅助的条件下直接激活MDA5.更重要的是,通过抑制剂抑制病毒复制过程中不同阶段(从而不同类型病毒核糖核酸的生产),我们发现负链核糖核酸的合成,即生产RF的这一步骤,是门戈病毒感染过程中诱导一型干扰素产生的先决条件.

第三章阐述了一种合成的含有5'三聚磷酸的核糖核酸转录子可通过激活RIG-I在细胞里激发有效的抗病毒反应.因为这一核糖核酸分子的序列来自于CVB3病毒基因组核糖核酸里的四叶草结构,从而被命名为CVB3四叶草核糖核酸.这一核糖核酸被转染后能够在细胞里诱导一型和三型干扰素,以及炎性细胞因子和趋化因子的产生.被CVB3四叶草核糖核酸预处理过的细胞还能够抵抗登革热病毒,水泡性口炎病毒和肠道病毒71的感染.

无论我们人类体内抗病毒效应是怎样的巧妙和有效,病毒其实是非常善于躲避人体内的抗病毒反应的,并以此在宿主体内恶劣的环境中成功扩散.第四和第五章阐述了CVB3,其他肠道病毒以及门戈病毒的逃逸机制.这些机制主要涉及了细胞的两种重要抗病毒系统——RLR介导的一型干扰素应答的信号通路和细胞应激反应.在第五章中,我们还探索了这两种细胞抗病毒通路之间可能存在的相互作用.

第四章的结果表明, CVB3和门戈病毒都能有效地抑制IRF3的磷酸化作用和激活,并从而抑制一型干扰素的生产.在被CVB3感染的细胞中, TBK1磷酸化被显著地抑制了. TBK1的磷酸化是对其对下游分子IRF3磷酸化和激活必不可少的.这一发现表明CVB3引起的RLR信号通路的阻断位于TBK1磷酸化这一步或者其上游.与这相反,门戈病毒能够显著增高TBK1的磷酸化水平,因此这一病毒在TBK1激活到IRF3磷酸化之间的某个过程对RLR信号通路表现出抑制作用.进一步研究表明, MDA5, MAVS和RIG-I在CVB3感染过程中发生了水解,但是这些蛋白在门戈病毒感染过程中却保持完好.与之前报道的一系列肠道病毒不同的是, CVB3诱导的MDA5的水解不是由细胞内半胱天冬酶或蛋白酶体(两组细胞蛋白酶)执行的.相反,病毒自身的蛋白酶是这一任务的执行者. MDA5和MAVS的水解模式可以被重组的CVB3蛋白酶2A再现出来,而RIG-I的水解模式可以被3C重组蛋白酶再现出来.随后,我们将肠病毒蛋白酶插入门戈病毒的基因组,并利用这些重组门戈病毒研究了肠病毒属中不同种病毒的2A和3C蛋白酶的作用.这些试验的结果表明MDA5和MAVS可以被三种不同种的肠病毒的2A蛋白酶水解,这些分别为肠病毒A种里的肠道病毒71, B种里的CVB3,以及C种里的小儿麻痹症病毒. RIG-I的水解相反依赖于这些病毒的3C蛋白酶的活性.

第五章的研究表明,除了干扰RLR介导的一型干扰素的生产, CVB3和门戈病毒都能阻碍细胞的应激反应. 以门戈病毒为例, 应激反应的抑制归因于病毒L蛋白的活性. 携带突变的L蛋白的重组病毒在被感染的细胞当中导致了大量应激颗粒的产生, 而野生型病毒并不引起应激颗粒的产生. 应激颗粒的形成对CVB3和门戈病毒的复制都具有抑制作用, 虽然这个作用比一型干扰素的抗病毒效应微弱. 但是, 这个应激反应诱导的抗病毒作用似乎和RLR介导的一型干扰素的生产并没有直接联系. 有趣的是, 我们发现MDA5会聚集于被突变L蛋白的门戈病毒感染, 热处理或氧化应激产生的应激颗粒上. 但MDA5的这个亚细胞定位对于应激颗粒的形成并不是必须的, 它也并不影响门戈病毒的核糖核酸识别过程和病毒应起的一型干扰素的生产过程. 至于微小核糖核酸病毒感染引起的应激反应的确切抗病毒机制仍旧需要进一步阐明.

结束语

病毒和宿主的抗病毒免疫反应之间的相互作用是极其复杂的. 在本论文中, 我们研究了MDA5识别微小核糖核酸病毒的过程, 以及这些病毒逃避抗病毒反应的途径. 我们提供了MDA5在生理条件下识别微小核糖核酸病毒核糖核酸的第一个实验证据, 并且还论证了肠病毒2A蛋白酶在这些病毒抑制MDA5介导的一型干扰素的生产途径中的中心作用. 同时, 我们还对门戈病毒L蛋白对一型干扰素系统的逃避机制提供了新的线索——TBK1磷酸化和IRF3的激活之间的一步被L蛋白抑制. 另外, 我们还部分阐明了细胞应激反应的抗病毒活性, 以及细胞应激反应和RLR介导的一型干扰素的生产途径之间的相互作用. 最后, 我们通过使用一个合成的5'三聚磷酸的核糖核酸转录子表明, RLR的激活具有抗病毒治疗和预防的潜能. 这些新的发现对未来对抗小核糖核酸病毒这个大家族的抗病毒治疗研究和疫苗的开发有重要价值.

Dankwoord
Acknowledgements

致谢词

Dankwoord / Acknowledgements / 致谢词

Nou nou ... Hier zijn we dus!

Dit proefschrift was nooit mogelijk geweest zonder veel hulpen, veel steun van veel mensen die ik hier wil van hart bedanken.

Mijn promotor Frank van Kuppeveld. Frank, Frank, Frank, waar zal ik mee beginnen? Bedankt om me in de fascinerende wereld van virussen te introduceren. Bedankt voor al je hulp met mijn opleidingen, zelfs vóór dat ik jouwe AIO werd. Bedankt om mij op aard te houden wanneer ik te ver wou vliegen, en mij weer even duwen als ik te lang op grond heb gezeten. Ik weet dat het veel makkelijker gezegd is dan gedaan! En bedankt voor alle andere dingen die ik hier niet ga noemen, in en buiten het lab! Ik zal nooit vergeten wat je voor me hebt gedaan. We houden contact!

P.S. Hoe dan ook we over je klachten (sorry, dat doen we dus af en toe wel :P), eind van de dag ben je een geweldig baas! Dat wil ik ook een keer gezegd worden.

Mijn twee paranimfen en vrienden - Hilde & Martijn. Hilde, het is hartstikke fijn om je op het kamer te hebben om af en toe even te ventileren, om mee te kletsen, en om goede én slechte nieuws te delen! Onze kleine brainstormsessies waren ook erg hulpvol om een net ander inzicht te krijgen, en dat wil ik ook blijven doen zolang als we beide in onderzoek zitten!! En natuurlijk heel erg bedankt voor al je hulp met dit proefschrift - het meedenken over mijn Discussie, alle taalhulp, en trucjes voor het opmaken!! Martijn, wat fijn was it om met een collega als jij samen te werken!! Je bent open, je bent fair, en bovendien, je bent altijd eerlijk en direct in wat je denkt. Dát waardeer ik heel erg, en wil je daarvoor eerst bedanken! En dan natuurlijk ook bedankt voor alle experimenten die je hebt meegeholpen, en voor alle technische en emotionele steun in de afgelopen jaren!

Joep, mijn promotor voor de eerste 3 jaren en mijn commissielid. Je zat toen niet echt bij ons op het lab in Nijmegen, maar je probeerde toch altijd aanwezig te zijn als ik praatjes moest geven bij groep besprekingen, en out-of-the-box vragen te stellen. Bedankt voor je belangstelling en steun! En ook bedankt om met me mee te gaan naar het Mozaiek laureate feestje! Was leuk!

Ellie, my mentor since the very early days. I was not all that long in your group, but somehow found a deep connection with you. Thank you for all your support and advice through out all these years, especially when time is tough. Your passion for the polio(post)eradiation program, and your strong sense of ethics will forever stay with me. And thank you, for showing me a "human" side of science and doing science.

Mijn kamergenoten, Rachel en Jim. Rachel, een van de fijnst consequenties van onze verhuizing is dat ik kon jij beter leren kennen! Ik ben altijd onder de indruk hoeveel van alles je weet, en ik heb al onze projectjes thuis zeker heel erg van genoten, en heel veel ervan geleerd! Bedankt daarvoor! Ik wens je ook heel veel succes met je volgende stap! Ik weet zeker dat je het kan, allen moet jij dat nog willen geloven :-). Jim, je bent zeker een bijzonder, en van hart welkom, toevoeging aan het kamer. Bedankt voor alle gezelligheid die je met opzet creëert, en die die je onbewust voor zorgt :D. Ik heb je gezelschap erg van genoten! En heel veel succes met je eigen

promotieonderzoek! Het komt allemaal goed!

De rest van de Picorna's :-). Jan en Stanley, jullie hebben allebei aan projecten die in dit proefschrift zijn gekomen gewerkt! Bedankt voor jullie bijdrage, steun, en alle leuk discussies die we hebben gehad, over werk of anders :-). Kjerstin, ons groepje in Nijmegen kon echt niet zonder jou! Bedankt om het lab zo goed georganiseerd en draaiende te houden! En natuurlijk ook bedankt voor al je hulp in mijn eerste 3 jaren op het lab, en je bijdrage aan Hoofdstuk 4!! Hendriek, mijn bier held, even een bijzonder bedankje aan jou, om de spontane borrels levend te houden door bijzondere en lekkere Belgische biertjes op voorraad te houden :D! Ik heb er heel erg van genoten! Mag ik bij je in België nog op bezoek ;-)? Matthijn, Huib, Cristina, Lucian, Lonneke en Jeroen - we did not get the chance to really work closely together. But, nonetheless, we do have a warm group, not without bumpiness, but warm at the end of the day anyways. That is, for me, an important part of the job, and I thank you all for being part of it and shaping it in your own ways along the way. Best of luck with your PhD's and post-doc's!!

Mijn relatieve nieuwe collega's in Utrecht. Nou, ik ga jullie niet één voor één noemen want er zijn er zo veel :-)! Ik wil jullie allemaal bedanken om ons warm te ontvangen toen we hier naar toe verhuisden! Vrieziers ontruimen is nooit leuk maar jullie hadden het toch voor ons gedaan! Ik ben heel blij dat ik de kans heb gehad om jullie allemaal te leer kennen! En ik heb ook veel nieuwe filosofie, kennis en technisch dingetjes van jullie geleerd! Ook hartelijk daarvoor bedanken! Hopelijk komen we elkaar nog tegen op congressen of feestjes. Het is maar een heel kleine wereld :-). 卉卉, 文涛, 秋实, 虹波, 美玲, 谢谢你们帮我翻译中文概述! 也祝愿你们在你们读博剩下的时间内成功, 好运!

The RNAi group from my beloved Nijmegen - Ronald, Sarah, Joël, Koen, Gijs, Pascal and Walter. It was a pleasure to have all of you as colleagues. Thank you for all the discussions in the lab and during our joint group meetings, and all the fun we had during borrels and football games! It was a shame that we had to say an early goodbye. But sometimes parting is the only way to truly realize what you really feel about someone and some place. I have missed you. Joël, mijn U'tje genoot voor 3 jaren, ook nog bedankt om al mijn rosé, fluffy spullen toe te staan :D ! En heel veel succes en plezier met de volgende stap van je leven, in jullie nieuwe huis!

I also owe many thanks to quite a number of students that worked with me along the way. Mai, Marie, Yasemin, Zilin, Dirk and Irene. Thank you all for your enthusiasm and hard work on your respective projects! I hope I have done you fair; sometimes a supervisor is just as unsure as the student :P. Good luck with your studies and PhD's!! I look forward to seeing your own theses!

My many many collaborators on various projects during the years - Thomas Michiels, Rick Lloyd, John Hiscott, David Olagnier, Robin van der Lee, Martijn Huynen, Safia Deddouche, Caceano Reis e Sousa, Richard Virgin-Slane, Bert Semler, Alys Peisley and Sun Hur. It was a pleasure to work with all of you. Thank you for your kind advice as well as technical and intellectual contributions to this thesis!

Of course, the past 4^{1/2} years were not spent entirely in the lab. My many many friends saw to it that I didn't drown in the ever-growing to-do lists and the inevitable frustrations that come with a PhD. Nina, Jurjen, Keke, 张岩, Jessica, Hilde, Sarah, Kjerstin, Rachel, and Arthur, thank you all

Dankwoord / Acknowledgements / 致谢词

for all the fun we had together, and for being there for me during all the good times, and all the bad ones! I promise I'll come up to visit as often as I can! And of course you are always welcome at our new home in Zurich!

爸爸妈妈, 爷爷奶奶, 姥姥姥爷, 感谢你们从小到大对我的养育, 培育, 和教育! 以及这些年来给我的支持和鼓励! 姥爷, 谢谢你把你科学的热爱从小就传递给了我! 我把这篇论文献给你. 希望你喜欢!

Last but not least, my dear Andi. It is public knowledge that it is no light job to be the partner of a PhD candidate (as we both know :P), just as it is public knowledge that you are the sweetest guy a girl can hope for :-). Thank you for all the love and support you've given me, and for keeping things in perspective for me. And before you complain, thank you for your professional support and advice on all screen-related matters. They were always deeply appreciated ;-). I look forward to finally having a home with you! Love.

Dankwoord / Acknowledgements / 致谢词

Curriculum Vitae

Curriculum Vitae

Qian Feng was born on 21 June 1985 in Beijing, China. Having received her high school diploma from the High School Affiliated to Renmin University of China in Beijing in 2003, she began her higher education in biochemistry at the Hogeschool van Arnhem en Nijmegen (HAN) in Nijmegen, the Netherlands. During this study she performed a four-month internship at the department of Molecular Animal Physiology at the Radboud University Nijmegen. Under the supervision of Karen van Loo and Prof. Dr. Gerard Martens, she studied associations between the genetic and epigenetic changes in the BDNF and TrkB genes and schizophrenia. For her thesis project, she went to the National Institutes of Health in Bethesda, USA, and performed 9 months research in the laboratory of Dr. Ellie Ehrenfeld, where she worked on the involvement of three cellular ArfGEF proteins in poliovirus infection under the supervision of Dr. Georgiy Belov.

After obtaining her Bachelor's degree in Biology and Medical Laboratory Research in 2007, she went on to further her education by participating in the Master's program Molecular Mechanisms of Diseases at the Radboud University Nijmegen Medical Centre. During this study she joined the group of Dr. Frank van Kuppeveld at the Department of Medical Microbiology, Section Virology for 6 months, and with help of Stanleyson Hato, studied picornavirus recognition by the RIG-I-like receptors. For her Master's thesis project, she went to the group of Prof. Dr. Charles Rice at the Rockefeller University in New York, USA. There, under the supervision of Dr. Alexander Ploss, she studied the tissue and species tropism of the hepatitis C virus and contributed to the development of a small animal model for hepatitis C. In 2009, she obtained her M.Sc. degree *summa cum laude* from the Radboud University Nijmegen.

Thereafter, with support of Dr. Frank van Kuppeveld, she obtained a personal PhD grant from the Netherlands Organisation for Scientific Research (NWO), and joined Frank's group at the Radboud University Nijmegen as a PhD student to continue to study the interaction between picornaviruses and innate antiviral responses. In 2012, she moved with Frank's group to the University of Utrecht, and joined the Virology section at the Department of Infectious Diseases and Immunology, Faculty of Veterinary Medicine, to continue her PhD work.

From December 2014 onwards, she will join the group of Dr. Benoit Kornmann at De Eidgenössische Technische Hochschule (ETH) in Zurich as a post-doc to study communication between intracellular membranous organelles.

LIST OF PUBLICATIONS

Feng, Q., Langereis, M.A., van Kuppeveld F.J.M. 2014. Induction and Suppression of Innate Antiviral Responses by Picornaviruses. *Cytokine and growth factor reviews*. Submitted upon invitation.

Feng, Q., Langereis, M.A., Olnagier, D., Chiang, C., van de Winkel, R., van Essen, P., Zoll, J., Hiscott, J., van Kuppeveld, F.J.M. 2014. Coxsackievirus Cloverleaf RNA Containing a 5' Triphosphate Triggers an Antiviral Response via RIG-I Activation. *PLoS One*. 9(4)

Deddouche, S., Goubau, D., Rehwinkel, J., Chakravarty, P., Begum, S., Maillard, P.V., Borg, A., Matthews, N., **Feng, Q.**, van Kuppeveld, F.J.M., Reis e Sousa, C. 2014. Identification of an LGP2-Associated MDA5 Agonist in Picornavirus Infected Cells. *eLife*. 3

Feng, Q., Langereis, M.A., Lork, M., Nguyen, M., Hato, S.V., Lanke, K., Emdad, L., Bhoopathi, P., Fisher, P.B., Lloyd, R.E., van Kuppeveld, F.J.M. 2014. Enterovirus 2A^{pro} Targets MDA5 and MAVS in Infected Cells. *Journal of Virology*. 88(6)

Langereis, M.A., **Feng, Q.**, Nelissen, F.H., Virgen-Slane, R., van der Heden van Noort, G.J., Maciejewski, S., Filippov, D.V., Semler, B.L., van Delft, F.L., van Kuppeveld, F.J. 2014. Modification of Picornavirus Genomic RNA Using 'Click' Chemistry Shows That Unlinking of the VPg Peptide is Dispensable For Translation and Replication of the Incoming Viral RNA. *Nucleic Acids Research*. 42(4)

Langereis, M.A., **Feng, Q.**, van Kuppeveld, F.J.M. 2013. MDA5 Localizes to Stress Granules, But This Localization is Not Required for the Induction of Type I Interferon. *Journal of Virology*. 87(11)

Feng, Q.*, Hato, S.V.*, Langereis, M.A., Zoll, J., Virgen-Slane, R., Semler, B.L., van Rij, R., van Kuppeveld, F.J.M. 2012. MDA5 Detects the Double-Stranded RNA Replicative Form in Picornavirus-Infected Cells. *Cell Reports*. 2(5)

Dorner, M., Horwitz, J.A., Robbins, J.B., Barry, W.T., **Feng, Q.**, Mu, K., Jones, C.T., Schoggins, J.W., Catanese, M.T., Burton, D.R., Law, M., Rice, C.M., Ploss, A. 2011. A genetically humanized mouse model for hepatitis C virus infection. *Nature*. 474(7350)

Belov, G., **Feng, Q.**, Nicovics, K., Jackson, C.L. & Ehrenfeld, E. 2008. A Critical Role of a Cellular Membrane Traffic Protein in Poliovirus RNA Replication. *PLoS Pathogens*. 4(11)

Lanke, K.H.W., van der Schaar, H.M., Belov, G.A., **Feng, Q.**, Duijsings, D., Jackson, C.L., Ehrenfeld, E., & van Kuppeveld, F.J.M. 2009. GBF1, a Guanine Nucleotide Exchange Factor for Arf, Is Crucial for Coxsackievirus B3 RNA Replication. *Journal of Virology*. 83(22)

